DOCTORAL THESIS

entitled:

Feasibility of treated wastewater on crops irrigation and its quality improvement through environmentally sustainable treatments

This thesis is submitted in fulfilment of the requirements

of the degree of Doctor in Chemistry

by

Zaineb Bakari

Supervisors:

Prof. **Boubaker Elleuch: University of Sfax, Tunisia**

Prof. **Massimo Del Bubba: University of Florence, Italy**

*Defense date:**25*** **June 2022**

Jury composition

President: Prof. Mahmoud Trabelsi, Faculty of sciences of Sfax, University of Sfax, Tunisia

Reppoter: Prof. Ilaria Palchetti, University of Florence, Italy

Prof. Moncef Zairi, National Engineering of Sfax, University of Sfax, Tunisia

Examiner: Prof. Anna Maria Papini, University of Florence, Italy

LR16ES19 LGEET, Ecole Nationale d'Ingénieurs ENIS, Université de Sfax, Sfax, Tunisie
Depatment of chemistry 'Hugo Schiff', Università degli Studi Di Firenze, Italia

Dedication

This work is dedicated to

My mother and my father,

whose great love has always been a propelling energy for all my success.

My sister and my brother Faika and Yassin

My close friends Amani and Sana

And everyone who helped me in any way.

Acknowledgments

I would like to express my appreciation and gratitude for my supervisors, professor Massimo Del Bubba and professor Boubaker Elleuch.
Their invaluable help, guidance and advice to me have been essential in the completion of this thesis
with their encouragement and positivity throughout the course of my PhD. Thank you for the opportunity I had to work with your teams.
I am grateful to Prof. Del Bubba for his time, effective supervision, constructive advice and above all for his trust and his patience. I can't thank you enough for all the help that you've bestowed upon me.

I was lucky enough to be co-supervised by Dr. Nesrine Boujelben I learned a lot from her. I am extremely thankful to her and I appreciate her efforts to provide all the necessary means for the completion of this thesis.

I would like to thank professor Mahmoud Trabelsi for accepting to chair the jury of my thesis.
I would like to thank the committee members, professor Ilaria Palchetti and professor Moncef Zairi for giving me the honour of being the referees of my thesis.
I associate with these acknowledgments, professor Anna Maria Papini for agreeing and taking the time to review my PhD thesis. I have a deep respect for their careers and works.

I present my sincere thanks to all the staff and laboratory technicians GEET and LARSEN at the National School of Engineers of Sfax. I am hugely grateful to Leonardo Checchini, his guidance, patience and assistance were very important while undertaking my experiments in the lab in the university of Florence.
I would like to extend my thanks to my colleagues who participated somehow to this work.

LIST OF ABBREVIATIONS AND ACRONYMS

AAS Atomic Absorption Spectrophotometry

ANOVA Analysis Of Variance

AB Activated Biochar

AC Activated Carbon

APnEOs Ethoxylated Alkylphenols

Aps Alkylphenols

BC Biochar

BET Brunauer-Emmet-Teller

BJH Barret-Joyner-Halenda

BOD_5 Five-Days Biological Oxygen Demand

C_e Equilibrium Concentration

C_i Initial Concentration

COD Chemical Oxygen Demand

EC Electrical Conductivity

FAO Food and Agriculture Organization of the United Nations

FC *Faecal Coliform*

FTIR Fourier Transform InfraRed

FW Fresh Weight

GW Groundwater

HI Hazard Index

MAC Mineral Activated Carbon

MB Methylene Blue

MQL Method Quantification Limit

NT Tunisian Norm

OM Organic Matter

PAH Polycyclic Aromatic Hydrocarbons

PCBs Polychlorinated Biphenyls

P_t Total Phosphorus

Q_t Adsorption Capacity

Q_m Maximum Adsorption Capacity

SAR Sodium Adsorption Ratio

SEM Scanning Electron Microscopy

SSA Sewage Sludge Ash

TC Total Coliform

THQ Target Hazard Quotients

TOC Total Organic Carbon

TSS Total Suspended Solids

TWW Treated Wastewater

VAC Vegetal Activated Carbons

WDPT Water Droplet Penetration Time

WHO World Health Organization

WW Wastewater

WWTP Wastewater Treatment Plant

LIST OF FIGURES

LIST OF TABLES

TABLE OF CONTENTS

General objectives

General objectives

The fast increase in the world population is accompanied by a growing demand of foods and energy that in turn requires an increase in the industrial and agricultural activities. The agriculture is considered to be the main water consumer with around 70% of the total world water use (Guadie et al., 2021). Water shortages are expected to affect 40% of the population by 2050, also because of climate change. Therefore, tackling water scarcity and saving fresh water are becoming an urgent need around the world. On the other hand, the rapid demographic and productive development generates huge amounts of wastewater (WW) and sewage sludge, which are at the same time are wastes but also contain important resources that should be reused. Important strategies for the management of these matrices are the reuse of treated wastewater (TWW) in the agricultural sector in order to decrease the pressure applied on fresh water resources and the management of sewage sludge to produce sorbent materials that can be used in the reduction of the contamination of TWW.

Indeed, the decrease in the availability of water of good quality for agricultural irrigation and increasing competition from other water use sectors (Mesa-Jurado et al., 2012, Milano et al., 2012), make TWW a valuable alternative source of irrigation water (Hamilton et al., 2007). However, TWW should be reused with caution and regularly monitored, as it may contain chemical and biological contaminants that may pose negative environmental and health impacts (Singh et al., 2004, Hamilton et al., 2006, Muchuweti et al., 2006, Fatta-Kassinos et al., 2011). From an agronomic point of view, WW irrigation was found to affect the yield and quality of agricultural products, as TWW may contain significant amounts of nutrients and heavy metals, depending on sewage origin and treatment technology applied.

To ensure the protection of crops from possible contamination when TWW is used for irrigation, the European Commission has set a series of limits and risk assessment strategies deriving from the reuse of such waters (Rizzo et al., 2018). Strawberries and olives are fruits with high commercial and nutraceutical added value, characterized by large production and consumption in the Mediterranean regions, by virtue of their climate, which is suitable to their cultivation (Akhatou et al., 2016; Giampieri et al. 2012) and that occur nutraceutical and economical values. Based on studies elsewhere reported (Christou et al., 2016; Renai et al., 2021), which demonstrated the safety of strawberry fruits obtained by irrigation with TWW, in this work it was analysed the effect on soil and plants of TWW used for crop irrigations. Considering the sensitivity of strawberries to salinity (Suarez and Grieve, 2013), the objective of this study was to evaluate the impact of different dilution percentages of TWW in comparison with groundwater on strawberry quality and safety, particularly for soil, plants and productivity and fruits metals compositions.

Moreover, additional treatments are useful to improve the removal of hazardous substances from TWW and the use of sewage sludge-based sorbent to pursue this goal would be a win-win solution. Indeed, huge attention has been given worldwide to the use and management of sludge, and a copious legislation has been promulgated in this regard. For example, in Italy, the legislative Decree 152/2006 issued by the regional administrative courts made the management of sludge even more complex, requiring for its spreading onto soil the satisfaction of a number of contamination threshold concentrations.

In this research, a comprehensive strategy was adopted to overcome the sludge management problems by producing a carbonaceous material from sawdust and mixtures of sewage sludge and sawdust to be used as sorbent as an economically advantageous alternative for WW treatment compared to traditional solutions to remove organic and inorganic pollutants such as dyes, ethoxylated alkylphenols and heavy metals.

In this study three part will be investigate:

i) Evaluation of the reuse of TWW for olive and strawberry for irrigation and its effect on soil, plant and heavy metals content in fruits.

ii) Performance of sewage sludge ash in the removal of inorganic pollutant (copper) using quality by design.

iii) Sewage sludge-based biochar development and their environmental importance in the pollution management through water and/or WW purification from organic contaminants.

Literature review

I. Water scarcity problem

1. Global situation

Fresh water is the basic resource for life on the planet, vital for human being and environment needs (Link et al., 2016). Recently, climate system perturbation and human socioeconomic fast evolution intensify the global use of water modifying the aquatic cycles and producing consequently water scarcity especially in regions that are arid or semi-arid (Kirby et al., 2014). Climatic changes produce the water evaporation by global warming and alter the global precipitation rhythms, which cause floods in some regions and droughts in others (Catorci et al., 2021; Prudhomme et al., 2014). Besides the considerable increase of the world population, just the same, industrial progress and dietary shift reduces considerably drinking and unpolluted water resources (Wada et al., 2016).

The increase of the global population from 7.6 to around 9.8 billion by 2050 will increase the demand of fresh water (UN, 2017). In fact, almost 50% of the current world population lives in regions suffering from water scarcity (i.e., about 3.6 billion people), and it is expected that by 2050 this number will increase to between 4.8 and 5.7 billion people (WWAP, 2018; Chakraborti et al., 2019).

The agricultural sector is considered the highest consumer of water (Sinha et al., 2017). Furthermore, fresh water available for each individual is continuously decreasing and its renewal is limited (Vanham et al., 2018), thus making water scarcity the most important public issue worldwide (van Vliet et al., 2021).

To moderate this water crisis, many studies are focused on sustainable solutions and alternative resources of water. The treatment of roof rainwater (Du et al., 2022) and different kind of non-conventional technologies used for desalting seawater such as such as reverse osmosis, electrodialysis and distillation (Alkhadra et al., 2020; Schiermeier, 2008) are convenient for extensive fresh water supply. The electrical or thermal electrical power leading seawater desalination needs high energy accompanied with an important capital cost that depends on the capacity of treatment plant and region' s characteristics (Pan et al., 2020). Distillation-based desalination, which consists of series of heat exchangers is much less efficient by about 5kWh/m^3 than reverse osmosis, which however has some drawbacks such as the low degrees of decontamination and water recovery, which represent of course an environmental problem (Shannon et al., 2009). TWW is also considered as an attractive solution across several broader unconventional industries and goals in all over the world (Mu'azu et al., 2020). As an example,

unconventional oil and gas production required a huge volume of fresh water. The treatment and reuse of its WW can be a promoted solution to minimize water scarcity risk and high economic cost (Robbins et al., 2022).

2. Water situation in Tunisia

Time and space rainfall scales in Tunisia are characterized by a certain irregularity, which are increasesd in the winter season. The rainfall trend records variable levels between north, centre and south with values respectively around 594, 289 and 156 mm and therefore a total water volume of about 4.8 billion m^3 (Chebil et al., 2019). Potential water resources derived from surface water (about 2.7 billion m^3) and groundwater (2.1 billion m^3) are unevenly distributed among the different regions of Tunisia with ratios of about 60, 27 and 22% in the north, centre and south, respectively (ITES, 2018). Considerable infrastructures are used to mobilize surface water including 698 artificial lakes, 182 hill dams and 27 large dams. Concerning the groundwater, about 212 and 267shallow and deep aquifers are available, respectively, including renewable and weakly renewable or fossil reserves (MA, 2016). Considerable pressure is maintained to the use of shallow aquifers especially in the coast and in the center of Tunisia, in the private irrigated regions that use particularly wells, which have been increased more than doubled between 1980 and 2015 (DGRE 2017). In fact, the irrigation of southern oases is essentially based on groundwater. The over exploitation of this water in private areas produces critical effects on fresh water supply, on the availability of water for irrigation and on salinity and/or soil degradation.

In fact, the analysis of the availability of water resources determined by the Tunisian Institute for Strategic Studies (ITES, 2018) has shown that starting from 2030, Tunisia will suffer from an absolute water shortage, and its level will drop by about 350 m^3/per capita/year. According to the World Health Organization the waters stress starts when water availability is less than 1000 m^3 per capita, per year. In 2018, this amount was 400 m^3/per capita/year, thus demonstrating the critical situation of the water shortage (Siddiqi and Anadon, 2011; UNDP, 2006). The water demand from the agricultural, urban, industrial, and tourism sectors is expected to be around 2770 million m^3 in 2030 (IETS, 2018). The agricultural sector, which covers approximately 450,000 hectares, uses about 80% of the total water for irrigation utilized in all Tunisia (Dhehibi et al. 2014; Chebil et al., 2019). As consequence, the Tunisian agricultural products increased with the expansion of these irrigated crops.

3. Water management in Tunisia

Efficient water resource management is required to manage the water demand in the future. An integrated water policy keeps in balance all the requests of the various sectors enhancing the exploiting of non-conventional water resources such as desalinization and WW treatment.

3.1.Water desalinization

Tunisia, having limited water and energy resources, considers desalination as a way to reduce the difference between water supply and demand, by providing water management rather than integrating solution for water penury (Affi et al., 2021). More than 100 facilities have been constricted essentially for domestic water supply with a desalinization capacity of about 200,000 m^3/ day in 2016. Brackish groundwater desalinization by reverse osmosis is generally used in the south and centre of Tunisia. This method has both environmental and economic benefits compared to the desalinization of seawater that is more expensive, mainly due to the initial investment required and subsequent operation and maintenance costs, as well as for the higher energy consumption (Ghaffour et al., 2013).

3.2.Wastewater treatment

The use of TWW for irrigation is considered an advantageous and sustainable alternative to the use of fresh water in agriculture, which is the sector with the greatest water consumption. This alternative is used in Tunisia since 1987 in the olive growing sector, such as in the El Hajeb region, in Central–Eastern Tunisia (34°43N, 10°41E). The reuse of TWW has environmental and economic benefits, such as the over exploitation of fresh water resources and the use of external fertilizing inputs, due to the high content of nutrients, necessary for plant growth and production (Hentati et al., 2014). However, some studies focusing on reuse of TWW demonstrated the possible drawbacks of irrigation using TWW such as soil salinization, plants damage and microbiological contamination with *Escherchia coli* (Bedbabis et al., 2015)

The TWW quantities have been increased from 6 Mm^3/year in 1975 to 284 Mm^3/year in 2019 in agreement with the increase in the number of wastewater treatment plants (WWTPs), which went from 5 in 1975 to 122 in 2019 (ONAS, 2019).

II. Treated wastewater composition

WW reuse represents an advantageous alternative to the lack of fresh water and its high demand, especially in countries having problems of water scarcity. Agricultural sector is responsible for 70% of the worldwide consumption of FW (FAO, 2005) imposing then a severe burden on water sources

in arid and semi-arid areas. Important efforts are made to generalize the use of TWW as an advantageous alternative hydraulic resource for irrigation in the agricultural, industrial and municipal sectors. The principal aim of the sewage treatment is to allow the final effluent to be disposed without any dangerous effect to human health and environmental safety. After the preliminary treatment, three processes should be used for the WW purification, which are primary, secondary and tertiary treatments (Massé and Masse, 2000). Sewage treatment aims to removing or reducing conventional pollutants such as organic matter, total suspended solids, phosphorus, and nitrogen, in order to ensure that the effluent does not have any toxic risks for the receiving environment.

WW generally contains solids, dissolved substances and microorganisms, which are the cause of the main restrictions on the reuse of TWW. In fact, the regulations distinguish between quality levels for TWW, determined mainly by organic matter concentration and occurrence of pathogenic microorganism or microorganisms acting as indicator of pathogens presence. It is therefore essential to know the composition of TWW in order to define the possible reuse areas and levels of restriction.

1.1.Microorganisms

Sewage contains all the microorganisms excreted with the faeces. Pathogenic organisms such as *Legionella* spp., *Salmonella* spp., intestinal Nematodes and *Escherichia coli* accompanies the normal enteric flora. All these organisms can be classified into four large groups; bacteria, virus, protozoa and helminths characterising by a great potential for the appearance of different variety of diseases and illnesses (Al-Nakshabandi et al., 1997; Calci et al., 1998).

1.2.Metallic trace elements

There are multiple sources of metals in aquatic environments, which are mainly differentiated based on their natural or anthropogenic origin. Indeed, metals are naturally present in soils (geochemical origin) as major (Al) or important (Fe, Mn) constituents of the structures of minerals. The main natural phenomena leading to the spreading of metals in environmental compartments are volcanic activity and rock weathering (Pettinger, 2008). In addition to geochemical backgrounds, aquatic environments are enriched in metals by human activities. Metals are used by humans as materials and as reagents in industry (e.g., surface treatment, and reaction intermediate). Industrial activities, as well as vehicular traffic, emit fine metallic particles into the atmosphere, mainly in urban areas (Azimi et al., 2005). Thus, disseminated metals are transferred in various environmental compartments such as water plants and soils. Metals disposed on the ground can however reach the

watercourses by runoff during the rainy periods.

In the case of an unitary WW collection network, urban WW is made up of a mixture of domestic WW, industrial WW and water runoff. The metals contained in the runoff come from atmospheric deposits also from the corrosion of the rusting surfaces (roofing, gutters…) (Gromaire et al., 2001). In fact, most metals in runoff are mainly associated with suspended matter or colloids. In industrial WW, metals result directly from their utilization in industrial processes. This WW is characterized by a significant variability of its pollution level. However, the metal level in domestic water is cyclical because it results from the daily activity of households. The metals contained in domestic WW originate, on the one hand, from the corrosion of drinking water pipes and, on the other hand, from the use of metals in domestic activities and in household products.

In some regions, mine wastes also constitute a significant point source of metallic trace elements (Kang et al., 2018). Urban WW is one of the main sources of metal supply to aquatic ecosystems (Rai, 2008). At the entrance of WWTPs, a large part of metals contained in WW is bound with dissolved organic matter. The metals present in the TWW (e.g., cadmium, copper, molybdenum, nickel, and zinc) can pose a significant health risk to human being and, in the long term, they can also affect crops irrigated by TWWs by their accumulation in the soil (FAO, 2005). However, it should be noted that metallic trace elements in TWW are generally low and do not represent a factor limiting the reuse of TWW in irrigation. In fact, most of these metals are retained in the sludge from WWTPs during the treatment of WW (Faby et al., 1999). Exceptions to this general low hazard are the presence of very polluting industrial activities connected directly to the sewage network or the reuse of WW containing metallic trace elements, without any treatment (Toze, 2006).

1.3.Nutrients

Nutrients are commonly found in large quantities in TWW. They constituted an important quality parameter for the evaluation of these waters in agriculture and in landscape management (Hamoda, 2004). The most common nutrients in TWW are nitrogen, phosphorus and sometimes potassium, zinc, boron and sulphur (Lubello et al., 2004; Adrover et al., 2013). These elements were found in appreciable quantities, but in strongly variable proportions, either in treated or raw WW (Hussain and Al- Saati, 1999; Kiziloglu et al., 2008).

1.4.Dyes

TWW can contain dark colour produced essentially by dyeing industry WW, which could cause serious pollution phenomena (Forgacs et al., 2004; Lim et al., 2010). Synthetic dyes can cause serious and harmful effects on humans and organisms in hydraulic medium, such as mutagenic,

carcinogenic, and teratogenic effects (Khandare and Govindwar, 2015). Dyes could also reduce photosynthesis and light penetration in aquatic medium (Aksu and Tezer, 2000). Therefore, synthetic dyes should be removed before their release into the environment (Feng et al., 2011). The treatment of dyeing WW is therefore an important issue and a "hot-spot" of the WW treatment, commonly managed using biological or membrane treatments, photo-degradation treatment, chemical oxidation, and adsorption approaches (Anastopoulos and Kyzas, 2014).

1.5. Suspended matter and organic matter

Suspended solids are mostly biodegradable in nature. Most of pathogenic microorganisms contained in TWW are associated with TSS (FAO, 2005).

The presence of organic matter does not represent in general an obstacle to the reuse of TWW. On the contrary, it contributes to soil fertility. However, the presence of organic micropollutants (OMPs) in TWWs can represent an issue of high environmental concern. A plethora of OMPs can be present in TWW as the result of domestic and industrial activities. As regard the latter origin, ethoxylated alkylphenols (APnEOs) are used mainly in the textile industry as non-ionic surfactants, as well as antioxidants in a number of industrial applications (OSPAR Commission, 2009), and their presence in this kind of industrial effluent is of some concern, especially considering that one of their most abundant metabolites is the alkylphenol, which is characterized by a significant toxicity (Asimakopoulos et al., 2012; Vega-Morales et al., 2010).

III. Reuse of treated wastewater

TWW reuse is an opportunity to greatly extend reservoirs of fresh water contrasting water scarcity (Maizel and Remucal, 2017; Margenat et al., 2017; Fongaro et al., 2016). The use of TWW for non-potable urban applications such as street cleaning, vehicle washing, and toilets flushing, as well as for industrial needs (e.g., for washing products or aggregates and for recycling cooling towers) are examples of these opportunities (Guest et al., 2009).

Recently, TWW has been considered as an important water source for agriculture sector that consumes the higher amount of water compared to the other sectors. TWW is used for irrigation of crops, public parks and golf courses. Many studies (Oron et al., 2007; Ghasemi et al., 2011) have verified the benefits of using TWW for irrigation as a permanent and cheap water resource that reduces the cost as well as the use of chemical fertilizers, provides water characterized by good quality for other uses and minimizes the possible negative effect of TWW disposal on the aquatic resources.

In many regions, especially those arid and semi-arid, that have limited resources of fresh water, it is

necessary to use TWW as an alternative to clean water in many sectors, such as the irrigation of crops. As an example, the irrigation of crops with TWW in the USA was started from 1930 in Texas and Arizona (US EPA, 2016) and until today this water is reused to irrigate different kind of crops such as cotton, wheat, citrus, alfalfa and others plants (SVWP, 2020). Another example is in California and north of Monterey, where around 12,000 acres of raw eaten crops are irrigated with TWW. The use of the drip irrigation method is the most expensive form used for salad and plants sensitive to possible microbial contamination from TWW, which make it safer than other irrigation methods (Fine et al., 2006).

The water scarcity problem obliges to find alternative resources of water for irrigation purposes. TWW is characterized by high availability compared to fresh water resources. Even with a low public acceptance level, recently the irrigation using TWW was enhanced in regions suffering from water shortage like Mexico, Morocco, Pakistan, and Ghana where many crops are irrigated with TWW (Pedrero et al., 2010; Lydecker and Drechsel, 2010; El Ghadraoui et al., 2021).
Many countries in Mediterranean region such as Italy, Greece and Spain, where the problem of water shortage is severe, the TWW reuse ranges from 5 to 12% while the average use of TWW in Europe is 2.4% of the total TWW volume. In Italy, TWW are widely used in agriculture such as the irrigation of tomatoes and eggplant (Cirelli et al., 2012), and has been tested in research studies for the cultivation of strawberry (Scordo et al., 2020) and olive (Renai et al.,2021). This use increased the crop productivity and reduces the water scarcity problem (Pollice et al., 2004; Cirelli et al., 2012).

Since 1965, TWWs are used for irrigation of citrus and its utilization has been authorized for many crops such as palms, olive, grapevine, wheat, and barley (Khabou et al., 2009; Werfelli et al., 2021). The irrigation with TWW of olive trees showed a favourable and efficient response (Celano et al., 1999; Ghrab et al., 2013). In fact, olive moderately tolerate to water salinity as reported by many researches (Wiesman et al., 2004; Sairam and Tyagi, 2004; Melgar et al., 2009). Ghrab et al., (2013) verified the absence of negative effects on olive yield and fruits after nine years of irrigation using saline water of trees cultivated in sandy soil and in an arid region (Sfax, Tunisia). The reuse of TWW has been declared as a national goal in Tunisia, while a rate of TWW' utilization about 24% was intended for irrigation to replace the use of well water in agriculture (FAO, 2017).
At the same time as the increase in agricultural water needs and the reduction of groundwater resources, the irrigation using TWW may present an improvement in the water balance of areas when used correctly. Furthermore, proper use of TWW can be realized by irrigation of crops and/or artificial regeneration of groundwater aquifers, which makes it useful in the agricultural sector,

ensuring compliance with the standards limits set for the reuse of TWW in this sector (**Table 1**). In fact, the use of TWW in Tunisia in agriculture was regulated in 1989 decree (Decree No. 89-1047). This practice was developed and by 2013, 110 WWTPs recycled approximately 230 million m^3 per year of TWW, 26% of which was reused to irrigate agricultural land of about 8100 ha (ONAS, 2013).

Table 1. Tunisian standard for treated wastewater uses in agriculture (NT 106.03) and for effluents discharge in hydraulic natural flows (NT 106.02) (INNORPI, 1989).

Parameter	Maximum allowed content in the NT 106. 03 for agricultural sector	Maximum allowed content in the NT 106. 02 for maritime public domain
pH	6.5 – 8.5	6.5 – 8.5
Electrical conductivity (EC) (µS cm^{-1})	7	-
Chemical oxygen demand (COD)	90 [a,b]	90
Biochemical oxygen demand during five days (BOD_5)	30 [a,b]	30
Total suspended solids (TSS)	30[b]	30
Calcium (Ca)	-	-
Magnesium (Mg)	-	2000
Sodium (Na)	-	-
Chloride (Cl)	2000	
Fluoride (F)	0.001	5
Halogenated hydrocarbons	0.1	10
Arsenic (As)	0.1	0.1
Boron (B)	3	20
Cadmium (Cd)	0.01	0.005
Cobalt (Co)	0.1	0.05
Chromium (Cr)	0.1	2
Copper (Cu)	0.5	1.5
Iron (Fe)	5	1
Manganese (Mn)	0.5	1
Mercury (Hg)	0.001	0.001
Nickel (Ni)	0.2	2
Lead (Pb)	1	0.5
Selenium (Se)	0.05	0.5
Zinc (Zn)	5	10
Faecal coliforms (per 100mL)	-	2000
Faecal streptococcus (per 100mL)	-	1000
Salmonella Intestinal nematodes (per 100 mL)	-	Absent
Intestinal nematodes (arithmetic mean for the number of eggs per liter)	<1	-

All units are in mg/L, unless differently specified. [a] 24h made up sample. [b] Except special authorization

Olive cultivation represents one of the most important sectors in the Tunisian economy. More in

detail, 65 million olive trees are cultivated in 1.6 million hectares (Hannachi et al., 2007).
Chemlali is the mainly cultivated olive, grown especially in northern and central regions that produces about 80% of the total Tunisian oil (Baccouri et al., 2007). The TWW irrigation proves olive plant growths and its physiological performance and oil quality as reported in many studies (Bedbabis et al., 2009; Tak et al., 2013; Tekaya et al., 2016)).

IV. Limits and proposed solution

1. Effects on public health

TWW can exert chemical and/or biological toxicity through the presence of organic and inorganic chemical pollutants, and pathogens that can contaminate the food chain (Balkhair and Ashraf, 2016). These biological and chemical contaminants may cause dangerous issues (Khalid et al., 2018) to the human health of the producers, distributors and consumers, mainly by inhalation and ingestion, especially in the absence of proper management (Yi et al., 2011).

1.1.Effects of pathogenic organisms

The different kinds of microorganisms such as protozoans, viruses and bacteria, existing in the untreated sewage, may be present also in the final treated effluent, especially in the case of absence of advanced filtration and/or disinfection process during the water recycling process. Enteric viruses (prevalently the adenovirus) were found in secondary treated effluents (Fabres et al., 2017; Schlindwein et al., 2010). Therefore, many norms and regulations were made to ensure the safety of TWW from these pathogens and reduce their negative effects on the public health. However, pathogens are frequently presenting in TWWs, especially when the legislation is not correctly applied. Microorganisms were revealed at different concentrations in many TWWs used for irrigation in several studies. For example, Libutti et al. (2018) used secondary TWW characterized by a high concentration of *Escherichia coli*, faecal enterococci and coliforms, for broccoli and tomatoes irrigation, with the *E. coli* concentration even above the limit set for reuse. Analogous characteristics of TWW have been reported by Gatta et al. (2016), who found concentrations of *E. coli* above the limit set by Italian authorities. Mcheik et al. (2017) verified that the faecal coliforms and *Escherichia coli* in secondary treated effluents, used for vetch and barley irrigation in Lebanon and Jordan, respectively, were above the required limits proposed by the World Health Organization. However, the literature did not show any pathogenic contamination of the edible part of the plant. These observations may be the result of the absence of real contact between fruits/vegetables and the effluent used for irrigation. Authors have been suggested that the higher contamination degree could affect more farmers than consumers by the direct exposure to TWW,

rather than by the consumption of crops. Moreover, many studies have been verified the effect of contaminated foods by enteric viruses in the spread of diseases and epidemics (Richards, 2001; Martinez et al., 2008) while other studies have been showed the effect of sewage treatment on the removal of some bacteriophages and enteric viruses such as hepatitis A virus, rotavirus and poliovirus (Arraj et al., 2005).

Therefore, as mentioned above, with the absence of adequate protection methods, it may not be possible to control many public health consequences of irrigation with TWW. Harmoniously with the EU Regulation 2020/741 commands, total TWW reuse in agriculture for irrigation purposes must be controlled to ensure its disinfection before utilization (European Commission, 2020). It was also recommended to avoid the real contact between TWW and fruits or vegetable to avoid the possibility contamination of crops production.

1.2. Effects of heavy metals

Heavy metals contained in TWW can be transferred to food chain and cause public health problems (Cherfi et al., 2015). The concentrations of heavy metals in TWW depend essentially on the origin of WW and the treatment process performed. Generally, even with low amounts of these non-biodegradable pollutants in the effluent, there are risks of heavy metals accumulation after long term of irrigation using TWW (Kim et al., 2015). These contaminants accumulate into soil and induce toxicological effects regarding agriculture products through the plant uptake of these elements (Kumar et al., 2015). The bioavailability of metals in soil increases their environmental risks that depend on soil contamination level and plants species (Werfelli et al., 2021; Dickin et al., 2016, Guala et al., 2001). Heavy metals can affect the plants growth by modifying the photosynthesis and metabolism systems (Parveen et al., 2015) and may influence microbial community and produce phytotoxicity (Becerra-Castro et al., 2015). The uptake of heavy metals by plants from contaminated soil could occur through various mechanisms, such as precipitation-dissolution redox reactions and ion exchange. It depends on different factors such as soil minerals (hydroxide, oxide, carbonates), soil organic matter content (fulvic acid, humic acids, organic acid, polysaccharides), cations exchange capacity (Rezapour et al., 2019), trace elements content, soil physical and mechanical characteristics, soil pH, nutrient balance, humidity, and temperature. (Kim et al., 2015, Tarradellas et al., 1996). Furthermore, many studies have reported that the accumulation of these pollutants differs according to the species (Dickin et al., 2016; Krstic et al., 2007), age (Naser et al., 2011) tissue (Filipović-Trajković et al., 2012) and organs of plants (Jolly et al., 2013).

Different plant parts can contain different heavy metals concentrations, being the highest in roots

and leaves, and the lowest in fruits and seeds. The non-uniformity of heavy metal availability is related to the adaptation of plants to the different environmental properties higher content in roots compared to the areal parts in many species. (Ilić et al., 2015; Parveen et al., 2015). Contamination of vegetables and fruits with heavy metals introduces serious health problems for humans such as malnutrition, mental development retardation, kidney damage, neurotoxicity, gastrointestinal tumours, as well as lung, kidney, bladder and skin cancer (Jarup, 2003, Turkdogan et al., 2003; Hu et al., 2013; Cherfi et al., 2015; Gress et al., 2015; Al-Saleh et al., 2017; Rai et al., 2019). Many researches highlighted the possible transfer of heavy metals from WW to food chain. Ying-ping et al. (2011) have demonstrated the transfer of Cr from WW used for irrigation to soil that increases plant uptake. Hough et al. (2004) have been verified the effect of irrigation with WW on the contamination of food by Ni that affect the renal functioning and integral components of urease enzyme in kidney. Chary et al. (2008) have verified that even with low Pb transfer from soil, the accumulation of Pb in plant increased with rising its level in soil. The Pb intake by human was generally provided from food contamination although those higher concentrations were found in roots parts (Chary et al., 2008). However, many studies (Qureshi et al., 2016; Parveen et al., 2015) found that the concentrations of heavy metals in plants should be considered safe for public health, in accordance with the limits set by regulations.

2. Effects on soil

2.1.Micronutrients contents

Irrigation with TWW is considered as a fertility source of soil (Bedbabis et al., 2014). In fact, the use of TWW enhances the amount of soil micro and macronutrients such as nitrogen, phosphorus, potassium (Singh et al., 2012; Heinze et al., 2014; Ganjegunte et al., 2017), copper, iron, manganese and zinc (Galavi et al., 2010; Qadir and Scott, 2010). TWW nutrients supplement is important for plants considering the important roles of these elements in the plant growth, development and productivity (Morgan and Connolly, 2013). Therefore, the use of TWW in crops irrigation is considered a key factor for sustaining and enhancing the quality of arable soils, fundamental medium to produce food.

Nitrogen is a fundamental nutrient for plants and an essential soil fertilizer. Nitrogen can occur as organic form, usually predominant, or as inorganic form, the most relevant for soil fertility and uptake by crops. A good management of nitrogen fertilization to maximize the crop production and reduce its possible negative effects is mandatory (Quemada et al., 2016; Bloom, 2015). Nitrogen promotes the vegetative growth of stems and leaves, enters in the vegetative biochemical process

and influences the uptake of potassium and phosphorus by plants (Leghari et al., 2016). It has an essential role in the production of chlorophyll used for light harvesting in the photosynthesis (Leghari et al., 2016). The nitrogen deficiency in soil causes stunted development, chlorosis, reduction in seed protein quantity, crop yield and efficiency of radiation use (Leghari et al., 2016). The irrigation using TWW may enhance the availability of nitrogen, which improves the soil fertility and facilitates the uptake of nitrogen by plants (Quemada et al., 2016). TWW irrigation can supply the amount of nitrogen, which is necessary to ensure the agriculture sustainability and food security.

Phosphorus is another important plant nutrient, characterized by its immobility in soil and high mobility within plants. Its involvement in many crops' biological mechanisms, such as roots and stalks developments, maintenance of membrane structures, carbohydrate metabolism, cell division, metabolic and phosphorylation reactions make it an indispensable plant nutrient (Malhotra et al., 2018; Delgado et al., 2016; Jones and Olson-Rutz, 2016). Accordingly, deficiency of phosphorus reduces crops yield and leaves deterioration (Razaq et al., 2017). The reuse of TWW for irrigation enhances the soil phosphorus content and improves the vegetal growth. It is considered as a source of phosphorus and also potassium for plants which avoids their lack in soil. Potassium is also characterized by its mobility in soil and high plant uptake of its cationic form (Delgado et al., 2016). Potassium affects the resistance of crops from diseases and drought problems (Crouse, 2018). Potassium controls the osmotic adjustment (Osakabe et al., 2013) and enters in many phenomena such as photosynthesis and functionalization of interesting enzymes.

Micronutrients are essential for plant in low quantities. They have many important roles; in fact, they fix nitrogen, participate in the chlorophyll synthesis, control of oxidation-reduction process and regulate metabolic systems (Jones and OlsonRutz, 2016). Moreover, crops growth and production need essential nutrients that are provided in soil and can be added by TWW irrigation which maintain sufficient amount for plant needs then assure the agriculture sustainability (Parikh and James, 2012).

2.2. Organic matter content

TWW has a high organic matter content compared to other water resources used in agriculture. Thus, irrigation with TWW could promote crops development by its content of organic carbon, as demonstrated in many studies (Galavi et al., 2010; Farhadkhani et al., 2018). The amount of organic carbon affects soil characteristics such as stability and aggregation. In fact, organic carbon is a microbial nourishment which, by promoting the development of microorganisms in the soil,

improves their aggregation. Furthermore, the increase in the organic matter content of the soil decreases its tendency to erosion, in turn improving the availability of nutrients and the possibility of agronomic use of the soil (Murphy, 2015).

2.3.Sodium adsorption ratio

Sodium adsorption ratio (SAR) of soils increases with TWW application, comparing to the use of conventional water for irrigation, as mentioned in many researches (Bedbabis et al., 2014; Ganjegunte et al., 2017). Many parameters can affect the SAR of soils irrigated by TWWs such as WW origin and composition, quantity used of irrigation and soil characteristics. High SAR values exert toxicity of plants and reduce vegetal growth (Aamer Maqsood et al., 2015).

In fact, the high availability of sodium in soil could damage its structural stability by clay deflocculation and movement as reported in literature (Smith et al., 2016). Soil permeability reduces with increasing SAR which causes the decrease of water conduct to roots and can even destroyed the plants (Arienzo et al., 2012)

2.4. Salinization effect

The accumulation of salts, sodium, calcium, magnesium, chloride or iron causes the soil salinization (Rojas et al., 2016) that consequently reduces the productivity (Isayenkov and Maathuis, 2019). These elements are highly provided by TWW, leading to an increase in soil salinity by irrigation for short or long-time scale with these waters (Vergine et al., 2017[a]). In fact, many studies have demonstrated the salinization after TWW irrigation of crops (Farhadkhani et al., 2018; Shakir et al., 2017). The increase of EC reduces the external water potentials for plants and modifies its physiology, reducing the vegetal productivity (Karan and Subudhi, 2012; Munns and Tester, 2008; Hussain et al., 2016). High soil salinity could lead to osmotic and ionic stresses that reduce the plant growth (Heidari, 2012; Djanaguiraman and Prasad, 2013). The effect of salinity on plant depends on its salt tolerance ability. Therefore, before using TWW in irrigation, it is mandatory to check its level of salinity to avoid any possible danger or destruction of soil and vegetal productivity and quality.

2.5. Microbial content

Frenk et al. (2014) have demonstrated the safety overall long-term effect of using TWW on the soil bacterial community composition. Moreover, Heinze et al. (2014) have verified the effect of irrigation with TWW in the N-availability in top-crust soil enhancement, due to the high development and activity of microorganisms, such as cyanobacteria, lichens.

3. Effects on plant

Irrigation using TWW is a double-edged sword, which, on the one hand, supports plant growth by

satisfying its water needs and providing essential nutrients (Shtull-Trauring et al., 2022), but which on the other hand can provide an excess of nutrients that can be toxic for plant and crops (Lu et al., 2015; Yuan et al., 2019[a]).

More in details, TWW provided plants with the necessary amount of nutrients, which increased the leaves area index, high yield biomass compared to the plants irrigated with conventional water as reported by many authors (Urbano et al., 2017; Vergine et al., 2017[a]; Zema et al., 2012). The irrigation using TWW increases the availability of both macro- and micronutrients for plants. The uptake of nutrients depends on its content, its charged form (ionic or uncharged state) and the root system (Jones and Olson-Rutz, 2016). As an example, nitrogen and phosphorus elements are easily up taken by plants in the forms of nitrates and orthophosphate and are available to plant irrigated with TWW, thus improving crop growth and productivity (Aziz and Farissi, 2014; Vergine et al., 2017[a]).

Moreover, by growing crops and successive harvests, soil nutrient contents can be reduced which requires the use of fertilizers to avoid this deficiency. However, the increases in macronutrients, micronutrients and organic compounds in soil can also cause serious problems that such as the pollution of water and air by leaching or greenhouse gas emission and can negatively affect the biodiversity (Parveen et al., 2015; Becerra-Castro et al., 2015; Zheng et al., 2019). As stated above, the accumulation of these elements can also induce toxicity for both soil and crops and its effect depend on soil properties, plant absorption ability and TWW supply level of these elements (Hussain et al., 2016; Alghobar and Suresha., 2016). As an example, low germination, chlorosis of leaves and older leaves wilting could be caused by the excess absorption of zinc (Crouse,2018). An excess of nitrogen can cause a delay in ripening, while an excess of phosphorus and potassium can be responsible for an inhibition of potassium and zinc absorption, respectively (McCauley et al., 2009). These drawbacks are quite hazardous since their origin are essential nutrients used by plant to promote its growth (under the danger threshold).

Furthermore, plant toxicity could be caused by the excess of TWW organic xenobiotic contents like pharmaceuticals, personal care products, etc. (Becerra-Castro et al., 2015).

4. Effects on water resources

The use of TWW on agricultural land is one of the techniques of artificial groundwater recharge commonly used in arid and semi-arid regions (Jaramillo and Restrepo, 2017). The use of TWW minimizes the fresh water scarcity problems. Balkhair et al. (2013) have verified that the use of TWW irrigation conserved 60% of groundwater in Saudi Arabia.

The irrigation using TWW can also preserve the quantity of fresh water (Becerra-Castro et al., 2015) and reduce water pollution by minimizing the use of chemical fertilizers (Shtull-Trauring et al., 2022; Ungureanu et al., 2018).

Overall, it has been reported by Zhang and Shen, (2019) that a volume of water of approximately 5500 billion m^3 is polluted annually by WW's sewage. Indeed, WW discharges could worsen the quality of the receiving water body, introducing large amounts of nutrients, nanoparticles, organic compounds or heavy metals, resulting in toxicity and even death of fish from oxygen depletion (Khan et al., 2018; Ji, 2017). Possible leaching of nutrients into groundwater may be the result of increased discharge of treated effluents (Narr et al., 2019). Consumption of nitrate-contaminated water can cause stomach cancer in adults and methemoglobinemia (Nolan et al., 2002; Wolfe and Patz, 2002). Increasing the application of TWW for crop irrigation can increase the salinity of soil and groundwater (Mirzavand et al., 2020). Furthermore, biological pollutants such as bacteria and viruses such as SARS-CoV-2 (Kitajima et al., 2020) can persist in WW at concentrations that depend on the effectiveness of the treatment processes to destroy these biological contaminants (Jaramillo and Restrepo, 2017). It can be concluded that the use of TWW for irrigation reduces water pollution by decreasing its discharge into receiving water bodies and replacing, at least in part, agricultural fertilizers. However, its use should be accompanied by measures to prevent any possible phenomenon of environmental contamination.

5. Effects on economic

In general, reusing TWW is expensive compared to using fresh water from natural resources, although it is cheaper than seawater desalination. In many arid and semi-arid regions, fresh water resources will be minimized due to their high demand. Therefore, the comparison of the cost of reuse of TWW should be made with the use of other water sources. The cost of reusing TWW depends on many factors such as the region, the energy cost, the treatment process (Lam et al., 2017) and many other parameters (Hosseinzadeh et al., 2017)

The reuse of TWW in irrigation provides organic matter and essential nutrients useful to maintain fertilization and soil productivity, which replace the use of chemical fertilizers (N, P and K) (Rusan et al., 2007). For example, approximately 45% and 94% reductions in fertilizer use were recorded from TWW irrigation of wheat and alfalfa crops, respectively, as reported by Balkhair et al. (2013). The reuse of TWW can solve the water shortage problem by reducing the use of fresh water, thus resulting in an economic advantage for farmers. The irrigation of tomato cultivation with TWW allowed to save about € 280/ha, as estimated by another work (Vergine et al., 2017 [b]). The use of TWW in irrigation can increase crop productivity (Ouda et al., 2016; Zalesny et al., 2011) and

provide continuous access to water even during rainless periods (Verlicchi et al., 2012).

6. Proposed solutions

TWW may contain, as previously mentioned, environmentally toxic organic or inorganic pollutants that require urgent treatment before being returned to the environment or reused (Kannan and Sundaram, 2001; Swami and Buddhi, 2006; Crini, 2006). Among the TWW purification techniques, the removal process using biochar or modified biochar sorbents is the most efficient for removing different types of contaminants (Yang and Jiang, 2014; Wang et al., 2017[b]; Wang et al., 2017[a]).

On the other hand, sewage sludge production increased rapidly globally and was about 5×10^7 t y^{-1} in Europe Union and 3×10^7 t y^{-1} in China (about 20% of total solid waste) (Xiao et al., 2018).

Part of sewage sludge is recycled for the biological WW treatment process. Indeed, sewage sludge-based adsorbents could be a sustainable economic alternative for the purification of TWW from different kinds contaminants such as heavy metals (Bouzid and al., 2008) organic micro-pollutants (Zhang et al., 2018[a]). Sewage sludge is a renewable resource for biochar production. The high mineral content (Ca, K, Mg, and P) of sewage sludge increases the ash content of biochar (Li and Jiang, 2017) and reduces its specific surface area. In fact, sewage sludge can contain many toxic elements such as, polycyclic aromatic hydrocarbons (PAHs), polychlorinated biphenyls (PCBs), dioxins, microplastics, per- and polyfluoroalkyl substance phthalate, polybrominated diphenyl ethers; synthetic steroids, detergent residues, endogenous hormones, and pharmaceuticals (Smith 2009; Fijalkowski et al. 2017) that could be removed by pyrolysis, as reported in many studies (Zielińska et al., 2015; Hoffman et al., 2016; Ni et al., 2020; Mosko et al., 2021; Mercl et al., 2021; Kundu et al., 2021; Buss, 2021). Furthermore, biochar derived from sewage sludge are usually characterized by a high content of toxic metals. However, much research has shown that co-pyrolysis of different raw materials improves the surface properties of the biochar and avoids the limiting effects produced by the normal carbonization of the biochar primitive materials (Ahmed and Hameed, 2020). Therefore, co-pyrolysis of sewage sludge with biomass could be the right way to reduce ash and heavy metal content, thereby improving specific surface area and carbon content compared to biochar produced from sewage sludge (Huang et al., 2017; Konczak and Oleszczuk, 2020). Recently, great attention has been paid to biochar with regards to its surface properties, cost-effectiveness and ion-exchange capacity. Biochar can adsorb organic and inorganic pollutants from WW through its porous structure (Peiris et al., 2019; Karunanayake et al., 2018).

V. Generality on the adsorption process

Adsorption is the process in which molecules or atoms in a fluid, called adsorbate, attach or bind to

the surface of a solid, called an adsorbent. During this phenomenon, the compounds dissolved in the liquid or gas are transported by diffusion to the porous material and are adsorbed at its area (Dubinin, 1966). The transfer of pollutants is governed by several physicochemical phenomena (Crini and Badot, 2010). Adsorption is an exothermic phenomenon: the adsorption capacity increases with the decrease of temperature. The concentration in the adsorbate is also a factor in the adsorption capacity (McKay et al, 1996). In case of presence of a mixture in the liquid, the adsorption capacity is modified with competition between the different compounds.

Adsorption is either a chemical reaction (chemisorption), with a transfer of electrons and the creation of chemical bonds, or a physical attraction (physisorption). Physical adsorption occurs through non-specific physical interaction forces of the Van der Waals type. It does not involve any modification of the adsorbate molecular structure. The physisorption is reversible. Adsorbate can be desorbed without being altered by changing the equilibrium conditions (decrease of the concentration in the liquid solution or increase in temperature).

Conversely, chemical adsorption is more specific, because it is a chemical reaction with an electron transfer between the adsorbate and the adsorbent. This reaction results in the formation of covalent bonds and therefore it is generally irreversible. The energy required for chemisorption is much more important than that necessary for physisorption (Crittenden et al., 2012).

1. Isotherms

The adsorption capacity of an adsorbent is described by an isotherm that is the set of equilibrium states at a given temperature. It represents the capacity of an adsorbent to adsorb one or several adsorbate(s). An isotherm is therefore characteristic of an adsorbent/adsorbate pair at a given temperature. In water treatment, equilibrium states are concentrations of the pollutant at equilibrium between the liquid phase and the adsorbed phase. The IUPAC classification lists six types of isotherms (**Figure 1**).

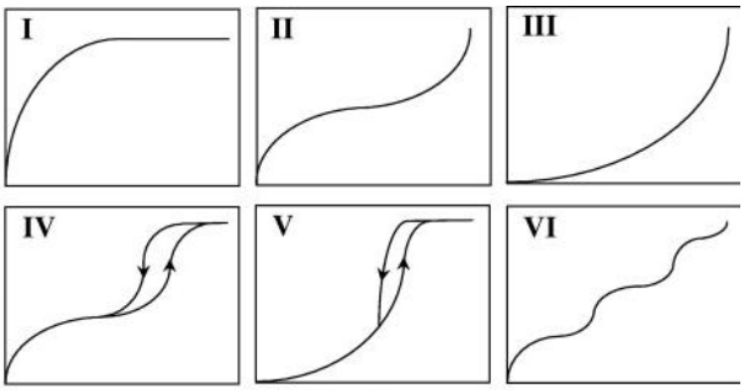

Figure 1. Classification of adsorption isotherms given by IUPAC (Crittenden et al., 2012).

The types of isotherms define different behaviours.

Type I: this type of isotherm is characterized by a horizontal plateau until saturation. This plateau represents the saturation of the adsorbent despite the increase in concentration. It's a consequence of a structure mainly composed of micropores. It is essentially a single-layer adsorption. Possible strong interactions are involved in the process (i.e., chemisorption).

Type II: this isotherm is very common for non-porous or macroporous solids. The absence of a horizontal plateau is clearly identifiable and a continuous rise in the adsorbed quantity are a sign of progressive thickening of the adsorbed layer. This isotherm is a characteristic of a multilayer adsorption.

Type III: this isotherm is rare. They correspond to non-porous or macroporous solids, characteristic of weak adsorbate/adsorbent interactions.

Type IV: it is characterized by a saturation level and is obtained with the filling of mesopores in which capillary condensation occurs (hysteresis).

Type V: There is filling of mesopores and capillary condensation in the pores, like for type IV, but the adsorbate/adsorbent interactions are weaker as for type III.

Type VI: This type of isotherm is very rare: it is only found for very homogeneous surfaces (Crittenden et al., 2012).

2. Isotherm models

Several isothermal models have been developed to estimate the adsorption capacities of adsorbents. They are based on adsorbent / adsorbate interaction mechanisms, the properties of surface and specific surface of the adsorbents. The most common models for estimating capacity of adsorption are the Langmuir and Freundlich equations.

2.1. Langmuir isotherm

The Langmuir isotherm is a theory of single-layer adsorption on an ideal surface developed in 1918 (Crittenden et al., 2012). The surface of the adsorbent is assumed to be homogeneous; adsorption energy is constant whatever the site and all the adsorption sites are equivalent. Adsorption on surface is also assumed to be localized, implying that no interaction exists between the adsorbed molecules. The expression of the Langmuir model is reported in equation (Eq.I. 1) (Cabrera-Lafaurie et al., 2014).

$$q = \frac{Q_m.b.C}{1+b.C} \quad \text{(Eq.I.1)}$$

Where:

q: adsorbate amount of adsorbate on the adsorbent (mg/g)

Q_m: maximum adsorbed quantity of adsorption per quantity of adsorbent (mg/g)

b: adsorption affinity constant, or Langmuir constant (L/mg), depends on the adsorbent / adsorbate pair and on the temperature

C: concentration of adsorbate in solution (mg/L).

2.2. Freundlich isotherm

Freundlich's model was proposed as an empirical model in 1906 to describe heterogeneous adsorbents such as activated carbon (I.2) (Erto et al., 2013).

$$q = F \,.\, C^{\frac{1}{n}} \qquad \text{(Eq.I.2)}$$

Where:

F: Freundlich adsorption quantity parameter (L/g)

n: dimensionless Freundlich adsorption intensity parameter (-).

In general, n is greater than 1. The larger n is, the more the isotherm is nonlinear and approaches a rectangular shape, representative of irreversible isotherms (Do, 1998).

3. Characteristics of adsorbent materials

The total surface area of a porous solid is defined as the sum of its internal and external surfaces. It is usually called the specific surface area that defines the ratio between the area and the mass of the adsorbent. This quantity can be considered as a first step as a reference for quickly estimating the storage capacity of an adsorbent (McKay et al., 1996). It depends on adsorbent texture characteristics. Porous materials with a very large specific surface are potentially the most efficient for storing compounds by adsorption. A porous material is characterized by cavities, called pores, the walls of which increase the specific surface area. The properties of a porous solid mainly depends on the geometry, size and distribution of its pores. According to their diameters, pores are classified into three groups by the IUPAC (International Union of Pure and Applied Chemistry): macropores (diameter higher than 50 nm), mesopores (pore diameter between 2 and 50 nm) and micropores (pore diameter below 2 nm). The pore size is selective to fix certain classes of compounds and prevent the adsorption of others.

The best adsorbents are those with significant specific surfaces, which exist in powder or granular form. Most common adsorbents used in the industry are activated carbon, silica gels, activated alumina and zeolites (Ferreira et al., 2011; Hauchhum and Mahanta, 2014; Álvarez-Hernández et al., 2018).

Zeolites have the particularity of having a crystalline structure with regular micropores uniform in size, called molecular sieves (Do, 1998). This crystalline structure is a tetrahedron sequence of SiO_4 and AlO_4, which is uniform and without size distribution. Zeolites usually have ionic structures that

affect adsorption properties. If its structure is rich in aluminum, it has a great affinity for water and other polar molecules. However, if it is poor in aluminum, it is rather hydrophobic. The adsorption on zeolites is selective in terms of size and polarity of the compounds to be separated. The small size of its pores excludes the filtration of some organic compounds.

Silica gels are obtained by precipitation of silica by reacting a solution of sodium silicate with mineral acid (sulfuric or hydrochloric). Silica gels are a hard glassy substance and their surface is polar due to hydroxyl groups. Gels preferably adsorb polar molecules and main uses of these adsorbents are drying, separation of aromatics and treatment of natural gas.

Activated alumina are porous aluminum oxide (Al_2O_3) (Bhatnagar and Sillanpää, 2010). Their surface is, like silica gels, polar and they are mainly used in drying for desiccations. Activated alumina have the disadvantage of a low specific surface area, therefore a limited adsorption capacity.

Activated carbon is the older and more largely used removal support in industry compared to the other adsorbents. Owing to its textural structure, large specific surface area and great adsorption capacity of different pollutants (Dąbrowski, 2001; Dąbrowski et al., 2005; Crini and Badot, 2010) commercial activated carbon are considered the efficacious support used for TWW purification in secondary or tertiary treatment step. After adsorption using packed beds of activated carbon or through batch system, the output generally characterized by reduction or even disappearance of the considered contaminant quantity such as organic elements, metals, dyes, PAHs and phenolic derivatives. Activated carbon participates with its microporous structure to the biological removal of organic matter through bacteria fixed in its surface, which regenerates the adsorbent material. This treatment type is coupled generally with the ozonation step of treatment that leads to detoxify the effluent filled with ions and reduce of total organic matter or chemical and biochemical oxygen demands (Radovic et al., 2000).

However, the technology of purification using activated carbon have economical and nonselective problems. The high cost of its production, including the pyrolysis and activation, its fast saturation and expensive regeneration restricted the use of activated carbon especially in medium and small-scale industries (Li et al., 2010). Therefore, many researches have been performed to substitute commercial activated carbon by different adsorbents such as natural (such as wood, cotton, lignin, peat) agricultural (sawdust), industrial (such as slag, red mud, fly ash, sludge.) and biological by products (such as bacteria) (Aydin and Yavuz, 2004; Vijayaraghavan and Yun, 2008; Sudha and Giri Dev, 2007; Tang et al., 2007, Sanghi and Verma, 2013; Del Bubba et al., 2020). These non-conventional materials are characterized by their abundance in the environment, availability in high

quantity and their low-cost, which promotes their use in the adsorption process (Crini et al., 2019). The last decades have revealed an increase in producing new adsorbents that enclosed biochar development from wastes and non-conventional products.

VI. Biochar preparation

Biochar is a term that mainly defines a porous carbonaceous material (Wathudura et al., 2020), resulting from the carbonization of vegetal biomasses (Del Bubba et al.,2020; Singh et al., 2015), animal wastes (Elzobair et al., 2016), industrial by-product or non-conventional materials under limited oxygen conditions (Sun et al., 2014; Lehmann and Joseph, 2015). Regarding to its surface properties, biochar could be used in the adsorption of pollutants from WW (Karunanayake et al., 2018; Peiris et al., 2019) and also for the remediation of soil contamination (Ahmad et al., 2014; Mohan et al., 2014; Jayawardhana et al., 2019). Biochar structure is rich in mineral compounds permit their use as amendment for increasing the soil fertility (Mukherjee and Zimmerman, 2013). According to the pyrolysis temperature, Verheijen et al. (Verheijen et al., 2009) have identified four main transformations occurring in biochar. For pyrolysis temperatures less than 250°C, the crystalline character of the origin feedstock is preserved. Between 250°C and 350°C, a mixed carbonaceous matrix is formed after the thermal degradation of cellulose. From 330°C, poly-aromatic graphene sheets start to growing laterally until reach their coalescence. Above 600°C, most non-carbonaceous matter is removed and the percent carbon content increased up to 90% (by weight) in the case of biochar obtained from wood (Demirbas, 2004).

VII. Biochar activation

The activation of biochar produces a low cost and eco-friendly product with high potential applications in different fields like chemical, petroleum, nuclear, alimental and pharmaceutical sectors (Tan et al., 2017).

In the interest of producing biochar with best features, researchers tested the influences of various modification approaches on biochar properties. The chemical and the physical activation of biochar are aspects included in the investigations carried out in this Doctoral thesis, in order to pursue the aforementioned goals. Many parameters can affect the characteristics of biochar such as the activation time and temperature, activating agent and soaking duration.

1. Chemical Oxidation

The oxidation of the biochar surface augments the functional groups containing oxygen atoms like

OH, -CO, and –COOH. This chemical oxidation causes the increase in the biochar hydrophilicity. Simultaneously, the pore structure and specific surface area of the material would be modified; in the end, its sorption ability for the polar compounds would be improved. The frequently oxidants are acid such as nitric acid, hydrochloric acid, phosphoric acid (Dong et al., 2017; Zhao et al., 2017). However, the modification of the specific surface area using HCl and HNO_3 is different from what is made by the activation using HCl only, in fact, HNO_3 increase the sorption capacity of NH_3-N and enriches the biochar by functional groups contain acidic oxygen (Ho et al., 2014).

2. Chemical reduction

The modification of the surface of biochar surface could be performed using a chemical reduction, also called alkali change method. Chemical reduction enhances the non-polarity character of the surface explained by the effect of reducing agents, which minimizes the surface functional groups. This modification may enhance the surface porosity and then improve the adsorption ability of non-polar pollutants. The chemical reduction could be done using KOH (Qu et al., 2021), NaOH (Zhang et al., 2017) or other agents (Sizmur et al., 2017).

The suitable chemical modification could be with acid or basic treatment; for that reason, Li et al. (2011) tested different oxidizing and reducing agents to analyse their effects in the adsorption of volatile compounds by the biochar produced from coconut shell. Results showed that, in contrast to acidic treatments, the alkali modification of carbon using NaOH and NH_4OH produced a decrease in surface oxygen containing functional groups and an increase of pore volume and specific surface area, which in turn increases the adsorption ability of volatile organic compounds. However, the acid modification using H_3PO_4, HNO_3 and H_2SO_4 reduced the adsorption capacity of the organic compounds. Others studies, such as the work done by Pouretedal and Sadegh (2014), based on an alkali-treatment, has other effects. In their work NaOH, KOH, $ZnCl_2$, NaCl and HNO_3 were used to remove some antibiotics from aqueous solutions. NaOH and KOH have the higher removal efficiency. However, the KOH activation produces the intercalation of potassium among the crystalline carbon layers, which becomes more predominant in case of highly ordered carbon, while, there is hardly possibility to the interactions between Na and carbon.

3. Metal impregnation

The impregnation with a suitable metal can enhance the chemical reactivity of the biochar. This surface modification improves the adsorption efficiency of the biochar by increasing the specific surface area and by possible reactions between impregnated reagents and the adsorbate (Liu et al., 2017). The impregnating agent that can be used are cobalt (Nguyen et al., 2019), copper (Liu et a.,

2017), iron (Yin et al., 2018), magnesium (Li et al., 2016), manganese (Wan et al., 2018), molybdenum (Li et al., 2018), silver (Wu and Feng, 2017), and zinc (Angın et al., 2013), also various organic compounds like pyridine and some amines could be used for carbon impregnation (Shao et al., 2018).

4. Other's surface modification

The surface of biochar could be modified also using ozone oxidation (Jimenez-Cordero et al., 2015) or by grafting organic matter (Wang et al., 2018[a]). The modification by low-temperature plasma improves the polarity of the surface of carbon material. This modification refers to the collection between plasmas and C=C and the oxidation of plasmas to surface oxygen (Tendero et al., 2006; Wu et al., 2012). These modification methods are not commonly applicable because of their difficult process and their high cost.

VIII. Application of biochar in water purification and soil Remediation

Biochar and activated biochar can be obtained from sewage sludge, which solves the problem of sludge management, respecting environmental safety (Barry et al., 2019) also reducing the sludge valorisation cost. In more details, sewage sludge could be managed through its use as soil amendment in agriculture, land filling and incineration (Kelessidis and Stasinakis, 2012).

1. Application of biochar in water purification

The activated biochar known for its high porosity, high surface area, large variation in surface functions that conduct to important reactivity degree, important mechanical strength (Sahu et al., 2010), showed high potential to remove organic and inorganic pollutants from aqueous or gaseous phases. These pollutants could be polar or non-polar elements such as heavy metals (Li et al., 2017), pharmaceutical compounds, detergents, pesticides (Zhang et al., 2013), organic compounds such as aromatic hydrocarbons and hydrophobic organic pollutants (Wang et al., 2018[b]). The structure of activated biochar is characterized by the presence of heteroatoms such as nitrogen, oxygen, halogen, sulphur or others (Puziy et al., 2008). These elements are responsible of the surface character like acidity or basicity. Oxygen content in biochar depends on the feedstock used in the process and the activation method (Nzediegwu et al., 2021). Oxygen could be also present in the functional groups like lactone, phenols, carboxyl and other functions (Gaur and Shankar, 2008). Moreover, the high alkalinity, stability and specific surface area of biochar allowed its effective application of metals adsorption from WW (Ippolito et al., 2017; Alam et al., 2018,). Biochar obtained from animals or vegetal wastes could remove trace metals from WW (Inyang et al., 2012**;** Zhang et al., 2017; Zhang

et al., 2020).

2. Adsorption of soil persistent organic pollutants

The TWW irrigation and the use of organochlorine pesticides bring organic contaminants to agricultural soil such as PAHs, phenolic compounds and PCB. Recent researches showed the efficiency adsorption capacity of biochar for organic contaminants. Wu et al. (2019) showed that the Oxyfluorfen degradation is faster in soil amended with biochar, produced from rice husk, compared to the non-amended soil. The oxyfluorfen sorption by soybean plants decreased by 18-63%, in presence of biochar which decrease the adsorption capacity of this compound by the plants. Rombolà et al. (2015) demonstrated that the PAHs concentrations in contaminated vine yard decrease with time with using biochar obtained from orchard pruning biomass, this change resulted more important for light PAHs. However, Bielská et al. (2018[b]) analysed the positive and negative effects of tow biochar obtained from Mixed wood shavings rice husk into the pyrene, polychlorinated biphenyl and dichlorodiphenyldichloroethylene sorption, bioavailability, and ecotoxicity. Results showed negative sublethal effects resulting from the biochar itself, especially when added at higher doses (N10%) At the highest biochar dose (10%), bioavailability and bioaccessibility decreased by 37% and 41%, respectively, compared to unamended soils.

Biochar obtained from mixture corn straw and pig manure was used by Zhang et al. (2018) to study the sorption and the evaluation of thiacloprid existing in black soil. Results indicated that the biodegradation of thiacloprid was enhanced. This amelioration was due to the microbial community changes made by the modification of the physicochemical properties of soil by using biochar.

The activated biochar can also reduce the organic pollutants from soil and this was verified by Kołtowski et al. (2017) that applied activated willow biochar by CO_2, H_2O and microwave, in the adsorption of PAHs. In fact, the concentrations of PAHs reduced by 86%, by using the activated biochar with best effects, the concentration of PAHs dissolved in bitumen plant soil, asphalt soil (industrial waste deposit) and coal plant soil near cooking plant battery soil, decreased from 174 to 24 ng/L, 52 to 16 ng/ L and 153 to 22 ng/ L, respectively.

Generally, biochar may enhance the sorption capacity of organic pollutants and decrease their leaching and their flow and desorption in soil. Biochars enhance the soil physicochemical characteristics and also the microbial activity by providing essential nutrients to soil.

3. Amelioration of soil

Biochar improves the macro and micro-nutrients content in the soil such as N, P, K, Ca, Mn and Al (Atkinson et al., 2010; Brennan et al., 2014; Lui et al., 2018), and it may be used for soil

amendment for their nutrients contents and as a consequence, biochar promote growth plants and crop yield (Hasan, 2018; Huang et al., 2019). Regarding the porous structure of biochar, the fertilizing retention and the aeration increase, these enhance physio-chemicals characteristics of the soil. Application of biochar in soil may increase the adsorption of organics elements that enhance the formation and the polymerizations of organic molecules, and due to the long period of the biochar destruction, soil fertilization will be promoting in for the long haul (Yuan et al., 2019[b]).

Zhang et al. (2019) demonstrated that biochar improves soil respiration; however, the soil respiration depends on the nitrogen addition to the soil. In fact, the surface functional groups can be oxidated with the volatile matter using biochar that produce after its interaction with soil matrixes that enhance the nitrogen and nutrients removal ability (Zhang et al., 2012).

Biochar may reduce soil carbon emission caused by future climate warming. Biochar can also increase the microbial availability and activity in the soil (Oleszczuk et al., 2014, Yadav et al., 2019). In fact, Wang et al. (Wang et al., 2019) showed the increase activities of invertase, urease, proteinase, neutral phosphatase, catalase, and polyphenol oxidase, increased in the soil treated with biochar as results of highest soil humus, the improvement of soil by high viability microbes, high humus content and fast C and nutrient cycling (Fan et al., 2018).

Previous studies demonstrated that in one side biochar remediate soil pollution and decrease nutrient losses in other side, biochar improve organic Carbon content in soil, crop yield and water storage capacity (Hagemann et al., 2017; Dahlawiet al., 2018; Huang et al., 2018; Paetsch et al., 2018).

Moreover, the use of biochar increases metal complex contents in both acid and basic soil such as complex iron especially in sandy alkali soil like demonstrated by Quan at al. (Quan et al., 2020), in fact they demonstrated that biochar improved the complexation mechanisms, such as Ca- and Fe/Al-bound complexes, and enhanced sedimentation processes of organo-mineral complexes and then reduced the soil pollution caused by heavy metal.

For aged biochar, carbonyl, carboxyl and phenolic groups could be formed due to their higher oxidation degree (Yadav et al., 2019), and then improve the formation of complexes with alkaline earth metals which increase the availability of nutrients in soil.

Other researchers studied the reasons of these complexations after adding biochar to soil and they demonstrated that due to the surface functional groups of biochar improve interactions that may enhance the production of organo-mineral complexes, these interactions could be H-bonding, and π- π-bonding with aromatics or exchanging ligands (Feng et al., 2014 ; Weng et al., 2018).

Biochar has also positives effects on the resistance to the soil acidification by suppressing nitrification and increasing the pH buffering capacity by the protonation of carboxyl on the surface

of biochar (Shi et al., 2019).

IX. Potential risks of biochar using

However, some toxic compounds such as polycyclic aromatic hydrocarbons (PAHs), pharmaceutical compounds and heavy metals could be present in the waste feedstock used for the production of biochar such as sewage sludge or manure waste (Rombolà et al., 2015; Wang et al., 2018[b]; dos Santos Pereira et al., 2020). PAHs could be formed during the carbonization process (Liu et al., 2008, Verheijen et al., 2010). Because of the capacity of some PAHs metabolites to bind DNA, EU and United States Environmental Protection Agency (US EPA) considered PAHs as carcinogenic, mutagenic and teratogenic compounds (Wassenberg and Giulio, 2004; Mirsadeghi et al., 2011). These pollutants could be present with significant amounts in the produced biochar. The release of these contaminants is possible during the biochar' use and then another contamination could be caused. Hence, it is important to focus on the liberation of PAHs by materials before their use.

Different researches have analysed the liberation of organic pollutants and heavy metals from biochar obtained from mineral feedstock like sewage sludge (Feng et al., 2018). Potential release of toxic compounds is strongly related to the operative conditions of producing biochar, such as temperature and time of pyrolysis. Metal elements liberation is also related to the feedstock used in the fabrication of biochar (Al-Wabel et al., 2018). In fact, previous studies demonstrated that biochar that contain toxic elements such as As, Cu, Cr, Pb and Zn, were produced from coconut shells (Anyika et al., 2016), municipal sewage sludge (Jin et al.2016), plants grown on contaminated land, food waste or demolition wood (Buss et al., 2016). During the production of the biochar from sewage sludge, heavy metals such as Cr, Cu, Mn, Ni, Pb and Zn could be concentrated in the formed biochar (Jin et al., 2016).

The accumulation of these toxic minerals and organic pollutants has dangerous drawbacks; on the long-term, the cumulating of these elements in biochar and regarding its stability in the environment that could reach 10,000 years (Kong and Zhou, 2013), it is important to limit the liberation ability of toxic elements from biochar. In this context, some methods have been used to decrease the release of pollutants from biochar such as the production of biochar from mixture biomass with sewage sludge (Jin et al., 2017; Godlewska et al., 2019; Kończak et al., 2019) and biochar activation using acid (Jin et al., 2018), basic (Dehkhoda et al., 2016; Feng and Zhu, 2018) or other agents such as KMO_4 or H_2H_2 (Wongrod et al., 2018).

Biochar and activated biochar can be obtained from sewage sludge which resolves the problem of sludge management with respecting environment safety reducing then the sludge valorisation cost (Barry et al., 2019). However, all these strategies have a number of drawbacks and limitations, such as high cost and possible environmental impacts (Marra et al., 2018).

For these reasons, huge national and international attention was given to the use and management of sludge by setting up proper legislative actions. As an example, in Italy, the legislative Decree 152/2006 issued by the regional administrative courts made the management of sludge even more complex, requiring for the spreading in the soil the satisfaction also for the sludge of contamination threshold concentrations.

X. Bibliography

Aamer Maqsood, M., Khawar Khan, M., Asif Naeem, M., Hussain, S., Aziz, T., Schoenau, J., 2015. High sodium in irrigation water caused B toxicity at low soil solution and shoot B concentration in maize (Zea mays L.). J. Plant Nutr. 38, 728–741.

Adrover, M., Moyà, G., Vadell, J., 2013. Use of hydroponics culture to assess nutrient supply by treated wastewater. Journal of environ. Manage. 127, 162-165.

Adegoke, A. A., Amoah, I.D., Stenström, T. A., Verbyla, M. E., Mihelcic, J.R., 2018. Epidemiological Evidence and Health Risks Associated With Agricultural Reuse of Partially Treated and Untreated Wastewater: A Review. Front. Public Health 6, 337

Affi, S., Cherif, H., Belhadj, J., 2021. Smart system management and techno-environmental optimal sizing of a desalination plant powered by renewables with energy storage. Int. J. Energy Res. 45, 7501-7520.

Ahmad, M., Rajapaksha, A.U., Lim, J.E., Zhang, M., Bolan, N., Mohan, D., Vithanage, M., Lee, S.S., Ok, Y.S., 2014. Biochar as a sorbent for contaminant management in soil and water: a review. Chemosphere 99, 19–23.

Ahmed, M. J., Hameed, B. H., 2020. Insight into the co-pyrolysis of different blended feedstocks to biochar for the adsorption of organic and inorganic pollutants: A review. J. Clean. Prod. 265, 121762.

Akhatou, I., González-Domínguez, R., Fernández-Recamales, Á., 2016. Investigation of the effect of genotype and agronomic conditions on metabolomic profiles of selected strawberry cultivars with different sensitivity to environmental stress. Plant Physiol. Biochem.101, 14-22.

Aksu, Z., Tezer, S., 2000. Equilibrium and kinetic modeling of biosorption of Ramazol Black B by R. arrhizus in a batch system: effect of temperature. Process Biochem. 36, 431-439.

Alam, M. S., Gorman-Lewis, D., Chen, N., Flynn, S. L., Ok, Y. S., Konhauser, K. O., Alessi, D. S., 2018. Thermodynamic analysis of nickel (II) and zinc (II) adsorption to biochar. Environ Sci Technol. 52, 6246-6255.

Alghobar, M. A., Suresha, S., 2016. Effect of wastewater irrigation on growth and yield of rice crop and uptake and accumulation of nutrient and heavy metals in soil. Appl. Ecol. Environ. Res. 4, 53-60.

Alkaisi, A., Mossad, R., Sharifian-Barforoush, A., 2017. A review of the water desalination systems integrated with renewable energy. Energy Procedia, 110, 268-274.

Alkhadra, M. A., Gao, T., Conforti, K. M., Tian, H., Bazant, M. Z., 2020. Small-scale desalination of seawater by shock electrodialysis. Desalination, 476, 114219.

Al-Nakshabandi, G. A., Saqqar, M. M., Shatanawi, M. R., Fayyad, M., Al-Horani, H., 1997. Some environmental problems associated with the use of treated wastewater for irrigation in Jordan. Agric. Water Manag. 34, 81-94.

Al-Saleh, I., Al-Rouqi, R., Elkhatib, R., Abduljabbar, M., Al-Rajudi, T., 2017. Risk assessment of environmental exposure to heavy metals in mothers and their respective infants. Int. J. Hyg. Environ. Health 220, 1252–1278.

Al-Wabel, M. I., Hussain, Q., Usman, A. R., Ahmad, M., Abduljabbar, A., Sallam, A. S., Ok, Y. S., 2018. Impact of biochar properties on soil conditions and agricultural sustainability: A review. Land

Degrad. Dev. 29, 2124-2161.

Álvarez-Hernández, M. H., Artés-Hernández, F., Ávalos-Belmontes, F., Castillo-Campohermoso, M. A., Contreras-Esquivel, J. C., Ventura-Sobrevilla, J. M., Martínez-Hernández, G. B., 2018. Current scenario of adsorbent materials used in ethylene scavenging systems to extend fruit and vegetable postharvest life. Food Bioproc Tech. 11, 511-525.

Anastopoulos, I., Kyzas, G.Z., 2014. Agricultural peels for dye adsorption: a review of recent literature, J. Mol. Liq. 200, 381–389.

Ang, W.L., Wahab Mohammad, A., Johnson, D., Hilal, N., 2019. Forward osmosis research trends in desalination and wastewater treatment: A review of research trends over the past decade. J. Water Process. Eng. 31, 100886.

Angelakis, A., Gikas, P., 2014. Water reuse: Overview of current practices and trends in the world with emphasis on EU states. Water Util. J. 8, e78.

Angın, D., Altintig, E., Köse, T. E., 2013. Influence of process parameters on the surface and chemical properties of activated carbon obtained from biochar by chemical activation. Bioresour. Technol. 148, 542–549.

Anyika, C., Majid, Z. A., Isa, A. B., Ismail, N., Zakaria, M. P., Yahya, A., 2016. Toxic and nontoxic elemental enrichment in biochar at different production temperatures. J. Clean. Prod. 131, 810-821.

Arienzo, M., Christen, E.W., Jayawardane, N.S., Quayle, W.C., 2012. The relative effects of sodium and potassium on soil hydraulic conductivity and implications for winery wastewater management. Geoderma 173, 303–310.

Arraj, A., Bohatier, J., Laveran, H., Traore, O., 2005. Comparison of bacteriophage and enteric virus removal in pilot scale activated sludge plants. J. Appl. Microbiol. 98, 516-524.

Asimakopoulos, A. G., Thomaidis, N. S., Koupparis, M. A., 2012. Recent trends in biomonitoring of bisphenol A, 4-t-octylphenol, and 4-nonylphenol. Toxicol. Lett. 210, 141-154.

Atkinson, C. J., Fitzgerald, J. D., Hipps, N. A., 2010. Potential mechanisms for achieving agricultural benefits from biochar application to temperate soils: a review. Plant and soil. 337, 1-18.

Aydın, A. H., Yavuz, Ö., 2004. Removal of acid red 183 from aqueous solution using clay and activated carbon.

Azimi, S., Rocher, V., Muller, M., Moilleron, R., Thevenot, D. R., 2005. Sources, distribution and variability of hydrocarbons and metals in atmospheric deposition in an urban area (Paris, France). Sci. Total Environ. 337, 223-239.

Aziz, F., Farissi, M., 2014. Reuse of treated wastewater in agriculture: solving water deficit problems in arid areas (review). Ann. West Univ. Timisoara Ser. Biol. 17, 95–110.

Baccouri, B., Ben Temime, S., Taamalli, W., Daoud, D., Msallem, M., Zarrouk, M., 2007. Analytical characteristics of virgin olive oils from two new varieties obtained by controlled roscsing on Meski variety. Food Chem. 14, 19–34.

Balkhair, K. S., Ashraf, M. A., 2016. Field accumulation risks of heavy metals in soil and vegetable crop irrigated with sewage water in western region of Saudi Arabia. Saudi J. Biol. Sci. 23, S32-S44.

Balkhair, K.S., El-Nakhlawi, F.S., Ismail, Al-Solimani, S.G., 2013. Treated wastewater use and its effect on water conservation, vegetative yield, yield components and water use efficiency of some

vegetable crops grown under two different irrigation systems in Western Region, Saudi Arabia. Eur. Sci. J. 9, 21.

Banik, C., Lawrinenko, M., Bakshi, S., Laird, D. A., 2018. Impact of pyrolysis temperature and feedstock on surface charge and functional group chemistry of biochars. J. Environ. Qual., 47, 452-461.

Becerra-Castro, C., Lopes, A.R., Vaz-Moreira, I., Silva, E.F., Manaia, C.M., Nunes, O.C., 2015. Wastewater reuse in irrigation: a microbiological perspective on implications in soil fertility and human and environmental health. Environ. Int. 75, 117–135.

Bedbabis, S., Trigui, D., Ahmed, C. B., Clodoveo, M. L., Camposeo, S., Vivaldi, G. A., Rouina, B. B., 2015. Long-terms effects of irrigation with treated municipal wastewater on soil, yield and olive oil quality. Agric. Water Manag. 160, 14-21.

Bedbabis, S., Rouina, B. B., Boukhris, M., Ferrara, G., 2014. Effect of irrigation with treated wastewater on soil chemical properties and infiltration rate. J. Environ. Manage. 133, 45-50.

Bedbabis, S., Palese, A.M., Ben Rouina, B., Rhouma, A., Gargouri, K., Boukhris, M., 2009. The effect of irrigation with treated wastewater on “chemlali” olive oil quality. J. Food Qual. 32, 141–157

Bhatnagar, A., Sillanpää, M., 2010. Utilization of agro-industrial and municipal waste materials as potential adsorbents for water treatment - A review. Chem. Eng. J. 157, 277–296.

Bielská, L., Škulcová, L., Neuwirthová, N., Cornelissen, G., Hale, S. E., 2018. Sorption, bioavailability and ecotoxic effects of hydrophobic organic compounds in biochar amended soils. Sci. Total Environ. 624, 78–86.

Bloom, A. J., 2015. The increasing importance of distinguishing among plant nitrogen sources. Curr. Opin. Plant Biol. 25, 10–16.

Borsani, R., Rebagliati, S., 2005. Fundamental and costing of multi stage flash desalination plants and comparison with other technologies. Desalination. 182, 29.

Bouzid, J., Elouear, Z., Ksibi, M., Feki, M., Montiel, A., 2008. A study on removal characteristics of copper from aqueous solution by sewage sludge and pomace ashes. J. Hazard. Mater. 152, 838-845.

Brennan, A., Jiménez, E. M., Puschenreiter, M., Alburquerque, J. A., Switzer, C., 2014. Effects of biochar amendment on root traits and contaminant availability of maize plants in a copper and arsenic impacted soil. Plant and soil. 379, 351-360.

Buss, W., 2021. Pyrolysis solves the issue of organic contaminants in sewage sludge while retaining carbon—making the case for sewage sludge treatment via pyrolysis. ACS Sustain. Chem. Eng. 9, 10048-10053.

Buss, W., Graham, M. C., Shepherd, J. G., Mašek, O., 2016. Suitability of marginal biomass-derived biochars for soil amendment. Sci. Total Environ. 547, 314-322.

Cabrera-Lafaurie, W. A., Román, F. R., Hernández-Maldonado, A. J., 2014. Removal of salicylic acid and carbamazepine from aqueous solution with Y-zeolites modified with extraframework transition metal and surfactant cations: Equilibrium and fixed-bed adsorption. J. Environ. Chem. Eng. 2, 899-906.

Calci, K. R., Burkhardt III, W., Watkins, W. D., Rippey, S. R., 1998. Occurrence of male-specific bacteriophage in feral and domestic animal wastes, human feces, and human-associated

wastewaters. Appl. Environ. Microbiol. 64, 5027-5029.

Catorci, A., Lulli, R., Malatesta, L., Tavoloni, M., Tardella, F. M., 2021. How the interplay between management and interannual climatic variability influences the NDVI variation in a sub-Mediterranean pastoral system: Insight into sustainable grassland use under climate change. Agric Ecosyst Environ. 314, 107372.

Campisano, A., Butler, D., Ward, S., Burns, M.J., Friedler, E., DeBusk, K., Fisher-Jeffes, L.N., Ghisi, E., Rahman, A., Furumai, H., 2017. Urban rainwater harvesting systems: Research, implementation and future perspectives. Water Res. 115, 195–209.

Celano, G., Dichio, B., Montanaro, G., Nuzzo, V., Palese, A.M., Xiloyannis, C., 1999. Distribution of dry matter and amount of mineral elements in irrigated and non-irrigated olive trees. Acta Hortic. 474, 381–384.

Chakraborti, R. K., Kaur, J., Kaur, H., 2019. Water Shortage Challenges and a Way Forward in India. Journal: American Water Works Association, 111.

Chary, N. S., Kamala, C. T., Raj, D. S. S., 2008. Assessing risk of heavy metals from consuming food grown on sewage irrigated soils and food chain transfer. Ecotoxicol. Environ. Saf. 69, 513-524.

Chebil, A., Souissi, A., Frija, A., Stambouli, T., 2019. Estimation of the economic loss due to irrigation water use inefficiency in Tunisia. Environmental Science and Pollution Research, 26, 11261-11268.

Cherfi, A., Achour, M., Cherfi, M., Otmani, S., Morsli, A., 2015. Health risk assessment of heavy metals through consumption of vegetables irrigated with reclaimed urban wastewater in Algeria. Process Saf. Environ. Prot. 98, 245–252.

Christou, A., Maratheftis, G., Elia, M., Hapeshi, E., Michael, C., Fatta-Kassinos, D., 2016. Effects of wastewater applied with discrete irrigation techniques on strawberry plants' productivity and the safety, quality characteristics and antioxidant capacity of fruits. Agric. Water Manag. 173, 48-54.

Cirelli, G.L., Consoli, S., Licciardello, F., Aiello, R., Giuffrida, F., Leonardi, C., 2012. Treated municipal wastewater reuse in vegetable production. Agric. Water Manag. 104, 163–170.

Crini, G., Lichtfouse, E., Wilson, L. D., Morin-Crini, N., 2019. Conventional and non-conventional adsorbents for wastewater treatment. Environ. Chem. Lett. 17, 195-213.

Crini, G., Badot, P. M. (Eds.). (2010). Sorption processes and pollution: conventional and non-conventional sorbents for pollutant removal from wastewaters. Presses Univ. Franche-Comté.

Crini, G., 2006. Non-conventional low-cost adsorbents for dye removal: a review. Bioresour Technol. 97, 1061-1085.

Crittenden, J. C., Trussell, R. R., Hand, D. W., Howe, K. J., Tchobanoglous, G., 2012. MWH's water treatment: principles and design. John Wiley & Sons.

Crouse, D.A., 2018. Soils and plant nutrients. In: Moore, K.A., Bradley, L.K. (Eds.), North Carolina Extension Gardener Handbook. NC State Extension, Raleigh, NC (Chapter 1).

Dahlawi, S., Naeem, A., Rengel, Z., Naidu, R., 2018. Biochar application for the remediation of salt-affected soils: Challenges and opportunities. Sci. Total Environ. 625, 320-335.

Dąbrowski, A., Podkościelny, P., Hubicki, Z., Barczak, M., 2005. Adsorption of phenolic compounds by activated carbon—a critical review. Chemosphere. 58, 1049-1070.

Dąbrowski, A., 2001. Adsorption—from theory to practice. Adv. Colloid Interface Sci. 93, 135-224.

Dehkhoda, A. M., Gyenge, E., Ellis, N., 2016. A novel method to tailor the porous structure of KOH-activated biochar and its application in capacitive deionization and energy storage. Biomass and Bioenergy. 87, 107-121.

Del Bubba, M., Anichini, B., Bakari, Z., Bruzzoniti, M.C., Camisa, R., Caprini, C., Checchini, L., Fibbi, D., El Ghadraoui, A., Liguori, F., Orlandini, S., 2020. Physicochemical properties and sorption capacities of sawdust-based biochars and commercial activated carbons towards ethoxylated alkylphenols and their phenolic metabolites in effluent wastewater from a textile district. Sci. Total Environ. 708, 135217.

Delgado, A., Quemada, M., Villalobos, F. J., Mateos, L., 2016. Fertilization with phosphorus, potassium and other nutrients. In Principles of agronomy for sustainable agriculture (pp. 381-405). Springer, Cham.

Demirbas, A., 2004. Effects of temperature and particle size on bio-char yield from pyrolysis of agricultural residues. J. Anal. Appl. Pyrol. 72, 243-248.

Denno, D. M., Klein, E. J., Young, V. B., Fox, J. G., Wang, D., Tarr, P. I., 2007. Explaining unexplained diarrhea and associating risks and infections. Anim. Health Res. Rev. 8, 69-80.

Dhehibi, B, Frija, A, Aw-Hassan, A., 2014. Performances, policies, challenges and opportunities of the Tunisian agriculture sector from natural resources management perspective a SWOT analysis. Am Eurasian J Agric Environ Sci. 14,1351–1358.

Dickin, S.K., Schuster-Wallace, C.J., Qadir, M., Pizzacalla, K., 2016. A review of health risks and pathways for exposure to wastewater use in agriculture. Environ. Health Perspect. 124, 900–909.

Djanaguiraman, M., Prasad, P.V.V., 2013. Effects of salinity on ion transport, water relations and oxidative damage. In: Ahmad, P., Azooz, M., Prasad, M. (Eds.), Ecophysiology and Responses of Plants Under Salt Stress. Springer, New York, NY, pp. 89–114

Do, D. D., 1998. Adsorption analysis: Equilibria and kinetics (with cd containing computer MATLAB programs) (Vol. 2). World Scientific.

Dong, H., Deng, J., Xie, Y., Zhang, C., Jiang, Z., Cheng, Y., Hou, K., Zeng, G. 2017. Stabilization of nanoscale zero-valent iron (nZVI) with modified biochar for Cr (VI) removal from aqueous solution. J. Hazard. Mater. 332, 79–86.

dos Santos Pereira, I., Bamberg, A. L., de Sousa, R. O., Monteiro, A. B., Martinazzo, R., Silveira, C. A. P., de Oliveira Silveira, A., 2020. Agricultural use and pH correction of anaerobic sewage sludge with acid pH. J. Environ. Manage. 275, 111203.

Du, X., Wang, Z., Liu, Y., Ma, R., Lu, S., Lu, X., Liu, L., Liang, H., 2022. Gravity-driven membrane bioreactor coupled with electrochemical oxidation disinfection (GDMBR-EO) to treat roofing rainwater. Chem. Eng. Sci. 427, 131714.

Dubinin, M. M., 1966. Porous structure and adsorption properties of activated carbons. In: Walker PL (ed) Chemistry and physics of carbon, vol 2. Marcel Dekker, New York, pp 51–120.

EEA (European Environmental Agency) (2009). Water resources across Europe—confronting water scarcity and drought, report No 2/2009.

El Ghadraoui, A., Ouazzani, N., Saf, C., Ahmali, A., Hejjaj, A., Aziz, F., Del Bubba, M., Mandi, L., 2021. Behaviour of physicochemical and microbiological characteristics of vertical flow

constructed wetland substrate after treating a mixture of urban and olive mill wastewaters. Environ. Sci. Pollut. Res. 28, 55433-55445.

Elzobair, K. A., Stromberger, M. E., Ippolito, J. A., Lentz, R.D, 2016. Contrasting effects of biochar versus manure on soil microbial communities and enzyme activities in an Aridisol. Chemosphere, 142, 145-152.

EPA. 1999. Ultraviolet disinfection. Water technology fact sheet. EPA water Resources Centre, Washington DC.

Erto, A., Giraldo, L., Lancia, A., Moreno-Piraján, J. C., 2013. A comparison between a low-cost sorbent and an activated carbon for the adsorption of heavy metals from water. Water Air Soil Pollut. 224, 1-10.

European Comission, 2020. Regulation (EU) 2020/741 of the European Parliament and of the Council of 25 May 2020 on minimum requirements for water reuse. Off. J. Eur. Union. L 177, 32–55.

Fabres, R. B., da Luz, R. B., Soliman, M. C., Staggemeier, R., Fleck, J. D., Nascimento, C. A. D., Nascimento, F. T. D., Spilki, F. R., 2017. Evaluation of virus recovery methods and efficiency of tannin-derived coagulants in removing total coliforms, E. coli and enteric viruses in effluents of a domestic sewage treatment plant. Water Sci. Technol. 76, 2195-2202.

Faby, J. A., Brissaud, F., Bontoux, J., 1999. Wastewater reuse in France: Water quality standards and wastewater treatment technologies. Water Sci. Technol. 40, 37-42.

Fan, Q., Cui, L., Quan, G., Wang, S., Sun, J., Han, X., Wang, J., Yan, J., 2018. Effects of wet oxidation process on biochar surface in acid and alkaline soil environments. Materials. 11, 2362.

FAO. 2017. AQUASTAT website. Rome (IT).
[cited 2017 July 10]. http://www.fao.org/nr/water/aquastat/main/index.stm.

FAO, 2005. Water use in agriculture, Food and Agriculture Organization of the United Nations, Rome.

Farhadkhani, M., Nikaeen, M., Yadegarfar, G., Hatamzadeh, M., Pourmohammadbagher, H., Sahbaei, Z., Rahmani, H.R., 2018. Effects of irrigation with secondary treated wastewater on physicochemical and microbial properties of soil and produce safety in a semi-arid area. Water Res. 144, 356–364

Fatta-Kassinos, D., Kalavrouziotis, I. K., Koukoulakis, P. H., Vasquez, M. I., 2011. The risks associated with wastewater reuse and xenobiotics in the agroecological environment. Sci. Total Environ. 409, 3555-3563.

Feng, M., Zhang, W., Wu, X., Jia, Y., Jiang, C., Wei, H., Qiu, R., Tsang, D. C., 2018. Continuous leaching modifies the surface properties and metal (loid) sorption of sludge-derived biochar. Sci. Total environ. 625, 731-737.

Feng, Z., Zhu, L., 2018. Sorption of phenanthrene to biochar modified by base. Front Environ Sci Eng. 12, 1-11.

Feng, W., Plante, A. F., Aufdenkampe, A. K., Six, J., 2014. Soil organic matter stability in organo-mineral complexes as a function of increasing C loading. Soil Biol. Biochem. 69, 398-405.

Feng, Y. Yang, F., Wang, Y., Ma, L., Wu, Y., Kerr, P. G., Yang, L., 2011. Basic dye adsorption onto an agro-based waste material—sesame hull (Sesamum indicum L.), Bioresour. Technol. 102,

10280–10285.

Ferreira, D., Magalhaes, R., Taveira, P., Mendes, A., 2011. Effective adsorption equilibrium isotherms and breakthroughs of water vapor and carbon dioxide on different adsorbents. Ind. Eng. Chem. Res. 50, 10201-10210.

Fijalkowski K., Rorat A., Grobelak A., Kacprzak M.J., 2017. The presence of contamination in sewage sludge – the current situation. J. Environ. Manage. 203, 1126–1136.

Filipović-Trajković, R., Ilić, S. Z. Šunić, L., 2012. The potential of different plant species for heavy metals accumulation and distribution. J. Food Agric Environ. 10, 959-964.

Fine, P., Halperin, R., Hadas, E., 2006. Economic considerations for wastewater upgrading alternatives: An Israeli test case. J. Environ. Manage. 78, 163-169.

Fongaro, G., Kunz, A., Magri, M. E., Schissi, C. D., Viancelli, A., Philippi, L. S., Barardi, C. R. M., 2016. Settling and survival profile of enteric pathogens in the swine effluent for water reuse purpose. Int. J. Hyg. Environ. Health. 219, 883-889.

Forgacs, E., Cserhati, T., Oros, G., 2004. Removal of synthetic dyes from wastewaters: a review, Environ. Int. 30, 953–971.

Frenk, S., Hadar, Y., Minz, D., 2014. Resilience of soil bacterial community to irrigation with water of different qualities under M editerranean climate. Environ. Microbiol. 16, 559-569.

Fytili, D., Zabaniotou, A., 2008. Utilization of sewage sludge in EU application of old and new methods—A review. Renew. Sust. Energ. Rev. 12, 116-140.

Galavi, M., Jalali, A., Ramroodi, M., Mousavi, S. R., Galavi, H., 2010. Effects of treated municipal wastewater on soil chemical properties and heavy metal uptake by sorghum (Sorghum bicolor L.). J. Agric. Sci. 2, 235.

Ganjegunte, G., Ulery, A., Niu, G., Wu, Y., 2017. Effects of treated municipal wastewater irrigation on soil properties, switchgrass biomass production and quality under arid climate. Ind. Crop. Prod. 99, 60–69.

Gao, P., Xu, W., Sontag, P., Li, X., Xue, G., Liu, T., Sun, W., 2016. Correlating microbial community compositions with environmental factors in activated sludge from four full-scale municipal wastewater treatment plants in Shanghai, China. Appl. Microbiol. Biotechnol. 100, 4663-4673.

Gatta, G., Libutti, A., Beneduce, L., Gagliardi, A., Disciglio, G., Lonigro, A., Tarantino, E., 2016. Reuse of treated municipal wastewater for globe artichoke irrigation: Assessment of effects on morpho-quantitative parameters and microbial safety of yield. Sci. Hortic. 213, 55-65.

Gaur, V. and Shankar, P., 2008. Surface modification of activated carbon for the removal of water impurities. Water. Cond. Purif.1–5.

Ghasemi, S., Danesh, S., Alizade, A., 2011. Evaluating the potential of providing irrigation water and fertilizer values of wastewater of urban wastewater treatment plants. J. Water Soil. 25, 1172-1183.

Ghernaout, D., 2018. Increasing trends towards drinking water reclamation from treated wastewater. World J. Appl. Chem. 3, 1–9.

Ghaffour, N., Missimer, T. M., Amy, G. L., 2013. Technical review and evaluation of the economics of water desalination: current and future challenges for better water supply

sustainability. Desalination. 309, 197-207.

Ghrab, M., Gargouri, K., Bentaher, H., Chartzoulakis, K., Ayadi, M., Mimoun, M. B., Masmoudi, M. M., Mechila, N. B., Psarras, G.,2013. Water relations and yield of olive tree (cv. Chemlali) in response to partial root-zone drying (PRD) irrigation technique and salinity under arid climate. Agri.Water Manag. 123, 1-11.

Giampieri, F., Tulipani, S., Alvarez-Suarez, J. M., Quiles, J. L., Mezzetti, B., Battino, M., 2012. The strawberry: Composition, nutritional quality, and impact on human health. Nutr. 28, 9-19.

Godlewska, P., Siatecka, A., Kończak, M., Oleszczuk, P., 2019. Adsorption capacity of phenanthrene and pyrene to engineered carbon-based adsorbents produced from sewage sludge or sewage sludge-biomass mixture in various gaseous conditions. Bioresour. Technol. 280, 421-429.

Gress, J., de Oliveira, L.M., da Silva, E.B., Lessl, J.M., Wilson, P.C., Townsend, T., Ma, L.Q., 2015. Cleaning-induced arsenic mobilization and chromium oxidation from CCA-wood deck: potential risk to children. Environ. Int. 82, 35–40.

Guadie, A., Yesigat, A., Gatew, S., Worku, A., Liu, W., Ajibade, F.O., Wang, A., 2021. Evaluating the health risks of heavy metals from vegetables grown on soil irrigated with untreated and treated wastewater in Arba Minch. Ethiopia. Sci. Total Environ. 761, 143302.

Guala, S. D., Vegaa, F. A. and Covelo, E. F., 2001. The dynamics of heavy metals in plant-soil interactions. Ecol. Model. 221, 1148-1152

Guest, J.S., Skerlos, S.J., Barnard, J.L., Beck, M.B., Daigger, G.T., Hilger, H., Jackson, S.J., Karvazy, K., Kelly, L., Macpherson, L., Mihelcic, J. R., Pramanik, A., Raskin, L., Van Loosdrecht, M. C. M., Yeh, D., Love, N.G., 2009. A new planning and design paradigm to achieve sustainable resource recovery from wastewater. Environ. Sci. Technol. 43, 6126-6130.

Gude, V. G., 2016. Desalination and sustainability–an appraisal and current perspective. Water Res. 89, 87-106.

Gromaire, M. C., Garnaud, S., Saad, M., Chebbo, G., 2001. Contribution of different sources to the pollution of wet weather flows in combined sewers. Water Res. 35, 521-533.

Hagemann, N., Joseph, S., Schmidt, H.P., Kammann, C.I., Harter, J., Borch, T., Young, R.B., Varga, K., Taherymoosavi, S., Elliott, K.W., McKenna, A., Albu, M., Mayrhofer, C., Obst, M., Conte, P., Dieguez-Alonso, A., Orsetti, S., Subdiaga, E., Behrens, S., Kappler, A., 2017. Organic coating on biochar explains its nutrient retention and stimulation of soil fertility. Nat. Commun. 8, 1 - 11.

Hamilton, A. J., Stagnitti, F., Xiong, X., Kreidl, S. L., Benke, K. K., Maher, P., 2007. Wastewater irrigation: the state of play. Vadose Zone J. 6, 823-840.

Hamilton, A. J., Stagnitti, F., Premier, R., Boland, A. M., Hale, G., 2006. Quantitative microbial risk assessment models for consumption of raw vegetables irrigated with reclaimed water. Appl. Environ. Microbiol. 72, 3284-3290.

Hamoda, M. F., Al-Ghusain, I., Al-Mutairi, N. Z., 2004. Sand filtration of wastewater for tertiary treatment and water reuse. Desalination, 164, 203-211.

Hannachi, H., Msallem, M., Ben Elhadj, S., El Gazzah, M., 2007. Influence du site biologique sur les potentialités agronomiques et technologiques de l'olivier (Olea europea L.) en Tunisie. C. R. Biol. 330, 135–142.

Harada, S., Okada, M., Yahiro, S., Nishimura, K., Matsuo, S., Miyasaka, J., Nakashima, R.,

Shimada, Y., Ueno, T., Ikezawa, S., Shinozaki, K., Katayama, K., Wakita, T., Takeda, N., Oka, T., 2009. Surveillance of pathogens in outpatients with gastroenteritis and characterization of sapovirus strains between 2002 and 2007 in Kumamoto Prefecture, Japan. J. Med Virol. 81, 1117-1127.

Hasan, Z., 2018. A new approach to soil solarization: Addition of biochar to the effect of soil temperature and quality and yield parameters of lettuce, (Lactuca Sativa L. Duna). Sci. Hortic. 228, 153-161.

Hauchhum, L., Mahanta, P., 2014. Carbon dioxide adsorption on zeolites and activated carbon by pressure swing adsorption in a fixed bed. Int. J. Energy Environ. 5, 349-356.

Heidari, M., 2012. Effects of salinity stress on growth, chlorophyll content and osmotic components of two basil (Ocimum basilicum L.) genotypes. Afr. J. Biotechnol. 11 (2), 379–384.

Heinze, S., Chen, Y., El-Nahhal, Y., Hadar, Y., Jung, R., Safi, J., Safi, M., Tarchitzky, J., Marschner, B., 2014. Small-scale stratification of microbial activity parameters in Mediterranean soils under freshwater and treated wastewater irrigation. Soil Biol. Biochem. 70, 193-204.

Hentati, O., Chaker, S., Wali, A., Ayoub, T., Ksibi, M., 2014. Effects of long-term irrigationwith treated wastewater on soil quality, soil-borne pathogens, and living organisms: case study of the vicinity of El Hajeb (Tunisia). Environ. Monit. Assess. 186, 2671–2683.

Hernández-Maldonado, A. J., Yang, R. T., 2003. Desulfurization of liquid fuels by adsorption via π complexation with Cu (I)− Y and Ag− Y zeolites. Ind. Eng. Chem. Res. 42, 123-129.

Hilal, N., Wright, C. J., 2018. Exploring the current state of play for cost-effective water treatment by membranes. npj Clean Water. 1, 1-4.

Ho, P.H., Lee, S. Y., Lee, D., Woo, H. C. 2014. Selective adsorption of tert-butylmercaptan and tetrahydrothiophene on modified activated carbons for fuel processing in fuel cell applications. Int. J. Hydrogen Energy. 39, 6737–6745.

Hoffman, T. C., Zitomer, D. H., McNamara, P. J., 2016. Pyrolysis of wastewater biosolids significantly reduces estrogenicity. J. Hazard. Mater. 317, 579-584.

Hosseinzadeh, S., Bonarrigo, G., Verheust, Y., Roccaro, P., Van Hulle, S., 2017. Water reuse in closed hydroponic systems: Comparison of GAC adsorption, ion exchange and ozonation processes to treat recycled nutrient solution. Aquac. Eng. 78, 190-195.

Hough, R.L., Breward, N., Young, S.D., Crout, N.M., Tye, A.M., Moir, A.M., Thornton, I., 2004. Assessing potential risk of heavy metal exposure from consumption of homeproduced vegetables by urban populations. Environ. Health Perspect. 112, 215–221.

Hu, J., Wu, F., Wu, S., Cao, Z., Lin, X., Wong, M.H., 2013. Bioaccessibility, dietary exposure and human risk assessment of heavy metals from market vegetables in Hong Kong revealed with an in vitro gastrointestinal model. Chemosphere 91, 455–461.

Huang, M., Zhang, Z., Zhu, C., Zhai, Y., Lu, P., 2019. Effect of biochar on sweet corn and soil salinity under conjunctive irrigation with brackish water in coastal saline soil. Sci. Hortic. 250, 405-413.

Huang, M., Fan, L., Chen, J., Jiang, L., Zou, Y., 2018. Continuous applications of biochar to rice: effects on nitrogen uptake and utilization. Sci. Rep. 8, 11461.

Huang, H. J., Yang, T., Lai, F. Y., Wu, G. Q., 2017. Co-pyrolysis of sewage sludge and sawdust/rice straw for the production of biochar. J. Anal. Appl. Pyrolysis. 125, 61-68.

Hussain, Z., Khattak, R. A., Irshad, M., Mahmood, Q., An, P., 2016. Effect of saline irrigation water on the leachability of salts, growth and chemical composition of wheat (Triticum aestivum L.) in saline-sodic soil supplemented with phosphorus and potassium. J. Soil Sci. Plant Nutr. 16, 604-620.

Hussain, G., Al-Saati, A. J., 1999. Wastewater quality and its reuse in agriculture in Saudi Arabia. Desalination. 123, 241-251.

Ilić, S. Z., Mirecki, N., Filipović-Trajković, R., Kapoulas, N., Milenković, L. Šunić, L., 2015. Effect of Pb on seed germination and his translocation in different seed tissues during sprouting. Fresenius Environ. Bull. 24, 670-675.

INNORPI, 1989. Normes de réutilisation des eaux usées (NT 106. 03).

Institut Tunisienne des Etudes Stratégiques (ITES), 2018. Management of water resources in Tunisia. Bilan and prespective of the future. ITES, Tunis

Inyang, M., Gao, B., Yao, Y., Xue, Y., Zimmerman, A. R., Pullammanappallil, P., Cao, X., 2012. Removal of heavy metals from aqueous solution by biochars derived from anaerobically digested biomass. Bioresour. Technol.110, 50-56.

Ippolito, J. A., Berry, C. M., Strawn, D. G., Novak, J. M., Levine, J., Harley, A., 2017. Biochars reduce mine land soil bioavailable metals. J. Environ. Qual. 46, 411-419.

Isayenkov, S. V., Maathuis, F. J., 2019. Plant salinity stress: many unanswered questions remain. Front. Plant Sci. 10, 80.

Jamali, M. K., Kazi, T. G., Arain, M. B., Afridi, H. I., Jalbani, N., Kandhro, G. A., Shah, A. Q., Baig, J. A., 2009. Heavy metal accumulation in different varieties of wheat (Triticum aestivum L.) grown in soil amended with domestic sewage sludge. J. Hazard. Mater. 164, 1386-1391.

Jaramillo, M.F., Restrepo, I., 2017. Wastewater reuse in agriculture: a review about its limitations and benefits. Sustainability 9, 1734.

Jarup, L., 2003. Hazards of heavy metal contamination. Br. Med. Bull. 68, 167–182.

Jayawardhana, Y., Gunatilake, S.R., Mahatantila, K., Ginige, M. P., Vithanage, M., 2019. Sorptive removal of toluene and m-xylene by municipal solid waste biochar: simultaneous municipal solid waste management and remediation of volatile organic compounds. J. Environ. Manag. 238, 323 330.

Ji, Z. G., 2017. Hydrodynamics and water quality: modeling rivers, lakes, and estuaries. John Wiley & Sons .

Jimenez-Cordero, D.; Heras, F.; Alonso-Morales, N.; Gilarranz, M.A.; Rodriguez, J.J., 2015. Ozone as oxidation agent in cyclic activation of biochar. Fuel Process. Technol. 139, 42–48.

Jin, J., Li, S., Peng, X., Liu, W., Zhang, C., Yang, Y., Han, L., Du, Z., Sun, K., Wang, X., 2018. HNO3 modified biochars for uranium (VI) removal from aqueous solution. Bioresour. Technol. 256, 247-253.

Jin, J., Wang, M., Cao, Y., Wu, S., Liang, P., Li, Y., Zhang, J., Zhang, J., Wong, M.H., Shan, S., Christie, P., 2017. Cumulative effects of bamboo sawdust addition on pyrolysis of sewage sludge: biochar properties and environmental risk from metals. Bioresour. Technol. 228, 218–226.

Jin, J., Li, Y., Zhang, Jianyun, Wu, S., Cao, Y., Liang, P., Zhang, Jin, Wong, M.H.,Wang, M., Shan, S., Christie, P., 2016. Influence of pyrolysis temperature on properties and environmental safety of

heavy metals in biochars derived from municipal sewage sludge. J. Hazard Mater. 320, 417 -426.

Jolly, Y. N., Islam, A., Akbar, S., 2013. Transfer of metals from soil to vegetables and possible health risk assessment. SpringerPlus. 2, 385.

Jones, C., Olson-Rutz, K., 2016. Plant nutrition and soil fertility. Nutr. Manag. Module 2, 4449–4452.

Kabwama, S. N., Bulage, L., Nsubuga, F., Pande, G., Oguttu, D. W., Mafigiri, R., Kihembo, C., Kwesiga, B., Masiira, B., Okullo, A. E., Kajumbula, H., Matovu, J., Makumbi, I., Wetaka, M., Kasozi, S., Kyazze, S., Dahlke, M., Hughes, P., Sendagala, J. N., Musenero, M., Nabukenya, I., Hill, V. R., Mintz, E., Routh, J., Gómez, G., Bicknese, A., Zhu, B. P., 2017. A large and persistent outbreak of typhoid fever caused by consuming contaminated water and street-vended beverages: Kampala, Uganda, January–June 2015. BMC public health, 17, 1-9.

Kalavrouziotis, I.K., Koukoulakis, P., Kostakioti, E., 2012. Assessment of metal transfer factor under irrigation with treated municipal wastewater. Agric. Water Manag. 103, 114–119

Kang, X., Song, J., Yuan, H., Li, X., Li, N., Duan, L., 2018. Historical trends of anthropogenic metals in sediments of Jiaozhou Bay over the last century Mar. Pollut. Bull. 135, 176-182.

Kannan, N., Sundaram, M. M., 2001. Kinetics and mechanism of removal of methylene blue by adsorption on various carbons—a comparative study. Dyes Pigm. 51, 25-40.

Karan, R., Subudhi, P.K., 2012. Approaches to increasing salt tolerance in crop plants. In: Ahmad, P., Prasad, M.N.V. (Eds.), Abiotic Stress Responses in Plants: Metabolism, Productivity and Sustainability. Springer Science + Business Media, LLC, pp. 63–88.

Karunanayake, A. G., Todd, O.A., Crowley, M., Ricchetti, L., Pittman Jr., C.U., Anderson, R., Mohan, D., Mlsna. T., 2018. Lead and cadmium remediation using magnetized and nonmagnetized biochar from Douglas fir. Chem. Eng. J., 331, 480-491.

Kelessidis, A., Stasinakis, A. S. (2012). Comparative study of the methods used for treatment and final disposal of sewage sludge in European countries. Waste manage. 32, 1186-1195.

Khabou, W., Ben Amar, F., Rekik, H., Beghir, M., Touir, A., 2009. Performance evaluation in olive trees irrigated by treated wastewater. Desalination. 246, 329–336.

Khalid, S., Shahid, M., Natasha, Bibi, I., Sarwar, T., Shah, A.H., Niazi, N. K., 2018. A review of environmental contamination and health risk assessment of wastewater use for crop irrigation with a focus on low and high–income countries. Int. J. Environ. Res. Public Health. 15, 895.

Khan, M. N., Mobin, M., Abbas, Z. K., Alamri, S. A., 2018. Fertilizers and their contaminants in soils, surface and groundwater. Anthropocene. 5, 225-240.

Khandare, R. V., Govindwar, S. P., 2015. Phytoremediation of textile dyes and effluents: Current scenario and future prospects. Biotechnol. Adv.33, 1697-1714.

Kim, H.K., Jang, T.I., Kim, S.M., Park, S.W., 2015. Impact of domestic wastewater irrigation on heavy metal contamination in soil and vegetables. Environ. Earth Sci. 73, 2377–2383.

Kirby, J. M., Connor, J., Ahmad, M. U. D., Gao, L., Mainuddin, M., 2014. Climate change and environmental water reallocation in the Murray–Darling Basin: Impacts on flows, diversions and economic returns to irrigation. J. Hydrol. 518, 120-129.

Kitajima, M., Ahmed, W., Bibby, K., Carducci, A., Gerba, C.P., Hamilton, K.A., Haramoto, E., Rose, J.B., 2020. SARS-CoV-2 in wastewater: state of the knowledge and research needs. Sci. Total

Environ. 739, 139076.

Kiziloglu, F. M., Turan, M., Sahin, U., Kuslu, Y., Dursun, A., 2008. Effects of untreated and treated wastewater irrigation on some chemical properties of cauliflower (Brassica olerecea L. var. botrytis) and red cabbage (Brassica olerecea L. var. rubra) grown on calcareous soil in Turkey. Agric. Water Manag. 95, 716-724.

Kołtowski, M., Hilber, I., Bucheli, T.D., Charmas, B., Skubiszewska- Zięba, J., Oleszczuk, P., 2017. Activated biochars reduce the exposure of polycyclic aromatic hydrocarbons in industrially contaminated soils. Chem. Eng. J. 310, 33–40.

Kong, L. L., Zhou, Q. X., 2013. Influences of biochar aging processes by eco-environmental conditions. Adv. Mat. Res. 790, 467-470.

Kończak, M., Oleszczuk, P., 2020. Co-pyrolysis of sewage sludge and biomass in carbon dioxide as a carrier gas affects the total and leachable metals in biochars. J. Hazard. Mater. 400, 123144.

Kończak, M., Oleszczuk, P., Różyło, K., 2019. Application of different carrying gases and ratio between sewage sludge and willow for engineered (smart) biochar production. J. CO2 Util. 29, 20-28.

Krstic, B., Stankovic, D., Igic, R. Nikolic, N., 2007. The potential of different plant species for nickel accumulation. Biotechnol. Biotechnol. Equip. 21, 431-436.

Kumar, A., Ahirwal, J., Maiti, S. K., Das, R., 2015. An assessment of metal in fly ash and their translocation and bioaccumulation in perennial grasses growing at the reclaimed opencast mines. Int. J. Environ. Res. 9, 1089-1096.

Kundu, S. K., Patel, S., Halder, P., Patel, T., Hedayati Marzbali, M., Pramanik, B. K., Paz-Ferreiro, J., de Figueiredo, C. C., Bergmann, D., Surapaneni, A., 2021. Removal of PFAS from Biosolids by a Semi-Pilot Scale Pyrolysis Reactor and the Application of Biosolids Derived Biochar for the Removal of PFAS from Contaminated Water. Environ. Sci. Water Res. Technol. 7, 638 - 649.

Kuntz Maykot, J., Ghisi, E., 2020. Assessment of A Rainwater Harvesting System in A Multi-Storey Residential Building in Brazil. Water. 12, 546.

Lam, C. M., Leng, L., Chen, P. C., Lee, P. H., Hsu, S. C., 2017. Eco-efficiency analysis of non-potable water systems in domestic buildings. Appl. Energy. 202, 293-307.

Leghari, S.J., Wahocho, N.A., Laghari, G.M., Hafeez Laghari, A., Mustafa Bhabhan, G., HussainTalpur, K., Lashari, A.A., 2016. Role of nitrogen for plant growth and development: a review. Adv. Environ. Biol. 10, 209–219

Lehmann, J., Joseph, S. (Eds.), 2015. Biochar for environmental management: an introduction. In: Biochar for environmental management: Science, technology and implementation. Routledge, London, 1–14.

Li. R., Shahbazi. A., Wang. L., Zhang. B., Chung. C.C., Dayton. D., Yan. Q., 2018. Nanostructured molybdenum carbide on biochar for CO2 reforming of CH4. Fuel. 225, 403-410.

Li, D. C., Jiang, H., 2017. The thermochemical conversion of non-lignocellulosic biomass to form biochar: a review on characterizations and mechanism elucidation. Bioresour Technol. 246, 57-68.

Li, H., Dong, X., da Silva, E. B., de Oliveira, L. M., Chen, Y., Ma, L. Q., 2017. Mechanisms of metal sorption by biochars: Biochar characteristics and modifications. Chemosphere, 178, 466–478.

Li, R., Wang, J.J., Zhou, B., Awasthi, M.K., Ali, A., Zhang, Z., Gaston, L.A., Lahori, A.H., Mahar,

A., 2016. Enhancing phosphate adsorption by Mg/Al layered double hydroxide functionalized biochar with different Mg/Al ratios. Sci. Total Environ. 559, 121–129.

Li, L., Liu, S., Liu, J., 2011. Surface modification of coconut shell based activated carbon for the improvement of hydrophobic VOC removal. J. Hazard. Mater. 192, 683–690.

Li, L., Liu S., Zhu, T., 2010. Application of activated carbon derived from scrap tires for adsorption of Rhodamine B. J Environ Sci. 22,1273–1280.

Libutti, A., Gatta, G., Gagliardi, A., Vergine, P., Pollice, A., Beneduce, L., Disciglio, G., Tarantino, E., 2018. Agro-industrial wastewater reuse for irrigation of a vegetable crop succession under Mediterranean conditions. Agric. Water Manag. 196, 1-14.

Lim, S. L., Chu, W.L., Phang, S.M., 2010. Use of Chlorella vulgaris for bioremediation of textile wastewater. Bioresour Technol. 101, 7314-7322,

Link, P.M., Scheffran, J., Ide, T., 2016. Conflict and cooperation in the water-security nexus: a global comparative analysis of river basins under climate change. Wiley Interdiscip. Rev.: Water, 3, 495-515.

Liu. Q., Zhang. Y., Liu. B., Amonette. J.E., Lin. Z., Liu. G., Ambus. P., Xie. Z., 2018. How does biochar influence soil N cycle? A meta-analysis. Plant Soil. 426, 211-225

Liu, S., Xu, W. H., Liu, Y.G., Tan, X. F., Zeng, G. M., .Li, X., Liang, J., Zhou, Z., Yan, Z.L., Cai, X.X., 2017. Facile synthesis of Cu (II) impregnated biochar with enhanced adsorption activity for the removal of doxycycline hydrochloride from water. Sci. Total Environ. 592, 546-553.

Liu, G., Niu, Z., Niekerk, D.V., Xue, J., Zheng, L., 2008. Polycyclic aromatic hydrocarbons (PAHs) from coal combustion: emissions, analysis and toxicology. Rev. Environ. Contam. Toxicol. 192, 1-28

Lu, Y., Song, S., Wang, R., Liu, Z., Meng, J., Sweetman, A.J., Jenkins, A., Ferrier, R.C., Li, H., Luo, W., Wang, T., 2015. Impacts of soil and water pollution on food safety and health risks in China. Environ. Int. 77, 5–15

Lubello, C., Gori, R., Nicese, F. P., Ferrini, F., 2004. Municipal-treated wastewater reuse for plant nurseries irrigation. Water res. 38, 2939-2947.

Lydecker, M., Drechsel, P., 2010. Urban agriculture and sanitation services in Accra, Ghana: the overlooked contribution. Int J Agric Sustain. 8, 94–103.

Lyu, H., Zhang, Q., Shen, B., 2020. Application of biochar and its composites in catalysis. Chemosphere 240, 124842.

Maizel, A. C., Remucal, C. K., 2017. The effect of advanced secondary municipal wastewater treatment on the molecular composition of dissolved organic matter. Water Res.122, 42-52.

Malhotra, H., Sharma, S., Pandey, R., 2018. Phosphorus nutrition: plant growth in response to deficiency and excess. In Plant nutrients and abiotic stress tolerance (pp. 171-190). Springer, Singapore.

Margenat, A., Matamoros, V., Díez, S., Cañameras, N., Comas, J., Bayona, J. M., 2017. Occurrence of chemical contaminants in peri-urban agricultural irrigation waters and assessment of their phytotoxicity and crop productivity. Sci. Total environ. 599, 1140-1148.

Marra, R., Vinale, F., Cesarano, G., Lombardi, N., d'Errico, G., Crasto, A., Mazzei, P., Piccolo, A., Incerti. G., Sheridan, L. W., Scala, F., Bonanomi, G., 2018. Biochars from olive mill waste have

contrasting effects on plants, fungi and phytoparasitic nematodes. PLoS One, 13 e0198728.

Martinez, A., Dominguez, A., Torner, N., Ruiz, L., Camps, N., Barrabeig, I., Arias, C., Alvarez, J., Godoy, P., Balaña,P. J., Pumares, A., Bartolome, R., Ferrer, D., Perez, U., Pinto, R., Buesa, J., 2008. Epidemiology of foodborne norovirus outbreaks in Catalonia, Spain. BMC nfect. Dis. 8, 1-7.

Massé, D. I., Masse, L., 2000. Treatment of slaughterhouse wastewater in anaerobic sequencing batch reactors. Can. Agric. Eng. 42, 131–137.

McCauley, A., Jones, C., Jacobsen, J., 2009. Plant nutrient functions and deficiency and toxicity symptoms. Nutrient management module, 9, 1-16.

Mcheik, M., Toufaily, J., Haj Hassan, B., Hamieh, T., Abi Saab, M. T., Rouphael, Y., Ferracin, E., da shio, B., Bashabshah, I., Al Hadidi, L., 2017. Reuse of treated municipal wastewater in irrigation: a case study from Lebanon and Jordan. Water Environ J. 31, 552-558.

McKay, G., El Geundi, M., Nassar, M. M., 1996. Pore diffusion during the adsorption of dyes onto bagasse pith. Process Saf. Environ. Prot. 74, 277-288.

McKay, G., 1996. Senseless acts of beauty: Cultures of resistance since the sixties. Verso.

Medeiros, R. C., Daniel, L. A., de Oliveira, G. L., Hoffmann, M. T., 2019. Performance of a small-scale wastewater treatment plant for removal of pathogenic protozoa (oo) cysts and indicator microorganisms. Environ. Technol. 40, 3492-3501.

Melgar, J. C., Mohamed, Y., Serrano, N., García-Galavís, P. A., Navarro, C., Parra, M. A., Benlloch, M., Fernández-Escobar, R., 2009. Long term responses of olive trees to salinity. Agric. Water Manag. 96, 1105-1113.

Meng, J., Liang, S., Tao, M., Liu, X., Brookes, P. C., Xu, J., 2018. Chemical speciation and risk assessment of Cu and Zn in biochars derived from co-pyrolysis of pig manure with rice straw. Chemosphere, 200, 344-350.

Meng, J., Feng, X., Dai, Z., Liu, X., Wu, J., Xu, J., 2014. Adsorption characteristics of Cu (II) from aqueous solution onto biochar derived from swine manure. Environ. Sci. Pollut. Res. 21, 7035–7046.

Menegaki, A.N., Hanley, N., Tsagarakis, K.P., 2007. The social acceptability and valuation of recycled water in Crete: A study of consumers' and farmers' attitudes. Ecol. Econ. 62, 7–18.

Mercl, F., Kosnar, Z., Marsik, P., Vojtisek, M., Dusek, J., Szakova, J., Tlustos, P., 2021. Pyrolysis of Biosolids as an Effective Tool to Reduce the Uptake of Pharmaceuticals by Plants. J. Hazard. Mater. 405, 124278.

Mesa-Jurado, M. A., Martin-Ortega, J., Ruto, E., Berbel, J., 2012. The economic value of guaranteed water supply for irrigation under scarcity conditions. Agric. Water Manag. 113, 10-18.

Mezzanotte, V., Antonelli, M., Citterio, S., Nurizzo, C., 2007. Wastewater disinfection alternatives: chlorine, ozone, peracetic acid, and UV light. Water Environ. Res. 79, 2373-2379.

Milano, M., Ruelland, D., Fernandez, S., Dezetter, A., Fabre, J., Servat, E., 2012. Facing climatic and anthropogenic changes in the Mediterranean basin: What will be the medium-term impact on water stress?. C. R. - Geosci. 344, 432-440.

Ministry of Agriculture (MA), 2016. Survey on irrigated areas, Tunisia.

Mirsadeghi, S.A., Zakaria, M.P., Yap, C.K., Shahbazi, A., 2011. Risk assessment for the daily intake of polycyclic aromatic hydrocarbons from the ingestion of cockle (Anadara granosa) and

exposure to contaminated water and sediments along the west coast of Peninsular Malaysia. J. Environ. Sci. (Beijing, China). 23, 336–345.

Mirzavand, M., Ghasemieh, H., Sadatinejad, S.J., Bagheri, R., 2020. An overview on source, mechanism and investigation approaches in groundwater salinization studies. Int. J. Environ. Sci. Technol. 17, 2463–2476.

Mohan, D., Sarswat, A., Ok, Y.S., Pittman, C.U., 2014. Organic and inorganic contaminants removal from water with biochar, a renewable, low cost and sustainable adsorbent – a critical review. Bioresour. Technol. 160, 191–202.

Monterey County Water Resources Agency, Salinas Valley Water Project (SVWP), Monterey County Water Resources Agency, Salinas, CA, USA, 2020, https://www.co.monterey.ca.us/government/government-links/water-resources agency/projects-facilities/salinas-valley-water-project-svwp.

Morgan, J. Á., Connolly, E. Á., 2013. Plant-soil interactions: nutrient uptake. Nat. Sci. Knowl. 4, 2.

Mosko, J., Pohorely, M., Cajthaml, T., Jeremias, M., RoblesAguilar, A. A., Skoblia, S., Beno, Z., Innemanova, P., Linhartova, L., Michalikova, K., Meers, E., 2021. Effect of Pyrolysis Temperature on Removal of Organic Pollutants Present in Anaerobically Stabilized Sewage Sludge. Chemosphere. 265, 129082.

Mu'azu, N. D., Abubakar, I. R., Blaisi, N. I., 2020. Public acceptability of treated wastewater reuse in Saudi Arabia: implications for water management policy. Sci. Total Environ. 721, 137659.

Muchuweti, M., Birkett, J. W., Chinyanga, E., Zvauya, R., Scrimshaw, M. D., Lester, J. N., 2006. Heavy metal content of vegetables irrigated with mixtures of wastewater and sewage sludge in Zimbabwe: implications for human health. Agric Ecosyst Environ. 112, 41-48.

Mukherjee, A., Zimmerman, AR., 2013. Organic carbon and nutrient release from a range of laboratory produced biochars and biochar-soil mixtures. Geoderma 193, 122–130.

Munns, R., Tester, M., 2008. Mechanisms of salinity tolerance. Annu. Rev. Plant Biol. 59, 651-681.

Murphy, B., 2015. Key soil functional properties affected by soil organic matter-evidence from published literature. IOP Conf. Ser. Earth Environ. Sci. 25, 012008.

Narr, C. F., Singh, H., Mayer, P., Keeley, A., Faulkner, B., Beak, D., Forshay, K. J., 2019. Quantifying the effects of surface conveyance of treated wastewater effluent on groundwater, surface water, and nutrient dynamics in a large river floodplain. Ecol. Eng. 129, 123-133.

Naser, H. M, Sultana, S., Mahmud, N. U., Gomes, R. Noor, S., 2011. Heavy metal levels in vegetables with growth stage and plant species variations. Bangladesh j. agric. res. 36, 563-574.

Nguyen, V.T., Nguyen, T.B, Chen, C.W., Hung, C.M., Huang, C.P., Dong, C. D., 2019, Cobalt impregnated biochar (Co-SCG) for heterogeneous activation of peroxymonosulfate for removal of tetracycline in water. Bioresour. Technol. 292,000 121954.

Ni, B. J., Zhu, Z. R., Li, W. H., Yan, X., Wei, W., Xu, Q., Xia, Z., Dai, X., Sun, J., 2020. Microplastics Mitigation in Sewage Sludge through Pyrolysis: The Role of Pyrolysis Temperature. Environ. Sci. Technol. Lett. 7, 961−967.

Nolan, B. T., Hitt, K. J., Ruddy, B. C., 2002. Probability of nitrate contamination of recently recharged groundwaters in the conterminous United States. Environ. Sci. Technol. 36, 2138-2145.

Nzediegwu, C., Arshad, M., Ulah, A., Naeth, M. A., Chang, S. X., 2021. Fuel, thermal and surface

properties of microwave-pyrolyzed biochars depend on feedstock type and pyrolysis temperature. Bioresour. Technol. 320, 124282.

Oatley-Radcliffe, D. L., Walters, M., Ainscough, T. J., Williams, P. M., Mohammad, A. W., Hilal, N., 2017. Nanofiltration membranes and processes: A review of research trends over the past decade. J. Water Process. Eng. 19, 164-171.

Office National de l'Assainissement (ONAS), 2013. Rapport annuel de l'ONAS, Tunisie.

Oleszczuk, P., Jośko, I., Futa, B., Pasieczna-Patkowska, S., Pałys, E., Kraska, P., 2014. Effect of pesticides on microorganisms, enzymatic activity and plant in biochar-amended soil. Geoderma, 214, 10-18.

ONAS (National Office of Sanitation) 2019. Annual report.

Oron, G., Gillerman, L., Bick, A., Mnaor, Y., Buriakovsky, N., Hagin J., 2007. Advanced low quality waters treatment for unrestricted use purposes: imminent challenges. Desalination, 213, 189-198.

Osakabe, Y., Arinaga, N., Umezawa, T., Katsura, S., Nagamachi, K., Tanaka, H., Ohiraki, H., Yamada, K., Seo, S-U, Abo, M., Yoshimura, E., Yamaguchi E., Shinozaki, K., 2013. Osmotic stress responses and plant growth controlled by potassium transporters in Arabidopsis. Plant Cell. 25, 609-624.

OSPAR Commision. Background Document on nonylphenol/nonylphenol ethoxylates, 2009.

Ouda, S., El-Latif, K. A., Khalil, F., 2016. Water requirements for major crops. In : Major crops and water scarcity in Egypt. Springer, Cham. 25-32.

Paetsch, L., Mueller, C. W., Kögel-Knabner, I., Von Lützow, M., Girardin, C., Rumpel, C., 2018. Effect of in-situ aged and fresh biochar on soil hydraulic conditions and microbial C use under drought conditions. Sci. Rep. 8, 1-11.

Pal, D. B., Singh, A., Jha, J. M., Srivastava, N., Hashem, A., Alakeel, M. A., Abd_Allah, E. F., Gupta, V. K., 2021. Low-cost biochar adsorbents prepared from date and delonix regia seeds for heavy metal sorption. Bioresour. Technol. 339, 125606.

Palmer, T. N., Räisänen, J., 2002. Quantifying the risk of extreme seasonal precipitation events in a changing climate. Nature. 415, 512-514.

Pan S-Y, Haddad AZ, Kumar A, Wang S-W., 2020. Brackish water desalination using reverse osmosis and capacitive deionization at the water-energy nexus. Water Res. 183, 116064.

Paranychianakis, N.V., Salgot, M., Snyder, S.A., Angelakis, A.N., 2015. Water Reuse in EU States: Necessity for Uniform Criteria to Mitigate Human and Environmental Risks. Crit. Rev. Environ. Sci. Technol. 45, 1409–1468.

Paranychianakis, N. V., Angelakis, A. N., Leverenz, H., Tchobanoglous, G., 2006. Treatment of wastewater with slow rate systems: a review of treatment processes and plant functions. Crit. Rev. Environ. Sci. Technol. 36, 187-259.

Parikh, S.J., James, B.R., 2012. Soil: the foundation of agriculture. Nat. Educ. Knowl. 3, 2.

Parveen, T., Hussain, A., Rao, M.S., 2015. Growth and accumulation of heavy metals in turnip (Brassica rapa) irrigated with different concentrations of treated municipal wastewater. Hydrol. Res. 46, 60–71.

Pazda, M., Kumirska, J., Stepnowski, P., Mulkiewicz, E., 2019. Antibiotic resistance genes

identified in wastewater treatment plant systems—A review. Sci. Total Environ. 697, 134023.

Pedrero, F., Kalavrouziotis, I., Alarcòn, J.J., Koukoulakis, P., Asano, T., 2010. Use of treated municipal wastewater in irrigated agriculture: Review of some practices in Spain and Greece. Agric. Water Manage. 97, 1233–1241.

Peiris, C., Nayanathara, O., Navarathna, C.M., Jayawardhana, Y., Nawalage, S., Burk, G., Karunanayake, A.G., Madduri, S.B., Vithanage, M., Kaumal, M.N., Mlsna, T.E., Hassan, E.B., Abeysundara, S., Ferez, F., Gunatilake, S. R., 2019. The influence of three acid modifications on the physicochemical characteristics of tea-waste biochar pyrolyzed at different temperatures: a comparative study RSC Adv. 9, 17612-17622.

Pettinger, A., 2008. Caviar and toast. Food Cult. Soc., 11, 133-148.

Pollice, A., Lopez, A., Laera, G., Rubino, P., Lonigro, A., 2004. Tertiary filtered municipal wastewater as alternative water source in agriculture: a field investigation in Southern Italy. Sci. Tot. Environ. 324, 201–210

Pouretedal, H., Sadegh, N., 2014. Effective removal of Amoxicillin, Cephalexin, Tetracycline and Penicillin G from aqueous solutions using activated carbon nanoparticles prepared from vine wood. J. Process. Eng. 1, 64–73.

Prudhomme, C., Giuntoli, I., Robinson, E. L., Clark, D. B., Arnell, N. W., Dankers, R., Fekete, B. M., Franssen, W., Gerten, D., Gosling, S. N., Hagemann, S., Hannah, D. M., Kim, H., Masaki, Y., Satoh, Y., Stacke, T., Wada, Y., Wisser, D., 2014. Hydrological droughts in the 21st century, hotspots and uncertainties from a global multimodel ensemble experiment. PNAS 111, 3262-3267.

Puziy, A. M., Poddubnaya, O. I., Socha, R. P., Gurgul, J., Wisniewski, M., 2008. XPS and NMR studies of phosphoric acid activated carbons. Carbon, 46, 2113-2123.

Qadir, M., Scott, C.A., 2010. Non-pathogenic trade-offs of wastewater irrigation. In: Dreschsel, P., Scott, C.A., Raschid-Sally, L., Redwood, M., Bahri, A. (Eds.), Irrigation and Health: Assessing and Mitigating Risk in Low-Income Countries. EarthscanTaylor & Francis Group, pp. 101–126.

Qu, J., Wang, Y., Tian, X., Jiang, Z., Deng, F., Tao, Y., Jiang, Q., Wang, L., Zhang, Y. (2021). KOH-activated porous biochar with high specific surface area for adsorptive removal of chromium (VI) and naphthalene from water: Affecting factors, mechanisms and reusability exploration. J. Hazard. Mater. 401, 123292.

Quan. G., Fan. Q., Sun. J., Cui. L., Wang. H., Gao. B., Yan. J., 2020. Characteristics of organo-mineral complexes in contaminated soils with long-term biochar application. J. Hazard. Mater. 384, 121265.

Quemada, M., Delgado, A., Mateos, L., Villalobos, F.J., 2016. Nitrogen fertilization I: the nitrogen balance. In: Villalobos, F.J., Fereres, E. (Eds.), Principles of Agronomy for Sustainable Agriculture. Springer International Publishing AG, Chapter 24.

Qureshi, A.S., Hussain, M.I., Ismail, S., Khan, Q.M., 2016. Evaluating heavy metal accumulation and potential health risks in vegetables irrigated with treated wastewater. Chemosphere. 163, 54–61.

Radovic, L. R., Moreno-Castilla, C., Rivera-Utrill, J., 2000. Carbon materials as adsorbents in aqueous solutions. Chem. Phys. Carbon. 27, 227–405.

Rai, P. K., Lee, S. S., Zhang, M., Tsang, Y. F., Kim, K. H., 2019. Heavy metals in food crops: Health risks, fate, mechanisms, and management. Environ. Int. 125, 365-385.

Rai, P. K., 2008. Heavy metal pollution in aquatic ecosystems and its phytoremediation using

wetland plants: an ecosustainable approach. Int. J. Phytoremediation. 10, 133-160.

Razaq, M., Zhang, P., Shen, H. L., 2017. Influence of nitrogen and phosphorous on the growth and root morphology of Acer mono. PloS one, 12, e0171321.

Renai, L., Tozzi, F., Scordo, C. V., Giordani, E., Bruzzoniti, M. C., Fibbi, D., Mandi, L., Ouazzani, N., Del Bubba, M., 2021. Productivity and nutritional and nutraceutical value of strawberry fruits (*Fragaria* x *ananassa* Duch.) cultivated under irrigation with treated wastewaters. J. Sci. Food Agric. 101, 1239-1246.

Rezapour, S., Atashpaz, B., Moghaddam, S.S., Damalas, C.A., 2019. Heavy metal bioavailability and accumulation in winter wheat (Triticum aestivum L.) irrigated with treated wastewater in calcareous soils. Sci. Total Environ. 656, 261–269.

Richards, G. P., 2001. Enteric virus contamination of foods through industrial practices: a primer on intervention strategies. J. Ind. Microbiol. Biotechnol. 27, 117-125.

Rivera-Utrilla, J., Méndez-Díaz, J., Sánchez-Polo, M., Ferro-García, M. A., Bautista-Toledo, I., 2006. Removal of the surfactant sodium dodecylbenzenesulphonate from water by simultaneous use of ozone and powdered activated carbon: Comparison with systems based on O3 and O3/H2O2. Water Res. 40, 1717-1725.

Rizzo, L., Krätke, R., Linders, J., Scott, M., Vighi, M., de Voogt, P., 2018. Proposed EU minimum quality requirements for water reuse in agricultural irrigation and aquifer recharge: SCHEER scientific advice. Curr. Opin. Environ. Sci. 2, 7-11.

Robbins, C. A., Du, X., Bradley, T. H., Quinn, J. C., Bandhauer, T. M., Conrad, S. A., Carlson, K. H., Tong, T., 2022. Beyond treatment technology: Understanding motivations and barriers for wastewater treatment and reuse in unconventional energy production. Resour Conserv Recycl. 177, 106011.

Robinson, T., McMullan, G., Marchant, R., Nigam, P., 2001. Remediation of dyes in textile effluent: a critical review on current treatment technologies with a proposed alternative. Bioresour. Technol. 77, 247-255.

Rojas, R.V., Achouri, M., Maroulis, J., Caon, L., 2016. Healthy soils: a prerequisite for sustainable food security. Environ. Earth Sci. 75, 1–10.

Rombolà, A.G., Meredith, W., Snape, C.E., Baronti, S., Genesio, L., Vaccari, F.P., Fabbri, D., 2015. Fate of soil organic carbon and polycyclic aromatic hydrocarbons in a vineyard soil treated with biochar. Environ. Sci. Technol. 49, 11037–11044.

Rusan, M. J. M., Hinnawi, S., Rousan, L., 2007. Long-term effect of wastewater irrigation of forage crops on soil and plant quality parameters. Desalination, 215, 143-152.

Sabri, N.A., Schmitt, H., Van der Zaan, B., Gerritsen, H.W., Zuidema, T., Rijnaarts, H.H.M., Langenhoff, A. A. M., 2020. Prevalence of antibiotics and antibiotic resistance genes in a wastewater effluent-receiving river in the Netherlands. J. Environ. Chem. Eng. 8, 102245.

Sahu, S. G., Sarkar, P., Chakraborty, N., Adak, A. K., 2010. Thermogravimetric assessment of combustion characteristics of blends of a coal with different biomass chars. Fuel Process. Technol. 91, 369-378.

Saifullah, Dahlawi, S., Naeem, A., Rengel, Z., Naidu, R., 2018. Biochar application for the remediation of salt-affected soils: challenges and opportunities. Sci. Total Environ. 625, 320-335.

Sairam, R.K., Tyagi, A., 2004. Physiology and molecular biology of salinity stress tolerance in

plants. Curr. Sci. 86, 407–421.

Sanghi, R., Verma, P., 2013. Decolorisation of aqueous dye solutions by low-cost adsorbents: a review. Color. Technol. 129, 85-108.

San Miguel, G., Lambert, S. D., Graham, N. J. D., 2001. The regeneration of field-spent granular-activated carbons. Water Res. 35, 2740-2748.

Schiermeier, Q., 2008. Water: Purification with a pinch of salt. Nature 452, 260–261.

Schlindwein, A.D., Rigotto, C., Simões, C.M.O., Barardi, C.R.M., 2010. Detection of enteric viruses in sewage sludge and treated wastewater effluent. Water Sci. Technol. 61, 537–544.

Scordo, C. V. A., Checchini, L., Renai, L., Orlandini, S., Bruzzoniti, M. C., Fibbi, D., Mandi, L., Ouazzani, N, Del Bubba, M., 2020. Optimization and validation of a method based on QuEChERS extraction and liquid chromatographic–tandem mass spectrometric analysis for the determination of perfluoroalkyl acids in strawberry and olive fruits, as model crops with different matrix characteristics. J. Chromatogr. A. 1621, 461038.

Sgroi, M., Vagliasindi, F. G., Roccaro, P., 2018. Feasibility, sustainability and circular economy concepts in water reuse. Curr. Opin. Environ. Sci. 2, 20-25.

Shakir, E., Zahraw, Z., Al-Obaidy, A.H.M.J., 2017. Environmental and health risks associated with reuse of wastewater for irrigation. Egypt. J. Pet. 26, 95–102.

Shannon, M. A., Bohn, P. W., Elimelech, M., Georgiadis, J. G., Marinas, B. J., Mayes, A. M., 2009. Science and technology for water purification in the coming decades. Nanoscience and technology: a collection of reviews from nature Journals. 337-346.

Shao, J., Zhang, J., Zhang, X., Feng, Y., Zhang. H., Zhang, S., Chen, H., 2018. Enhance SO2 adsorption performance of biochar modified by CO2 activation and amine impregnation. Fuel. 224, 138-146.

Shi, R. Y., Ni, N., Nkoh, J. N., Li, J.Y., Xu, R. K., Qian, W., 2019. Beneficial dual role of biochars in inhibiting soil acidification resulting from nitrification. Chemosphere, 234, 43 – 51.

Shi, R.Y., Hong, Z. N., Li, J.Y., Jiang, J., Baquy, M. A. A., Xu, R. K., Qian, W., 2017. Mechanisms for increasing the pH buffering capacity of an acidic Ultisol by crop residue-derived biochars. J. Agric. Food Chem. 65, 8111-8119.

Shtull-Trauring, E., Cohen, A., Ben-Hur, M., Israeli, M., Bernstein, N., 2022. NPK in treated wastewater irrigation: Regional scale indices to minimize environmental pollution and optimize crop nutritional supply. Sci. Total Environ. 806, 150387.

Singh, R., Babu, J.N., Kumar, R., Srivastava, P., Singh, P, Raghubanshi, A.S., 2015. Multifaceted application of crop residue biochar as a tool for sustainable agriculture: an ecological perspective. Ecol. Eng. 77, 324-347.

Singh, P.K., Deshbhratar, P.B., Ramteke, D.S., 2012. Effects of sewage wastewater irrigation on soil properties, crop yield and environment. Agric. Water Manag. 103, 100–104.

Singh, K. P., Mohan, D., Sinha, S., Dalwani, R., 2004. Impact assessment of treated/untreated wastewater toxicants discharged by sewage treatment plants on health, agricultural, and environmental quality in the wastewater disposal area. Chemosphere. 55, 227-255.

Sizmur, T., Fresno, T., Akgül, G., Frost, H., Jiménez, E.M., 2017. Biochar modification to enhance sorption of inorganics from water. Bioresour. Technol. 246, 34–47.

Smith, C. J., Oster, J. D., Sposito, G., 2015. Potassium and magnesium in irrigation water quality assessment. Agric. Water Manag. 157, 59-64.

Smith, S. R., 2009. Organic contaminants in sewage sludge (biosolids) and their significance for agricultural recycling. Philos. Trans. Royal Soc. A. 367, 4005-404.

Sonune, A., Ghate, R., 2004. Developments in wastewater treatment methods. Desalination, 167, 55-63.

Suarez, D. L., Grieve, C. M., 2013. Growth, yield, and ion relations of strawberry in response to irrigation with chloride-dominated waters. J. Plant Nutr. 36, 1963-1981.

Sudha, S., Giri Dev, V. R., 2007. Low cost-sorbents—an overview. Synth Fibres 36, 5–9.

Suh, Y. J., Rousseaux, P., 2002. An LCA of alternative wastewater sludge treatment scenarios. Resour Conserv Recycl. 35, 191-200.

Sun, Y., Gao, B., Yao, Y., Fang, J., Zhang, M., Zhou, Y., Chen, H., Yang, L., 2014. Effects of feedstock type, production method, and pyrolysis temperature on biochar and hydrochar properties Chem. Eng. J. 240, 574-578.

Swami, D., Buddhi, D., 2006. Removal of contaminants from industrial wastewater through various non-conventional technologies: a review. Int. J. Environ. Pollut. 27, 324-346.

Tak, H.I., Babalola, O.O., Huyser, M.H., Inam, A., 2013. Urban wastewater irrigation and its effect on growth, photosynthesis and yield of chickpea under different doses of potassium. Soil Sci. Plant Nutr. 59, 156–167.

Tan, X.F, Liu, S., Liu, L., Gu, Y., Zeng, G., Hu, X., Wang, X., Liu, S., Jiang, J., 2017. Biochar as potential sustainable precursors for activated carbon production: Multiple applications in environmental protection and energy storage. Bioresour. Technol. 227, 359-372.

Tang, D., Zheng, Z., Lin, K., Luan, J., Zhang, J., 2007. Adsorption of p-nitrophenol from aqueous solutions onto activated carbon fiber. J. Hazard. Mater. 143, 49-56.

Tarradellas, J., Bitton, G., Rossel, D., 1996. Soil ecotoxicology. CRC press.

Tekaya, M., Mechri, B., Dabbaghi, O., Mahjoub, Z., Laamari, S., Chihaoui, B., Bounah, D., Hammami, M., Chehab, H., 2016. Changes in key photosynthetic parameters of olive trees following soil tillage and wastewater irrigation, modified olive oil quality. Agric. Water Manag. 178, 180–188.

Tendero, C., Tixier, C., Tristant, P., Desmaison, J., Leprince, P., 2006. Atmospheric pressure plasmas: A review. Spectrochim. Acta B: At. Spectrosc. 61, 2–30.

Toze, S., 2006. Reuse of effluent water—benefits and risks. Agric. Water Manag. 80, 147-159.

Turkdogan, M.K., Fevzi, K., Kazim, K., Ilyas, T., Ismail, U., 2003. Heavy metals in soil, vegetables and fruits in the endemic upper gastrointestinal cancer region of Turkey. Environ. Toxicol. Pharmacol. 13, 175–179.

Tzanakakis, V. A., Paranychianakis, N. V., Angelakis, A. N., 2020a. Water supply and water scarcity. Water. 12, 2347.

Tzanakakis, V., Angelakis, A., Paranychianakis, N., Dialynas, Y., Tchobanoglous, G., 2020b. Challenges and Opportunities for Sustainable Management of Water Resources in the Island of Crete, Greece. Water. 12, 1538.

UN, 2017. United Nations. World Population Prospects: The 2017 Revision, Key Findings and Advance Tables. Working paper no. ESA/P/WP/248 (Department of Economic and Social Affairs, Population Division, United Nations, New York, 2017).

Ungureanu, N., Vlăduț, V., Dincă, M., Zăbavă, B. Ș., 2018. Reuse of wastewater for irrigation, a sustainable practice in arid and semi-arid regions. In Proceedings of the 7th International Conference on Thermal Equipment, Renewable Energy and Rural Development (TE-RE-RD), Drobeta-Turnu Severin, Romania. Vol. 31, 379-384.

United States Environmental Protection Agency, Water Topics, US EPA, Washington, D.C., USA, 2016, https://www.epa.gov/environmental-topics/water-topics.

Urbano, V.R., Mendonça, T.G., Bastos, R.G., Souza, C.F., 2017. Effects of treated wastewater irrigation on soil properties and lettuce yield. Agric. Water Manag. 181, 108–115.

Vijayaraghavan, K., Yun, Y. S., 2008. Bacterial biosorbents and biosorption. Biotechnol. Adv. 26, 266-291.

Verheijen, F.G.A., Jeffery, S., Bastos, A.C., van der Velde, M., and Diafas, I., 2009. Biochar Application to Soils - A Critical Scientific Review of Effects on Soil Properties, Processes and Functions. EUR 24099 EN, Office for the Official Publications of the European Communities, Luxembourg, 149.

van Vliet, M. T., Jones, E. R., Flörke, M., Franssen, W. H., Hanasaki, N., Wada, Y., Yearsley, J. R., 2021. Global water scarcity including surface water quality and expansions of clean water technologies. Environ. Res. Lett. 16, 024020.

Vanham, D., Hoekstra, A. Y., Wada, Y., Bouraoui, F., De Roo, A., Mekonnen, M. M., van de Bund, W. J., Batelaan, O., Pavelic, P., Bastiaanssen, W. G. M., Kummu, M., Rockström, J., Liu, J., Bisselink, B., Ronco, P., Pistocchi, A., Bidoglio, G., 2018. Physical water scarcity metrics for monitoring progress towards SDG target 6.4: An evaluation of indicator 6.4. 2 “Level of water stress”. Sci. Total Environ. 613, 218-232.

Vega-Morales, T., Sosa-Ferrera, Z., Santana-Rodríguez, J. J., 2010. Determination of alkylphenol polyethoxylates, bisphenol-A, 17α-ethynylestradiol and 17β-estradiol and its metabolites in sewage samples by SPE and LC/MS/MS. J. Hazard. Mater. 183, 701-711.

Vergine, P., Lonigro, A., Salerno, C., Rubino, P., Berardi, G., Pollice, A., 2017a. Nutrient recovery and crop yield enhancement in irrigation with reclaimed wastewater: a case study. Urban Water J. 14, 325–330.

Vergine, P., Salerno, C., Libutti, A., Beneduce, L., Gatta, G., Berardi, G., Pollice, A., 2017b. Closing the water cycle in the agro-industrial sector by reusing treated wastewater for irrigation. J. Clean. Prod. 164, 587–596.

Verheijen, F., Jeffery, S., Bastos, A.C., van der Velde, M., Diafas, I., 2010. Biochar application to soils. A Critical Scientific Review of Effects on Soil Properties, Processes and Functions. European Commission, Italy.

Verlicchi, P., Al Aukidy, M., Galletti, A., Zambello, E., Zanni, G., Masotti, L., 2012. A project of reuse of reclaimed wastewater in the Po Valley, Italy: polishing sequence and cost benefit analysis. J. Hydrol. 432, 127–136.

Voutchkov, N., 2018. Energy use for membrane seawater desalination—Current status and trends. Desalination. 431, 2–14.

Wada, Y., Flörke, M., Hanasaki, N., Eisner, S., Fischer, G., Tramberend, S., Satoh, Y., van Vliet M. T. H., Yillia, P., Ringler, C., Burek, P., Wiberg, D., 2016. Modeling global water use for the 21st century: The Water Futures and Solutions (WFaS) initiative and its approaches. Geosci. Model Dev. 9,175-222.

Wada, Y., Gleeson, T., Esnault, L., 2014. Wedge approach to water stress. Nat. Geosci. 7, 615-617.

Wan, S., Wu, J., Zhou, S., Wang, R., Gao, B., He, F., 2018. Enhanced lead and cadmium removal using biochar-supported hydrated manganese oxide (HMO) nanoparticles: Behavior and mechanism. Sci.Total Environ. 616, 1298-1306.

Wang, Y., Ma, Z., Wang, X., Sun, Q., Dong, H., Wang, G., Chen, X., Yin, C., Han, Z., Mao, Z., 2019. Effects of biochar on the growth of apple seedlings, soil enzyme activities and fungal communities in replant disease soil. Sci. Hortic. 256, 108641.

Wang, T., Liu, J., Zhang, Y., Zhang, H., Chen, W. Y., Norris, P., Pan, W. P., 2018a. Use of a non-thermal plasma technique to increase the number of chlorine active sites on biochar for improved mercury removal. Chem. Eng. Sci. 331, 536-544.

Wang, J., Xia, K., Waigi, M. G., Gao, Y., Odinga, E. S., Ling, W., Liu, J., 2018b. Application of biochar to soils may result in plant contamination and human cancer risk due to exposure of polycyclic aromatic hydrocarbons. Environ. Int. 121, 169-177.

Wang, B., Wang, Z., Jiang, Y., Tan, G., Xu, N., Xu, Y., 2017a. Enhanced power generation and wastewater treatment in sustainable biochar electrodes based bioelectrochemical system. Bioresour Technol. 241, 841–848.

Wang, P., Tang, L., Wei, X., Zeng, G. M., Zhou, Y. Y., Deng, Y. C., Wang, J. J., Xie, Z. H., Fang, W., (2017b). Synthesis and application of iron and zinc doped biochar for removal of p-nitrophenol in wastewater and assessment of the influence of co-existed Pb (II). Appl. Surf Sci. 392, 391–401.

Warner, N. R., Christie, C. A., Jackson, R. B., Vengosh, A., 2013. Impacts of shale gas wastewater disposal on water quality in western Pennsylvania. Environ. Sci. Technol. 47, 11849-11857.

Wassenberg, D. M., Di Giulio, R. T., 2004. Synergistic embryotoxicity of polycyclic aromatic hydrocarbon aryl hydrocarbon receptor agonists with cytochrome P4501A inhibitors in Fundulus heteroclitus. Environ. Health Perspect. 112, 1658-1664.

Wathudura, P. D., Peiris, C., Navarathna, C. M., Mlsna, T. E., Kaumal, M. N., Vithanage, M., Gunatilake, S. R., 2020. Microwave and open vessel digestion methods for biochar. Chemosphere. 239, 124788.

Weng, Z. H., Van Zwieten, L., Singh, B. P., Tavakkoli, E., Kimber, S., Morris, S., Macdonald, A., Cowie, A., 2018. The accumulation of rhizodeposits in organo-mineral fractions promoted biochar-induced negative priming of native soil organic carbon in Ferralsol. Soil Biol. Biochem. 118, 91-96.

Werfelli, N., Ben Ayed, R., Abassi, M., Béjaoui, Z., 2021. Contamination Assessment of Durum Wheat and Barley Irrigated with Treated Wastewater through Physiological and Biochemical Effects and Statistical Analyses. J. Food Qual.1–10.

Wiesman, Z., Itzhak, D., Ben Dom, N., 2004. Optimization of saline water level for sustainable Banea olive and oil production in desert conditions, Sci. Horticul. 100, 257–266.

Wolfe, A. H., Patz, J. A., 2002. Reactive nitrogen and human health: acute and long-term implications. Ambio. 31, 120-125.

Wongrod, S., Simon, S., van Hullebusch, E. D., Lens, P. N., Guibaud, G., 2018. Changes of sewage

sludge digestate-derived biochar properties after chemical treatments and influence on As (III and V) and Cd (II) sorption. Int. Biodeterior. Biodegradation. 135, 96-102.

Wu, C., Liu, X., Wu, X., Dong, F., Xu, J., Zheng, Y., 2019. Sorption, degradation and bioavailability of oxyfluorfen in biochar-amended soils. Sci. Total Environ. 658, 87-94.

Wu, H., Feng, Q., 2017. Fabrication of bimetallic Ag/Fe immobilized on modified biochar for removal of carbon tetrachloride. J. Environ. Sci. (China). 54, 346-357.

Wu, G. Q., Zhang, X., Hui, H., Yan, J., Zhang, Q. S., Wan, J. L., Dai, Y., 2012. Adsorptive removal of aniline from aqueous solution by oxygen plasma irradiated bamboo-based activated carbon. Chem. Eng. J. 185, 201–210.

WWAP (World Water Assessment Program), 2018. The United Nations World Water Development Report 2018: Nature-Based Solutions for Water. United Nations Educational, Scientific and Cultural Organization, Paris. https://unesdoc.unesco.org/ark:/48223/pf0000261424_eng (accessed Dec. 7, 2018).

Xiao, B., Dai, Q., Yu, X., Yu, P., Zhai, S., Liu, R., Guo, X., Liu, J., Chen, H.,2018. Effects of sludge thermal-alkaline pretreatment on cationic red X-GRL adsorption onto pyrolysis biochar of sewage sludge. J. Hazard. Mater. 343, 347-355.

Yadav, V., Jain, S., Mishra, P., Khare, P., Shukla, A. K., Karak, T., Singh, A. K., 2019. Amelioration in nutrient mineralization and microbial activities of sandy loam soil by short term field aged biochar. Appl. Soil Ecol. 138, 144-155.

Yang, G. X., Jiang, H., 2014. Amino modification of biochar for enhanced adsorption of copper ions from synthetic wastewater. Water Res. 48, 396–405

Yannopoulos, S., Giannopoulou, I., Kaiafa-Saropoulou, M., 2019. Investigation of the current situation and prospects for the development of rainwater harvesting as a tool to confront water scarcity worldwide. Water. 11, 2168.

Yi, L., Jiao, W., Chen, X., Chen, W., 2011. An overview of reclaimed water reuse in China. J. Environ. Sci. 23, 1585–1593.

Yin, Z., Liu, Y., Liu, S., Jiang, L., Tan, X., Zeng, G., Li, M., Liu, S., Tian, S., Fang, Y., 2018. Activated magnetic biochar by one-step synthesis: Enhanced adsorption and coadsorption for 17β-estradiol and copper. Sci. Total Environ. 639, 1530–1542.

Ying-ping, L., Zhen-Xing, W., Zhi-Hui, Y., Li-Yuan, C., Jian-qun, C., Ping-Fu, Y., 2011. Migration and transfer of chromium in soil-vegetable system and associated health risks in vicinity of ferro-alloy manufactory. Trans. Nonferrous Met. Soc. China. 21, 2520-2527.

Yuan, Y., Xiang, M., Liu, C., Theng, B. K., 2019a. Chronic impact of an accidental wastewater spill from a smelter, China: a study of health risk of heavy metal (loid) s via vegetable intake. Ecotoxicol. Environ. Saf. 182, 109401.

Yuan, P., Wang, J., Pan, Y., Shen, B.X., Wu, C.F., 2019b. Review of biochar for the management of contaminated soil: Preparation, application and prospect. Sci. Total Envion. 659, 473-490.

Yuan, S. J., Dai, X. H., 2017. Sewage sludge-based functional nanomaterials: development and applications. Environ. Sci. Nano. 4, 17-26.

Zalesny Jr, R. S., Stanturf, J. A., Evett, S. R., Kandil, N. F., Soriano, C., 2011. Opportunities for woody crop production using treated wastewater in Egypt. I. Afforestation strategies. Int. J.

Phytoremediation. 13, 102-121.

Zema, D.A., Bombino, G., Andiloro, S., Zimbone, S.M., 2012. Irrigation of energy crops with urban wastewater: effects on biomass yields, soils and heating values. Agric. Water Manag. 115, 55–65.

Zerva, I., Alexandropoulou, I., Panopoulou, M., Melidis, P., Ntougias, S., 2018. Antibiotic Resistance Genes Dynamics at the Different Stages of the Biological Process in a Full-Scale Wastewater Treatment Plant. Proceedings 2, 650.

Zhang, J., Shao, J., Jin, Q., Zhang, X., Yang, H., Chen, Y., Zhang, S., Chen, H., 2020. Effect of deashing on activation process and lead adsorption capacities of sludge-based biochar. Sci. Total Environ. 716, 137016.

Zhang, Y., Shen, Y., 2019. Wastewater irrigation: past, present, and future. Wiley Interdisciplinary Reviews. Water, 6, e1234.

Zhang. J., Li. Q., Wu. J., Song. X., 2019. Effects of nitrogen deposition and biochar amendment on soil respiration in a Torreya grandis orchard. Geoderma. 355, 113918.

Zhang, F., Wu, K., Zhou, H., Hu, Y., Sergei, P., Wu, H., Wei, C., 2018a. Ozonation of aqueous phenol catalyzed by biochar produced from sludge obtained in the treatment of coking wastewater. J. Environ Manag. 224, 376–386.

Zhang, P., Sun, H., Min, L., Ren, C., 2018b. Biochars change the sorption and degradation of thiacloprid in soil: Insights into chemical and biological mechanisms. Environ. Pollut. 236, 158–167.

Zhang, Q. P., Liu, Q. C., Li, B., Yang, L., Wang, C.-Q., Li, Y.-D., Xiao, R., 2017. Adsorption of Cd (II) from aqueous solutions by rape straw biochar derived from different modification processes. Chemosphere 175, 332–340.

Zhang, J., Zhang, L., Wang, P., Huang, Q.W., Yu, G., Li, D.C., Shen, Q., Ran, W., 2013. The role of non-crystalline Fe in the increase of SOC after long-term organic manure application to the red soil of southern China. Eur. J. Soil Sci. 64, 797–804.

Zhang, A., Bian, R., Pan, G.X., Cui, L.Q., Hussain, Q., Li, L.Q., Zheng, J.W., Zhang, X.H., Han, X.J., Yu, X.Y., 2012. Effects of biochar amendment on soil quality, crop yield and greenhouse gas emission in a Chinese rice paddy: A field study of 2 consecutive rice growing cycles. Field Crops Res. 127, 253-160.

Zhao, L., Zheng, W., Mašek, O., Chen, X., Gu, B., Sharma, B.K., Cao, X., 2017. Roles of Phosphoric Acid in Biochar Formation: Synchronously Improving Carbon Retention and Sorption Capacity. J. Environ. Qual. 46, 393.

Zheng, F., Zhu, D., Giles, M., Daniell, T., Neilson, R., Zhu, Y.-G., Yang, X.-R., 2019, Mineral and Organic Fertilization Alters the Microbiome of a Soil Nematode Dorylaimus Stagnalis and Its Resistome. Sci. Total Environ. 680, 70–78.

Zhou, Y., Tol, R. S. J., 2005. Evaluating the costs of desalination and water transport. Water Resour. Res. 41, 1–10.

Zielińska, A., Oleszczuk, P., Charmas, B., Skubiszewska-Zięba, J., Pasieczna-Patkowska, S., 2015. Effect of sewage sludge properties on the biochar characteristic. J. Anal. Appl. Pyrolysis. 112, 201-213.

Experimental part

I. Irrigation by treated wastewater of olive and strawberry plants

This work was managed to evaluate the short-term impact on soil, olive and strawberry plants of irrigation using different types of water. The cultivation of plant was done under greenhouse at the national engineering school of Sfax in Tunisia.

1. Area study

Sfax is a Tunisian city that is located at 270 km southeast of Tunis (latitude: 34.44° N, longitude: 10.46° E, elevation: 41 m above the sea level, heating design temperature: 8.96 and cooling design temperature: 31.96) (Baklouti et al., 2012). Sfax is an important industrial city also it is the first producer and exporter of olive oil in Tunisia. Sfax provides 11% of the National olive oil revenues, 34% of the processing capacity, and contributes to 37% to the National production and 68% to the exports of olive oil (Ministry of Agriculture, 2015). Its location characterized by warmest areas experiencing frequent and cyclic warm winter each 3–4 years (Benmoussa et al., 2017; Ghrab et al., 2014) and the global water shortage problem and also sandy to sandy loam soil characteristics (Belaid et al., 2010; Rouina et al., 2007) are considered reasons to reuse the TWW in Sfax as an alternative approach for the irrigation with of fresh water.

2. Olive plantation

Olive cultivation has been carried out starting from January 2018 to December 2019. Plants were irrigated with groundwater (GW) or TWWs that were taking from three WWTPs (TWW1, TWW2 and TWW3) that treated essentially industrials effluents. For each type of water, three plots contained 15 Kg of soil were planted by four months olive trees (*Olea europaea* L. cv. Koroneiki'). The first triple was irrigated with GW and others plants were irrigated with TWWs; each triple by a particular TWW (TWW1, TWW2 or TWW3). Soil samples were taken before and after olive irrigation. Plant growth was conducted continuously.

3. Strawberry plantation

Young fresh strawberry plants (*Fragaria* x *ananassa* cv Camarosa) were transplanted into 5 liters PVC pots (23 cm diameter, 17.6 cm deep) filled with 5 kg of substrate (soil mixed with peat (1/3; 2/3)) and placed in a greenhouse starting from January to June 2018. Since strawberry requires cool and moist climates, the climatic condition in the greenhouse were set to have a temperature of 25/12°C (day/night). Four experimental series of eight pots were considered for each type of irrigation water; one series of pots was irrigated with GW and three other series were irrigated with diluted TWWs at 60% (D60), 40% (D40) and 20% (D20). Harvest was performed at the end of June

and the plants were washed, divided into two parts (areal parts and roots), and stored at -20°C for analysis. After each harvesting, fruits were washed with distilled water and dried using paper towel.

4. Physicochemical and microbiological analysis of well water and treated wastewater

4.1.pH

Water pH was measured by the electrochemical method using a pH meter Mettler Toledo (MP 220). The glass electrode is immersed in water, its pH was displayed on the pH-meter screen. The electrode must be well rinsed with distilled water and must be regularly calibrated to keep its precision.

4.2. Electrical conductivity

EC is an index of soluble salt content. The solution conductance value varies according to the presence of ions, their concentrations, their mobility and temperatures of the sample, which is linked to the concentration and nature of dissolved substances. In general, mineral salts are good conductor's contrary to organic and colloidal materials. To measure the EC according to AFNOR (NF 27888), an Inolab WTW conductivity meter was used. The cell was first rinsed with distilled water then immersed in the solution under agitation to ensure that the ionic concentration between the electrodes is identical to that of the ambient liquid.

4.3. Total suspended solids (TSS)

TSS represents the rate of undissolved, mineral or organic matter present in the water. TSS were determined according to the standard method (NF EN 872 (1996)). TSS, expressed in mg / L, were measured after filtration of a volume of water and filter drying in an oven at 105 ° C using the following equation (Eq.1):

$$TSS = \frac{W_1 - W_2}{V} \times 1000 \qquad \text{(Eq.1)}$$

Where;

W_1 is the weight of filter in mg,

W_2 is the weight of filter with suspended matters,

V is the Volume of sample in mL.

4.4. Chemical oxygen demand (COD)

DOC corresponds to the quantity of oxygen necessary to oxidize the organic matter and a part of the mineral matter under well-defined operating conditions. COD was measured referring to the AFNOR standard method (Rodier, 2009). The oxidation was carried out by potassium dichromate

characterizes by a powerful oxidizing power in hot and acidic medium. To estimate the water-soluble COD, UV - Visible spectrophotometry (Agilent Technologies-Cary 60-5 UV – Vis) was used at the absorbance of 254 nm.

4.5. Biochemical oxygen demand (BOD)

BOD was determined using the NF T 90-103. BOD is the amount of oxygen consumed by microorganisms to oxidize organic matter. The sample was placed in an Oxitop system (WTW) connected to a mercury manometer. The depression due to the oxygen consumption by microorganisms corresponds to BOD. The CO_2 formed by the respiration of bacteria is extracted from the gaseous medium by the KOH (45%) placed in the cap of the bottle. Throughout the experiment, the sample was constantly agitated during five days of incubation at 20 ° C.

4.6. Total nitrogen content

Total nitrogen, which is ammonium and organic Nitrogen was determined using Kjeldahl method by titrimetric determination after mineralization and distillation. The mineralization of organic nitrogen was carried out in a hot and sulfuric medium, in the presence of a catalyst prepared from a homogeneous mixture of potassium sulphate and selenium. The next step corresponds to the distillation of the ammoniacal salts previously moved to a basic medium in the form of ammonia. This ammonia is entrained in steam and then trapped in a solution of boric acid. The ammonia was finally titrated with sulfuric acid in the presence of the coloured indicator reagent.

The nitrate and nitrite contents were analysed by ion chromatography, which was carried out using a DIONEX ® apparatus using the Ion Pac AS18 ion exchange column. Ions or polar compounds were entrained by the mobile phase and separated by the effect of their interactions with the ionic sites of the stationary phase. The ion exchange layer of the stationary phase of the AS18 column consisted of quaternary ammonium. The eluent used was Na_2CO_3 (10 mM) and $NaHCO_3$ (7mM) solutions. The device was calibrated with a solution of comprising 50 and 100 mg / L of NO_2^- and NO_3^-. One milliliter was then injected using a syringe equipped with a 0.45 µm filter.

4.7. Metals contents

WW contains mineral salts with different proportions. There are two categories of mineral salts; major elements which are very numerous present in a relatively high concentration such as calcium, magnesium, sodium and potassium and minor or trace elements which are generally toxic such as arsenic, cadmium, chromium, mercury nickel. First, the determination of metals concentrations required their mineralization. This step was carried out by an attack acid to release organic matter and release heavy metals. Then the water is filtered and the metals are measured by atomic

absorption. The atomic absorption spectrophotometer used is a Hermoquert Fisher Scientific.

4.8. Biological analysis

The search for the main indicators of microbiological pollution was carried out by carrying out the analysis of the enumeration or presence of coliforms, faecal streptococci and *Salmonella*.

For the detection of total and faecal coliforms, a presumptive test is carried out on a lactose broth with bromocresol purple. The successive decimal dilutions prepared and seeded were from 10-5 to 10 -3. Samples were incubated at 30 ° C for 48 hours. The confirmatory test was carried out by subculturing on lactose broth with bile and brilliant green (Merck). After incubation at 44 ° C for 24 hours, positive faecal coliform indicator tubes are those which show acidification of the medium reflected by the colour change from the medium to yellow with production of the gas trapped in the Durham bell.

This confirmatory test makes it possible to determine the number of faecal coliforms per 100 mL of suspensions following the determination of the most probable number.

Streptococcal count was performed on two liquid culture media (Most Probable Number Technique): Rothe's medium and Litsky's medium (Pronadisa), serving respectively as a presumptive test and a confirmatory test. Three tubes were used for dilution. Incubation of these media is done at 37 ° C for 48 hours.

50 mL of sample was enriched for 24 hours at 37 ° on double selenite concentrated medium. The selectivity of this medium is based on the ability of *Salmonella* to multiply in the presence of selenite. If a suspected *Salmonella* is noted, an analysis of the suspension is plated on SS agar and incubated for 24 hours at 37 ° C. Finally, a single characteristic colony per dish was transferred to another medium (SS agar at 37°C for 24 hours). To this colony, usually black in colour with a transparent outline, the urea- Hajna test was applied. Salmonellae were urea-, glucose +, H2S +, gas +, lactose - and ONPG-. Once there is a match between its characteristics and the isolated colony, a biochemical characterization (API 20E) confirms the preliminary results.

The used technique for the detection of helminth eggs in WW is that of Bailenger (El Guamri and Belghyti, 2007)

The technique was modified by using a buffer at pH of 4.5, which allowed a concentration of all the usual species found in the WW. It is a two-phase method that is based on the difference in density between the parasites and annoying debris which sediment in an immiscible buffer, while the fat remains in an ethereal interphase solution.

Five-liter samples were taken from the outlet of the WWTP and stored by adding 10% formalin (2 mL L^{-1}) in sterile vials. In the laboratory, TWW samples were placed in 2-liter test tubes, then left

to settle for 12 hours. The obtained pellet was carefully transferred in one or more tubes. The test tube racks were rinsed with the Tween 80 solution and the rinsing product is added to the sediment previously collected. Thus, the obtained tubes were centrifuged at 10000 rpm for 15 min. After centrifugation, the supernatant is removed with a suction pump. To the pellet obtained, acetoacetic tampon and ether were added, after stirring for 5 minutes, microscopic observation allowed a qualitative and quantitative analysis of the helminth eggs.

The total number of helminth eggs per liter of TWW was calculated using the following formula

$$N = \frac{A \times X}{P \times V} \quad \text{(Eq.2)}$$

Where:

N is the number of eggs per liter of TWW;

A is the number of eggs counted on the cell (average of the numbers found in three cells);

X is the volume of final product (mL);

P is the capacity of the cell (mL);

V is the volume of the initial TWW sample to be analysed (5 letters).

5. Physicochemical analysis of the substrate

Substrate samples were collected after each three months and after the harvest from all pots. The samples were dried for one week at room temperature. 2 mm sieved substrates were chosen for further characterizations. For the pH and EC of the saturated paste measurements, substrate suspension was prepared with a ratio of substrate/water ratio 1/2.5 and 1/5 (W/V) respectively according to the protocol used by Belaid et al. (2012). The suspension was stirred for one hour and left 24h for decantation, the pH was then measured in the supernatant using a laboratory pH meter.

Organic matter was determined by the Walkey and Black modified method (Verma et al., 2013). The sample was oxidized with concentrated sulfuric acid in the presence of potassium dichromate. The quantity of excess $K_2Cr_2O_7$ was dosed back by a standard solution of Mohr's salt (ferrous sulphate) in the presence of redox indicator (ferroin).

Total nitrogen was analysed using the Kjeldahl method using Büchi B-315 apparatus. This method started with the mineralization of organic matter which was carried out using concentrated sulphuric acid in the presence of a catalyst (K_2SO_4 and $CuSO_4$). After mineralization the nitrogen transform into NH_4^+. A distillation step was necessary to transform the ammonium ions into ammonia. The latter was then collected in a boric acid solution in order to be trapped and then neutralized with a calibrated solution of strong acid (HCl or H_2SO_4) (Sáez-Plaza, et al., 2013).

Total phosphorus contained in the substrate can be measured after mineralization by sulfonitric acid attack of a sample in the presence of ammonium molybdate forming a complex phosphomolybdic anion, which after reaction with ascorbic acid ($C_6H_8O_6$, 99%) gives a blue colour. Optical density is measured at 880 nm. Chlorine was determined in saturated substrate paste extract using the Mohr's titration method. To assess heavy metals content, 1g of substrate was calcined at 500 ° C in a muffle furnace for two hours. The sample was taken up to 10 mL of 50% hydrofluoric acid and dried again in a Teflon beaker on a sand bath. The residue obtained was dissolved by adding 7.5 mL of hydrochloric acid and 2.5 mL of nitric acid. The beaker was covered with a watch glass and then dried on a hot plate until the redhead vapours, indicator of the complete mineralization, disappear. The solution obtained was then brought to a final volume of 10 mL with distilled water. Mineralization blanks was carried out jointly, the metals were then analysed by Flame Atomic Absorption Spectrometer (Belaid et al., 2012).

6. Determination of chlorophyll content

The chlorophyll a and b contents were determined according to the method of Lichtenthaler and Welburn (1983). The method consists of the extraction of chlorophylls from 100 mg of fresh leaves in 80% acetone. The extract was centrifuged then the recovered supernatant was adjusted to a volume of 2 ml with acetone (80%). The chlorophylls a, b and total chlorophyll contents were evaluated with a spectrophotometer (HACH DR 4000/U) at different wavelengths: 645 and 663 nm. The chlorophyll a and b contents are expressed in µg / g fresh weight as follows (Eq. 3, 4 and 5):

$$Chlorophyll\ a = (12.7 \times OD\ 663nm) - (2.6 \times OD\ 645nm) \times V / M \quad \text{(Eq.3)}$$

$$Chlorophyll\ b = (22.9 \times OD\ 663nm) - (4.68 \times OD\ 663nm) \times V / M \quad \text{(Eq.4)}$$

$$Total\ chlorophyll = chlorophyll\ a + chlorophyll\ b \quad \text{(Eq.5)}$$

Where:

V: volume of acetone added to the supernatant.

M: mass of the fresh leaves.

OD: Optical density.

7. Plants and fruits metal content

All plants and fruits samples were washed with distilled water and were dried at 60 ° C for one day then crushed and sieved at 500 µm on a nylon sieve. To determine the mineral contents (Mn, Zn, Cu, Cr and Ni), fruit and plant samples were calcinated in a muffle oven at 450°C. Ashes were then digested with 1M nitric acid and the suspension was filtrated using cellulose filter. Filtered samples

were then analysed using atomic absorption spectrometry.

8. Fruit dry matter, total soluble solids, and ascorbic acid content

Dry matter was determined by drying strawberry fruits until constant mass at 70°C in ventilated oven. Total soluble solids were measured using a refractometer and expressed in % of strawberry fresh weight. Ascorbic acid (AA) was determined using a refractometer (Merck, Darmstadt, Germany) with an AA test strip and expressed in mg of AA in 100 mg of fruit fresh weight.

9. Health risk assessment

Possible risks to public health by human intake of heavy metal contamination from fruits and vegetables was determined using the U.S. Environmental Protection Agency's Health Risk Handbook. Health risk assessment indices were given by the target hazard quotient (HQ) and the hazard index (HI) that measured for carcinogenic and non-carcinogenic heavy metals as described in equations (Eq. 6) and (Eq.7).

Hazard quotient can be identified as the proportion of the probable exposure to a chemical or element and level that does not presents any expectable negative risk. If the quotient is lower than 1, this implies no predictable risk resulting from the exposure to the mentioned element. However, when THS is higher than 1, hazardous health problems are expected (Bermudez et al., 2011).

Additive risks can be resulted from the display to many contaminants. Therefore, the hazard index (HI) presents the sum of the target hazard quotients that assesses generally the effects of two or more pollutants. Similar to the THQ, a HI higher than 1 demonstrates adverse health impacts from cons consumption contaminants from a foodstuff.

$$THQ = \frac{C_M \times D_{Fuit} \times E_F \times E_D}{B_w \times AT_n \times RfD} \quad \text{(Eq. 6)}$$

$$HI = \sum THQ \quad \text{(Eq. 7)}$$

Where C_M is the concentration of metal in the fruit (mg kg–1), D_{Fruit} is the daily consumption of fruit (0.057 kg d^{-1} $person^{-1}$), E_F represents the exposure frequency (365 d $year^{-1}$), E_D is the exposure duration (74.68 years) and B_w is the mean human body weight (60 kg). AT_n represents the average time of exposure to heavy metals (E_D× 365 days $year^{-1}$) (Qureshi et al., 2016, Chen et al 2021). The oral reference doses (RfD) are the daily oral allowed dose of heavy metals without inducing any harmful impacts throughout the lifespan (Akoto, et al., 2014). RfD of Cr, Mn, Zn, Cu and Ni are 1.5, 0.14, 0.3, 0.04 and 0.02 mg kg^{-1} d^{-1} respectively (Ferré-Huguet et al., 2008; Guadie et al., 2021).

10. Statistical analysis

The influence of irrigation with TWW on strawberry crops and soil was evaluated using a statistical assessment implying comparison of result's mean, and analysis of regression and correlation data by a software IBM SPSS Statisticas 20 and using Tukey's post hoc test.

II. Preparation of sewage sludge ash and its application in copper adsorption using quality by design approach

1. Wastewater sampling and analysis

Effluent WW and sludge were collected in the Sfax WWTP located in the northern area of the city of Sfax (Tunisia). The TWW was analysed for pH and Electrical conductivity (EC) determined according to the protocols of AFNOR (° NF T 90-008 and NF EN 27888) using a multi parameter probe model HI 9829 (HANNA, Woonsocket, RI, USA). Total suspended solids (TSS), chemical oxygen demand (COD) and five-days biological oxygen demand (BOD_5) were measured according to AFNOR protocols (NF T 90-018, NF EN 872, NF T 90-103, NF EN 1189), total phosphorus (P_{tot}), and ammonium (NH_4^+) were analysed according to the AFNOR methods (AFNOR, 1997). Nitrate (NO_3^-), sulphates (SO_4^{2-}), chloride (Cl^-), sodium (Na^+), potassium (K^+), magnesium (Mg_2^+), calcium (Ca^{2+}), bicarbonate (HCO_3^-), total copper (Cu^{2+}), iron (Fe^{2+}), Manganese (Mn^{2+}), Zinc (Zn^{2+}), cadmium (Cd^{2+}), chromium (Cr^{3+}), lead (Pb^{2+}) were analysed following the RODIER methods using Hitachi Z-6100 Polarized Zeeman Flame Atomic Absorption Spectrophotometer (Hitachi, Berks). Results of TWW characterization are illustrated in supplementary part (**Table S 2.1**)

2. Preparation of the ash sorbent

Ash was produced by incineration of dehydrated sludge collected in the aforementioned WWTP, according to the protocol described by Elouear et al. (2009). More in detail, the sludge was placed in a muffle furnace ventilated with normal atmosphere for two hours at 600 °C.

After production, the ash was sieved at 100 µm, washed with distilled water and dried overnight in oven at 105 °C.

3. Physicochemical characterization of the ash sorbent

3.1.Determination of the specific surface area

The specific surface was determined using an ASAP 2020 Accelerated Surface Area and Porosimetry System (Micromeritics, Norcross, GA, USA) from the nitrogen adsorption isotherm at

-196.15 °C, based on the theory of Brunauer, Emmett and Teller (BET) (Brunauer et al. 1938). Pore volumes and pore size distribution were evaluated by the Barrett, Joyner and Halenda method (BJH) (Barrett et al. 1951), from obtained isotherms of the complete adsorption/desorption cycle. In practical, 100 mg of ash were degassed at 200 °C for 2 hours under vacuum and then BET and BJH adsorption/ desorption nitrogen isotherms were performed.

3.2.Scanning electron microscopy (SEM)

In order to highlight the morphological aspect of the prepared sorbent a Philips XL30 environmental scanning electron microscope was used (Philips, Amsterdam, Netherland).

3.3. Metal contents

For the determination of metal contents in SSA, a known mass of the material was calcinated in muffle furnace for 2h at 550°C. After calcination, the crucible was placed in sand bath at 200°C and nitric acid was used to perform acid digestion. The solution was then filtered using 0.47µm filter and the filtrate was analysed using Hitachi Z-6100 Polarized Zeeman Flame Atomic Absorption Spectrophotometer (Hitachi, Berkshire, United Kingdom).

3.4. pH of point of zero charge

The pH point of zero charge (pH_{pcz}) was determined by adding a 0.1 g of SSA to a series of bottles containing 50 mL of NaCl (0.1 N), the pH of the solutions was then adjusted to be from 2 to 12 by the addition of HNO_3 0.1 M or NaOH 0.1 M. These samples were then stirred for 24 hours and the pH values were measured at the end of the test. The difference between the final and the initial pH of suspension (ΔpH) is represented as a function of the initial pH of the solutions.

3.5. Boehm titration

Boehm's method (Boehm, 1994) was used to determine and differentiate surface acid and basic groups of the adsorbents. The acid groups (carboxylic acids, lactones, phenols and carbonyls) and the basic groups were neutralized using NaOH and HCl solutions, respectively. $NaHCO_3$, Na_2CO_3, NaOH and HCl (0.1 N) solutions were prepared and 1 g of the ash was mixed with 50 ml of each solution. The mixture was shaken at room temperature for 72 hours then centrifuged at 3500 rpm for 6 minutes. A volume of 10 mL of each supernatant was titrated with a 0.1N HCl and NaOH (0.1 N) in order to determine the remaining base and acid, respectively. For the calculations, it was considered that NaOH neutralizes all the acid groups of the adsorbent (carboxylic, lactonic and phenolic), Na_2CO_3 neutralizes carboxylic and lactonic groups, $NaHCO_3$ neutralizes only the carboxylic groups, and HCl neutralizes all of the basic surface groups. From the titration curves (pH as a function of the volume of the titrating solution), the quantities of acid or basic functions were

calculated as milliequivalents per gram.

3.6. Fourier Transform InfraRed spectroscopy (FTIR)

The surface functional organic groups and structure were determined by a spectrometer Fourier transform infrared (FTIR) spectrometer Shimadzu IR 470s (Shimadzu, Kyoto, Japan) using potassium bromide pellet method. FTIR spectra were recorded between 400 and 4000 cm^{-1}.

4. Adsorption isotherm

In order to perform the adsorption isotherm, TWW from the Sfax WWTP was fortified using a synthetic stock solution of copper prepared from copper sulphate pentahydrate ($Cu\ SO_4.\ 5H_2O$). The stock solution was added in order to have following final concentrations of copper: 10, 20, 30, 40, and 50 mg/L. The pH of the solutions was adjusted to the desired value by adding nitric acid (HNO_3) or sodium hydroxide (NaOH). Aliquots (100 mg) of ash sorbent and TWW (100 mL) spiked at different copper concentrations were then mixed and stirred for 2 hours at 15, 25 and 40°C in order to study the effect of temperature on the adsorption of copper ions. Samples were then filtered using a 0.47µm filter and analysed by atomic absorption spectrometer (HITACHI Z-6100). The Langmuir and Freundlich isotherms were used for fitting the results obtained for each temperature.

5. Response surface methodology and the design of experiments

To study the influence of different variables on copper removal using SSA, a BOX-BEHNKEN Design was established by considering the adsorption capacity (Q_e) of copper ions present in model solutions as response variable. The considered variables are: contact time (X_1), pH of the reaction medium (X_2), mass of the adsorbent (X_3) and concentration of the solution in copper ions (X_4). The fundamental level and the factors variation interval are presented in **Table 2.1**. In order to assess the significance of the studied operational variables, a statistical analysis of the experimental data was carried out by the analysis of variation (ANOVA).

Table 2. Experimental region.

	Factor	Unit	Center	variable step
U1	Time	min	60	30
U2	pH		4	1
U3	Adsorbent mass	g	1.1	1
U4	Copper concentration	mg/g	30	20

Twenty-four experiments corresponding to all possible combinations of variable factors plus four experiments at the center point and five test experiments were adopted to constitute the best

experimental conditions from the considered variables. The mathematical polynomial model that translates the relationship between the studied variables is the response function in this case, the equation of the estimated model Y is there:

$$Y_1 = b_0 + \sum_{i=1}^{n} biXi + \sum_{i=1}^{n} bii\ Xi^2 + \sum_{i=1}^{n-1} \sum_{j=i+1}^{n} bij\ Xi\ Xi \quad \text{(Eq. 8)}$$

where b_0 is the model constant, b_i are the linear coefficients, b_{ii} are the quadratic coefficients, b_{ij} are the interaction coefficients and X_i and X_j are the experimental values of the aforementioned variables.

III. Physicochemical properties of sawdust and sewage-based biochars

Full details of the reagents, standards and materials used in this research, as well as preparation of stock solutions of target analytes, are reported in paragraph **S.3.1** of the Supplementary material, in which CAS numbers, structure formulas and log Kow values of the investigated AP_nEOs and APs are also shown (**Table S.3.1**).

1. Sawdust-based biochar production

Three biochars (BC450, BC650 and BC850) were produced via pyrolysis of sawdust, in a muffle furnace (Gefran 1001, Vittadini Strumentazione, Milano, Italy), at 450, 650 and 850° C, respectively, with a contact time of 60 min. The following yield percentages (mean ± standard deviation) were registered in the 15 pyrolysis processes performed for each temperature: BC450 – 23 ± 3; BC650 – 20.0 ± 0.7; BC850 – 18.1 ± 0.5. The temperature of 450 °C was chosen since it represents a minimum temperature value allowing the pyrolysis process to fully proceed on woody matrices. In fact, wood contains large amounts of lignin, the complete decomposition of which only occurs at around 500 °C (Ok et al., 2018). The highest temperature limit was selected as intermediate between the maximum values investigated in literature (i. e., 800–900 °C) (Li et al., 2017), whereas the value of 650 °C was equally spaced between 450 and 850 °C.

The muffle furnace was properly modified to allow the heating process in N_2-saturated conditions. The sawdust was obtained from a local sawmill and consisted of a mixture of waste biomass from broad-leaved and coniferous plants. The water content of sawdust and concentrations of selected toxic heavy metals are reported in **Table S3.2** of the Supplementary material. Metal analysis was performed by acidic-oxidant digestion (Doumett et al., 2011) followed by ICP-MS analysis, with the only exception of Cr (VI) which was determined according to Bruzzoniti et al. (Bruzzoniti et al., 2017). Full details of these analyses are reported in paragraph S.3.3 of the Supplementary material.

Virgin mineral activated carbon (MAC) was obtained from Arkema (Colombes, France). Virgin

vegetal activated carbon (VAC) was purchased from SICAV (Chieti, Italy).

All chars were pre-treated before being characterized and used in isotherm studies. More specifically, the materials were sieved at 45 mm and then repeatedly washed with Milli-Q water according to the ASTM D-5919–96 method (American Society for Testing and Material, 1996).

2. Sewage sludge-based biochars production

2.1.Pyrolysis materials

Two varieties of woody biomass (oak and poplar) were chosen according to their availability in the Tuscan region. Sludge used in the production of biochar were provided by two WWTPs in the cities of Calice and Vernio. Sludge and vegetal feedstock were dried at 105° C overnight before use.

2.2.Biochar production

Subsequently, 12 biochars were produced using biological sludge mixed with woody biomass waste (Oak or Poplar), as reported in the experimental plan described in **Table 3**. The "Quality by Design" approach made it possible producing a matrix consisting of 12 production experiments, each one characterized by appropriate values of the following parameters: type of vegetable waste (poplar, oak), origin of sludge (Calice and Vernio WWTPs), pyrolysis temperature (in the range 450-850 ° C), contact time (60-120 minutes) and percentage of sludge (0-30%) in the pyrolizer feed mixture (**Table 3**). The 12 biochars produced were named BC1-BC12.

Table 3. Biochars preparation conditions.

Simple	Type of Biomass	Sludge type	Sludge Percentage (%)	Pyrolysis temperature (°C)	Contact time (min)
BC1	Oak		0	450	120
BC2	Oak		0	650	60
BC3	Poplar		0	850	120
BC4	Poplar	CALICE	15	450	60
BC5	Oak	VERNIO	15	650	160
BC6	Poplar	VERNIO	15	850	60
BC7	Oak	VERNIO	30	450	60
BC8	Poplar	CALICE	30	650	120
BC9	Oak	CALICE	30	850	60
BC10	Poplar	VERNIO	0	850	120
BC11	Oak	CALICE	30	850	60
BC12	Poplar	CALICE	30	650	120

2.3. Acidic modification of biochar

The biochar was washed using an acid solution that is the waste product of a gasification process of vegetable biomass. Numerous preliminary tests were carried out to fix the washing conditions of these materials by varying the weight/ volume ratio between the biochar and washing solution, as

well as their contact time. The optimized conditions foresee a biochar / washing solution ratio 1/10 (W/ V) (g/mL) and a contact time of 30 minutes. After acidic washing, the materials were centrifugated and finally washed with deionized water until reaching a pH value similar to that of the deionized water.

2.4. Biochar activation

The activation of BC8 and BC11 (biochars contained 30% of SS) was carried out in a furnace (BIO class, Italy) under nitrogen flow at 650°C during two hours. After carbonation, biochars were washed using milli Q water and then dried at 105°C overnight. The two activated biochars were named ABC8 and ABC11. In brief, the overall process of activated biochars production included three major operations: pre-treatment carbonation, acidic washing using gasification WW, carbonation under N_2 atmosphere.

3. Chars' physicochemical characterization

3.1. Elemental analysis

The analyses of C, H, N and S were performed using a FlashEA 1112 elemental analyser Thermo Fisher Scientific (Waltham, MA) equipped with a thermal conductivity detector. Aliquots of about 2 mg of finely grinded samples, dried at 120 °C for 24 hours, were analysed in triplicate using a FlashEA® 1112 elemental analyser Thermo Fisher Scientific (Waltham, MA) equipped with a thermal conductivity detector. The percentage content of oxygen was determined by difference as follows: O (%) = 100 – (C% + H% + N% + S% + ash%) (Al-Wabel et al., 2013).

O/C vs H/C ratios were also determined.

3.2. Physisorption analyses

Physisorption analysis of biochars, and of commercial vegetal and mineral activated carbons (VAC and MAC) was performed via nitrogen adsorption and desorption experiments using a Porosity Analyser Micrometrics (Norcross, GA, USA) model ASAP 2020 (American Society for Testing and Materials, 2012, 2017). More in details, the textural properties of the biochars obtained at 450 °C (BC450), 650 °C (BC650) and 850 °C (BC850), MAC and VAC were determined by nitrogen adsorption and desorption experiments at -196°C. The surface area was calculated by using the Brunauer-Emmet-Teller (BET) and the Langmuir methods applied to nitrogen adsorption data in the relative pressure (P/P°) range of 0.06-0.40. The total pore volume was determined from the amount of nitrogen adsorbed at P/P°=0.98. The mesopore size distribution was determined by the Barret-Joyner-Halenda (BJH) model applied to desorption data and the assessment of microporosity was carried out by the t-plot method.

3.3. Porosity indexes

The analyses of the porosity indexes were performed following the official methods for activated carbons and regarded the determination of iodine (American Society for Testing and Materials, 1994), phenol (American Water Works Association, 1978) and methylene blue indexes (European Council of Chemical Manufacturers' Federation, 1986).

3.4. pH of the point of zero charge

The pH of the point of zero charge (pH_{pzc}) of biochars and MAC was determined using the pH drift method, which is a simple and widely used procedure, adopted for the evaluation of surface charge of both biochars (Chaukura et al., 2017) and activated carbons (Niasar et al., 2016). Stock solutions of 0.1 M NaCl were prepared at pH 2, 3, 4, 5, 6, 7, 8, 9, 10, and 11 (pH_i) by adding 1 M NaOH or 1 M HCl. Aliquots of 50 mL of these solutions were then transferred to a series of volumetric flasks and 0.1 g of each sorbent was added. The flasks were sealed and the suspensions orbital shaken at 150 rpm for 32 h before the final pH value (pH_f) of the supernatant was recorded. The difference between pH_i and pH_f (ΔpH) was plotted as a function of pH_i, and the point of the intersection of the resulting curve with pH_i axis was pH_{pzc}.

3.5. X-ray photoelectron spectroscopy (XPS) analysis

The chemical composition of the near surface sample portions of BCs and ACs were investigated by means of X-ray Photoelectron Spectroscopy (XPS) experiments carried out in an ultrahigh vacuum (UHV, 10^{-9} mbar) system equipped with a VSW HAC 500 hemispherical electron-energy analyser using a non-monochromatic Mg K-alpha X-ray source operating at 120 W power (10 kVx10 mA). The samples were fixed to the sample holder by means of a conductive carbon tape and introduced in the UHV under an inert gas (N_2) flux. Survey and high-resolution spectra were acquired in the constant analyser energy mode (CAE) at pass energy of 22 eV with a step size of 1.0 and 0.1 eV, respectively. The peaks were fitted using CasaXPS software employing Gauss-Lorentz curves after subtraction of a Shirley-type background. Experimental XPS peak areas were normalized using proper sensitivity factors (Moulder et al., 1992) in order to calculate the relative element percentages.

3.6. Fourier-transform infrared analysis

Fourier-transform infrared (FTIR) analyses were performed on a Shimadzu IRAffinity-1 Spectrometer equipped with a single reflection diamond ATR crystal on Zn Se plate (MIRacleTM Single Reflection ATR, PIKE Technologies). Samples were dried beforehand in a muffle furnace at 120 C for 24 h.

3.7. Ash content

Ash content was determined according to the EN 12902:2004 Official Method (European Committee for Standardization, 2004), which is adopted for the analysis of activated carbons.

3.8. Water-extractable substances

The following water extractable elements were determined: As, Cd, Cr, Hg, Ni, Pb, Sb, Se, Al, Ba, B, Ca, Fe, Mg, Mn, K, Cu, Na, Va and Zn. Moreover, the 16 PAHs included in the EPA mixture were analysed. The extraction of the aforementioned inorganic and organic species was performed according to the EN 12902:2004 standard method (European Committee for Standardization, 2004). 10 grams of char are put in contact with 1 L of extraction water and the solution is shaken for 24 hours at 25°C. Extraction water was a $NaHCO_3$ 0.5 mM, $CaCl_2$ 0.3 mM and $MgSO_4$ 0.2 mM aqueous solution (pH=7.5±0.2); Afterwards, the obtained suspension was filtered on 0.4 µm polycarbonate membranes (Sigma-Aldrich, St. Louis, MO, USA) and divided in two aliquots for metal and PAH analysis.

a. Analysis of water extractable metals

The analysis of the water-extractable metals was carried out by CP-MS, based on to the USEPA SW-846 test method 6020B (USEPA, 2014). The filtered water sample (100 mL aliquots) was treated with 1 mL of concentrated nitric acid, spiked with 1% Au 1000 mg L^{-1} solution and directly analysed by an ICP-MS model 7700X (Agilent Technologies, Santa Clara, CA, U.S.A.).

b. Analysis of water extractable PAHs

PAHs were determined by SPE extraction and GC–MS analysis as described in paragraph S.3. 4. PAHs were analysed according to the following internal method: 2.0 L of filtered solution were spiked with 5 mL of methanol, stirred and then loaded on a C18-SPE cartridge previously conditioned with (i) 4 mL of isopropyl alcohol, (ii) 4 mL of a 15/85 (*v/v*) isopropyl alcohol/water mixture and (iii) 25 mL of methanol. Afterward, the cartridge was dried under vacuum and the elution of the selected compounds was carried out with 6 mL of dichloromethane. The recovered solution was concentrated under a gentle nitrogen stream to 50 µL and analysed by a Shimadzu (Kyoto, Japan) gas chromatograph model GC2010 equipped with an AOC-20i auto-injector (Shimadzu) and an AOC-20s auto-sampler (Shimadzu) and coupled with a QP2010 Plus mass spectrometer (Shimadzu). The GC column employed was an SLB®-5ms fused silica capillary (10 m × 0.10 mm, 0.10 µm particle size) from Supelco.

The GC analysis was performed according to the following conditions: (i) 1 µL of sample was injected in splitless mode, (ii) injector temperature: 320°C, (iii) column flow: 1.2 mL min^{-1} and (iv)

constant linear velocity: 69.2 cm s^{-1}.

Temperature programme: 60 °C initial temperature for 2 min, from 60°C to 160 °C in 2.2 min, from 160°C to 200°C in 2.0 min, from 200°C to 210°C in 3.3 min, from 210°C to 225° C in 15.0 min. from 255°C to 244°C in 6.3 min, from 240°C to 320°C in 1.9 min, final isotherm for 1.0 min. MS conditions: ion source temperature: 230°C; interface temperature: 280°C; detector voltage: 0.5 kV; analysis mode: single ion monitoring (SIM), see **Table 3.4** for the complete list of the selected ions. Instrumental control and data processing were carried out by the GCMS Solution software, version 2.50 (Shimadzu). Figures of merit and apparent recovery of the method are shown in **Tables S 3.4** – **S 3.6** and **Figure S 3.1**.

4. Sorption properties of sawdust-based biochars and commercial activated carbon towards ethoxylated alkylphenols and their phenolic metabolites in treated wastewater from a textile district

4.1. Characteristics of the effluent wastewater

Kinetic and isotherm sorption studies were performed in a real effluent WW obtained from the Baciacavallo WWTP operating in the industrial textile district of Prato (Italy). The WWTP consisted in a primary sedimentation, biological oxidation, secondary sedimentation, clariflocculation and final ozonation treatment. The effluent WW was sampled in August 2018, during the summer closure of the industrial textile district in order to minimize the concentration of target analytes in the TWW (Berardi et al., 2019). The characterization of the effluent WWfor a number of routinely analysed parameters, as well as target analytes was determined.

4.2. Performance evaluation of chars as adsorbent materials

The evaluation of biochar and activated carbon adsorption performance towards APnEOs and APs was carried out by kinetic and isotherm tests, performed in triplicate. In line with the ASTM D-5919–96 (American Society for Testing and Material, 1996), suspensions (1 g L^{-1}) of each adsorbent material were prepared, stirred for 24 h and used to make solutions of biochar (10 mg L^{-1}) and MAC (1 mg L^{-1}) with proper APnEO and AP concentrations.

kinetic and isotherm adsorption tests were performed by maintaining in rotation (Reax 20, Heidolph Instruments, Schwabach, Germany) the bottles under the following experimental conditions: (i) 6 revolutions/minute; (ii) absence of light; (iii) room temperature (25±2°C). The suspensions were finally centrifuged at 30000 x g, for 10 minutes, at 10°C (MPW-351R, MPW Med. Instruments, Warsaw, Poland). A control sample without the sorbent was run in parallel.

Supernatant 1-mL aliquots were stored at +4°C until LC-MS/MS analysis was performed (in any

case not later than 24 h after the last collection), according to the following specifications and in accordance with the identification criteria proposed by the Commission Decision 2002/657/CE.

LC-MS/MS analysis of APnEOs and APs at the end of the tests was performed following the identification criteria proposed by the Commission Decision 2002/657/EC (The Commission of the European Communities, 2002), according to a method optimized specifically for this study.
Full details of LC-MS/MS method are provided in paragraph **S.3.5** and **Tables S 3.7** – **S 3.9** of the Supplementary material.

a. Kinetic adsorption tests

Kinetic adsorption tests of target compounds on biochars and MAC were performed using solutions of APs (40 mg L^{-1}), TritonTMX-45 and IGEPAL CO-520 technical mixtures (400 mg L^{-1}) in the aforementioned real effluent WW. These experiments were carried out by maintaining the test bottles in rotation at 20 °C with contact times of 1, 2, 4, 6, and 12 h.

b. Isotherm adsorption tests

Isotherm experiments were conducted using eleven different concentration levels of APnEO technical mixtures (i.e., 0, 5, 10, 25, 50, 75, 100, 150, 200, 300, and 400 mg L^{-1}) and APs (i.e., 0, 0.5, 1.0, 2.5, 5.0, 7.5, 10, 15, 20, 30, and 40 mg L^{-1}) in the aforementioned real effluent WW, keeping the concentration of the adsorbent materials constant. These experiments were carried out by maintaining the test bottles in rotation for 4 h at T = 20° C, in accordance with results of the kinetic tests.
Adsorption data were fitted by using both Langmuir and Freundlich equations. More specifically, the following Langmuir adsorption-isotherm equation (Eq. 9) was adopted:

$$Q_e = \frac{Q_m * k * C_e}{1 + (k * C_e)} \qquad \text{(Eq. 9)}$$

where C_e is the equilibrium adsorbate concentration (mg L^{-1}), Q_e the mass of adsorbate per mass unit of adsorbent at equilibrium (mg g^{-1}), Q_m the maximum mass adsorbed at saturation conditions per mass unit of adsorbent (mg g^{-1}) and k (L mg^{-1}) the empirical constant with units of inverse of concentration C_e. The linear form of the above-mentioned equation is reported in the Equation 10.

$$\frac{C_e}{Q_e} = \frac{1}{Q_m \cdot k} + \frac{1}{Q_m} \cdot C_e \qquad \text{(Eq.10)}$$

which represents a straight line with slope Q_m^{-1} and intercept (Q_m k^{-1}) (Del Bubba et al., 2003). Accordingly, linearized Langmuir adsorption-isotherm equation allows for estimating both the Q_m

and k, the latter representing the inverse of the equilibrium concentration of the adsorbate at half saturation and thereby giving a measure of the affinity of the compound for the material.

The Freundlich isotherm model can be written as following (Eq.11):

$$logQ_e = logK_F + \frac{1}{n} \cdot logC_e \quad \text{(Eq. 11)}$$

where Q_e and C_e have the same aforementioned meaning, whereas K_F and n are the Freundlich constants related to adsorption capacity and intensity, respectively (Sun et al., 2013).

c. Data treatment and computational analysis

The multiple comparison of the mean values of the sorption parameters was performed using the non-parametric Games-Howell test (Minitab®17.1.0, Minitab Inc., State College, PA, USA), which makes it possible to compare mean values and corresponding standard deviations without assuming equal variances of the measured variables. Molecular width of target analytes was calculated after energy minimization by Chem3D version 12.0.2.1076 (PerkinElmer Informatics, Waltham, MA, USA).

5. Adsorption study of methylene blue using sewage sludge-based biochars

5.1. Kinetic adsorption study

A stock solution of 1g/L of methylene blue (MB) was prepared. The stock solution was then diluted using MiliQ-water in order to produce concentrations of 25, 50, 75 and 100 mg/l of methylene blue solution. A fixed amount of biochar was added to the initial concentrations and stirred at room temperatures for 5, 10, 20, 30, 60, 180 and 240 min. Afterwards, the mixture was centrifuged at 3600 rpm for 6 min then the supernatant was collected and passed through 0.45 µm Sartorius Minisart SRP 25 syringe filters before to be analysed using UV-spectrophotometer HACH DR/4000 U. The quantity of MB adsorbed by the biochar at each time (qe) was determined using the following equation (Eq. 12):

$$q_e = (C_i - C_e) \cdot V / m \quad \text{(Eq.12)}$$

where:

Ce and Ci are equilibrium and initial concentrations of MB (ppm),

V is the volume of MB solution (L),

m is the weight of biochar (g).

The evaluation of the efficiency and mechanism of MB adsorption process can be carried out by adsorption kinetics study that give information concerning the chemical or physical interactions between biochar and adsorbate. Pseudo-first order, pseudo-second order and intra-particle diffusion

models were separately used to describe the mechanism of MB removal by biochar and to study the kinetic process.

The equations of these models are (Eq.13), (Eq.14) and (Eq.15):

$$Q_t = \frac{K_2 * {Q_e}^2 * t}{1 + K_2 * Q_e * t} \quad \text{(Eq.13)}$$

$$Q_t = Q_e * (1 - e^{-K_1 * t}) \quad \text{(Eq.14)}$$

$$Q_t = Q_i * t^{\frac{1}{2}} + C \quad \text{(Eq.15)}$$

Where:

Q_t is the adsorption capacity (mg/g) at a given time (t),

Q_e is the adsorption capacity at the equilibrium concentration (mg/g),

K_1 is the pseudo-first order rate constant (min^{-1}),

K_2 is the pseudo-second order rate constant (min^{-1}),

k_i is the intraparticle diffusion rate constant ($mg.\ g^{-1}\ min^{-1}$),

C is a constant.

5.2. Isotherm adsorption study

Isotherm study was determined by suspended 100 mg of biochar in 25 mL of MB at various concentrations; 25, 50, 75 and 100 mg L-1 and shaking for 180 min. Then, the filtrate was analysed with UV spectrophotometer HACH DR/4000 U at 660 cm-1.

Adsorption data were fitted using the Langmuir and Freundlich isotherm models to analyse the sorption process of MB solution onto biochars 8, 11 and activated carbon.

6. Column study

TWW used in the column study was provided from Baciacavallo WWTP treats industrial (textile) WW in Prato (Italy). A MB removal test was performed from a sample of wastewater treated by primary sedimentation, biological oxidation, secondary sedimentation and clariflocculation, fortified with sufficient dye to be achieved. The test was performed by passing the TWW through a column filled with 35 g of activated biochar 11 (ABC11) at an average flow of 180 mL per hour. A series of 5 columns and 5 in-line filter units (0.45 μm) were used. Each column was supplied with water to be treated using a multichannel peristaltic pump. Each column has an internal diameter of 21 mm and a total height of 15 cm. Glass wool was placed on the surface of the bed to prevent its disturbance during the continuous introduction of the dye solution. For each adsorption test, a series of fractions of solution leaving the column (effluent) were collected and the methylene blue

concentration was determined by UV–vis spectrophotometer HACH DR/4000 U.

7. Biochar regeneration

The exhausted biochar was regenerated using a thermal desorption. After column study, the biochar was dried in the oven at 105°C during 2h, then pyrolyzed for 2h in the muffle furnace under nitrogen flow at 650°C. After cooling in a desiccator, the specific surface area and pores volumes and size were determined using Micromeritics Instrument SORPTOMATIC 1990. This process was carried out to determine the reusability and regeneration of the exhausted activated biochar.

IV. Bibliography

AFNOR, 1997. Recueil de normes françaises: eau, méthodes d'essai, 2ème edition. Paris.

Akoto, O., Bismark Eshun, E.F., Darko, G., Adei, E., 2014. Concentrations and health risk assessments of heavy metals in fish from the Fosu Lagoon. Int. J. Environ. Res. 8, 403–410.

Al-Wabel, M. I., Al-Omran, A., El-Naggar, A. H., Nadeem, M., Usman, A. R. A., 2013. Pyrolysis temperature induced changes in characteristics and chemical composition of biochar produced from conocarpus wastes. Bioresour. Technol. 131, 374–379.

American Society for Testing and Materials. Standard Practice for Calculation of Pore Size Distributions of Catalysts and Catalyst Carriers from Nitrogen Desorption Isotherms (ASTM-D4641-17). West Conshohocken, PA: ASTM International, 2017.

American Society for Testing and Materials. Standard Test Method for Carbon Black—Total and External Surface Area by Nitrogen Adsorption (ASTM-D6556-10). West Conshohocken, PA: ASTM International, 2012.

American Society for Testing and Material. Standard Practice for Determination of Adsorptive Capacity of Activated Carbon by a Micro-Isotherm Technique for Adsorbates at ppb Concentrations (ASTM D5919-96). ASTM International, West Conshohocken, PA, 1996.

American Society for Testing and Materials. Standard Test Method for Determination of Iodine Number of Activated Carbon (ASTM-D4607-94). West Conshohocken, PA: ASTM International, 1994.

American Water Works Association. B600-78, Standard for Powdered Activated Carbon. AWWA, 1978.

Barrett, E. P., Joyner, L. G., Halenda, P. P., 1951. The determination of pore volume and area distributions in porous substances. I. Computations from nitrogen isotherms. J. Am. Chem. Soc. 73, 373-380.

Belaid, N., Neel, C., Lenain, J.F., Buzier, R., Kallel, M., Ayoub, T., Ayadi, A., Baudu, M., 2012. Assessment of metal accumulation in calcareous soil and forage crops subjected to long-term irrigation using treated wastewater: case of El Hajeb-Sfax. Tunisia. Agric. Ecosyst. Environ. 158, 83–93.

Belaid, N., Neel, C., Kallel, M., Ayoub, T., Ayadi, A., Baudu, M., 2010. Effects of treated wastewater irrigation on soil salinity and sodicity in Sfax (Tunisia): a case study. Revue des sciences de l'eau/ Water Sci. 23, 133-146.

Benmoussa, H., Ghrab, M., Mimoun, M. B., Luedeling, E., 2017. Chilling and heat requirements for local and foreign almond (Prunus dulcis Mill.) cultivars in a warm Mediterranean location based on 30 years of phenology records. Agric For Meteorol. 239, 34-46.

Berardi, C., Fibbi, D., Coppini, E., Renai, L., Caprini, C., Scordo, C. V. A., Checchini, L., Orlandini, S., Bruzzoniti, M. C., Del Bubba, M., 2019. Removal efficiency and mass balance of polycyclic aromatic hydrocarbons, phthalates, ethoxylated alkylphenols and alkylphenols in a mixed textile-domestic wastewater treatment plant. Sci. Total Environ. 674, 36-48.

Bermudez, G. M., Jasan, R., Pla, R., Pignata, M.L., 2011. Heavy metal and trace element concentrations in wheat grains: assessment of potential non-carcinogenic health hazard through their consumption. J. Hazard. Mater. 193, 264–271.

Boehm, H. P., 1994. Some aspects of the surface chemistry of carbon blacks and other carbons. Carbon. 32, 759-769.

Bouraoui, C., Ben Nejma, F., 2020. Numerical study of the greenhouse solar drying of olive mill wastewater under different conditions. Adv. Mech. Eng. 12, 1687814019889748.

Brunauer, S., Emmett, P. H., Teller, E., 1938. Adsorption of gases in multimolecular layers. J. Am. Chem. Soc. 60, 309-319.

Bruzzoniti, M. C., Abollino, O., Pazzi, M., Rivoira, L., Giacomino, A., Vincenti, M., 2017. Chromium, nickel, and cobalt in cosmetic matrices: an integrated bioanalytical characterization through total content, bioaccessibility, and Cr (III)/Cr (VI) speciation. Anal. Bioanal. Chem. 409, 6831-6841.

Chaukura, N., Murimba, E. C., Gwenzi, W., 2017. Sorptive removal of methylene blue from simulated wastewater using biochars derived from pulp and paper sludge. Environ. Technol. Innov. 8, 132-140.

Chen, Z., Muhammad, I., Zhang, Y., Hu, W., Lu, Q., Wang, W., Huang, B., Hao, M., 2021. Transfer of heavy metals in fruits and vegetables grown in greenhouse cultivation systems and their health risks in Northwest China. Sci. Total Environ. 766, 142663.

Del Bubba, M., Arias, C.A., Brix, H., 2003. Phosphorus adsorption maximum of sands for use as media in subsurface flow constructed reed beds as measured by the Langmuir isotherm. Water Res. 37, 3390-3400.

Doumett, S., Fibbi, D., Azzarello, E., Mancuso, S., Mugnai, S., Petruzzelli, G., Del Bubba, M., 2011. Influence of the application renewal of glutamate and tartrate on Cd, Cu, Pb and Zn distribution between contaminated soil and paulownia tomentosa in a pilot-scale assisted phytoremediation study. Int. J. Phytoremediation. 13, 1-17.

El Guamri, Y., Belghyti, D., 2007. Charge parasitaire des eaux usées brutes de la ville de Kénitra (Maroc). Afr. Sci. Rev. Int. Sci. Technol. 3(1).

Elouear, Z., Bouzid, J., Boujelben, N., 2009. Removal of nickel and cadmium from aqueous solutions by sewage sludge ash: study in single and binary systems. Environ. Technol. 30, 561-570.

Elloumi, O., Ghrab, M., Chatti, A., Chaari, A., Mimoun, M. B., 2020. Phenological performance of olive tree in a warm production area of central Tunisia. Sci. Hortic. 259, 108759.

European Committee for Standardization. EN 12902:2004, Products Used for Treatment of Water Intended for Human Consumption - Inorganic Supporting and Filtering Materials - Methods of Test, 2004.

European Council of Chemical Manufacturers' Federation. Test Method for Activated Carbon, 1986.

Ferré-Huguet, N., Martí-Cid, R., Schuhmacher, M., Domingo, J. L., 2008. Risk assessment of metals from consuming vegetables, fruits and rice grown on soils irrigated with waters of the Ebro River in Catalonia. Spain. Biol. Trace Elem. Res. 123, 66–79.

Ghrab, M., Mimoun, M. B., Masmoudi, M. M., Mechlia, N. B., 2014. Chilling trends in a warm production area and their impact on flowering and fruiting of peach trees. Sci. Hortic. 178, 87-94.

Guadie, A., Yesigat, A., Gatew, S., Worku, A., Liu, W., Ajibade, F.O., Wang, A., 2021. Evaluating the health risks of heavy metals from vegetables grown on soil irrigated with untreated and treated

wastewater in Arba Minch. Ethiopia. Sci. Total Environ. 761, 143302.

Li, H., Dong, X., da Silva, E. B., de Oliveira, L. M., Chen, Y., Ma, L. Q., 2017.Mechanisms of metal sorption by biochars: biochar characteristics and modifications. Chemosphere. 178, 466-478.

Lichtenthaler, H. K., Wellburn, A. R., 1983. Determinations of total carotenoids and chlorophylls a and b of leaf extracts in different solvents. Biochem. Soc. Trans. 11, 591–592.

Moulder, J. F., Stickle, W. F., Sobol, P. E., Bomben, K. D. Handbook of X-ray photoelectron spectroscopy. Eden Prairie, Minnesota, USA: Perkin-Elmer Corporation, 1992.

Niasar, H. S., Li, H., Kasanneni, T. V. R., Ray, M. B., Xu, C., 2016. Surface amination of activated carbon and petroleum coke for the removal of naphthenic acids and treatment of oil sands processaffected water (OSPW). Chem. Eng. Sci. 293, 189-199.

Ok, Y. S., Tsang, D. C., Bolan, N., Novak, J. M., 2018. Biochar from Biomass and Waste: Fundamentals and Applications. Elsevier.

Qureshi, A. S., Hussain, M. I., Ismail, S., Khan, Q. M., 2016. Evaluating heavy metal accumulation and potential health risks in vegetables irrigated with treated wastewater. Chemosphere. 163, 54–61.

Rodier, J., Bazin, C., Broutin, J. P., Chambon, P., Champsaur, H., Rodi, L., 2009. Water Analysis, 9th ed. Dunod, Paris, France, 1579.

Rouina, B. B., Trigui, A., d'Andria, R., Boukhris, M., Chaieb, M., 2007. Effects of water stress and soil type on photosynthesis, leaf water potential and yield of olive trees (Olea europaea L. cv. Chemlali Sfax). Aust. J. Exp. Agric. 47, 1484-1490.

Sáez-Plaza, P., Navas, M. J., Wybraniec, S., Michałowski, T., Asuero, A. G., 2013. An overview of the Kjeldahl method of nitrogen determination. Part II. Sample preparation, working scale, instrumental finish, and quality control. Crit. Rev. Anal. Chem. 43, 224-272.

Sun, L., Wan, S., Luo, W., 2013. Biochars prepared from anaerobic digestion residue, palm bark, and eucalyptus for adsorption of cationic methylene blue dye: characterization, equilibrium, and kinetic studies. Bioresour. Technol. 140: 406-413.

The Commission of the European Communities. Implementing Council Directive 96/23/EC concerning the performance of analyticalmethods and the interpretation of results. Off J Eur Commun., 2002.

USEPA. SW-846 Test Method 6020B: inductively coupled plasma - mass spectrometry, part of test

methods for evaluating solid waste, physical/chemical methods, Washington, D.C., 2014.

Verma, B. C., Datta, S. P., Rattan, R. K., Singh, A. K., 2013. Labile and stabilized fractions of soil organic carbon in some intensively cultivated alluvial soils. J. Environ. Biol. 34, 1069.

Results and discussion

Part 1

Assessment of the impacts of irrigation with municipal treated wastewater on soil, olive and strawberry chemical characteristics

I. Effects of irrigation with treated wastewater at different dilutions on growth, quality parameters and contamination transfer in strawberry (Fragaria x ananassa cv Camarosa) fruits and soil: health risk assessment

1. Characteristics of the irrigation waters

Physio-chemical characteristics of the used TWW are presented in **Table 1.1** The TWW is characterized with a neutral pH (pH=7.84). In term of electrical conductivity, **Table 1.1** shows a value of 5 mS/cm which is considered high for an effluent. Yet, this value remains below the Tunisian law (NT 106.03) related to the reuse of TWW in agriculture. The TWW used in the current study was characterized with concentration of COD and BOD_5 equal to 106.9 and 37 mg of O_2/L, respectively. These values are above the values dictated by the Tunisian law (NT 106.03) related to the reuse of TWW in agriculture which are 90 and 30 mg of O_2/L, respectively for COD and BOD_5.

Table 1.1. Average physicochemical characteristics of groundwater (GW) diluted TWW, D60, D40 and D20 used for strawberry irrigation.

	GW	TWW	D20	D40	D60	NT 106.03
pH	7.1 ± 0.2	7.8 ± 0.3	7.6 ± 0.4	7.5 ± 0.4	7.4 ± 0.4	6.5-8.5
EC (mS/cm)	0.5 ± 0.2	5.2 ± 0.4	4.6 ± 0.4	3.4 ± 0.4	2.7 ± 0.2	7
TSS (mg/L)	2.2 ± 0.2	30 ± 2	25 ± 1	18.8 ± 0.8	12 ±1	30
HCO3 (mg/L)	104 ± 2	283 ± 3	232 ± 3	176 ± 2	118 ± 3	-
COD (mg/L)	0	107 ± 3	89 ± 2	65 ± 3	44 ± 3	90
BOD5 (mg/L	0	37 ± 3	30 ± 3	22 ± 1	15 ± 2	30
Pt (mg/L)	0.6 ± 0.2	15.4 ± 0.8	13 ± 1	9.6 ± 0.4	6.4 ± 0.7	-
NTK (mg/L)	1.8 ± 0.4	56 ± 2	46 ± 2	35 ± 2	23 ± 3	-
Cl^- (mg/L)	257 ±19	1780 ± 56	1435 ± 31	1002 ± 11	742 ± 11	-
K (mg/L)	5 ± 0.9	30 ± 2	25 ± 2	19 ± 2	13 ± 2	-
Mg (mg/L)	28 ± 1	81 ± 3	68 ± 3	51 ± 3	34 ± 3	-
Na (mg/L)	32 ± 2	204 ± 2	170 ± 2	127 ± 2	85 ± 2	-
Ca (mg/L)	69 ± 2	107.2 ± 0.8	89 ± 1	67 ± 1.4	45 ± 2	-
SAR (m_{eq}/L)	n.d.	3 ± 0.1	2.5 ± 0.2	1.9 ± 0.2	1.3 ± 0.1	-
Mn (mg/L)	n.d.	3.4 ± 0.2	2.7 ± 0.1	2.1 ± 0.1	1.4 ± 0.2	0.5
Zn (mg/L)	n.d.	2.6 ± 0.3	2.1 ± 0.2	1.6 ± 0.2	1 ± 0.2	5
Cr (mg/L)	n.d.	14 ± 2	11.5 ± 0.5	8.6 ± 0.4	5.8 ± 0.4	0.1
Cu (mg/L)	n.d.	4.6 ± 0.1	3.7 ± 0.2	2.8 ± 0.1	1.9 ± 0.1	0.5
Ni (mg/L)	n.d.	0.17 ± 0.06	0.14 ± 0.05	0.10 ± 0.01	0.07 ± 0.01	0.2
Faecal coliform	n.d	n.d	n.d	n.d	n.d	-
Total coliform	n.d	n.d	n.d	n.d	n.d	-
Streptococcus	n.d	n.d	n.d	n.d	n.d	-
E. coli	n.d	n.d	n.d	n.d	n.d	-

n.d.= not detected

According to **Table 1.1**, potassium, total phosphate, and nitrogen which are essential for the growth of strawberry are present in sufficient concentration. In term of heavy metals, TWW demonstrate in the cases of Mn (3.4 mg/L), Cr (14.3 mg/L), and Cu (4.6 mg/L) values above those dictated by the Tunisian law (NT 106.03) related to the reuse of TWW in agriculture which are 0.5, 0.1 and 0.5 mg/L, respectively for Mn, Cr, and Cu. The dilution decreased significantly the amount of these elements with the increase in the dilution factor. **Table 1.1** shows also that concentrations of certain parameters such as COD and BOD decreased after the dilution to match Tunisian Law (NT 106.03). On the microbiological level, analysis on GW as well as TWW demonstrated the total absence of FC, TC as well as *E. coli*.

2. Substrate analysis

In **Table 1.2**, the physicochemical characteristics of the substrate at the initial status is demonstrated. The substrate used in this study was made my mixing sandy soil and peat (1/3; 2/3). In **Table 2.2** shows that the substrate is characterized with a neutral pH (pH=7.1), low conductivity (0.7 mS/cm) and TOC (28%).

Table 1.2. Main physicochemical characteristics of the used substrate for strawberry cultivation in pots.

Parameter	Substrate
pH	7.1 ± 0.4
EC (mS/cm)	0.7 ± 0.1
TOC (%)	28 ± 6
NTK (%)	0.28 ± 0.03
NH4+ (%)	0.04 ± 0.01
Cl^- (mg/kg d.w.)	44 ± 3
K (g/kg d.w.)	3.00 ±0.01
Mg (g/kg d.w.)	1.51 ± 0.003
Na (g/kg d.w.)	1.45 ±0.01
Ca (g/kg d.w.)	5.48 ± 0.01
Fe (mg/kg d.w.)	788 ± 9
Mn (mg/kg d.w.)	57 ± 3
Zn (mg/kg d.w.)	18 ± 4
Cr (mg/kg d.w.)	26 ± 4
Cu (mg/kg d.w.)	11 ± 4
Ni (mg/kg d.w.)	2.0 ±0.5

± Standard Deviation

The substrate was also characterized with high concentration of potassium (3 g/kg), magnesium (1.51 g/kg), sodium (1.45 g/kg), and calcium (5.48 g/kg), these concentrations are probably high due to their import from peat. Heavy metals such as Fe, Mn, Z, Cr, Cu, and Ni were detected at various level of abundance. Fe was dominating with a concentration of 788 mg/kg of dry weight. The concentration of the remaining metals was ranged between 2 and 57 mg/kg of dry weight.

3. Effect of the dilutions on plant growth parameters

3. 1. Morphological plant growth

The analysis of the plant lengths at the end of the experiment revealed no significant difference between plants irrigated with GW and those irrigated with D60 dilution. Results presented in **Figure. 1.1** show that the mean plants heights at the end of the experiment was 20.12 cm and 17

cm, respectively for plant treated with GW and D60 dilution.

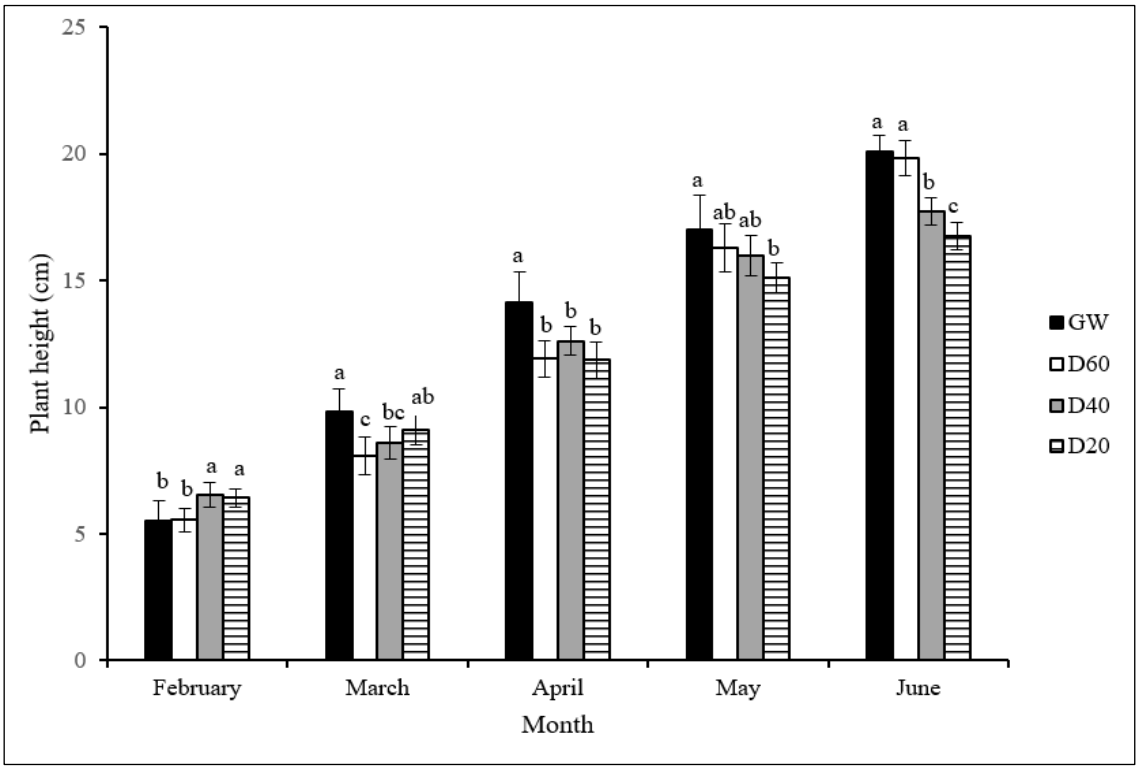

Figure 1.1. Effect of groundwater (GW) diluted treated wastewater D60, D40 and D20 on strawberry plant height according to time. Bars with different letters refer to differences (ANOVA, Tukey's test, $p < 0.05$) between treatments, where the same letter indicates no indicates no significant difference.

On the other hand, a significant difference was notified when comparing results from GW with D40 and D20 dilutions. Heights were lower in plants irrigated with D40 (14.4 cm) and D20 (12.4 cm) with reference to the control and D60. More in details, the noticed recorded decrease in the plant length with the increase of TWW dilution (**Figure 1.1**) could be explained by the decrease in carbohydrates and growth hormones level, the changes in enzyme activity, or the decrease photosynthesis rate which is directly related to the presence of high concentration of chloride (Dantas et al. 2005, Memon et al. 2010). Heavy metal might also cause stunted stem length (Srivastava et al., 2012).

In term of leaves number, results present in **Figure 1.2** show that the number of leaves was higher during the whole period of cultivation in plants irrigated with GW.

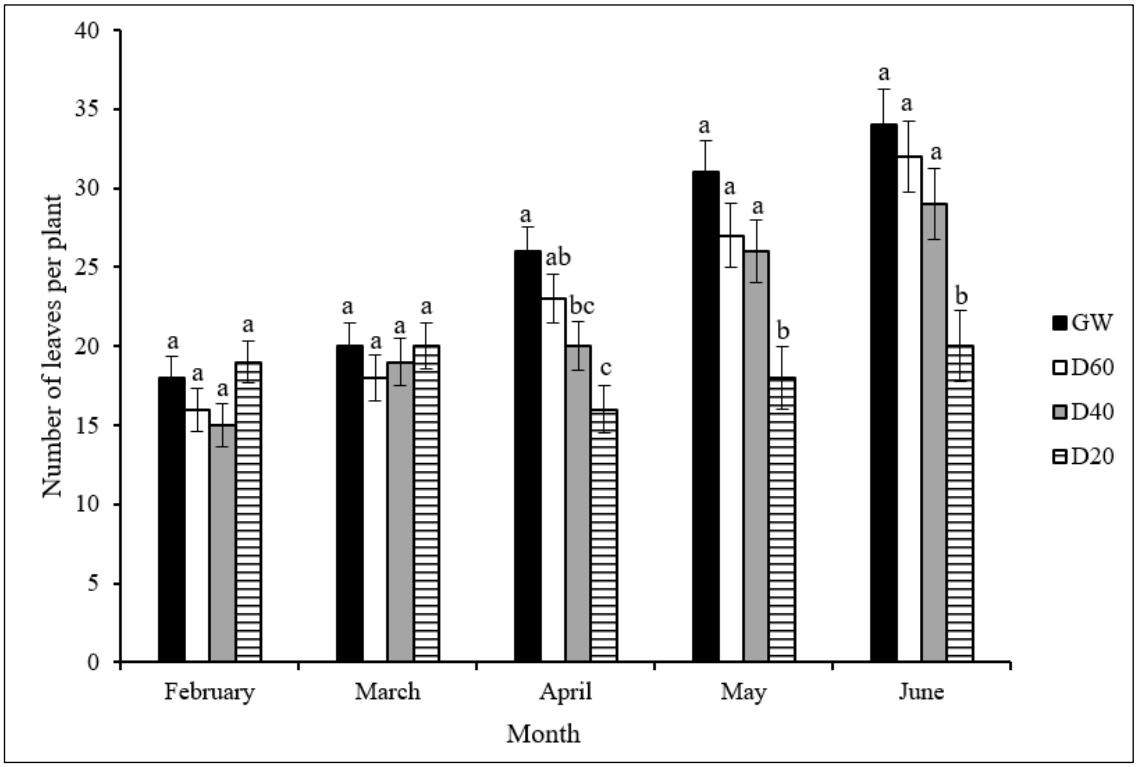

Figure 1.2. Effect of groundwater (GW) diluted treated wastewater D60, D40 and D20 on strawberry leaves number according to time. Bars with different letters refer to differences (ANOVA, Tukey's test, $p < 0.05$) between treatments, where the same letter indicates no significant difference.

Figure 1.2 shows that in plant irrigated with the dilution D60 demonstrated the highest leaves number followed by plants irrigated with D40 with no significant difference. Yet, plants irrigated with the D20 were characterized by low leaves number. This low number of leaves could be explained by the higher concentration of metals in D20, as heavy metals can delay the metabolism in plant tissues if present in inhibitory concentration causing chlorosis and a sharp reduction in leaves number (Singh et al., 2016). The toxic effect of D20 was also demonstrated in **Figure 1.3**.

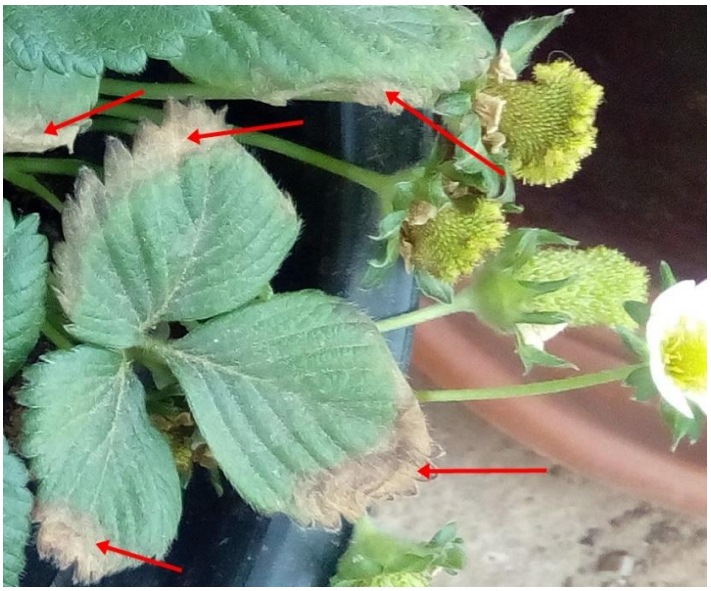

Figure 1.3. Brown edge in strawberry leaves irrigated with D20.

At the end of the experiment, leaves from strawberry shoots irrigated with D20 were characterized with brown edges (**Figure 1.3**). This phenomenon can be related to salts accumulation in roots, imbalances in ion ratio, lack of iron or high toxic levels of specific ions (Keutgen and Pawelzik, 2009) as high concentrations of chlorine ions can lead to several growth disorders generally observed at the level of leaves number or the quality of the fruit. These issues are mainly due to the destruction of the leaf metabolism and the reduction of nitrate uptake (Keutgen and Pawelzik, 2009). It was reported in literature that high concentration of chlorine can result in chlorotic discolorations and in the apparition of necrotic leaf edged (Geilfus, 2018).

3. 2. Total chlorophyll content

The analysis of the chlorophyll content in strawberry leaves is demonstrated in **Figure 1.4**. The determination of this parameter gives an idea on the chlorine or other trace element uptake by plant (Aggarwal et al., 2012; Ahmali et al., 2020;).

The results in **Figure 1.4** show that there is no significant difference between the chlorophyll content in leaves from plant irrigated with D60 and D40 with respect to plant irrigated with GW. Mean results were 274.9 µg/gFW, 265.5 µg/gFW, and 266.1 µg/gFW, respectively for GW, D60, and D40.

However, a lower chlorophyll content was observed in pots irrigated with D20 dilution where the chlorophyll content was significantly lower with a value of 218 µg/g FW.

According to Kato and Shimizu, (1985), the decrease in chlorophyll content was related to the

photoinhibition or reactive oxygen species formation. It was reported in the literature that excess in chlorine concentration might lead to a chlorosis at the leaf edges which is often explained by low chlorophyll content (Geilfus, 2018). Ahmali et al. (2020) reported a decrease in olive leaves chlorophyll content when irrigating with water with high content of chlorine. Moreover, the decrease in chlorophyll content could also be related to the high concentration of metals present in the dilutions. In fact, it is reported in the literature that metals such as Hg, Cu, Cr, Cd, and Zn have been found to decrease the chlorophyll content in various plants in most cases (Chandra and Kang, 2016). Maleva et al. (2012) have observed that Mn, Cu, Cd, Zn, and Ni caused a significant decrease in chlorophyll contents in *Elodea densa*. Heavy metals are characterized with high redox potential which can inhibit the reductive steps in the biosynthetic pathways of the chlorophyll (Chandra and Kang, 2016). Heavy metals can also inhibit the production of protochlorophyllide reductase which is a key enzyme involved in the reduction of protochlorophyll to chlorophyll (Küpper et al., 1996).

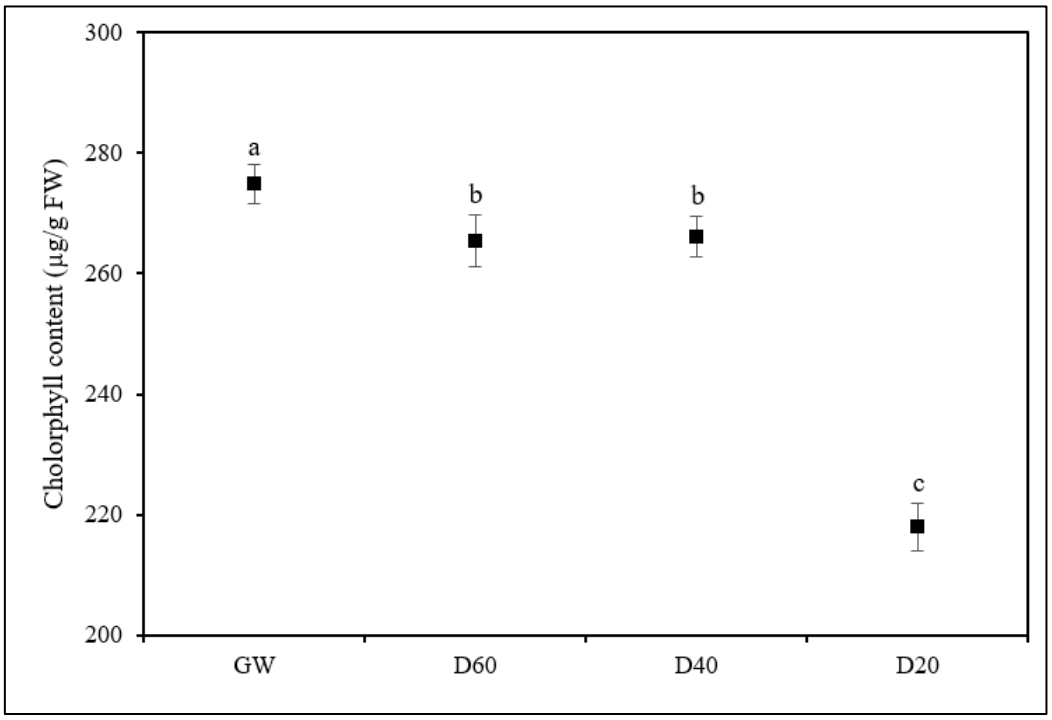

Figure 1.4. Total chlorophyll content in leaves of plants irrigated with groundwater (GW) diluted treated wastewater D60, D40 and D20. Bars with different letters are refer to differences (ANOVA, Tukey's test, $p < 0.05$) between treatments, where the same letter indicates no significant difference.

3. 3. Fruit yield and quality

The effect of the irrigation with GW and the various dilutions on strawberry yield, dry matter (%),

total soluble solids (%), and ascorbic acid (mg AA/ 100g FW) was studied, and results were reported in **Table 1.3**.

Strawberry mean production was significantly higher in plant irrigated with GW (118 g per plant) compared with plants irrigated with D20 (48 g per plant) and D40 (74 g per plant) ($p< 0.01$). However, no significant difference was recorded between the yield of plants irrigated by GW and D60. Mean production was very low for plants irrigated with D20.

Table 1.3. Effects of groundwater (GW) diluted treated wastewater D60, D40 and D20 applied for the strawberry plants' irrigation on fruits yield, dry matter, total soluble solids, and ascorbic acid contents. Different letters refer to differences (ANOVA, Tukey's test, $p < 0.05$) between treatments, where the same letter indicates no significant difference)

Parameters	GW	D60	D40	D20
Yield plant (g/plant)	118 ± 9 [a]	107 ± 11 [a]	74 ± 9 [b]	48 ± 8 [c]
Dry matter (%)	24 ± 5 [a]	17 ± 5 [ab]	15 ± 6 [b]	10 ± 4 [b]
Total Soluble solids (%)	7.68 ± 2 [a]	7.72 ± 3 [a]	7.76 ± 3 [a]	7.81± 3 [a]
Ascorbic acid (mg AA/ 100g FW)	40 ± 78 [a]	39 ± 7 [a]	39 ± 5 [a]	38 ± 6 [a]

± Standard Deviation

The same behaviour was notified for dry matter. Dry matter content was higher in plant irrigated with GW (24 %) compared with plants irrigated with D60 (17 %) and D40 (15 %). Mean production was very low for plants irrigated with D20 (10%).

As shown in **Table 1.3**, plant yield and dry matter were affected by the toxicity of the effluent, as their concentration decrease with the increase of the effluent pollutant's concentrations. Also, the reduction of production yield with the increase of dilution factor was related to various abiotic stress which can be caused by the presence of significant concentration of heavy metals in soil. It was demonstrated by Keunen et al. (2011) that plant growing in heavy metal-rich medium suffer from decreased yield.

4. Effect of the dilutions on substrate physicochemical parameters

The evolution of pH, EC, total phosphorus, TOC, NTK, and Cl^- of different substrates was evaluated and the results are demonstrated in **Table 1.4**.

As it is demonstrated in **Table 1.4** no significant changes occur between substrate for pH and NTK when treating with the various dilutions. For TOC content, a significant statistically difference ($p<0.05$) was recorded between the substrates irrigated with GW and D20. On the other hand, there

is significant statistically differences in EC, P_t and Cl^- between substrate irrigated with GW and different diluted TWWs.

Table 1.4. Effects of groundwater (GW) diluted treated wastewater D60, D40 and D20 applied for the strawberry plants' irrigation on some substrate chemical characteristics.

	pH	EC	P_t (mg/kg)	TOC (%)	NTK (%)	Cl^- (mg/kg)
GW	8 ± 1	0.8 ± 0.1*	225 ± 9*	24 ± 5	0.26 ± 0.06	68.9 ± 5.4*
D60	8 ± 1	1.2 ± 0.2*	360 ± 9*	29 ± 7	0.30 ± 0.06	134.5 ± 4.7*
D40	8 ± 1	1.9 ± 0.1*	424 ± 10*	30 ± 8	0.31 ± 0.07	210.9 ± 7*
D20	8 ± 1	2.3 ± 0.12*	479 ± 9*	32 ± 7	0.33 ± 0.07	283 ± 6*

* Indicate significant differences at a significance level of 5%.

A slighter increase was also observed in the substrate irrigated in D60; such rise proves the fertilizer effect of the TWW. The accumulation of salt in the soil is perfectly correlated to the increasing of EC in the substrate. The increase in such parameters in the substrate after a period of irrigation is totally normal which is usually due to the accumulation of particles present in the irrigation water at the level of the substrate. Similar results were reported by Ahmali et al., (2020). The authors demonstrated an increase in salt content and in the electrical conductivity in the substrate after a period of irrigation using a treated mixture of olive mill WW and urban WW. El Ghadraoui et al. (2020; 2021) has reported an increase of electrical conductivity, organic content, and total dissolved salts in the substrate of a pilot scale constructed wetland after a period of treatment of highly saline WW. These changes in the physicochemical parameters might be one of the factors in damaging crop productivity and affecting plant growth parameters especially in the case of shoots irrigated with D20 and D40, in which a significant difference when comparing to the control was demonstrated. In fact, the growth of sensitive plants may be significantly impacted when EC is within an interval of 2 - 4 mS/cm (Keutgen and Pawelzik, 2009). In this sense, Ondrašek et al., (2006) reported that the high conductivity of the soil induced to a sharp decrease in growth and the fresh fruit yield of strawberry. The author reported a decrease of 29%, 35%, and 59% in total yield when using substrate with an initial conductivity of 4 mS/cm, 6 mS/cm and 8 mS/cm, respectively (Ondrašek et al., 2006). Another study suggested that *Toro* and *Douglas* strawberry cultivars are sensitive to the specific action of the chlorine. These cultivars have demonstrated no negative impact at a soil conductivity level of 2 mS/cm. Yet, if the level is higher than this, the risk of leaf damage increases, due to the higher incidence of the hydric deficit, and also to an increase in sensitivity to the action of chlorine (Barroso and Alvarez, 1997).

Soil hydrophobicity is related to the soil surface contained different levels of coated hydrophobic

surface (Doerr et al., 2006). The result illustrated in **Figure 1.5** shows that all substrates were slightly hydrophobic. Moreover, the soil irrigated by water diluted to 20% had the maximum WDPT (31s) while the lowest value was obtained from the control soil (13s). According to ANNOVA results, there is a statistical difference between GW in one hand and D20, D40 and D60 in other hand. Another significant statistical difference was registered between D40 and D20. However, there are no significant statistical difference between D60 and D40 and between D60 and D20.

The increase of substrate water repellence demonstrated that the decrease of dilution of TWW used for irrigation increased the water resistance then disturbed the water dynamics. Further, substrate hydraulic properties were negatively affected by the use of TWW. These results are in agreement with the conclusions of Schacht et al. (2014) in their study focus on the impact of irrigation with TWW in Mediterranean soils.

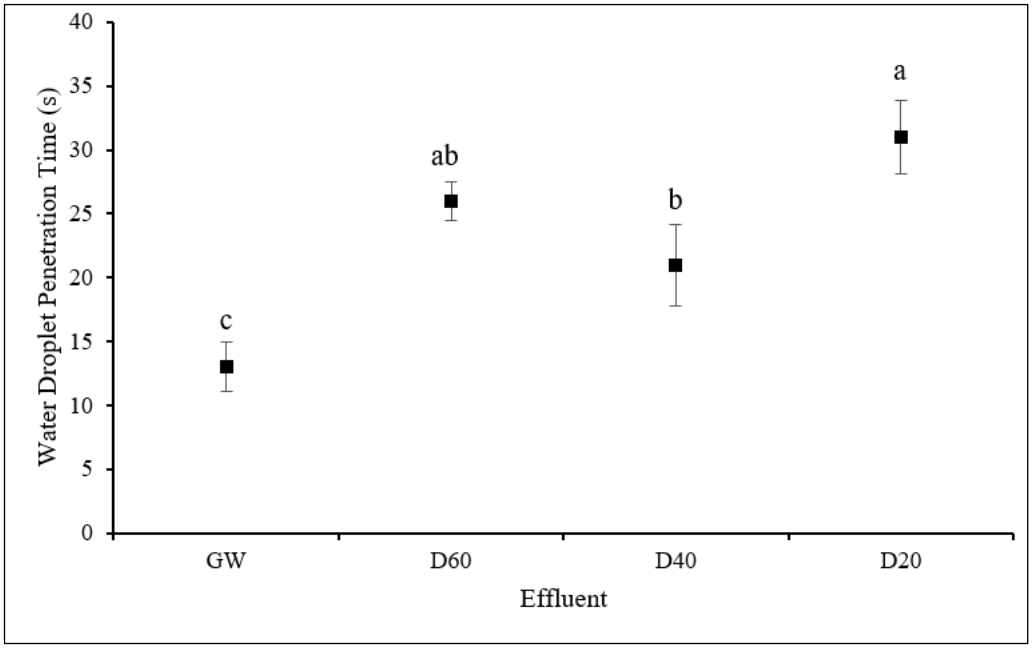

Figure 1.5. Effect of with groundwater (GW) diluted treated wastewater D60, D40 and D20 on substrate water droplet penetration time. Bars with different letters refer to differences (ANOVA, Tukey's test, $p < 0.05$) between treatments, where the same letter indicates no significant difference.

Substrates irrigated with 20% diluted TWW and contained the highest TOC content (**Table 1.4)** then highest amount of OM characterized by the highest degree of hydrophobicity. In fact, and as reported by Abegunrin et al (2016), the hydrophobicity is related to the high soil OM content. More in details, the OM molecules reacted by their polar groups with water and faced into the solution in wet soils pores that will be faced after that by hydrophobic groups within the soil drying. In this

phase OM polar groups faced the water and new hydrophobic surface were obtained on the soil (Doerr et al., 2005; Tarchitzky et al., 2007)

5. Heavy metal concentrations in the substrate and in the plant

5. 1. Heavy metals in the substrate

Table 1.5 shows that no significant difference in substrate heavy metals concentration was observed when irrigating with GW compared to the concentrations in raw substrate. The effect of heavy metals accumulation was significantly higher in substrate irrigated with D20 when compared to the substrate irrigated with D40, D60 and the raw substrate (**Table 1.5**).

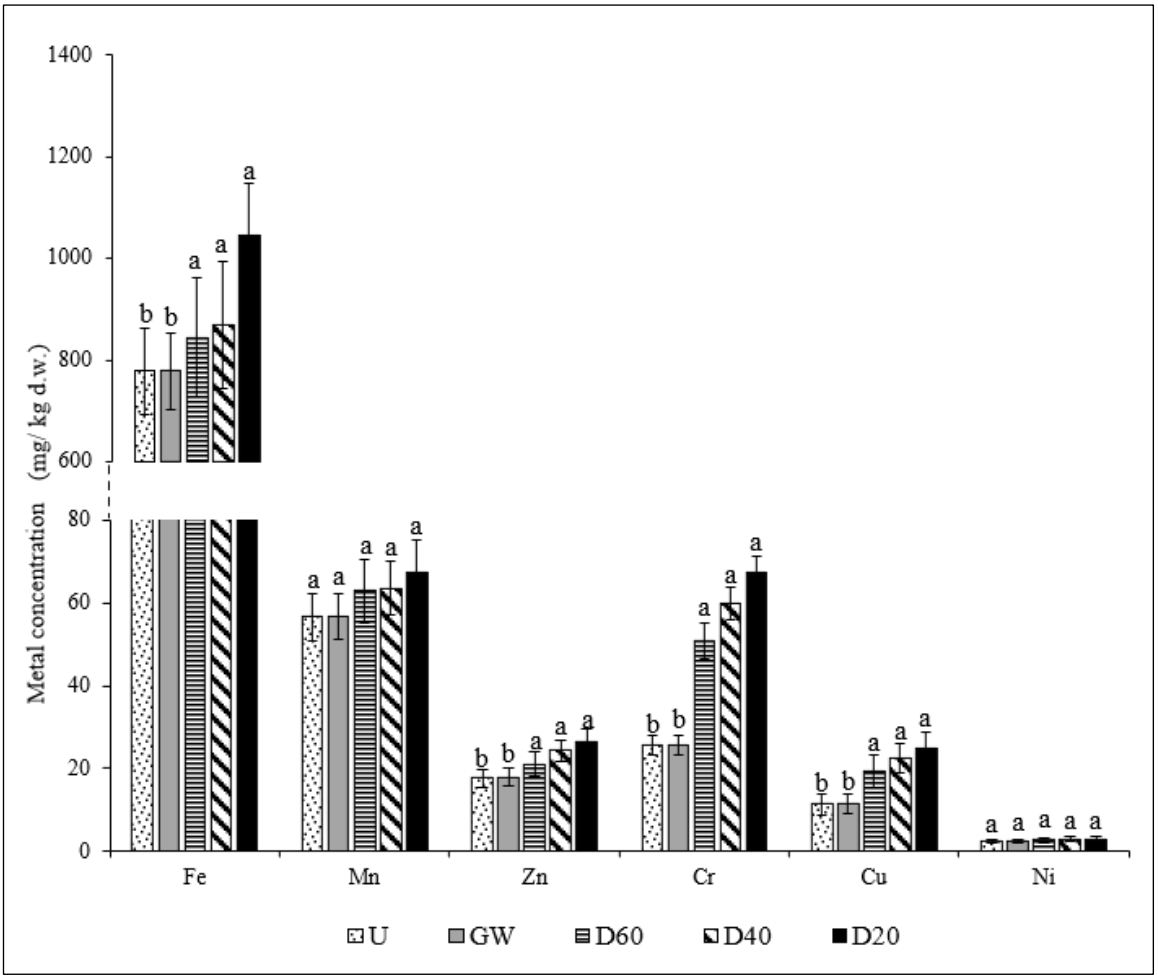

Figure 1.6. Metal contents in substrates before (U) and after irrigation with groundwater (GW) diluted treated wastewater D60, D40 and D20. (mg/kg d.w.). Bars with different letters refer to differences (ANOVA, Tukey's test, $p < 0.05$) between treatments, where the same letter indicates no significant difference.

This difference is obviously due to the concentration of these heavy metals in the irrigation waters. As demonstrated in **Table 1.1**, heavy metal concentrations were higher in D20. According the results in **Table 1.1** and **Figure 1.6**, the increase in substrate heavy metals in perfectly correlated with their concentration in the irrigation waters. The lowest heavy metals accumulation in the substrate when using TWW dilutions was observed in the case of D60.

The Ni, Cu and Zn total concentrations in soil increased without reaching 75, 140 and 300 mg kg^{-1}, respectively, which are the maximum permissible limits set by the EU Directive (McGrath et al., 1988). Moreover, in accordance with Sahay et al. (2019), in agriculture, the permissible limits for Cr concentration must be in the range of 75 - 100 mg kg^{-1}. Yet, in this study Cr concentration reached a maximum of 67 mg/ kg d.w. using the most polluted dilution (D20) (**Figure 1.6**) which will allow us to deduce that the irrigation using TWW did not record soil heavy metals contents above preferable levels. However, since heavy metals tend to accumulate and are persistent pollutant it is clear that the substrate can be used only one more time before reaching the limits.

The added concentration of heavy metals calculated according to the operating conditions (e.g., heavy metal concentration, number of irrigations, and quantity of water per batch) match with a slight difference to the concentration measured in substrate. The major part of heavy metals introduced to each pot were accumulated in the substrate, which indirectly means that only a small fraction was up taking by the plant.

5. 2. Heavy metals in the plant

The concentration of Mn, Zn, Cr, Cu, and Ni in the various part of the strawberry plant (root, stem, and fruit) were evaluated and the results are demonstrated in **Table 1.5**.

Table 1.5 shows that no significant difference in substrate heavy metals concentration was observed when irrigating with GW compared to the concentrations in raw substrate. The effect of heavy metals accumulation was significantly higher in substrate irrigated with D20 when compared to the substrate irrigated with D40, D60 and the substrate before irrigation.

Table 1.5. Heavy metal (Fe, Mn, Zn, Cu and Ni) contents of strawberry stem and roots irrigated with groundwater (GW) diluted treated wastewater D60, D40 and D20. Different letters refer to differences (ANOVA, Tukey's test, $p < 0.05$) between treatments, where the same letter indicates no significant difference)

Roots (µg/g d.w.)					
Sample	Fe	Mn	Zn	Cu	Ni
GW	29 ± 6 ^{c}	12 ± 2 ^{c}	1.6 ± 0.6 ^{b}	1.8 ± 0.5 ^{b}	0.5 ± 0.1 ^{b}
D60	35 ± 6 ^{bc}	14 ± 1 ^{b}	1.6 ± 0.5 ^{b}	2.0 ± 0.7 ^{b}	0.6 ± 0.1 ^{b}
D40	39 ± 8 ^{ab}	15 ± 1 ^{a}	2.7 ± 0.5 ^{a}	2.6 ± 0.8^{ab}	0.8 ± 0.1 ^{a}
D20	45 ± 7 ^{a}	17 ± 1 ^{a}	3.0 ± 0.8 ^{a}	3.2 ± 0.7 ^{a}	0.9 ± 0.1 ^{a}
Stem (µg/g d.w.)					
GW	11 ± 2 ^{c}	22 ± 4 ^{a}	6.0 ± 0.9 ^{b}	1.9 ± 0.7 ^{c}	0.8± 0.1 ^{b}
D60	15 ± 3 ^{bc}	24 ± 4 ^{a}	6.1 ± 0.8 ^{b}	2.7 ± 0.9 ^{bc}	1.4 ± 0.3 ^{a}
D40	18 ± 3 ^{b}	25 ± 5 ^{a}	6.9 ± 0.9 ^{ab}	3.4 ± 0.9 ^{ab}	1.6 ± 0.3 ^{a}
D20	22 ± 3 ^{a}	27 ± 6 ^{a}	7.9 ± 0.8 ^{a}	4.5 ± 1.1 ^{a}	1.7 ± 0.3 ^{a}

± Standard Deviation

When comparing the distribution of heavy metals in the different part of the plant, **Table 1.5** shows that all studied metals were found at higher concentrations in aerials parts except from Fe of which higher concentrations were detected in roots. In fact, essential trace elements such as Ni, Cu, and Zn involved in the plant metabolism processes are usually absorbed and translocated in the aerial parts. The results in **Table 1.5** show that plant's heavy metals accumulations were pronounced by the irrigation using higher percentage of TWW compared to the GW (D60% < D40% < D20%). These findings were confirmed by previous study in the irrigation of tomatoes conducted by Al-Lahham et al. (2007) in which results approve that for GW: TWW ratios {100%: 0%; 50%:50%; 25%:75%; 0%:100%} metals accumulation increased in the same order of dilution. The high level of metal contents in aerials part was explained by Sahay et al (2019) as a way to reduce these toxic elements from plants by the shedding of old leaves.

For the fruit, results presented in **Figure 1.7** show that metals accumulation depends strongly on the TWW dilution factor.

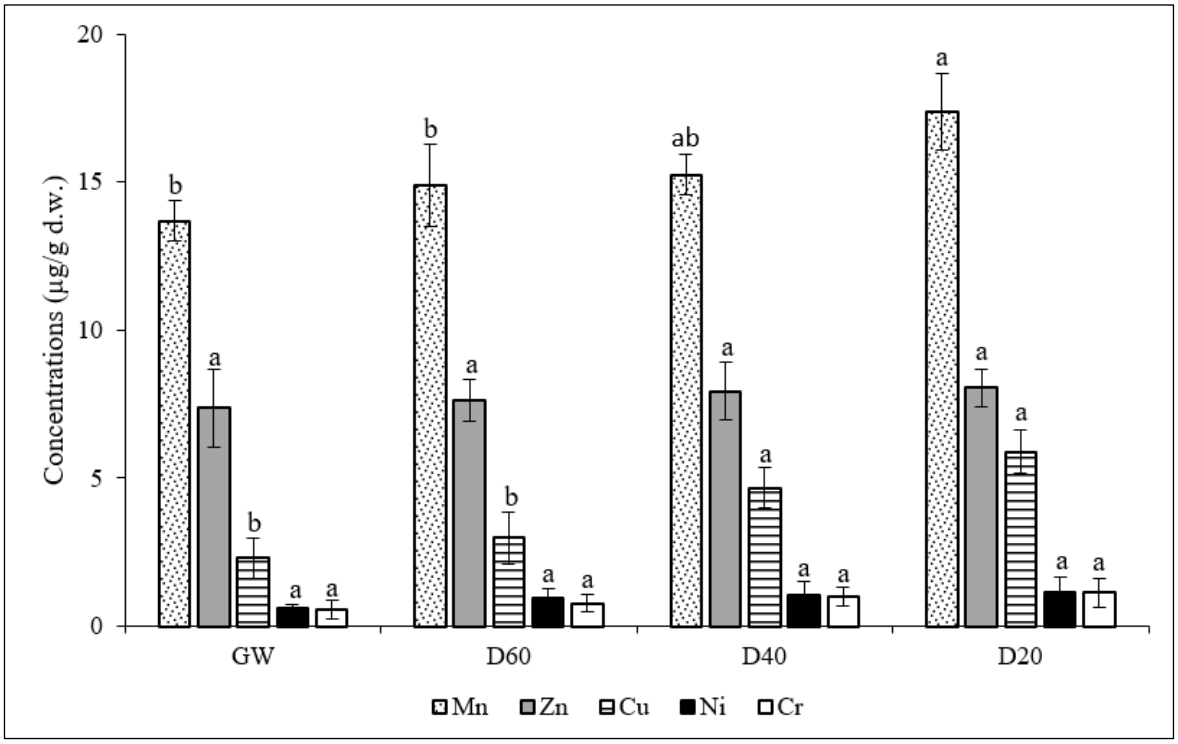

Figure 1.7. Heavy metal (Mn, Zn, Cu, Ni and Cr) contents in fruits of plants irrigated with groundwater (GW) diluted treated wastewater D60, D40 and D20. Bars with different letters refer to differences (ANOVA, Tukey's test, $p < 0.05$) between treatments, where the same letter indicates no significant difference.

Metal's concentration was lower in the fruits harvested from pots irrigated using GW. Cu and Mn concentrations showed high increase with the reduction of the dilution factor compared to Zn, Cr and Ni content. Moreover, the concentrations of Zn, Cu and Ni were lower than the limits set by the WHO/FAO Codex Committee on Food Hygiene. Therefore, and regarding the absence of microbial contamination by *E. coli*, Faecal Streptococci, *Salmonella* spp. in the used TWW, the suggested dilutions of TWW used in this study produced safe fruits considering the metals and microbial contaminations. These results were found also by Christou et al. (2016) that verified that advanced tertiary treated effluent as a valid alternative for the irrigation of strawberry crops.

6. Health risk assessment

The health risk assessment determined from the target hazard quotients (THQ) and hazard index (HI) was measured and results are presented in **Table 1.6**.

Table 1.6. The target hazard quotients (THQ) and hazard index (HI) values of strawberries irrigated with groundwater (GW) diluted treated wastewater D60, D40 and D20. Different letters refer to differences (ANOVA, Tukey's test, $p < 0.05$) between treatments, where

	THQ					HI
	Cr	Mn	Zn	Cu	Ni	
GW	0.0003±0.0002^{a}	0.093±0.005^{b}	0.023±0.004^{a}	0.05±0.02^{b}	0.03±0.01^{a}	0.20±0.03^{b}
D 60	0.0005±0.0002^{a}	0.101±0.009^{b}	0.024±0.002^{a}	0.07±0.02^{b}	0.05±0.02^{a}	0.24±0.05^{b}
D 40	0.0006±0.0002^{a}	0.103±0.004^{ab}	0.025±0.003^{a}	0.11±0.02^{a}	0.05±0.02^{a}	0.29±0.05^{ab}
D 20	0.0007±0.0003^{a}	0.118±0.009^{a}	0.025±0.002^{a}	0.14±0.02^{a}	0.06±0.03^{a}	0.34±0.05^{a}

± Standard Deviation

THQ and HI values were below than 1 that is present the standard of the health protection from serious risk. These results suggested the safety of the strawberry consuming on the public health from serious concern brought by heavy metals (Woldetsadik et al.,2017). THQ results demonstrated that the potential health risk of heavy metals was in the order Cu > Mn > Ni > Zn. However, adverse health risk could be raised with a consideration of many heavy metals' simultaneously. Indeed, results showed that HI was lower for the strawberry irrigated with groundwater (0.20) when compared with the one irrigated with D60 (0.24), followed by D40 (0.29). The highest HI value was obtained for D20 (0.34) which contained the higher concentration of heavy metals. However, all HI results were below 1, which evidence the safety of all fruits produced in this experiment according to the standard of the health protection from serious risk. HI was considered as an important way to estimate the possible multiple influences of the presence of heavy metals (Guadie et al., 2021).
Thus, all water resources used in this study did not demonstrate any possible negative health risk for consumers (Chen et al., 2021).

7. Conclusion

The possible effects of diluted TWW irrigation in strawberry productivity and safety, soil fertility and salinity and metals contamination, compared to GW were evaluated in this work.
Comparing with the GW irrigated plants, TWW improved the soil fertility by increasing total P, NTK and macro- and micronutrients.
Substrate salinity and metal contents in fruits, plant, and substrate showed a reduction with the dilution factor (D20 > D40 > D60). Substrate irrigated with D60 registered an EC that did not exceed 2 mS/cm, thus the use of D60 showed no significant differences with GW irrigated plants

and showed beneficial effects on the soil fertility and fruits safety compared to the other dilutions. According to the evaluation of different physicochemical properties of soil, plants growth and fruits yield and quality, the dilution D60 could be a sustainable management solution to use TWW for the irrigation of strawberry which is a saline sensitive plant. Moreover, the target hazard quotient (THQ) and hazard index (HI) revealed that consummation of strawberry fruits after the irrigation using diluted TWW will not exhibit any hazardous health risks. Therefore, this research insists administrators, environmentalists, and public health employee to use TWW on the irrigation of strawberry plants considering its safety aspect, hence reducing the fresh water shortage risk.

II. Effect of the irrigation of olive (Olea europaea L. cv. '*Koroneiki*') trees using treated wastewater

1. Characterization of treated wastewaters used for irrigation and soil

1.1. Groundwater and treated wastewaters characterization

Table 1.7 summarizes the characterisation of the waters used for olive trees irrigation as well as the Tunisian standards (NT 106.03) related to the reuse of these effluents in the agriculture sector for crop irrigation purpose.

The three TWWs have pH values from 7.84 to 7.95, which are in the range of effluent pH recommended by the Tunisian norm for crops irrigation. P_t contents were in the range from 10.3 to 25.5 mg/ L. The average value of the EC of the TWW1 was about 7.65 mS/cm, which is slightly higher than the Tunisian standards (NT 106.03) related to the reuse of TWW for irrigation (7 mS/cm). This high value could be due to the high sodium and chloride concentrations. However, this EC value could not assess any problem for olive tree that is considered as a moderately tolerant species to salinity (Chartzoulakis, 2005). TWW2 and TWW3 contained higher values of TSS (about 280 and 198 mg/ L respectively) compared to the Tunisian limits. TWW1 and TWW2 were characterised by COD values around 107 and 93 mg O_2/ L, respectively, and BOD_5 values of 48 and 37 mg O_2/ L respectively, which are higher than the NT 106.03 (90 and 30 mg O_2/ L respectively). However, the used TWWs contained high amount of nitrate, total phosphorus and potassium that demonstrated their possible amendment effect on soil. Fe, Mn, Zn, Cr and Cu in the three TWWs were above the NT 106.03standards limits.

Table 1.7. Physicochemical characterisations of groundwater (GW) and different treated wastewaters (TWW1, TWW2 and TWW3) used for irrigation and corresponding maximum limits (NT 106.03). All parameters are expressed as mg/L, unless differently specified.

Parameters	GW	TWW1	TWW2	TWW3	NT 106.03
pH	7.1 ± 0.1	7.8 ± 0.1	7.9 ± 0.2	7.9 ± 0.1	6.5-8.5
EC (mS/cm)	1.8 ± 0.1	7.6 ± 0.1	3.3 ± 0.1	6.99 ± 0.1	7
Total suspended matter	0	30 ± 2	280 ± 7	198 ± 9	30
Chemical oxygen demand	0	107 ± 2	93 ± 4	19.5 ± 1	90
Biological oxygen demand	0	48 ± 3	37 ± 3	12 ± 1	30
Nitrate	1.1 ± 0.1	20 ± 2	26 ± 3	100 ± 6	-
Nitrite	0	0	0	12 ± 1	-
Chloride	257 ± 4	1950 ± 12	540 ± 15	1780 ± 12	2000
Sulfate	251 ± 10	1600 ± 10	500 ± 8	1660 ± 5	-
Total phosphorus	0.02 ± 0.01	14 ± 2	10.3 ± 0.5	25 ± 4	-
Potassium	5 ± 1	175 ± 5	181 ± 4	102 ± 7	-
Sodium	162 ± 5	596 ± 5	394 ± 5	492 ± 2	-
Calcium	100 ± 2	242 ± 4	184 ± 4	287 ± 4	-
Magnesium	27 ± 3	280 ± 5	163 ± 6	241 ± 3	-
Hydrogenocarbonate	130 ± 3	240 ± 3	483 ± 4	300 ± 6	-
Iron	0.06 ± 0.03	97 ± 2	89 ± 4	102 ± 2	5
Manganese	0	3.4 ± 0.4	2.3 ± 0.2	3.3 ± 0.3	0.5
Zinc	0	1.4 ± 0.4	1.1 ± 0.1	1.3 ± 0.3	5
Chromium	0	2.2 ± 0.1	1.9 ± 0.2	2.1 ± 0.2	0.1
Copper	0	1.2 ± 0.1	0.97 ± 0.18	1.2 ± 0.3	0.5
Nickel	0	0.19 ± 0.04	0.13 ± 0.04	0.17 ± 0.05	0.2

± Standard deviation

As shown in the **Table 1.7** the concentration of Fe was significantly higher that the concentration of other metals. This high content could be probably due to the use of Fe-based chemical products, such as iron chloride in the procedure of WW treatment. The high content of Cu, Zn and Cr in TWWs is the results of the discharge of WW from metals-based industrials activities such as battery building, fabric printing, electroplating and metals surface treatment (Aghabarati et al. 2008).

1.2.Soil characterisation

Table 1.8 shows the properties of the soil used in this work. The soil was collected from El Hajeb plot located 10 km in the south west of Sfax city. The soil was characterized by an alkaline pH (8.43), an EC around 0.29 mS/cm, a low amount of organic matter and a very low quantity of nitrogen. The lack of OM and the nutrient deficiency can be compensated by the irrigation using TWWs. According to the results displayed in the table and the information given from the soil texture triangle it can be concluded that the soil used for olive cultivation is loamy sandy soil.

Table 1.8. Physicochemical characteristics of soil

Soil characteristic	Value ± Standard Error
pH	8.4 ± 0.2
EC (mS/ cm)	0.29 ± 0.02
Total Phosphorus (mg/ Kg)	28.5 ± 0.5
Organic matter (%)	0.64 ± 0.03
NTK (mg/ Kg)	24.7 ± 0.4
Mg (mg/ Kg)	168 ± 5
CEC (mol/Kg)	23.4 ± 0.2
K (mg/ Kg)	695 ± 10
Sand (%)	84.4 ± 0.4
Clay (%)	9.80 ± 0.05
Silts (%)	5.8 ± 0.1

2. Characterization of soil after irrigation with treated wastewater

Table 1.9 outlines the different effects of irrigation with GW and TWWs on EC, pH, OM and Pt contents in soil.

Table 1.9. pH, Electrical conductivity (EC) and organic matter (OM) and phosphorus total (P_t) contents in soil after one and two years of irrigation with groundwater (GW) and TWW1, TWW2 and TWW3. Different letters refer to differences (ANOVA, Tukey's test, $p < 0.05$) between treatments, where the same letter indicates no significant difference).

		pH	EC (mS/cm)	OM (%)	Pt (mg/Kg)
GW	1 year	8 ± 0.2^{a}	0.33 ± 0.02^{d}	0.5 ± 0.1^{c}	30 ± 1^{d}
	2 years	8 ± 0.1^{a}	0.36 ± 0.02^{d}	0.6 ± 0.1^{b}	31 ± 1^{d}
TWW1	1 year	8.1 ± 0.1^{a}	0.53 ± 0.02^{a}	0.6 ± 0.1^{bc}	60 ± 1^{b}
	2 years	8.0 ± 0.2^{a}	0.76 ± 0.03^{a}	0.7 ± 0.2^{b}	79 ± 1^{b}
TWW2	1 year	8.0 ± 0.1^{a}	0.38 ± 0.02^{c}	0.8 ± 0.1^{a}	44 ± 1^{c}
	2 years	8.1 ± 0.2^{a}	0.48 ± 0.02^{c}	1.0 ± 0.1^{a}	60 ± 1^{c}
TWW3	1 year	7.9 ± 0.2^{a}	0.49 ± 0.02^{b}	0.6 ± 0.1^{b}	81 ± 1^{a}
	2 years	8.0 ± 0.2^{a}	0.72 ± 0.02^{b}	0.9 ± 0.1^{a}	132 ± 2^{a}

± Standard deviation

No significant decrease in the soil pH was registered after irrigation with different TWWs. In fact, after irrigation the soil pH decreased slightly from 8.43 and varied in the range of 7.89 and 8.11. This result is in agreement with several works (Ben Rouina et al., 2011; Bedbabis et al., 2014) that showed a reduction of the alkalinity of sandy soil after irrigation using TWW in comparison with the irrigation by fresh water. However, Kumar et al. (2009) reported that the irrigation using TWW characterised by high concentrations of bicarbonate increased the soil pH, and the same findings were observed by Bedbabis et al. (2015) and Suarez et al. (2006). Gargouri (1998) verified that the

range of soil pH for olive development was from 7 to 8.5, therefore, the irrigation using the different TWWs did not have negative effect on the soil acidity. The reduction of soil pH can be explained by the effect of the OM accumulation and their decomposition, as reported by Belaid et al. (2019) and Rattan et al. (2005). The slight decrease of pH found in this work could be the result of a process that release protons. Khawla et al. (2019) explained the reduction of soil pH after irrigation using TWW by nitrification of ammonium or plant uptake of ammonia ions, leaching of basic cations or plant' OM exudation in the root zone.

As shown in **Table 1.9**, the EC of the soil saturated paste extract increased using the different TWWs from 0.29 to reach 0.759, 0.476 and 0.717 mS cm^{-1} using TWW1, TWW2 and TWW3, respectively after two years of olive trees plantation, i.e., increasing about 2.5 times after the irrigation using TWW1 and TWW3 and approximately 1.5 time using TWW2. Morugán-Coronado et al. (2011) demonstrated the 2.38 times increase in EC for soil after only one year of irrigation using secondary TWW. These results are in agreement with the high EC of TWW1 and TWW3, compared to TWW2, as reported in **Table 1.7**. Based on literature, EC of irrigation water affects soil salinity, but also texture, OM content, drainage operations and crop productivity (Jaramillo and Restrepo, 2017, Kiziloglu et al., 2008). Thus, the increases in EC due to the addition of salts from using TWWs for irrigation, could conduct to soil and plant productivity problems (Natsheh, 2021). However, after two years of irrigation using different TWWs, the EC did not exceed the salinity threshold of 4.00 dS m^{-1} elsewhere reported as critical for olive trees (Bedbabis et al., 2015).

Moreover, **Table 1.9** demonstrates different increases in the OM content using all TWWs for olive irrigation after one and two years. Rusan et al. (2007) have found a change in the OM value without significant difference after irrigation by TWW for 2 years. Moreover, the amounts of OM in soil irrigated by TWWs were slightly higher than that determined in soil irrigated with GW, which could also be related to the higher contents of OM in TWWs. These results were in agreement with those achieved by Valipour and Singh (2016), that found a level of OM of about 2% in soil irrigated with TWW compared to 0.74% in GW irrigated soil. As mentioned in a previous study (Rattan et al., 2005), an application of TWW for more than 20 years increased the soil OM content. Moreover, a significant enhancement of soil OM was registered also after a shorter irrigation period such as 2 years (Bedbabis et al., 2010) and 10 years (Assouline et al., 2016).

After 2 years of olive trees irrigation using TWW1, TWW2 and TWW3, P_t increased from 28.5 in soil non irrigated to 79, 60 and 132 mg Kg^{-1} respectively. The much higher increase in P_t in soil

irrigated with TWW3 is in agreement with the higher P-concentration in this TWW compared to the other TWWs. Statistically significant differences were observed between GW and TWWs in P_t contents ($p<0.05$) (**Table 1.9**). In fact, P_t contents in soils irrigated with TWW1, TWW2 and TWW3 were around 2.5, 2 and 4.3 times higher than that in GW irrigated soil. Similar results were found by Erel et al. (2019) in a soil used for olive trees cultivation, irrigated with TWW, which showed a two-fold increase in P_t compared to soil irrigated by fresh water. This P_t increase was verified also by Bar-Yosef (2011) in a sandy soil. Bedbabis et al. (2010) used a TWW containing 10.3 mg. L^{-1} of P_t for olive trees irrigation and showed an increase of P_t content in sandy soil from 66.3 to 76.6 mg kg^{-1} by the irrigation during 19 months using TWW, compared to a final concentration of 69.6 mg kg^{-1} using GW.

The improvement of P concentrations can increase the plants yield, thus potentially enhancing the olive oil productivity; in this regard, some researches showed the important effect of P availability in olive flowering and productivity processes (Jaramillo and Restrepo, 2017, Erel et al., 2016).

Ca, Mg, K and Na concentrations in soil are represented in **Figure 1.8**. The increase in metal concentrations due to the irrigation with TWWs instead of GW was clearly evidenced, even though at different irrigation time, depending on the metal and TWW considered. In this latter regard, the increase in Na, Ca and Mg concentrations were significantly lower in soil irrigated with TWW2 compared to the soil irrigated by the two other TWWs. These findings reflected the different concentrations of these metals in TWWs (see **Table 1.7**) and highlighted the fertilizing effect of the irrigation with TWW. Mg registered an important improvement that could be related to the lowest absorption of this element by the trees. This result was confirmed by Bedbabis et al. (2014) who showed even a decrease of Mg in soil irrigated with TWW after four years of treatment. This behaviour was probably related to the precipitation of this element as magnesite or other low-solubility magnesium salts (Laribi and Alzubaidi, 2007). Calcium concentrations were not significantly different in soil irrigated with GW and TWWs, except after eighteen and twenty-four months of irrigation. The Ca accumulation verified also that soil exchangeable complex adsorbs this element much more than its uptake by roots which was verified also by Bedbabis et al. (2014). The concentrations of K were lower in soil irrigated with TWW3 probably due to the lower supply by the water used for irrigation. Heidarpour et al. (2007) showed that the low accumulation of K in soil could be explained by its plant uptake. Petousi et al. (2015) verified similar improvement of Na, P and K concentrations in soils cultivated with olive (*Olea europaea* L. cv. 'Koroneiki') trees after two years of irrigation with TWWs compared to WW. Abegunrin et al. (2016) showed that the

irrigation using TWWs increased the Ca, Mg, and K, as well as OM. Indeed, the improvement of OM content increases the negatively charged surfaces and therefore the ability to attract more cations (Lines-Kelly, 2004). The soil OM has a basic function on many biological, chemical and physical activities and phenomena in soil such as the structure of the soil, its exchange capacity, and the retention of nutrients and pollutants (Bayer and Mielniczuk, 1999). More in details, the contents of TWWs in compostable and degradable elements increases OM by providing nourishment for microorganisms and thus improving microbial processes in the soil. Afterwards, the decomposition activities of OM result in an accumulation of humus and an increase in the nutrient content in the soil.

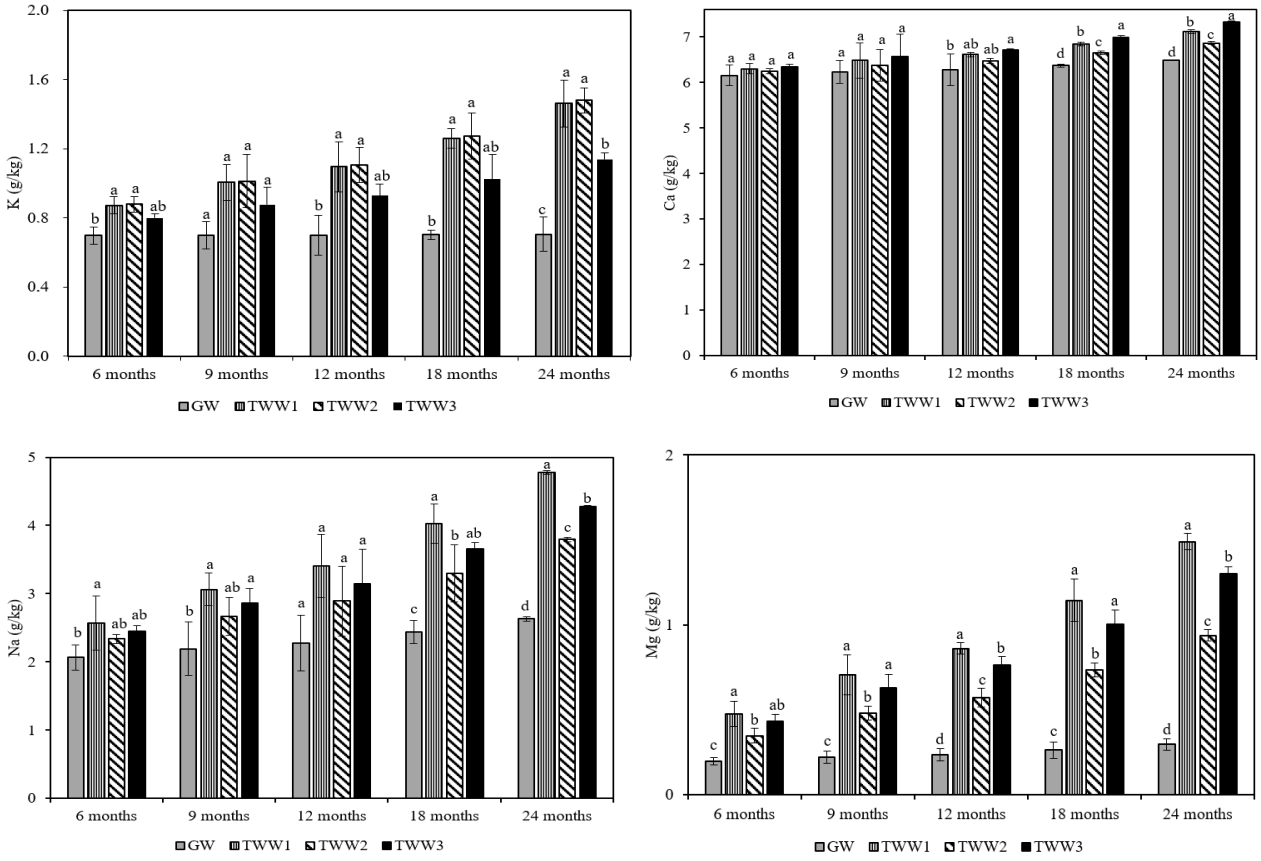

Figure 1. 8. Effect of the irrigation using groundwater (GW) and different treated wastewaters (TWW1, TWW2 and TWW3) in soil' sodium, potassium, magnesium and calcium contents. Bars with different letters refer to differences (ANOVA, Tukey's test, $p < 0.05$) between treatments, where the same letter indicates no significant difference.

3. Plant growth after irrigation using different water

The irrigation with TWWs showed different responses on the plant growth as represent in **Figure**

1.9. No significant differences in length of plants irrigated with GW and TWW3 were observed after 15 and 24 months of irrigation. TWW2 demonstrated the highest plant heights followed by TWW1, TWW3 and GW irrigated plants. This result can be related to the increase of heavy metals levels in soil irrigated by TWW1 and TWW3, that reduced the root development causing as consequence the decrease of the absorption of macronutrients by plants (Burton et al., 1983). In fact, as shown in **Table 1.7**, TWW2 contained the lowest metal contents compared to the other TWWs, therefore, olive trees irrigated with TWW2 recorded the highest plant growth.

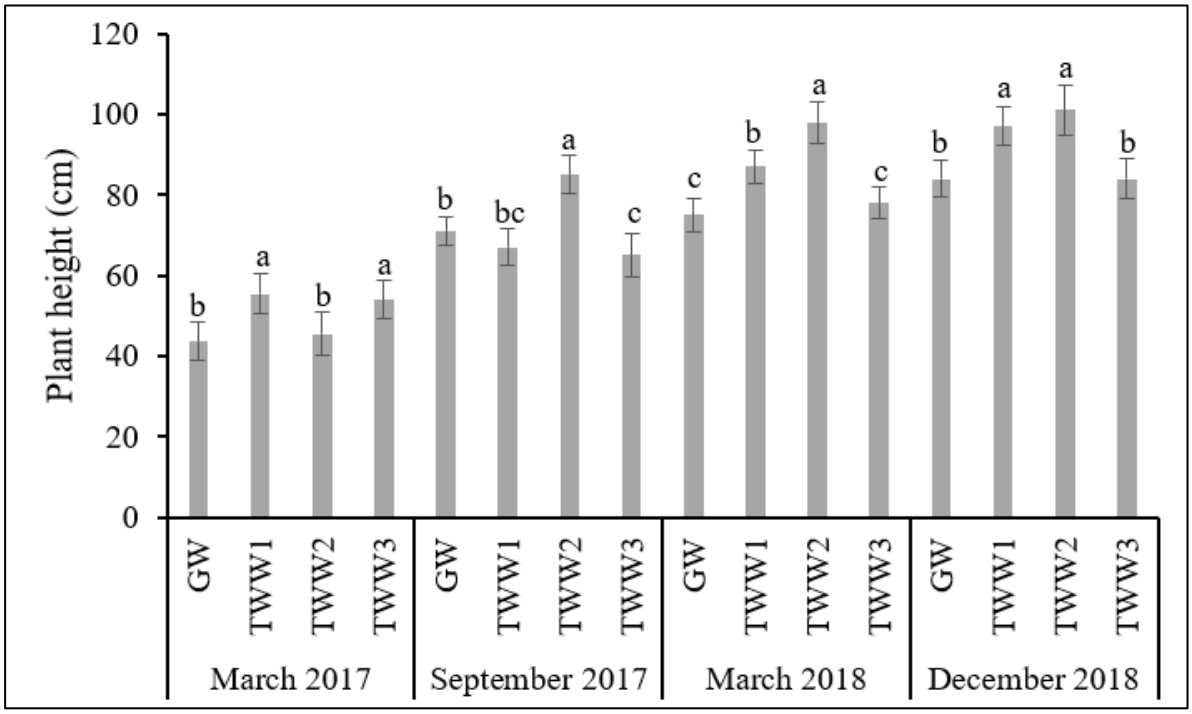

Figure 1. 9. Effect in the length of olive trees after irrigation using groundwater (GW) and different treated wastewaters (TWW1, TWW2 and TWW3). Bars with different letters refer to differences (ANOVA, Tukey's test, $p < 0.05$) between treatments, where the same letter indicates no significant difference.

4. Heavy metals content in soil and olive trees after irrigation

4.1.Heavy metals in soil

Metal concentrations in soil before and after two years of irrigation by GW and TWWs are shown in **Figure 1.10**. Statically significant differences in the heavy metal levels, except Mn and Ni, were registered between soil irrigated with TWWs compared to the soil not irrigated and irrigated with GW. As already mentioned, the TWWs contained high metals quantities compared to permitted

values. Moreover, OM content allowed to sequester trace metals and decrease their mobility and risk of leaching improving as reported by Gwenzi and Munondo (2008), which can enhance the soil quality.

More in detail, Ni showed the lowest concentrations, about 3 mg Kg^{-1}, Cu was in the range of 16-17 mg Kg^{-1}, Cr ranged from 21 to 22 mg Kg^{-1}, Zn from 20 to 22 mg Kg^{-1}, Mn from 50 to 56 mg Kg^{-1}, and Fe around 1.2 g/Kg, thus demonstrating by far the highest level compared to the other elements. The higher contents of Mn and above all Fe in the soil could depend on their lower uptake by plants or, more likely, on a greater accumulation of these metals caused by the TWW used for irrigation, as suggested in previous works (Al-Habahbeh et al., 2021; Dikinya and Areola, 2010). The concentrations of metals in soil were in all cases below the limits established by the European directive (2007/2/EC) (), which are 50-140, 150-300, and 30-75 mg kg^{-1} for Cu, Zn, Ni, respectively. The concentrations of Ni were also in full agreement with the guideline of WHO (107 mg Kg^{-1}) (WHO, 2006).

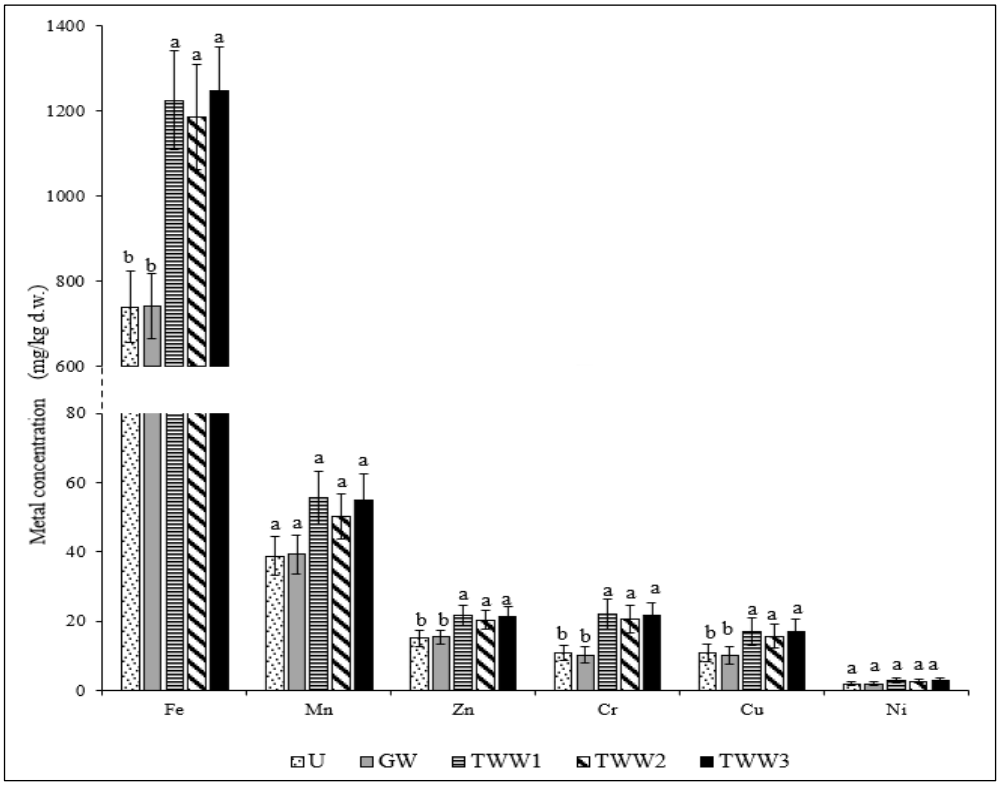

Figure 1.10. Metal contents in soil before (U) and after irrigation using groundwater (GW) and treated wastewaters (TWW1, TWW2 and TWW3). Bars with different letters refer to differences (ANOVA, Tukey's test, $p < 0.05$) between treatments, while the presence of the same letter indicates no significant difference.

The concentrations of Fe, Cu and Zn in soil increased significantly after irrigation with TWWs. This could be the result of the soil cumulative addition of these elements by irrigation as indicated in other researches (Rezapour et al., 2012; Akoto et al., 2015; Bedbabis et al., 2015;). The lowest increase in heavy metal concentrations was found for Mn (less than 30%in soil irrigated with TWW2) followed by Ni that increased by 45, 30 and 40% after irrigation with TWWs 1, 2 and 3, respectively. These results could be related to the lowest content on Ni in the TWWs used for irrigation and also the highest mobility of this element in alkaline soil (Aydin et al. 2015).

The content of Zn in soils irrigated with TWWs has undergone a significant increase compared to its level in soil irrigated with GW. This increase occurred in a shorter time than reported elsewhere. For example, Belaid et al. (2012) reported a significant accumulation of Zn after 17 years of irrigation with TWW. Similarly, Mapanda et al. (2005) found that the Zn content in the soil increased after 10 years of irrigation with TWW.

As regards the behaviour of chromium, previous studies Previous studies conducted by Sakthivel and Vivekanandan (2009) on soils contaminated with tannery waste, have shown that it exists in the soil in the trivalent form, accumulated in the surface layers of the soil, due to its low solubility. Conversely, hexavalent Cr can migrate into deeper soil layers, but usually at lower concentrations. Furthermore, as previously demonstrated, Cr (VI) has carcinogenic effects while Cr (III) is considered an essential trace element in the metabolic processes of cholesterol, glucose and nutrients of succulents (Herath et al., 2017). In our study, the mean total Cr was about 22, 20 and 22 mg/Kg d.w. in land irrigated with TWW1, TWW2 and TWW3 respectively, significantly higher values ($p < 0.05$) than that relating to irrigation with GW (about 10 mg Kg^{-1} d.w).

The results showed a significant difference in the Cu content in soil after irrigation by TWW compared to soil irrigated with GW. This evidence is in agreement with what reported by Abedi-Koupai et al. (2006). However, Saber et al. (1986) showed that irrigation with TWW for 7 years did not significantly affect the amount of Cu in the soil. Furthermore, the clay minerals of the soil, the content of OM and Al, Fe or Mn oxides could stabilize the Cu as verified by pervious work (Adriano, 2001).

In this study, the soil is alkaline (pH is around 8.43) and contains 9.8% clay. These properties should facilitate the absorption of heavy metals through the soil and in particular clay particles, the appearance of insoluble organic complexes or the precipitation of carbonates and metal hydroxides (Christou et al., 2014; Smith et al., 1996).

The phytoavailability of heavy metals depends on numerous condition such as the metal speciation,

the soil characteristics (pH, organic matter content, redox potential, texture, cation exchange capacity), the presence of organometallic chelates and soluble inorganic ion pair species and the species of cultivated plant (Peijnenburg and Jager, 2003; Tack, 2010; Kalavrouziotis et al., 2012). In this study, the soil is alkaline (pH is about 8.43) and contain 9.8% of clay. These properties should facilitate the absorption of heavy metals through the soil and in particular clay particles, the appearance of insoluble organic complexes or the precipitation of carbonates and metal hydroxides (Christou et al., 2014; Smith et al., 1996).

The use of industrial TWW for crop irrigation is a source of considerable concern regarding the possible accumulation of heavy metals contained in these effluents, since the accumulation of heavy metals in the soil determines a potential greater bioavailability for plants and therefore for the human being.

4.2. Heavy metals in plant

The content of heavy metals in shoot and root are presented in **Table 1.10**. The highest levels were registered for Fe in plants irrigated with different TWWs followed by Cu, Mn, Cr, Zn then Ni. The use of industrial TWWs for crops irrigation raises the concern of heavy metals absorption by plants (Heidarpour et al., 2007).

Table 1.10. Metal contents in different parts of olive tree after irrigation using groundwater (GW) and different treated wastewaters (TWWs). Different letters refer to differences (ANOVA, Tukey's test, $p < 0.05$) between treatments, where the same letter indicates no significant difference)

	Root (µg/g d.w.)					
	Fe	Mn	Zn	Cr	Cu	Ni
GW	19.2±0.7^{b}	2.1±0.3^{b}	1.0±0.3^{b}	2.4±0.3^{b}	1.2±0.2^{b}	0.053±0.005^{c}
TWW1	36.2±0.2^{a}	3.8±0.8^{a}	2.0±0.4^{a}	6.5±0.5^{a}	2.5±0.3^{a}	0.091±0.004^{a}
TWW2	36.0±0.4^{a}	3.1±0.3^{ab}	1.8±0.2^{ab}	5.9±0.2^{a}	2.0±0.2^{a}	0.074±0.006^{b}
TWW3	36.2±0.4^{a}	3.7±0.6^{a}	2.0±0.3^{a}	6.3±0.4^{a}	2.4±0.3^{a}	0.082±0.004^{ab}
	Shoot (µg/g d.w.)					
GW	17.4±1.0^{c}	5.2±0.7^{b}	4.4±0.4^{b}	1.4±0.3^{b}	3.1±0.6^{b}	0.2±0.1^{b}
TWW1	29.0±0.8^{a}	8.1±0.5^{a}	6.7±0.6^{a}	3.0±0.6^{a}	6.4±0.7^{a}	0.7±0.2^{a}
TWW2	26.0±0.7^{b}	7.3±0.8^{a}	6.2±0.8^{a}	2.7±0.5^{a}	5.8±0.5^{a}	0.5±0.2^{ab}
TWW3	28.4±0.5^{a}	7.9±0.5^{a}	6.5±0.7^{a}	2.9±0.5^{a}	6.3±0.6^{a}	0.6±0.2^{ab}

± Standard Deviation

Concentrations of Fe and Cr were higher in the roots than in the aerial parts. This result is in agreement with previous studies (Al-Habahbeh et al., 2021) and suggests the protective role of the roots. In fact, roots may act as a barrier that limits the absorption by plants of harmful heavy metals such as Cr or also essential elements, which are however characterized by a certain phytotoxicity (including Fe) and which could be less bioavailable due to their adsorption in the soil (Bazel et al., 1998). Indeed, such interpretations have been proposed in other research (Chen at al., 2016; Rezapour et al., 2019). Friedman et al. (2007) showed that the reduction in the concentration of Fe in the *celosia* leaf compared to that in the root was related to the low adsorption of this element caused by the high pH value and the high chloride content in the TWW used for the irrigation. In fact, TWW1 and TWW3 characterized by high chloride content about 1950 and 1780 mg L^{-1} respectively compared to TWW2 (540 mg L^{-1}). Fe content in shoots of plants irrigated by TWW1 and TWW3 (about 29 and 28 µg g^{-1} d. w) revealed a significant difference compared to those of plants irrigated with TWW2 (26 µg g^{-1} d.w.). However, Fe concentrations in shoot of trees irrigated by different TWWs were below the normal amounts between 40 -150 ppm (Marr and Cresser, 1983). Same result was verified for the Cu content which were about 6.4, 5.8 and 6.3 µg g^{-1} d.w. in shoot of plants irrigated by TWW1, TWW2 and TWW3 respectively. In fact, Cu contents were in

the normal range between 5 and 12 ppm (Marr and Cresser, 1983).

Fe, Mn and Cu contents increased with the increase of soil salinity which was reported also by the study done by Al-Gazzaz (1999) (**Table 1.9**; **Table 1.10**). Furthermore, the irrigation by TWWs increased the OM that could increase the bioavailability of metals. These results may be explained by the contribution of organic complexing molecules of low molecular in the distribution of micronutrients that improve the absorption of heavy metals (Chen and Aviad, 1990). Rupa et al. (2003) verified that the Zn uptake increased in wheat plants with the rise of soil' OM content. Thus, the trace element levels were varied according to the plant uptake, salinity and bio-availability

Moreover, olive tree was considered as an important Zn and Cu bio- accumulator when planted in soil contaminated or enriched by these elements (Wilson and Pyatt, 2007). Mn, Zn, Cu and Ni contents in areal parts were higher than those in roots. However, Zn, Cu and Ni that entrain in the plant' metabolisms, were translocated in shoots (Bidar et al., 2009). Similar results were investigated by Al Absi et al. (2009).

The lowest plant accumulation was recorded for Ni (**Table 1.10**). Indeed, as reported in the study done by Wuana and Okieimen (2011), the accumulation of this carcinogenic element was not known in plants. In fact, alkaline soil adsorbed Ni and reduced its mobility.

As mentioned by previous studies (Khan, 2001; Houben et al 2013; Herath et al., 2017), the cultivation of plant in metal contaminated soil such as Cu, Zn, Mn and Cr could accumulate high quantities of these pollutants in its different parts. The recommended permissible limit content of Cr in crop plant is 10 µg. g^{-1}(Alloway, 2013). Our results showed lower Cr content compared to this permissible value in plants irrigated with different TWWs (**Table 1.10**) Metals concentrations were in the range 8.8, 7.8, 8.7 µg g^{-1} d. w. for Cu; 8.8, 8, 8.5 µg g^{-1} d. w. for Zn and 0.8, 0.6, 0.7 µg g^{-1} d. w. of Ni in plant irrigated with TWW1, TWW2 and TWW3 respectively. All these values were below the permissible levels in crop plant parts which are 10, 100 and 10 ppm for Cu, Zn and Ni respectively (Kabata-Pendias and Mukherjee, 2007). These results verified the absence of particular concern after two years of irrigation by these three industrial TWWs.

4.3. Heavy metal translocation from soil to plant system

The translocation of metals from soil to plants depends on the bioavailability of the metals, which in turn is a function of several soil- or plant-related factors (Shukla et al., 2011). Soil pH, nitrogen bioavailability, soil moisture, temperature, and OM content have an impact on the uptake of heavy metals by plants (Aghabarati et al., 2008). The irrigation using TWWs increased the availability and

distribution of Fe in the soil. This finding was also demonstrated by Khawla et al. (2019). In general, and at a basic pH, Fe^{3+} is characterized by low solubility. Therefore, the Fe^{3+} chelate reductase that reduced Fe^{3+} to Fe^{2+}, increased the solubility and availability of Fe for plant uptake (Yi and Guerinot, 1996). A possible Fe blockage in the transfer process from soil to roots could observed as a result of reduction of Fe^{3+} chelate reductase activity in zone of roots deprived from Fe as demonstrated by Sun et al. (2007).

The mobility of heavy metals is restricted in soil having a pH value above 7, thus decreasing their adsorption by plant (Mapanda et al., 2005). The low plant uptake and low solubility of heavy metals permit its accumulation in soil matrix up to values that can become toxic for the vegetative growth (Chang et al., 1992). However, the plant metal uptake increased with the increase of soil heavy metal contents (**Figure 1.10** and **Table 1.10**) as a result to high apport of these nutrients contained in TWWs used for irrigation. This result is in accordance with previous woks (Yintao et al., 2015) that verified the translocation of these elements from soil to shoots, and by xylem vessels according to Oropeza-Garcia et al. (2014). The transportation of heavy metals has a long way in which these elements mobilized in xylem and stored in leaves cells vacuoles as verified by previous findings (Khawla et al., 2019). This mobilization depends on many parameters such as organic acids and phyto-chelating substances as mentioned by Yang et al. (1997).

5. Conclusion

The evaluation of the effects of irrigation by TWWs on sandy soil characterizations and olive trees growth in the intention of testing its safety for reuse in agriculture. TWWs contained high concentration of some metals that above ethe permissible limits. In addition, after two years of olive irrigation with TWWs characterized by high levels of heavy metals that above the maximum permissible limits, results showed modification of some soil properties such as the increase of EC, OM content, total P, Na, Ca, Mg and K after irrigation with TWWs compared to those in soil irrigated with GW. However, the pH value decreased slightly. Plant growth increased after the use of TWW in irrigation as well as the chlorophyll content that increased the macro and micro-nutrient in soil than in plant. Results include those heavy metal concentrations increased in soil as well as in olive trees, however, their levels did not reach the permissible limits. Based on this study, it may be summarized that the TWWs the short safe reuse of TWW in olive irrigation with the regular reviewer to control the metals accumulation in soil and plants, this TWW reuse may be a good solution for the water scarcity problem and to reduce the refuge to the chemical plant's fertility.

III. Bibliography

Abedi-Koupai, J., Mostafazadeh-Fard, B., Afyuni, M., Bagheri, M. R., 2006. Effect of treated wastewater on soil chemical and physical properties in an arid region. Plant Soil Environ. 52, 335.

Abegunrin, T. P., Awe, G. O., Idowu, D. O., Adejumobi, M. A., 2016. Impact of wastewater irrigation on soil physico-chemical properties, growth and water use pattern of two indigenous vegetables in southwest Nigeria. Catena 139, 167–178.

Adriano, D. C., 2001. Trace elements in terrestrial environments: biogeochemistry, bioavailability, and risks of metals (Vol. 860). New York: Springer.

Aghabarati, A., Hosseini, S. M., Maralian, H., 2008. Heavy metal contamination of soil and olive trees (*Olea europaea* L.) in suburban areas of Tehran, Iran. Res J Environ Sci. 2, 323-329.

Ahmali, A., Mandi, L., Loutfi, K., El Ghadraoui, A., El Mansour, T. E., El Kerroumi, A., Hejjaj, A., Del Bubba, M., Ouazzani, N., 2020. Agro-physiological responses of Koroneiki olive trees (*Olea europaea* L.) irrigated by crude and treated mixture of olive mill and urban wastewaters. Sci. Hort. 263, 109101.

Akoto, O., Addo, D., Baidoo, E., Agyapong, E. A., Apau, J., Fei-Baffoe, B., 2015. Heavy metal accumulation in untreated wastewater-irrigated soil and lettuce (*Lactuca sativa*). Environ. Earth Sci. 74, 6193-6198.

Al-Absi, K. M., Al-Nasir, F. M., Mahadeen, A. Y., 2009. Mineral content of three olive cultivars irrigated with treated industrial wastewater. Agric. Water Manag. 96, 616-626.

Al-Gazzaz, N.M., 1999. Long-term irrigation effect of Khirbit Es-Samra Effluent Water on soil and olive (*Olea europaea* L.) quality. MSc Thesis. Fac. of Sci., Univ. of Jordan.

Al-Habahbeh, K. A., Al-Nawaiseh, M. B., Al-Sayaydeh, R. S., Al-Hawadi, J. S., Albdaiwi, R. N., Al-Debei, H. S., Ayad, J. Y., 2021. Long-Term Irrigation with Treated Municipal Wastewater from the Wadi-Musa Region: Soil Heavy Metal Accumulation, Uptake and Partitioning in Olive Trees. Horticulturae, 7, 152.

Al-Lahham, O., El Assi, N. M., Fayyad, M., 2007. Translocation of heavy metals to tomato (*Solanum lycopersicom* L.) fruit irrigated with treated wastewater. Sci. Hort. 113, 250-254.

Alloway, B. J., 2013. Heavy metals and metalloids as micronutrients for plants and animals. In Heavy metals in soils (pp. 195-209). Springer, Dordrecht.

Assouline, S., Narkis, K., Gherabli, R., Sposito, G., 2016. Combined effect of sodicity and organic matter on soil properties under long-term irrigation with treated wastewater. Vadose Zone J. 15.

Aydin, M. E., Aydin, S., Beduk, F., Tor, A., Tekinay, A., Kolb, M., Bahadir, M., 2015. Effects of long-term irrigation with untreated municipal wastewater on soil properties and crop quality. Environ. Sci. Pollut. Res. 22, 19203-19212.

Bar-Yosef, B., 2011. Major minerals—phosphorus. Use of Treated Wastewater in Agriculture. Impacts on soil, Environment and Crop. Willey-Blackwell, UK, pp. 166–202.

Barroso, M. M., Alvarez, C. E., 1997. Toxicity symptoms and tolerance of strawberry to salinity in the irrigation water. Sci. Hort. 71, 177-188.

Bayer, C., Mielniczuk, J., 1999. Dinâmica e função da matéria orgânica. In: GA, S., FAO, C. (Eds.),

Matéria orgânica do solo: fundamentos e caracterização. Gênesis, Porto Alegre, pp. 9–26 (Abstract in English).

Bedbabis, S., Trigui, D., Ahmed, C. B., Clodoveo, M. L., Camposeo, S., Vivaldi, G. A., Rouina, B. B., 2015. Long-terms effects of irrigation with treated municipal wastewater on soil, yield and olive oil quality. Agric. Water Manag. 160, 14-21.

Bedbabis, S., Rouina, B. B., Boukhris, M., Ferrara, G., 2014. Effect of irrigation with treated wastewater on soil chemical properties and infiltration rate. J. Environ. Manage. 133, 45-50.

Bedbabis, S., Palese, A.M., Ben Rouina, B., Rhouma, A., Gargouri, K., Boukhris, M., 2009. The effect of irrigation with treated wastewater on "chemlali" olive oil quality. J. Food Qual. 32, 141–157.

Belaid, N., Feki, S., Cheknane, B., Frank-Neel, C., Baudu, M., 2019. Impacts of irrigation systems on vertical and lateral metals distribution in soils irrigated with treated wastewater: Case study of Elhajeb-Sfax. Agric. Water Manag. 225, 105739.

Belaid, N., Neel, C., Lenain, J. F., Buzier, R., Kallel, M., Ayoub, T., Ayadi, A., Baudu, M., 2012. Assessment of metal accumulation in calcareous soil and forage crops subjected to long-term irrigation using treated wastewater: case of El Hajeb-Sfax, Tunisia. Agric. Ecosyst. Environ.158, 83-93.

Rouina, B. B., Ch, B. A., Bedbabis, S., Baccari, M., Boukhris, M., 2011. Effects of long-term irrigation with treated wastewater on soil chemical properties, plant nutrient status, growth and oil quality of olive tree. Environment and ecology in the Mediterranean Region. Cambridge Scholars Publishing, Cambridge, 147-156.

Bezel, V. S., Zhuikova, T. V., Pozolotina, V. N., 1998. The structure of dandelion cenopopulations and specific features of heavy metal accumulation. Russ. J. Ecol. 29, 331-337.

Bidar, G., Pruvot, C., Garçon, G., Verdin, A., Shirali, P., Douay, F., 2009. Seasonal and annual variations of metal uptake, bioaccumulation, and toxicity in Trifolium repens and Lolium perenne growing in a heavy metal-contaminated field. Environ. Sci. Pollut. Res. 16, 42-53.

Burton, K. W., Morgan, E. Roig, A., 1983. The influence of heavy metals upon the growth of sitka-spruce in South Wales forests. Plant Soil, 73, 327-336.

Castro, E., Mañas, M. P., Heras, J. D. L., 2011. Effects of wastewater irrigation on soil properties and turfgrass growth. Water Sci. Technol. 63, 1678-1688.

Chandra, R., Kang, H., 2016. Mixed heavy metal stress on photosynthesis, transpiration rate, and chlorophyll content in poplar hybrids. For. Sci. Technol. 12, 55-61.

Chang, A.C., Granato, T.C., Page, A.L., 1992. A methodology for establishing phytotoxicity criteria for Cr, Cu, Ni and Zn in agricultural land application of municipal sewage sludge. J. Environ. Qual. 21, 521–536.

Chartzoulakis, K.S., 2005. Salinity and olive: growth, salt tolerance, photosynthesisand yield. Agric. Water Manage. 78, 108–121.

Chen, Z., Muhammad, I., Zhang, Y., Hu, W., Lu, Q., Wang, W., Huang, B., Hao, M., 2021. Transfer of heavy metals in fruits and vegetables grown in greenhouse cultivation systems and their health risks in Northwest China. Sci. Total Environ. 766, 142663.

Chen, H., Yuan, X., Li, T., Hu, S., Ji, J., Wang, C., 2016. Characteristics of heavy metal transfer and their influencing factors in different soil–crop systems of the industrialization region, China. Ecotoxicol. Environ. Saf. 126, 193-201.

Chen, Y., Aviad, T., 1990. Effects of humic substances on plant growth. Humic substances in soil and crop sciences: Selected readings, 161-186.

Christou, A., Maratheftis, G., Elia, M., Hapeshi, E., Michael, C., Fatta-Kassinos, D., 2016. Effects of wastewater applied with discrete irrigation techniques on strawberry plants' productivity and the safety, quality characteristics and antioxidant capacity of fruits. Agric. Water Manag. 173, 48-54.

Christou, A., Eliadou, E., Michael, C., Hapeshi, E., Fatta-Kassinos, D., 2014. Assessment of long-term wastewater irrigation impacts on the soil geochemical properties and the bioaccumulation of heavy metals to the agricultural products. Environ. Monit. Assess. 186, 4857-4870.

Dantas, B. F., Ribeiro, L. D. S., Aragão, C. A., 2005. Physiological response of cowpea seeds to salinity stress. Rev. Bras. Sementes. 27, 144-148.

Dikinya, O., Areola, O., 2010. Comparative analysis of heavy metal concentration in secondary treated wastewater irrigated soils cultivated by different crops. Int. J. Environ. Sci. Technol. 7, 337-346.

Directive 2007/2/EC of the European Parliament and of the Council of 14 March 2007 establishing an Infrastructure for Spatial Information in the European Community (INSPIRE) (OJ L 108, 25.4.2007, p. 1).

Doerr, S. H., Shakesby, R. A., Dekker, L. W., Ritsema, C. J., 2006. Occurrence, prediction and hydrological effects of water repellency amongst major soil and land-use types in a humid temperate climate. Eur. J. Soil Sci. 57, 741-754.

Doerr, S. H., Llewellyn, C. T., Douglas, P., Morley, C. P., Mainwaring, K. A., Haskins, C., Johnsey, L., Ritsema, C. J., Stagnitti, F., Allinson, G., Ferreira, A. J. D., Keizer, J. J., Ziogas, A. K, Diamantis, J., 2005. Extraction of compounds associated with water repellency in sandy soils of different origin. Soil Res. 43, 225-237.

EEC (1986). Council Directive of 12 June 1986 on the protection of the environment, and in particular of the soil, when sewage sludge is used in agriculture (86/278/EEC). http://eur-lex.europa.eu/legal-content/EN/TXT/PDF/?uri= CELEX:31986L0278&from=EN. Accessed 25 Jun 2013.

El Ghadraoui, A., Ouazzani, N., Saf, C., Ahmali, A., Hejjaj, A., Aziz, F., Del Bubba, M., Mandi, L., 2021. Behaviour of physicochemical and microbiological characteristics of vertical flow constructed wetland substrate after treating a mixture of urban and olive mill wastewaters. Environ. Sci. Pollut. Res. 1- 13.

El Ghadraoui, A., Ouazzani, N., Ahmali, A., El Mansour, T. E. H., Aziz, F., Hejjaj, A., Mandi, L., 2020. Treatment of olive mill and municipal wastewater mixture by pilot scale vertical flow constructed wetland. Desalination Water Treat. 198, 126-139.

Erel, R., Eppel, A., Yermiyahu, U., Ben-Gal, A., Levy, G., Zipori, I., Schaumann, G. E., Mayer, O., Dag, A., 2019. Long-term irrigation with reclaimed wastewater: Implications on nutrient management, soil chemistry and olive (*Olea europaea* L.) performance. Agric. Water Manag. 213, 324-335.

Erel, R., Yermiyahu, U., Yasuor, H., Cohen Chamus, D., Schwartz, A., Ben-Gal, A., Dag, A., 2016. Phosphorous nutritional level, carbohydrate reserves and flower quality in olives. PLoS One. 11, e0167591.

Friedman, H., Bernstein, N., Bruner, M., Rot, I., Ben-Noon, Z., Zuriel, A., Zuriel, R., Finkelstein, S., Umiel, N., Hagiladi, A., 2007. Application of secondary-treated effluents for cultivation of sunflower (*Helianthus annuus* L.) and celosia (*Celosia argentea* L.) as cut flowers. Sci. Hortic. 115, 62-69.

Gargouri, K., 1998. Fertilité des sols et nutrition phospho-potassique de l'olivier (Olea europaea L.) en Tunisie. Mémoire de fin d'études du cycle de spécialisation de l'INAT. 82 p. (Unpublished).

Geilfus, C. M., 2018. Review on the significance of chlorine for crop yield and quality. Plant Sci. J. 270, 114 – 122.

Guadie, A., Yesigat, A., Gatew, S., Worku, A., Liu, W., Ajibade, F. O., Wang, A., 2021. Evaluating the health risks of heavy metals from vegetables grown on soil irrigated with untreated and treated wastewater in Arba Minch, Ethiopia. Sci. Total Environ. 761, 143302.

Gwenzi, W., Munondo, R., 2008. Long-term impacts of pasture irrigation with treated sewage effluent on nutrient status of a sandy soil in Zimbabwe. Nutr. Cycl. Agroecosyst. 82, 197-207.

Heidarpour, M., Mostafazadeh-Fard, B., Koupai, J. A., Malekian, R., 2007. The effects of treated wastewater on soil chemical properties using subsurface and surface irrigation methods. Agric. Water Manag. 90, 87-94.

Herath, I., Iqbal, M. C. M., Al-Wabel, M. I., Abduljabbar, A., Ahmad, M., Usman, A. R., Ok, Y. S., Vithanage, M., 2017. Bioenergy-derived waste biochar for reducing mobility, bioavailability, and phytotoxicity of chromium in anthropized tannery soil. J. Soils Sediments. 17, 731-740.

Houben, D., Evrard, L., Sonnet, P., 2013. Beneficial effects of biochar application to contaminated soils on the bioavailability of Cd, Pb and Zn and the biomass production of rapeseed (*Brassica napus* L.). Biomass Bioenergy. 57, 196-204.

Jaramillo, M. F., Restrepo, I., 2017. Wastewater reuse in agriculture: A review about its limitations and benefits. Sustainability, 9, 1734.

Kabata-Pendias, A., Mukherjee, A. B., 2007. Trace elements of group 12 (Previously group IIb). Trace elements from soil to human, 283-319.

Kalavrouziotis, I. K., Koukoulakis, P., Kostakioti, E., 2012. Assessment of metal transfer factor under irrigation with treated municipal wastewater. Agric. Water Manag. 103, 114-119.

Kato, M., Shimizu, S., 1985. Chlorophyll metabolism in higher plants VI. Involvement of peroxidase in chlorophyll degradation. Plant Cell Physiol. 26, 1291-1301.

Keunen, E., Remans, T., Bohler, S., Vangronsveld, J., Cuypers, A., 2011. Metal-induced oxidative stress and plant mitochondria. Int. J. Mol. Sci. 12, 6894-6918.

Keutgen, A. J., Pawelzik, E., 2009. Impacts of NaCl stress on plant growth and mineral nutrient assimilation in two cultivars of strawberry. Environ. Exp. Bot. 65, 170-176.

Khan, A. G., 2001. Relationships between chromium biomagnification ratio, accumulation factor, and mycorrhizae in plants growing on tannery effluent-polluted soil. Environ. Int. 26, 417-423.

Khawla, K., Besma, K., Enrique, M., Mohamed, H., 2019. Accumulation of trace elements by corn (*Zea mays*) under irrigation with treated wastewater using different irrigation methods. Ecotoxicol. Environ. Saf. 170, 530-537.

Kiziloglu, F. M., Turan, M., Sahin, U., Kuslu, Y., Dursun, A., 2008. Effects of untreated and treated wastewater irrigation on some chemical properties of cauliflower (*Brassica olerecea* L. var. botrytis) and red cabbage (*Brassica olerecea* L. var. rubra) grown on calcareous soil in Turkey. Agric. Water Manag. 95, 716-724.

Kumar, A., Arienzo, M., Quayle, W. C., Christen, E., Grocke, S., Fattore, A., Doan, H., Gonzago, D., Zandonna, R., Bartrop, K., Smith, L., Correll, R., Kookana, R., 2009. Developing a systematic approach to winery wastewater management: Final report to Grape and Wine Research & Development Corporation. Project number: CSL05/02.

Küpper, H., Küpper, F., Spiller, M., 1996. Environmental relevance of heavy metal substituted chlorophylls using the example of water plants. J. Exp. Bot. 47, 259-266.

Laribi, A., Alzubaidi, A. H., 2007. Etat Du Magnesium Dans Quelques Sols Sales Du Sud Et Du Centre De L\'Irak. Agron. Afr. 19, 187-195.

Maleva, M. G., Nekrasova, G. F., Borisova, G. G., Chukina, N. V., Ushakova, O. S., 2012. Effect of heavy metals on photosynthetic apparatus and antioxidant status of *Elodea*. Russ. J. Plant Physiol. 59, 190-197.

Mapanda, F., Mangwayana, E. N., Nyamangara, J., Giller, K. E., 2005. The effect of long-term irrigation using wastewater on heavy metal contents of soils under vegetables in Harare, Zimbabwe. Agric Ecosyst Environ. 107, 151-165.

Marr, I. L., Cresser, M. S., 1983. Environmental chemical analysis. International Textbook Company (Blackie Publishing Group) New York, USA.

McGrath, S. P., Brookes, P. C., Giller, K. E., 1988. Effects of potentially toxic metals in soil derived from past applications of sewage sludge on nitrogen fixation by *Trifolium repens* L. Soil Biol. Biochem. 20, 415-424.

Memon, S.A., Hou, X., Wang, L.J., 2010. Morphological analysis of salt stress response of pak Choi. Elec. J. Env. Agricult. Food Chem. 9, 248-254.

Miltner, A., Bombach, P., Schmidt-Brücken, B., Kästner, M., 2012. SOM genesis: Microbial biomass as a significant source. Biogeochemistry, 111, 41–55.

Morugán-Coronado, A., García-Orenes, F., Mataix-Solera, J., Arcenegui, V., Mataix-Beneyto, J., 2011. Short-term effects of treated wastewater irrigation on Mediterranean calcareous soil. Soil Tillage Res. 112, 18-26.

Natsheh, B., 2021. Impact of Short Term Irrigation with Different Water Types on Some Chemical and Physical Soil Properties. Open J. Soil Sci. 11, 389-401.

Ondrašek, G., Romić, D., Romić, M., Duralija, B., Mustač, I., 2006. Strawberry growth and fruit yield in a saline environment. Agric. Conspec. Sci. 71, 155-158.

Oropeza-Garcia, N., Hausler, R., Glaus, M., Vega-Azamar, R., Romero-Lopez, R., 2014. Transport of heavy metals in materials with diameter analogous to xylem vessels. Int. J. Environ. Res. 8, 123–132.

Peijnenburg, W. J. G. M., Jager, T., 2003. Monitoring approaches to assess bioaccessibility and bioavailability of metals: matrix issues. Ecotoxicol. Environ. Saf. 56, 63-77.

Petousi, I., Fountoulakis, M. S., Saru, M. L., Nikolaidis, N., Fletcher, L., Stentiford, E. I., Manios, T., 2015. Effects of reclaimed wastewater irrigation on olive (*Olea europaea* L. cv. 'Koroneiki') trees. Agric. Water Manag. 160, 33–40.

Rattan, R. K., Datta, S. P., Chhonkar, P. K., Suribabu, K., Singh, A. K., 2005. Long-term impact of irrigation with sewage effluents on heavy metal content in soils, crops and groundwater—a case study. Agric Ecosyst Environ. 109, 310-322.

Rezapour, S., Atashpaz, B., Moghaddam, S. S., Damalas, C. A., 2019. Heavy metal bioavailability and accumulation in winter wheat (*Triticum aestivum* L.) irrigated with treated wastewater in calcareous soils. Sci. Total Environ. 656, 261-269.

Rezapour, S., Samadi, A., Khodaverdiloo, H., 2012. Impact of long-term wastewater irrigation on variability of soil attributes along a landscape in semi-arid region of Iran. Environ. Earth Sci. 67, 1713-1723.

Rupa, T. R., Rao, C. S., Rao, A. S., Singh, M., 2003. Effects of farmyard manure and phosphorus on zinc transformations and phyto-availability in two alfisols of India. Bioresour. Technol. 87, 279-288.

Rusan, M. J. M., Hinnawi, S., Rousan, L., 2007. Long-term effect of wastewater irrigation of forage crops on soil and plant quality parameters. Desalination, 215, 143-152.

Saber, M. S., 1986. Prolonged effect of land disposal of human wastes on soil conditions. Water Sci. Technol. 18, 371-374.

Sahay, S., Iqbal, S., Inam, A., Gupta, M., Inam, A., 2019. Waste water irrigation in the regulation of soil properties, growth determinants, and heavy metal accumulation in different *Brassica* species. Environ. Monit. Assess. 191,107.

Sakthivel, V., Vivekanandan, M., 2009. Reclamation of tannery polluted soil through phytoremediation. Physiol. Mol. Biol. Plants. 15, 175-180.

Schacht, K., Chen, Y., Tarchitzky, J., Lichner, L., Marschner, B., 2014. Impact of treated wastewater irrigation on water repellency of Mediterranean soils. Irrig. Sci., 32, 369-378.

Schmidt, M. W., Torn, M. S., Abiven, S., Dittmar, T., Guggenberger, G., Janssens, I. A., Kleber, M., Kögel-Knabner, I., Lehmann, J., Manning, D. A. C., Nannipieri, P., Rasse, D. P., Weiner S., Trumbore, S. E., 2011. Persistence of soil organic matter as an ecosystem property. Nature, 478, 49-56.

Shukla, S. K., Singh, K., Singh, B., Gautam, N. N., 2011. Biomass productivity and nutrientavailability of *Cynodon dactylon* (L) Pers. growing on soils of different sodicity stress. Biomass Bioenergy 35, 2440–3447.

Singh, S., Parihar, P., Singh, R., Singh, V. P., Prasad, S. M., 2016. Heavy metal tolerance in plants: role of transcriptomics, proteomics, metabolomics, and ionomics. Front. Plant Sci. 6, 1143.

Sinha, S., Saxena, R., Singh, S., 2002. Comparative studies on accumulation of Cr from metal solution and tannery effluent under repeated metal exposure by aquatic plants: its toxic effects. Environ. Monit. Assess. 80, 17-31.

Smith, C. J., Hopmans, P., Cook, F. J., 1996. Accumulation of Cr, Pb, Cu, Ni, Zn and Cd in soil following irrigation with treated urban effluent in Australia. Environ. Pollut. 94, 317-323.

Srivastava, G., Kumar, S., Dubey, G., Mishra, V., Prasad, S. M., 2012. Nickel and ultraviolet-B stresses induce differential growth and photosynthetic responses in *Pisum sativum* L. seedlings. Biol Trace Elem Res. 149, 86-96.

Suarez, D. L., Wood, J. D., Lesch, S. M., 2006. Effect of SAR on water infiltration under a sequential rain–irrigation management system. Agric. Water Manag. 86, 150-164.

Sun, B.T., Jing, Y., Chen, K.M., Song, L.L., Chen, F.J., Zhang, L.X., 2007. Protective effect of nitric oxide on iron deficiency-induced oxidative stress in maize (Zea mays). J. Plant Physiol. 164, 536–543.

Tack, F. M., 2010. Trace elements: general soil chemistry, principles and processes. Trace elements in soils, 9-37.

Tarchitzky, J., Lerner, O., Shani, U., Arye, G. L. A. A., Lowengart-Aycicegi, A., Brener, A., Chen, Y. J. E. J. O. S. S., 2007. Water distribution pattern in treated wastewater irrigated soils: hydrophobicity effect. Eur. J. Soil Sci. 58, 573-588.

WHO. Guidelines for the Safe Use of Wastewater, Excreta and Greywater; World Health Organization: Geneva, Switzerland, 2006; Volume 2.

Wilson, B., Pyatt, F. B., 2007. Heavy metal bioaccumulation by the important food plant, Olea europaea L., in an ancient metalliferous polluted area of Cyprus. Bull Environ Contam Toxicol. 78, 390-394.

Woldetsadik, D., Drechsel, P., Keraita, B., Itanna, F., Gebrekidan, H., 2017. Heavy metal accumulation and health risk assessment in wastewater-irrigated urban vegetable farming sites of Addis Ababa, Ethiopia. Int. J. Food Contam. 4, 1-13.

Wuana, R. A., Okieimen, F. E., 2011. Heavy metals in contaminated soils: a review of sources, chemistry, risks and best available strategies for remediation. International Scholarly Research Notices, 2011.

Yang, X.E., Baligar, V.C., Foster, J.C., Martens, D.C., 1997. Accumulation and transport of nickel in relation to organic acids in ryegrass and maize grown with different nickel levels. Plant Soil 196, 271–276.

Yi, Y.L., Guerinot, M.L., 1996. Genetic evidence that induction of root Fe (III) chelate reductase activity is necessary for iron uptake under iron deficiency. Plant J. 10, 835–844.

Yintao, L., Hong, Y., Dan, S., Yichen, J., Shichao, Z., Jun, Y., 2015. Heavy metal residues in soil and accumulation in maize at Long-term wastewater irrigation area in Tongliao. China J. Chem. 1–9.

Part 2

Evaluation of sewage sludge ash performance in the retention of copper ions from aqueous solution using quality-by-design approach

I. Characterization of sewage sludge ash

1. Specific surface area

The specific surface area of SSA is 17.94 m² /g and the pore average width is 11.92 nm. Based on literature data, the feedstock biomass used for the ash production seems to affect the porosimetry characteristics. In fact, fly ash prepared from the combustion of the lignite recovered from the cyclones and electrostatic filters of a power plant was about 10.20 m²/g (Papandreou et al. 2007), while the BET surface area of the bottom ash from the incineration of expired drugs was 18.42 m²/g (Benzaoui et al. 2018). Moreover, previous studies showed that the specific surface area is generally higher in ashes obtained from vegetal feedstocks such as rice husk (47.47 m²/g) (Wang et al. 2010), pomace (146.4 m²/g) (Bouzid et al. 2008) and bagasse (470 m²/g) (Gupta and Sharma, 2003), compared to those obtained from sewage sludge. In fact, ashes obtained by incineration of sewage sludge during 2 hours under 600°C had surface areas of 31.6 m²/g (El-Sheltawy et al. 2016), 50.85 m²/g (Bouzid et al. 2008) and 4.13 m²/g (Wang et al. 2019). It should be however mentioned that other experimental conditions, such as temperature may affect specific surface area of ash (Chandrasekhar and Pramada, 2006).

The Dubinin-Radushkevich (DR) equation (McEnaney, 1987) was the method commonly used for the calculation of micropores volume. However, the BET equation was employed for the analysis of the sorbent specific surface area. **Figure 2.1** represents the nitrogen adsorption/desorption isotherm which demonstrates the type IV isotherms and H3 hysteresis loop indicating ink-bottle pores structure (Ruthven, 1984) and showing the remarkable presence of mesopores (2 nm < pore diameter < 50 nm) in the ash, according to the IUPAC classification (Pezoti et al., 2014).

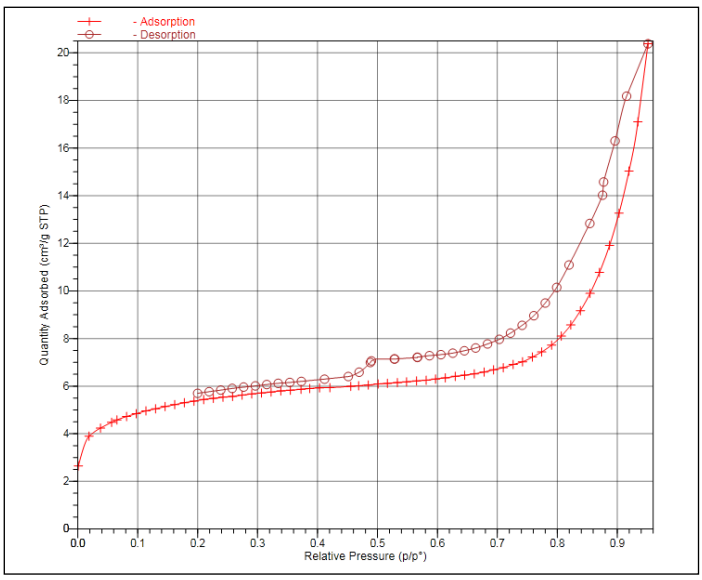

Figure 2.1. Nitrogen adsorption/desorption isotherm of sewage sludge ash.

2. Scanning electrical microscopy (SEM)

Figure 2.2 shows the morphology of the SSA, which was characterized by a remarkable irregular shape. In fact, the carbonization at 600°C released small percentage of volatile matter from the sewage sludge, which produced a partially porous surface (Asadieraghi and Wan Daud, 2014). SSA characterized by a granularity form with common feature of porous that could be the result of the significant melting points of SiO_2 and Fe_2O_3 as reported by Deng et al. (2020).

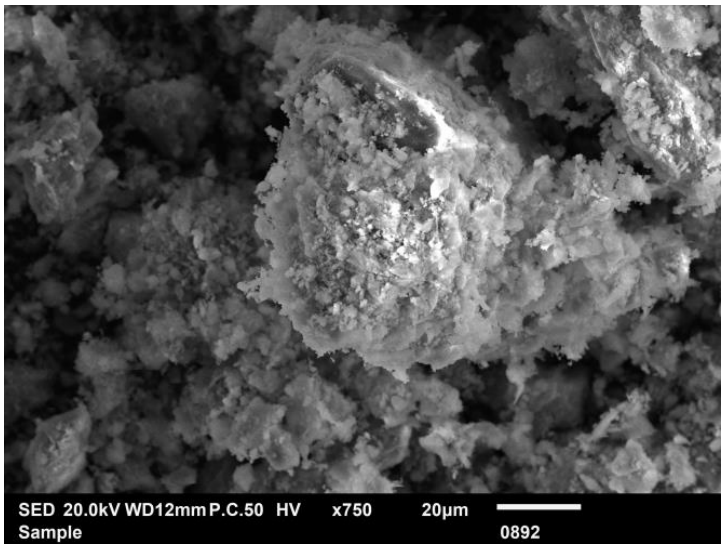

Figure 2.2. Scanning electron microscope image of sewage sludge ash.

3. Metal content

Table 2.1 shows the heavy metals content of SSA. No significant amounts of heavy metals were found in the prepared sorbent. This is probably due to the nature of WW entering the WWTP. The copper concentration of SSA was 1.51 mg/Kg, which was much lower than those reported by Pan et al (2003) and Khanbilvardi and Afahari (1994), being them about 3 and 19.3 g/Kg respectively.

Table 2.1. Metal contents of sewage sludge ash.

Metal	Pb	Ni	Cu	Cd	Zn
Concentration (mg/kg)	0.18	0.16	1.51	0.07	1.6

4. pH of the point zero charge

The pH of point zero charge corresponds to the pH value for which, the net charge of the surface of the adsorbents is zero. This parameter is very important in adsorption phenomena, especially when electrostatic forces are involved in the sorption mechanisms. Graphically, this parameter corresponds to the point of intersection of the curve obtained with the first bisector. **Figure 2.3** shows that the pH_{pzc} of the SSA is equal to 2.2**.** The adsorption of copper by SSA could be then effectuated by cation exchange mechanism as reported by Rio et al. (2005) and verified also by

Seredych and Bandosz (2006). These authors indicated that the sludge ash obtained at a carbonization temperature about 650°C contained Mg and Zn in the crystalline aluminosilicate phase produced during the thermal treatment, that can play a role in the cations exchange mechanism leading to the copper adsorption.

In particular, the incineration of SS resulted in the formation of oxides with an acidic (SiO_2), amphoteric (Fe_2O_3 and Al_2O_3) or basic character (MgO, CaO, Na_2O and K_2O). Indeed, in previous studies, for ash from silica, alumina, and iron oxide, pH_{pzc} were 2.0, 6.7, and 8.5, respectively (Stumm et Morgan, 1996; Elouear et al., 2009). Therefore, the low zero charge pH value can be attributed to the high presence of silica compared to alumina and iron oxide and the adsorption of copper on SSA could be explained by the interaction with silica, with low contributions of aluminium and iron oxides adsorption sites (Elouear et al., 2009).

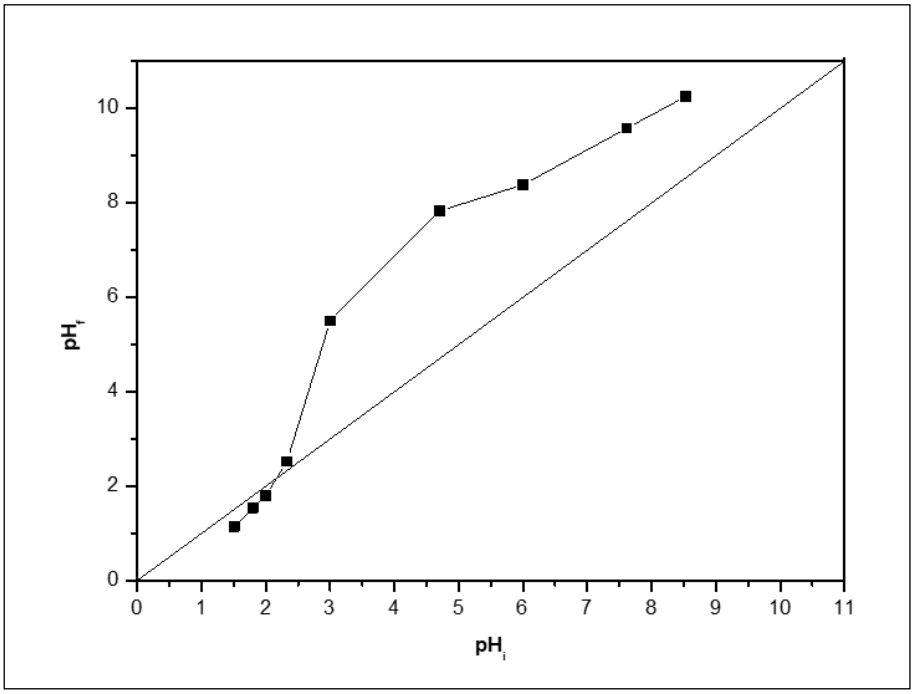

Figure 2.3. Value of the pH of point of zero charge of sewage sludge ash.

5. Fourier transform infrared spectroscopy

The analysis of materials by Fourier Transform Infrared Spectroscopy (FTIR) permits to identify the main chemical functions present on the surface of the adsorbent, as well as determining the possible changes of these functional groups' characteristic of the support after treatment of the basic material. These groups are often responsible for the adsorbent-adsorbate bonds. Infrared analysis spectra of raw materials and prepared ash are shown in **Figure 2.4**. The mass losses caused by the heating of the sewage sludge reduced the concentration of mineral components and modified the

structure of organic matter, which caused a difference between the spectra of ash and dry sludge FTIR (Cao and Harris, 2010).

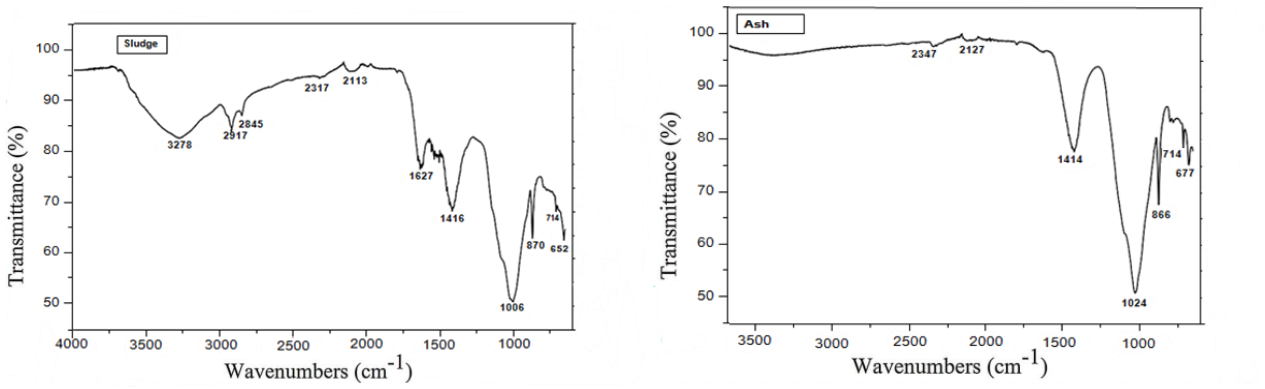

Figure 2.4. FTIR of the raw sewage sludge and the prepared sewage sludge ash.

The FTIR spectra of SS and SSA showed similar bands in the range 600-750 cm^{-1} that could be attributed to in-plane and out-plane aromatic ring deformation vibrations, C-C and C-H stretching (Jaria et al., 2017), a low intensity band at 714 cm^{-1} and moderate intensity bands around 1415 cm^{-1} probably related to CO_3 vibrations of calcium carbonate (El Ouazzani et al., 2012; Aboulayt et al., 2017). Also, strong elongation at 1004 and 1024 cm^{-1} in the FTIR spectra of SS and SSA respectively could be related to the vibrations of the Si-O bond (Xu et al., 2017).

Comparing the two spectra, incineration of sludge caused the disappearance of the following bands. (i) Band at 1627 that can be attributed to the stretching of C=C groups and/or the bending of N-H groups. (ii) Bands around 2845 and 2917 cm^{-1}, corresponding to the stretching of C-H bonds of saturated or unsaturated aliphatic groups (Zhang and Wang, 2018). (iii)

Broad band, observed around 3278 cm^{-1} in the sludge spectrum and attributable to the stretching of the hydroxyl group (Lautrette, 2004) and/or chemisorbed water (Calisto et al., 2014).

II. Adsorption

1. Effect of process parameters on the adsorption of copper ions

The matrix of the experimental design and the results obtained for the response variables are shown in **Table 2.2**. The methodology used for analysing results consists of establishing a mathematic model for the response parameter to estimate the coefficients of the established model (see **Table S2.2**) and to determine the residuals (differences between the obtained values and values predicted by the model) (See **Table S2.3**), based on the easy-to use least squares method implemented by specialized software.

Table 2.2. Experimental design matrix and corresponding responses.

Experiment	Time (min)	pH	Adsorbent mass (g)	Copper concentration (mg/L)	Adsorption capacity (mg/g)	Removal %
1	30	3	1.1	30	2.675	98.083
2	90	3	1.1	30	2.704	99.147
3	30	5	1.1	30	2.503	91.78
4	90	5	1.1	30	2.504	91.813
5	30	4	0.1	30	20.715	69.05
6	90	4	0.1	30	21.694	72.313
7	30	4	2.1	30	1.411	98.77
8	90	4	2.1	30	1.412	98.84
9	30	4	1.1	10	0.950	104.5
10	90	4	1.1	10	0.953	104.83
11	30	4	1.1	50	4.479	98.538
12	90	4	1.1	50	4.486	98.692
13	60	3	0.1	30	19.785	65.95
14	60	5	0.1	30	20.382	67.94
15	60	3	2.1	30	1.311	91.77
16	60	5	2.1	30	1.417	99.19
17	60	3	1.1	10	0.655	72.05
18	60	5	1.1	10	0.905	99.55
19	60	3	1.1	50	4.164	91.608
20	60	5	1.1	50	4.208	92.576
21	60	4	0.1	10	8.39	83.9
22	60	4	2.1	10	0.498	104.58
23	60	4	0.1	50	14.546	29.092
24	60	4	2.1	50	2.351	98.742
25	60	4	1.1	30	2.696	98.853
26	60	4	1.1	30	2.698	98.927
27	60	4	1.1	30	2.695	98.817
28	60	4	1.1	30	2.697	98.89
29	43	3.7	0.9	26	2.563	88.719
30	77	3.7	0.9	26	2.567	88.858
31	60	4.6	0.9	26	2.77	95.885
32	60	4	1.8	26	2.11	146.077
33	60	4	1.1	44	4.054	101.35

2. Statistical analysis of results: significance of the coefficients and model validity

The parametric statistical tests were based on the calculation of the standard deviation σ, estimated by repeatability tests, which allow to evaluate the quality of the model (descriptive and predictive), its validation (analysis of variance) and significance of the coefficients (Student test). **Table 2.3.** shows the coefficients values, their standard deviations, t-student and p-value. These parameters

allowed to determine the factors influencing the multiple regression model response.

Table 2.3. The significance of the operational variables on the adsorption capacity (coefficient analysis table)**.**

	Coefficient	Standard deviation	t. exp.	P-value %
b_0	2.302	0.000496	4643	< 0.01 ***
b_1	0.078	0.000364	215.33	< 0.01 ***
b_2	0.064	0.000364	176.92	< 0.01 ***
b_3	-7.874	0.000364	-21657.53	< 0.01 ***
b_4	1.93	0.000364	5310	< 0.01 ***
b_{11}	0.993	0.000487	2042	< 0.01 ***
b_{22}	0.596	0.000487	1225	< 0.01 ***
b_{33}	7.151	0.000486	14719	< 0.01 ***
b_{44}	-1.299	0.000485	-2678.18	< 0.01 ***
b_{12}	-0.0005	0.000641	-0.79	48.80
b_{13}	-0.239	0.000643	-373.07	< 0.01 ***
b_{23}	-0.131	0.000643	-203.92	< 0.01 ***
b_{14}	0.004558	0.000644	7.08	0.58
b_{24}	-0.057995	0.000644	-90.05	< 0.01 ***
b_{34}	-1.191464	0.000644	-1849.99	< 0.01 ***

* Significant with 95% (P<0.05); ** Significant with 99% (P<0.1); *** Significant with 99.9% (P<0.001)

The calculation of the factor's coefficients and their interactions and significance allowed to predict the polynomial model which is presented by the equation corresponding to the adsorption capacity.

The examination of **Table 2.3** reveals that for the linear coefficients, the factor X_3 is the most important coefficient in this model. The negative sign of the coefficient b_3 (-7.874) proves that for a low mass (X_3) the maximum capacity is optimal. The following significant factor is X_4 (b_4 = 1.93). The increase of this factor (X_4) is accompanied with the increase of the response Y_1. The coefficients b_1 and b_2 attributed respectively to the linear effects of X_1 and X_2 factors are of lesser importance compared to the linear effect of factor X_4 which shows that the contact time (X_1) and pH of the reaction medium (X_2) present less importance and less significance level than that caused by the concentration of the synthetic metalliferous solution (X_4). For the quadratic coefficients, the factor 3 (b_{33}) is the most influential parameter followed by X_4 (b_{44}). The interaction effects verify that for each interaction between parameter 3 and another parameter, the corresponding coefficient is quite large and its effect on the calculated response is significant. However, all the interactions between factors 1 and 2 (b_{12}, b_{14}) are not significant. These results confirm that the adsorbent mass factor (X_3) and copper ion concentration factor (X_4) represent the most important determinant factors of adsorption capacity.

To verify the validity of the model, it is necessary to ensure that there is no correlation between the data of the analysis. The residues which represent the vertical distance between each point of a

scatter plot and the regression line passing through the plot showed a random dispersion (See **Figure S2.1**), which leads to conclude the validity of the model.

3. Model quality evaluation

Analysis Of Variance or ANOVA allowed to compare the variances of the values calculated by the model and the residues. ANOVA is required to judge the representativeness of the model as well as the significance of the regression. In this analysis, it should be noted that, the sum of the squares attributed to the total variation evaluated with 32 degrees of freedom are divided into a sum of two variations. One of them is due to regression, which is estimated with 14 degrees of freedom, while the other regards the residual variation and is estimated with 18 degrees of freedom, as defined in **Table 2.4**.

Table 2.4. Regression analysis for response Y_1.

Sources of variation	Sum of squares	Degrees of freedom	Mean square	Report	P-value
Regression	1201	14	85.785	15.145	<0.01***
Residues	101.953	18	5.664		
Total	1302.95	32			

Fischer ratio (F) which is about 15.14, is higher than the critical value [$F_{0.\ 0.01}(14.18) = 3.27$] of the distribution F at 99% confidence level and at 14 and 18 degrees of freedom. Therefore, Regression is very significant and the model is considered representative of the process studied. Using the experimental data, the theorical mathematic model was created:

$$Y_1=2.302+0.078* X_1+0.064 * X_2-7.874 * X_3+1.98* X_4+0.993 * X_1^2 +0.596 * X_2^2+ 7.151 * X_3^2-1.299 * X_4^2- 0.239 * (X_1* X_3) -0.131 * (X_2 * X_3) - 0.058 * (X_2* X_4) - 1.191 * (X_3* X_4)$$

The coefficient of determination of the multilinear regression R^2 is equal to 0.92 and is higher than adjusted coefficient of determination R^2_{adj} which is 0.86. Then, the model exhibits a good fit for the measured response

4. Effects of different parameters on the copper removal from aqueous solution

Figure 2.5 shows that the iso-response curves described an elliptical shape, demonstrating that the adsorption of copper does not follow a simple linear trend as a function of pH and contact time, and highlighting the importance of the multivariate investigation for understanding this kind of processes. Based on the isoresoponse curve, the best contact time was in the low values of the investigated range (30-90 min). This result was confirmed by previous studies done by Banerjee et al., (2012) which explained that the rapidity of the copper ions removal is related to their mobility in the solution. Wang et al. (2019) explained this result by the saturation of the vacant sites on the

ash surface by metals in the first step of the adsorption process, followed by the establishment of repulsive forces among metal ions, thus limiting the fixation of more ions in the sorbent surface.

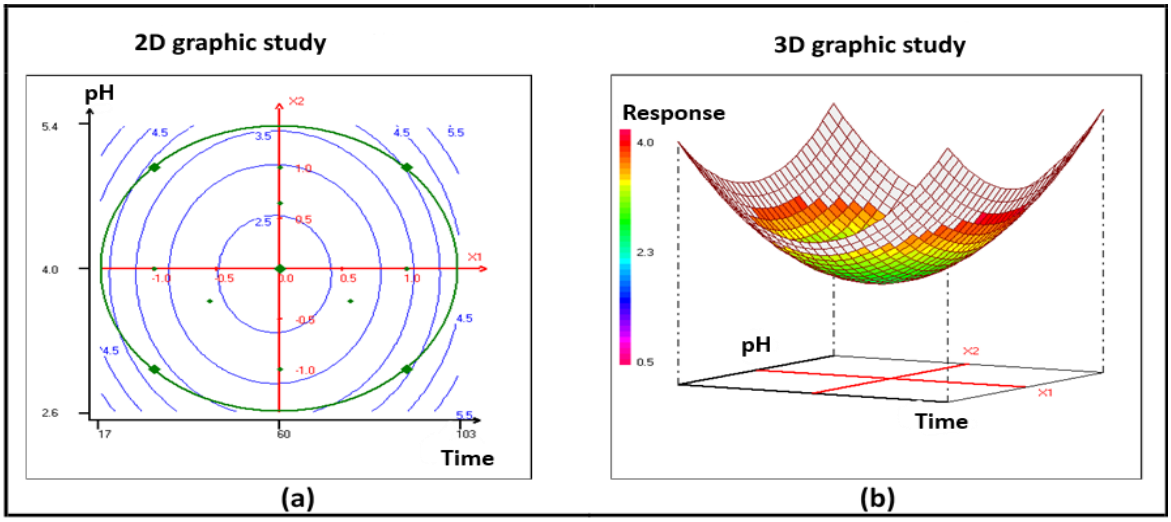

Figure 2.5. Isoresponse curves (a) and response surface (b) of the adsorption capacity (q_m (mg/g)) with the variation of contact time and pH using 1.1 g of SSA and 30 mg/L of copper ions.

According to these researchers, the short equilibrium time of copper adsorption could be related to the driving force for mass transfer from liquid phase to solid phase, which decreases with increasing contact time. Hence, contact time was considered a weak influence on the copper adsorption process since the adsorption equilibrium was reached even after a short contact time. **Figures 2.6**, **2.7,** and **2.8** show that the quantity of adsorbed ions varied considerably as a function of the adsorbent mass.

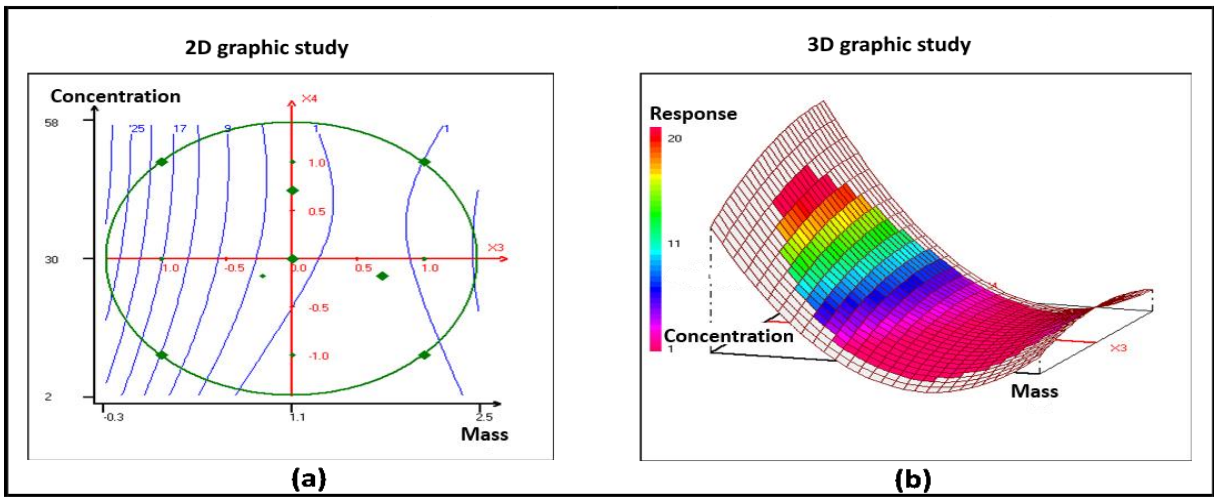

Figure 2.6. Isoresponse curves (a) and response surface (b) of the adsorption capacity (q_m (mg/g)) with the variation of SSA mass (g) and copper concentration (mg/L) using 60 min as contact time and pH=4.

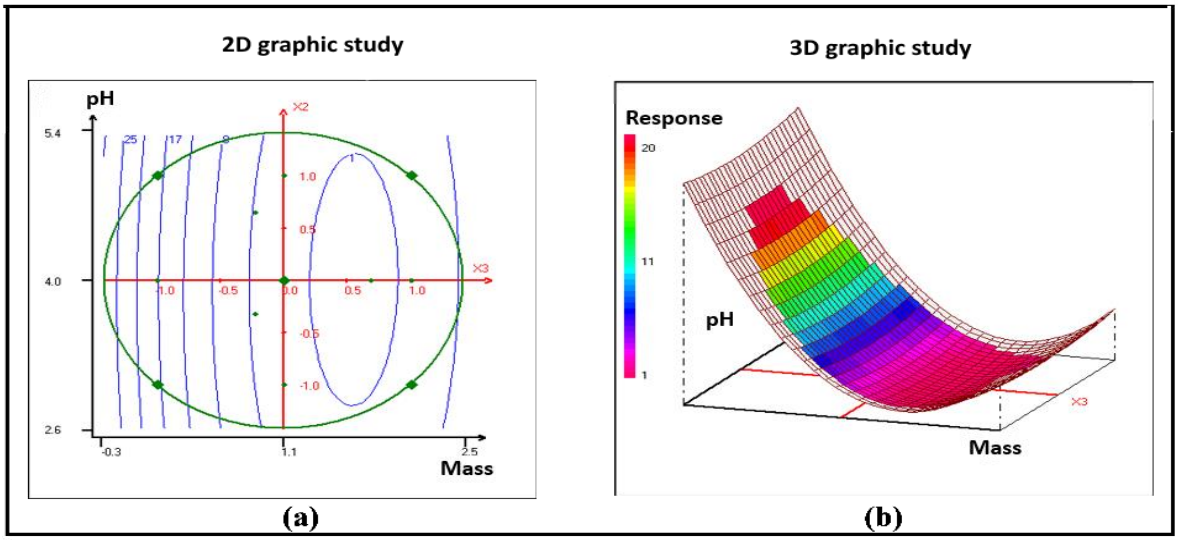

Figure 2.7. Isoresponse curves (a) and response surface (b) of the adsorption capacity (q_m (mg/g)) with the variation of SSA mass (g) and pH using 60 min as contact time and 30 mg/L as initial concentration of copper ions.

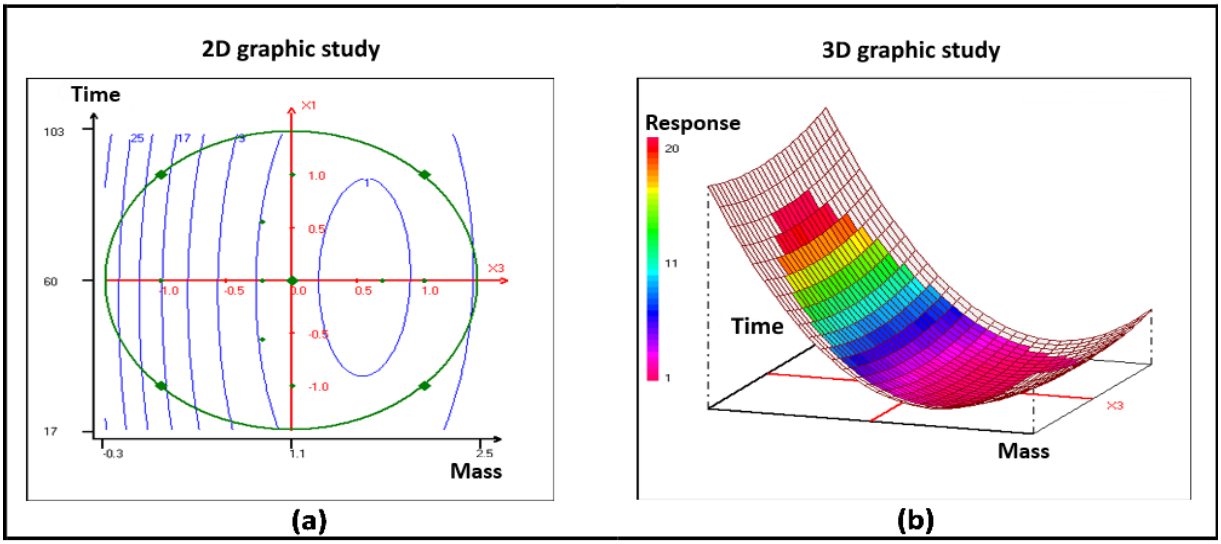

Figure 2.8. Isoresponse curves (a) and response surface (b) of the adsorption capacity (q_m (mg/g)) with the variation of SSA mass (g) and the contact time (min) at pH = 4 and 30 mg/L as initial concentration of copper ions.

The graphical study of the response surfaces corresponding to this model confirmed that the coefficient b_3 was the most important coefficient. The mass of the adsorbent (X_3) was therefore the most influencing factor. A reduction in the mass of adsorbent resulted in a marked improvement in the adsorption capacity of the ash towards copper ions, that could be mainly a result of increasing the unsaturation of adsorption sites through the adsorption process which was reported also in previous studies (Yu et al., 2003; Özacar and Şengil, 2005). This result is also translated by the

negative sign of the coefficient b_3. **Figure 2.7** shows the effect of the amount of ash and the pH of the effluent on the copper adsorption. The pH values were from 2.6 to 5.4 to avoid the negligible copper sorption at pH<3 or the metal precipitation at pH>5 (Xu et al. 2009). Results demonstrated that, for low amount of adsorbent, the quantity of adsorbed copper increased with the increase of pH. This could be explained by the fact that for an acidic pH around 3, the excess of H^+ ions competed with copper ions for the adsorption sites, while at higher pH values, this competition was attenuated and adsorption was increasingly promoted until copper precipitation occurs (Nguyen et al., 2018; Wang et al., 2019). The maximum adsorption was found at a value of pH equal to 4.

Figure 2.8 shows the influence of the adsorbent mass and contact time on the adsorption process. The maximum adsorption increased for an amount of 0.5g of SSA after a contact time about 60 min. In general, the graphical study of the adsorption potential of SSA as a function of the three factors time (X_1), pH (X_2) as well as the concentration of metallic element (X_4) showed that the effect of these three parameters seems rather weak compared to the influence of the dose of adsorbent (**Figures 2.6, 2.7** and **2.8**). **Figure 2.9** shows that the quantity of micropollutant adsorption varied in function of contact time and concentration of copper ions but with less importance and with lower level of significance than that caused by the amount of adsorbent, in fact the adsorption capacity did not exceed 5 mg / g.

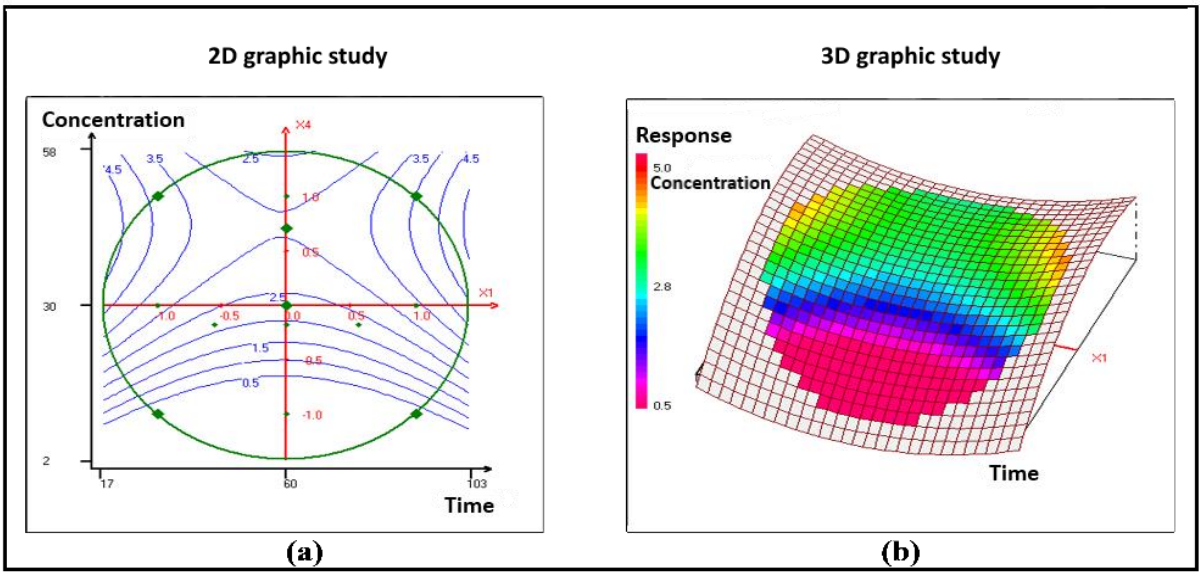

Figure 2.9. Isoresponse curves (a) and response surface (b) of the adsorption capacity (q_m (mg/g)) with the variation of contact time (min) and the copper concentration (mg/L) at pH equal to 4 and using 1.1 g of SSA.

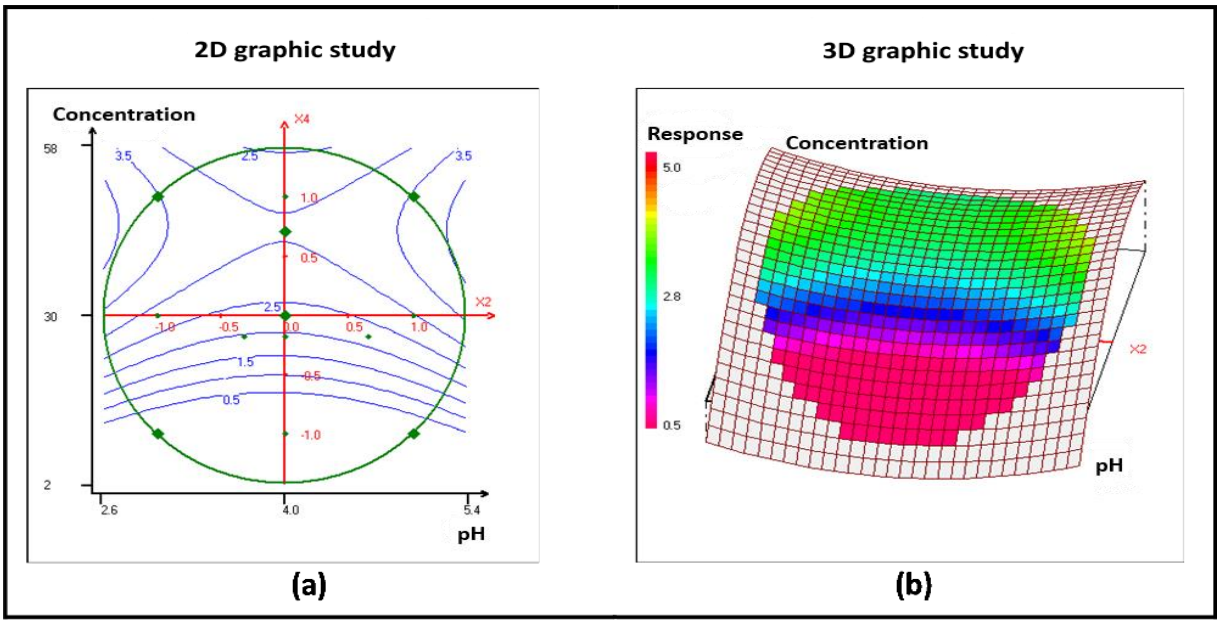

Figure 2.10. Isoresponse curves (a) and response surface (b) of the adsorption capacity (q_m (mg/g)) with the variation of pH and the copper concentration (mg/L) using 60 min as contact time and 1.1 g of SSA.

The optimum contact time was 60 min which was reported in previous study (Bouzid et al. 2008). Regarding the effect of the initial concentration of copper ions, Figures 2.6, 2.9 and 2. 10 demonstrates that the adsorption capacity increased with the increase of the initial concentration. This can be translated by an increase in the conductive force of the concentration gradient which is proportional to the initial concentration (Shaarani and Hameed, 2010).

5. Optimization of experimental conditions

The objective of this work is to determine the appropriate experimental conditions for optimizing the clarification yield of discharges rich in copper ions by the ash from sludge. Using the methodology of the experimental designs, the stirring time, the pH of reaction medium, the adsorbent amount and the concentration of micropollutant were determined.

The examination of the Box Behnken design results make it possible to select the optimal operating conditions listed in **Table 2.5**.

Table 2.5. Maximum coordinates.

Variable	Value	Factor	Real value
X_1	0.315	Time	69
X_2	0.158	pH	4.2
X_3	-1.032	Mass	0.1
X_4	0.885	Concentration	48

Desirability analysis has shown that a short contact time estimated at 69 min, a pH value equal to

4.2, an ash amount in the order of 0.1 g and a concentration of copper ions which don't exceed 48 mg L^{-1} were able to stimulate the adsorption capacity of sludge ash to reach an adsorption capacity of copper ions around 20 mg/g. According the maximum sorption characterization (**Table S2.4**), the copper removal quantity obtained according to the optimum conditions was 20 mg/g, this result demonstrated the useful aspect of prepared SSA in the treatment of WW contaminated by copper ions.

III. Adsorption isotherms

The adsorption isotherms measured at 10, 25 and 40°C are shown in **Figure 2.11**.

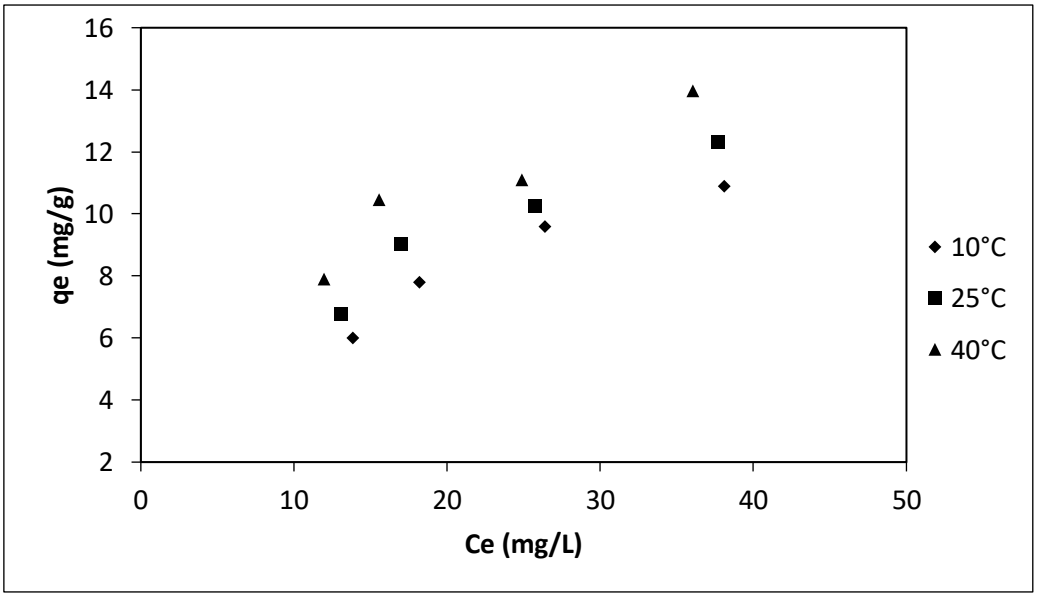

Figure 2.11. Direct isotherms of the adsorption of copper ions at 10, 25 and 40°C.

The direct adsorption isotherms show an "L" shape according to the classification of Giles, proving a relatively high affinity between adsorbate and adsorbent and suggesting an adsorption of monomolecular layer and a possibility of applying as well Langmuir's law than that of Freundlich (Babakhouya et al.,2010). To fully understand the adsorption mechanisms, it is important to model the direct adsorption isotherms. Indeed, this modelling provides information on the improvement of adsorbents, maximum adsorption capacity, affinity and binding energy between the adsorbate and adsorbent which confirms or not the existence of lateral interactions between molecules. Adsorption isotherms are used to estimate the adsorption process (monolayer or multilayers adsorption). The two most commonly used two-parameters models are Langmuir and Freundlich models that have been used to fit the experimental data. To find the best fitting model that describes the isotherms of experimental removal of copper by ash, linear regression was determined for each model.

Figure 2.12 presents the linear forms of Langmuir and Freundlich adsorption isotherms respectively

at 10°C, 25°C and 40°C.

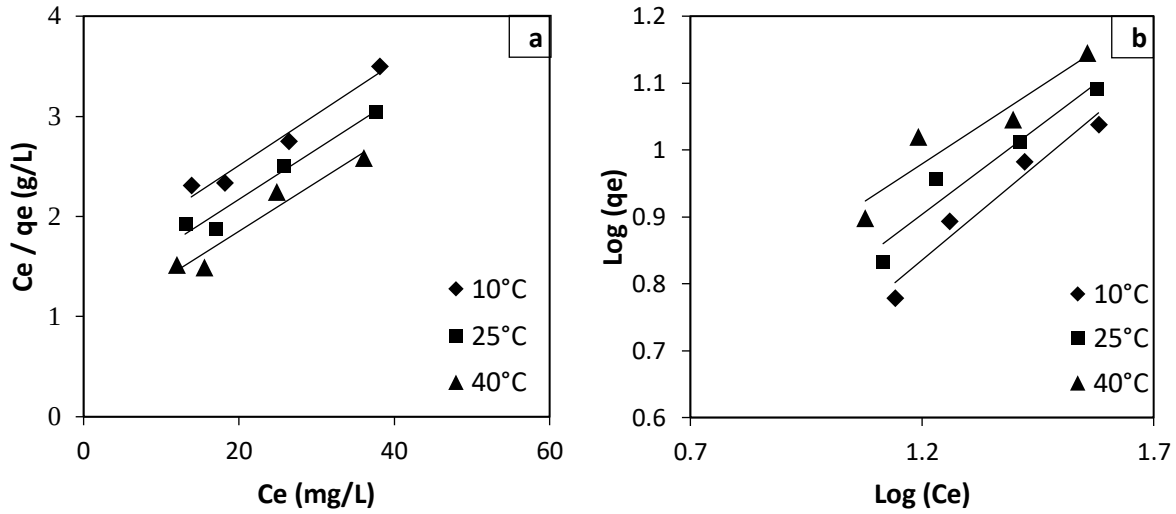

Figure 2.12. Linear fits of Langmuir (a) and Freundlich (b) adsorption isotherms at 10°C, 25°C and 40°C.

Examination of the results summarized in **Table 2.6** and corresponding to the parameters of Langmuir and Freundlich models allow to evaluate the adsorption mechanism, surface properties and adsorbent-adsorbate affinities. Indeed, correlation coefficients R^2 corresponding to the Langmuir model and Freundlich model were close to the unit. The regression coefficients relative to the Langmuir model were slightly higher than those corresponding to the Freundlich model.

Table 2.6. Adsorption isotherm parameters of copper on SSA for Langmuir and Freundlich models.

	10°C	25°C	40°C
Langmuir parameters			
Qm (mg/g)	19.60	20.00	20.40
(mg/g)	0.034	0.042	0.056
R^2	0.965	0.964	0.943
Freundlich parameters			
K_F (L/mg)	1.152	1.32	1.546
1/n	0.577	0.52	0.452
R^2	0.954	0.937	0.899

These results prove that the Langmuir model presents the best fit of the experimental data and can be considered as an adequate description of the phenomenon of copper adsorption by the sludge ashes. In fact, previous study verified that the removal data of copper on ash derived from Pomace ash was better described by Langmuir adsorption isotherm (Bouzid et al., 2008). The values of the Langmuir parameters are also important (R^2 = 0.96), this confirms that extra granular adsorption can also take place. This result directs us towards a physisorption type adsorption (Mimanne et al.

2014). Langmuir's model showed also that the ash surfaces are homogeneous on the energy plan and that the adsorption is of the monolayer type (Petrović et al., 2017, Yu and Luo, 2014). Furthermore, the maximum adsorption capacities were 19.6, 20 and 20.6 mg/g at 10°C, 25°C and 40°C respectively. These results denoted that the adsorption capacities increased with temperature which reflects the endothermicity of the adsorption reaction of copper ions by sludge ashes. The estimated maximum adsorption capacity using Langmuir model at ambient temperature (20 mg/g) was very close to the experimental data obtained by the quality by design (20.072 mg/g).

The evolution of the adsorption equilibrium constant (b) as a function of temperature showed that the affinity between the adsorbent and the adsorbate is more important at high temperatures. Moreover, values of Freundlich's constant (n) greater than 1, confirmed that the inorganic micropollutant trapping phenomenon on the ash from sludge is favourable and physical (Dawood and Sen, 2012). In fact, the affinity of the adsorbent material towards the removal of heavy metal ion is indicated by the value of n which must be higher than1 and less than 10 (Dada et al., 2013).

The results obtained in this study in terms of adsorption capacity (Q_m) can be compared with those obtained in other copper adsorption studies by SSA and other media. This comparison shows a high removal efficiency of the adsorbent prepared by the incineration of the sewage sludge in the removal of copper ions from aqueous solutions (see **Table 2.7**).

Table 2.7. Comparison of the adsorbed quantity of Cu^{2+} ions obtained in this study with previous studies.

Adsorbent	Q_m (mg/g)	Reference
Phosphate rock	10.8	Sarioglu et al., 2005
Brick waste covered by manganese oxides	5.66	Boujelben et al. 2011
Sewage sludge ash	2.56	El-Sheltawy et al., 2016
Bottom ash of expired drugs	13.33	Benzaoui et al. 2017
Agriculture residues fly ash	19.82	Xu et al. 2017
Coal industry fly ash waste	4.49	Nguyen et al., 2018
Iron industry blast furnace slag waste	5.22	Nguyen et al., 2018
Sewage sludge ash	7.2	Wang et al. 2019
Sewage sludge ash	20.07	This study

For example, the adsorbent prepared and used in this study has higher copper adsorption capacity (Q_m) compared to those investigated in previous researches using others sewage sludge ashes; in

fact, the adsorption capacities of copper found by Wang et al. (2019), El-Sheltawy et al. (2016), and Bouzid et al. (2008) were 8.26 mg/g, 2.56 mg/g and 5.71 mg/g respectively. This comparison highlights the advantages of the adsorbent prepared in this study.

Pan et al. (2003) explained the adsorption mechanism of copper using SSA by the electrostatic attraction between the negative charge of the surface in the effluent solution and the positive charge of the metal element. Also, they demonstrated the possible formation of surface complex between hydrous silicon oxide and aluminum oxide and copper ions. Possible cation exchange between ash surface and copper ions explained by the significant CEC of the SSA constituted a further important mechanism for copper sorption by the sludge ash.

IV. Desorption study

The regeneration of the sorbent using thermal activation could reduce the mass of adsorbent by 5-10% after each cycle, with an important use of energy (Rao et al., 2006). Hence, in this study, the regeneration of SSA was conducted using nitric acid, achieving a desorption efficiency of about 76%. Hence, the desorption process can be considered feasible, thus representing a positive characteristic of the sorbent. The incomplete regeneration of the material could be related to the presence of different types of interaction between Cu (II) and the adsorbent, some of which are reversible and others irreversible. Part of the adsorption probably occurs through physisorption mechanisms such as electrostatic attraction between the adsorbent and the adsorbate, and in this case the Cu ions would be easily desorbed. Conversely, other interactions may involve chemisorption mechanisms, thus involving irreversible sorption (Papandreou et al., 2007; Qian et al., 2009; Wang et al., 2011).

V. Conclusion

The objective of this work is to enhance the reuse of by-products of low economic value, to design a new efficient purification process to treat effluents rich in copper from industrial plants and produce water of good quality. In this way, it can be possible to allow the water discharge in the environment without any risk or its partial reuse in industrial aqueducts without affecting the operations or quality of manufactured products. This study was dedicated to the development of an adsorbent based on WWTP sludge intended for the adsorption of a metal-bearing micropollutant (i.e., copper), which may be present in industrial effluents. Box-Behnken Design was used to define the optimal conditions able to maximize the adsorption capacity of copper ions by sludge-based ash. It was observed that a time of 69 min, a pH=4.2 associated with an adsorbent dose of 0.1 g and a concentration of 48 mg/L results in an estimated maximum adsorption capacity of 20 mg/g.

The experimental research methodology made it possible to conclude that the dose of the adsorbent introduced is the most determining factor, among the other factors studied, suitable to orient the copper adsorption capacity towards an optimal value.

To model the adsorption isotherms of copper by sewage ash, Langmuir model and Freundlich model were used. The study showed that the adsorption process can be described by these two models, which confirms the monomolecular criterion of the copper trapping phenomenon.

At the end of this study, it is important to point out that the exploitation of this type of by-products appear as a major advantage, both from an economic and an environmental point of view, allowing a better purification of metalliferous waters and the reuse of ashes, in accordance with modern sustainable development strategies.

VI. Bibliography

Aboulayt, A., Riahi, M., Touhami, M. O., Hannache, H., Gomina, M., Moussa, R. J. A. P. T., 2017. Properties of metakaolin based geopolymer incorporating calcium carbonate. Adv. Powder Technol., 28, 2393-2401.

Akintelu, S. A., Folorunso, A. S., Folorunso, F. A., Oyebamiji. A. K., 2020. Green synthesis of copper oxide nanoparticles for biomedical application and environmental remediation. Heliyon 6.

Albuquerque, A. R. L., Angélica, R. S., Merino, A., Paz, S. P. A., 2021. Chemical and mineralogical characterization and potential use of ash from Amazonian biomasses as an agricultural fertilizer and for soil amendment. J. Clean. Prod. 126472.

Asadieraghi. M., Wang Daud. W.M.A., 2014. Characterization of lignocellulosic biomass thermal degradation and physiochemical structure: Effects of demineralization by diverse acid solutions. Energy Convers. Manag. 82, 71-82.

Azad, F. N., Ghaedi, M., Dashtian, K., Hajati, S., Pezeshkpour, V., 2016. Ultrasonically assisted hydrothermal synthesis of activated carbon-HKUST-1-MOF hybrid for efficient simultaneous ultrasound-assisted removal of ternary organic dyes and antibacterial investigation: Taguchi optimization. Ultrasonics Sonochem. 31, 383-393.

Banerjee, K., Ramesh, S. T., Gandhimathi, R., Nidheesh, P. V., Bharathi, K. S., 2012. A novel agricultural waste adsorbent, watermelon shell for the removal of copper from aqueous solutions. Iran. j. energy environ. 3, 143-156.

Babakhouya, N., Boughrara, S., Abad, F., 2010. Kinetics and thermodynamics of Cd (II) ions sorption on mixed sorbents prepared from olive stone and date pit from aqueous solution. Appl. Sci. 10, 2316-2321.

Barakat, M. A. 2011. New trends in removing heavy metals from industrial wastewater. Arab. J. Chem. 4361-377.

Benassai, E., Del Bubba, M, Ancillotti, C., Colzi, I., Gonnelli, C., Calisi, N., Salvatici, M. C., Casalone, E., Ristori., S., 2021. Green and cost-effective synthesis of copper nanoparticles by extracts of non-edible and waste plant materials from Vaccinium species: Characterization and antimicrobial activity. Mater. Sci. Eng. C. 119, 111453.

Bianchi, E., A. Biancalani, C. Berardi, A. Antal, D. Fibbi, A. Coppi, L. Lastrucci, N. Bussotti, I. Colzi, L. Renai, C. Scordo, M. Del Bubba, and C. Gonnelli. 2020. Improving the efficiency of wastewater treatment plants: Bio-removal of heavy-metals and pharmaceuticals by Azolla filiculoides and Lemna minuta. Sci. Total Environ, 746.

Brewer, G. J. 2010. Copper toxicity in the general population. Clinical Neurophysiology 121:459-460.

Cao, X., Harris W., 2010. Properties of dairy-manure-derived biochar pertinent to its potential use in remediation. Bioresour. Technol. 101, 5222-5228.

Chandrasekhar, S., Pramada, P. N., 2006. Rice husk ash as an adsorbent for methylene blue—effect of ashing temperature. Adsorption, 12, 27-43.

Cheng, W. C., Ding, C. C., Wu, Q. Y., Wang, X. X., Sun, Y. B., Shi, W. Q., Hayat, T., Alsaedi, A., Chai, Z. F., Wang, X. K.. 2017. Mutual effect of U(VI) and Sr(II) on graphene oxides: evidence from EXAFS and theoretical calculations (Retracted article. See vol. 7, pg. 1617, 2020). Environ. Sci. Nano, 4, 1124-1131.

Dil, E. A., M. Ghaedi, and A. Asfaram. 2017. The performance of nanorods material as adsorbent for removal of azo dyes and heavy metal ions: Application of ultrasound wave, optimization and modeling. Ultrasonics Sonochemistry 34, 792-802.

Donatello, S., Cheeseman, R.C., 2013. Recycling and recovery routes for incinerated sewage sludge ash (ISSA): A review. J. Waste Manag. 33, 2328-2340.

Grobelak, A., Jaskulak, M., 2019. Sludge multifunctions in a phytobiome—Forest and plantation application including microbial aspects. Pages 323-336 in M. N. V. Prasad, P. J. d. C. Favas, M. Vithanage, and S. V. Mohan, editors. Industrial and Municipal Sludge, Emerging Concerns and Scope for Resource Recovery. Butterworth-Heinemann.

Jaishankar, M., T. Tseten, N. Anbalagan, B. B. Mathew, and K. N. Beeregowda. 2014. Toxicity, mechanism and health effects of some heavy metals. Interdiscip Toxicol 7:60-72.

Jittin, V., Bahurudeen, A., Ajinkya S. D., 2020. Utilisation of rice husk ash for cleaner production of different construction products. J. Clean. Prod. 263.

Majumdar, D. 2021. Recent progress in copper sulfide based nanomaterials for high energy supercapacitor applications. J. Electroanal. Chem. 880.

Noszczynska, M., and Z. Piotrowska-Seget. 2018. Bisphenols: Application, occurrence, safety, and biodegradation mediated by bacterial communities in wastewater treatment plants and rivers. Chemosphere 201,214-223.

Özacar, M., Şengil, İ. A., 2005. Adsorption of metal complex dyes from aqueous solutions by pine sawdust. Bioresour. Technol. 96, 791-795.

Rajabi, M., Rezaie, A., Ghaedi. M., 2015. Simultaneous extraction and preconcentration of some metal ions using eucalyptus-wood based activated carbon modified with silver hydroxide nanoparticles and a chelating agent: optimization by an experimental design. Rsc Advances 5, 89204-89217.

Ruyters, S., Salaets, P., Oorts K., Smolders. E., 2013. Copper toxicity in soils under established vineyards in Europe: A survey. Sci. Total Environ. 443, 470-477.

Shah, K. W., Lu, Y.. 2018. Morphology, large scale synthesis and building applications of copper nanomaterials. Constr Build Mater. 180, 544-578.

Trakal, L., Sigut, R., Sillerova, H., Faturikova, D., Komarek, M., 2014. Copper removal from aqueous solution using biochar: Effect of chemical activation. Arab. J. Chem. 7,43-52.

Waris, A., Din, M., Ali, A., Ali, M., Afridi, S., Baset, A., Ullah Khan, A., 2021. A comprehensive review of green synthesis of copper oxide nanoparticles and their diverse biomedical applications. Inorg. Chem. Commun. 123,108369.

Yildiz, K., Atakan, M., 2020. Improving microwave healing characteristic of asphalt concrete by using fly ash as a filler. Constr Build Mater. 262.

Yu, L. J., Shukla, S. S., Dorris, K. L., Shukla, A., Margrave, J. L., 2003. Adsorption of chromium from aqueous solutions by maple sawdust. J. Hazard. Mater., 100, 53-63.

Zhang, Q., Wu, Y., Luo, J. Y., Cao, J.S., Kang, C. J., Wang, S. N., Li, K. Y., Zhao, J. N., Aleem, M., Wang. D. B., 2020. Enhanced volatile fatty acids production from waste activated sludge with synchronous phosphorus fixation and pathogens inactivation by calcium hypochlorite stimulation. Sci. Total Enviro. 712.

Zou, Y. D., X. X. Wang, A. Khan, P. Y. Wang, Y. H. Liu, A. Alsaedi, T. Hayat, and X. K. Wang. 2016. Environmental Remediation and Application of Nanoscale Zero-Valent Iron and Its Composites for the Removal of Heavy Metal Ions: A Review. Environ. Sci. Technol. 50,7290-7304.

Part 3

Study of physicochemical properties and sorption capacities of sawdust-based biochars and commercial activated carbon towards ethoxylated alkylphenols and their phenolic metabolites in effluent wastewater from a textile district

The effluent WW used in this study was obtained from the Baciacavallo WWTP operating in the textile industrial district of Prato (Italy). The characteristics of WW are shown in **Table S3.2**.
The results presented in **Table S3.2** showed that the WWTP effluent contained APs and APnEOs at different concentrations.
Based on log K_{OW} data (3.49-5.79) shown in **Table S3.1** of the Supplementary material, the target molecules covered a quite wide range of hydrophobicity, making the study informative of the adsorption properties of synthesized biochars for molecules characterized by low-to-medium polarity

I. Char characterization

Sorbent materials to be used for water and WW treatment are commonly characterized for their elemental composition, surface area and presence of functional groups both involved in the adsorption capacities towards the organic micropollutants. In this study, CHNS elemental analysis, BET total surface area, micropore and mesopore distribution, as well as pH_{pzc}, XPS and FTIR data on surface functionalization were provided. Furthermore, in water treatment plants (WTPs) and WWTPs the selection of activated carbons is performed via the determining of parameters related to sorption efficiency, porosity indexes (i.e., iodine, phenol and MB numbers) and ash content. The porosity indexes, which are still used in research papers for comparing sorption properties of activated carbons (Jian et al., 2018), were also evaluated and discussed in relation to the instrumental porosimetry results.

1. Elemental analysis

Data concerning C, H, N, S, and O analysis are presented in **Table 3.1** The results showed very small percentages of nitrogen in all the investigated materials. Furthermore, sulphur was only found in MAC, even though at very low percentages. As observed elsewhere, the abundance of these elements in biochar depends mainly on the feedstock characteristics (Ahmad et al., 2014). Pyrolysis temperature played a significant role in changing the biochar characteristics, as evaluated by elemental analysis. The carbon content strongly increased with the rise in the pyrolysis temperature and a corresponding loss of H, N, and O was recorded. More specifically, much higher percentage variations were found from 450 °C to 650 °C for C and O, whereas for H the percentage decrease was quite homogeneous among the three biochars. The increase in carbon content with a rise in temperature is attributed to an enhanced carbonization degree of the material, which is related to the increasing formation of well-organized graphitized layers (Ahmad et al., 2014). The decline in H,

N, and O can be ascribed to the defunctionalisation of the materials that involves a loss of polar groups.

Table 3.1. Elemental composition of biochars produced at pyrolysis temperatures of 450°C (BC450), 650°C (BC650), 850°C (BC850), vegetal activated carbon (VAC) and in mineral activated carbon (MAC). Data are presented as mean (n = 3) and standard deviation (in bracket).

Char	C (%)	H (%)	N (%)	S (%)	O (%)
BC450	67.2 (0.1)	2.7 (0.2)	0.1071 (0.0003)	< 0.05 [a]	27.8 (0.2)
BC650	80 (0.3)	2.1 (0.1)	0.086 (0.008)	< 0.05 [a]	16.1 (0.2)
BC850	82.7(0.3)	1.3 (0.4)	0.070 (0.01)	< 0.05 [a]	13.6 (0.7)
VAC	90.2(0.4)	0.55 (0.05)	0.097 (0.002)	< 0.05 [a]	7.0 (0.4)
MAC	77.66 (0.07)	1.21 (0.08)	0.235 (0.002)	0.64 (0.01)	12.5 (0.1)

[a] Detection limits

Accordingly, as shown by the van Krevelen diagram (**Figure 3.1**), lower molar H/C and O/C ratios are observed in biochar with a rise in the pyrolysis temperature. The diagram also highlights that between the two activated carbons considered, MAC is the one most similar to the biochars obtained in this study.

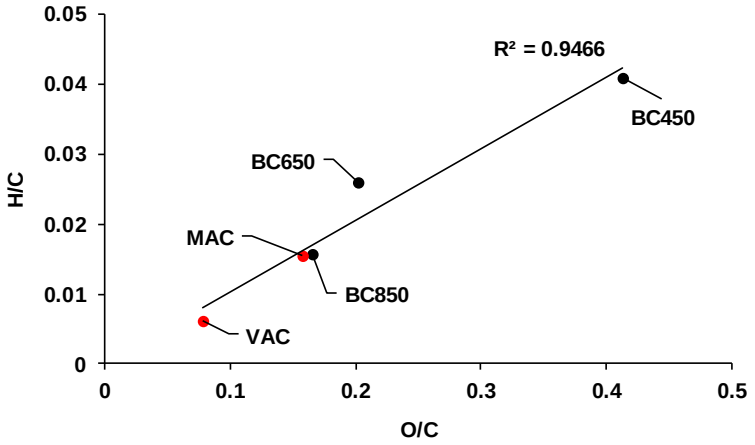

Figure 3.1. van Krevelen diagram for vegetal and mineral activated carbons (VAC and MAC, red points), and biochars produced at 450°C (BC450), 650°C (BC650), and 850°C (BC850) (black points).

2. Porosimetry results

Table 3.2 illustrates the results obtained for the porosimetry analyses (i.e., BET total surface area, t plot micropore surface area and BJH desorption cumulative mesopore surface area) of all the investigated materials. In accordance with data in literature (Inyang and Dickenson, 2015), biochar surface areas increased with a rise in the production temperature, from 102 to 419 m^2. g^{-1}. Hence, in

this study, the highest BET surface area measured for biochar was approximately half that wide range of temperatures from woody species, the temperature trends observed in this study for microporosity and mesoporosity were similar to those reported elsewhere for biochar deriving from maple and pine wood waste (Xiao and Pignatello, 2015; Zhu et al., 2018).

Table 3.2. Total surface area (BET method), surface area of micropores (t-plot method) and surface area of mesopores (BJH model − desorption cumulative surface area) determined in biochars produced by pyrolysis at 450 °C (BC450), 650 °C (BC650) and 850 °C (BC850), and in vegetal and mineral commercial activated carbons (VAC and MAC, respectively). Values of total surface area in bracket represent the instrumental standard deviation.

	Total Surface Area (m^2 g^{-1})	Micropore Surface Area (m^2 g^{-1})	Mesopore Surface Area (m^2 g^{-1})
BC450	102 (4)	73.9	20.9
BC650	319 (13)	253.4	28.9
BC850	419 (16)	296.4	80.8
VAC	785 (30)	474.6	192.0
MAC	1105 (34)	122.0	637.0

The iodine, phenol and MB indexes are commonly determined in activated carbons in order to evaluate their quality as sorbents, due to the relation between these indexes and pore distribution (Zhang et al., 2007). More in detail, iodine and phenol indexes should be related to the presence of micropores and therefore be informative of the effectiveness in removing small-size organic water pollutants. On the other hand, MB index should be linked to the abundance of mesopores and thus be a useful indicator of adsorption capacities for medium-large sized organic pollutants. Higher values of MB and especially iodine index, as well as corresponding enhanced adsorptions of phenol, were observed with a rise in the pyrolysis temperature (**Table 3.3**). It is worth noting that the three indexes showed a good linear correlation ($R^2 \geq 0.976$) with temperature.

Table 3.3. Mean values (n=3) and standard deviations (in brackets) of porosity indexes and ash percentage determined in each investigated char.

Char	Iodine index	Phenol index	Methylene blue index	Ash
BC450	102 (1)	18.9 (0.9)	2.2 (0.1)	2.11 (0.05)
BC650	157 (8)	9.5 (0.2)	2.9 (0.1)	1.74 (0.03)
BC850	190 (4)	2.4 (0.1)	3.6 (0.2)	2.30 (0.02)
VAC	964 (10)	1.9 (0.1)	16.6 (0.2)	2.13 (0.04)
MAC	1192 (9)	1.4 (0.1)	20.0 (0.1)	8.02 (0.03)

The behaviour of the iodine index is in line with other studies (e.g., for rice husk derived biochar) (Jian et al., 2018) The modest increase of the MB index with a rise in temperature was also in accordance with data reported elsewhere (Irfan et al., 2016; Jian et al., 2018). Very good linear correlations (R^2=0.928-0.996) were observed between surface area and adsorption indexes (**Figure 3.2 A-C**). Moreover, high correlations were found between iodine/phenol indexes and micropore surface area (R^2=0.932-0.962, **Figure 3.2 D-E**), as well as between the MB index and mesopore surface area (R^2=0.890, **Figure 3.2 F**), thus confirming the physical significance of these indexes in describing structural properties of sorbents. However, these correlations were only found to be strong when considering biochar produced in the same experimental conditions (e.g., same feedstock), with the only exception of the pyrolysis temperature. In fact, the inclusion of VAC and MAC, as well as other biochars produced in our laboratory from other feedstocks strongly lowered the correlations.

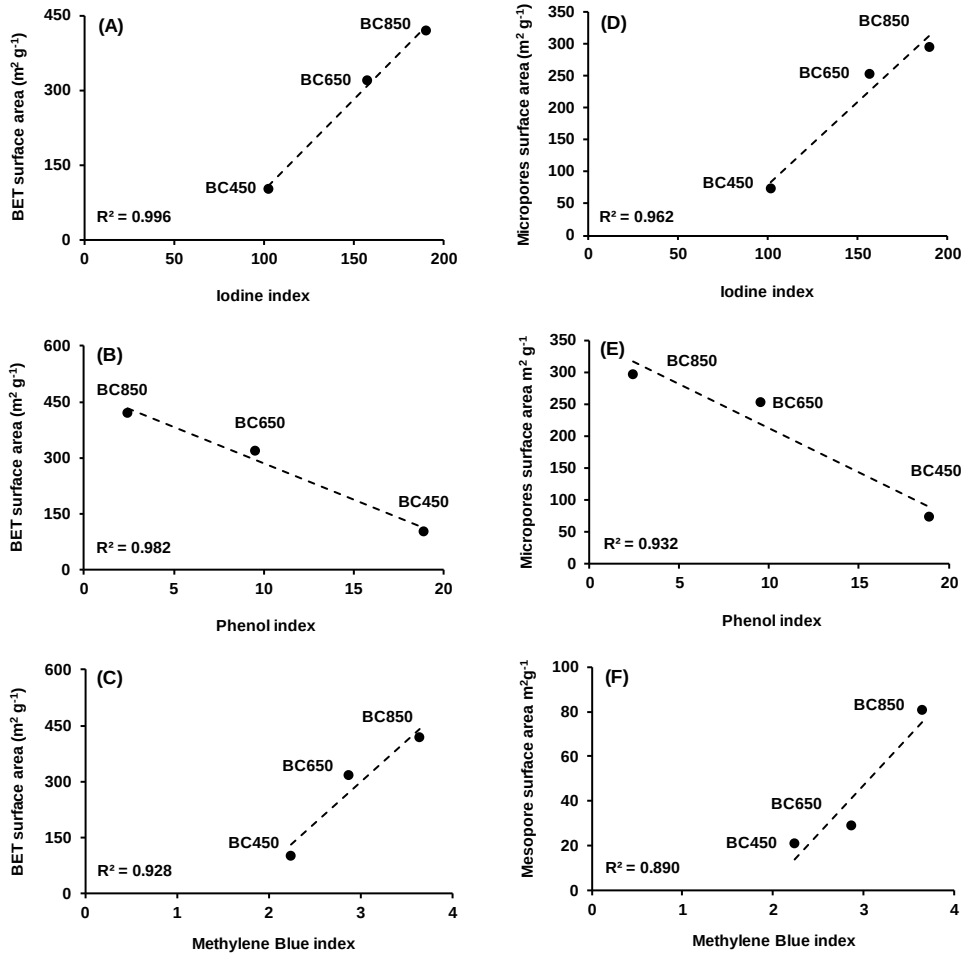

Figure 3.2. Plots of BET surface areas (A-C), t-plot micropore surface areas (D-E) and BJH mesopore surface area (F) as a function of porosity indexes determined in BC450, BC650 and BC850. Values of determination coefficients (R^2) are reported in the plots.

As regards VAC and MAC, porosimetry data highlighted a much higher total surface area and mesoporosity in the latter (**Table 3.2**). In this regard, literature data showed that APnEO adsorption by ACs is mainly related to the mesopore abundance (Liu et al., 2006) as well as surface area. Hence, considering also the results of the elemental analysis on VAC and MAC, the latter was selected as the reference material for the following investigations.

3. Point of zero charge

The results of the pH measurements at the point of zero charge of biochars and MAC (**Figure 3.3**) were included in quite a narrow range (7.15-7.78). Since the mean value of pH of the effluent WW used in this study was 7.46 (see **Table S 3.2**), it can be assumed that no significant charge was present at the surface of the investigated materials. It should also be noted that APnEOs do not have any dissociable acid-base groups in water. APs, which have the phenol group characterized by

a pKa value of about ten, are neutral at the pH of the effluent WW. Accordingly, sorption mechanisms based on ionic interactions are not present in the experimental conditions adopted here.

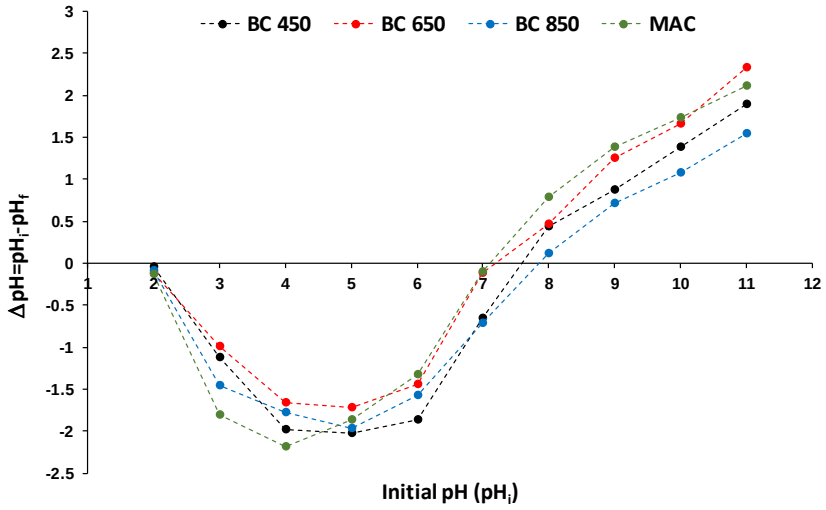

Figure 3.3. Point of zero charge of biochars produced by pyrolysis at 450 °C (BC450), 650 °C (BC650) and 850 °C (BC850), and of commercial mineral activated carbon (MAC).

4. XPS analysis

The results of the XPS analyses for the elements carbon and oxygen in BC450, BC650, BC850 and MAC are reported in **Figure 3.4**. The assignment of the various XPS binding energy peaks can be performed according to practical guidelines for the interpretation of XPS spectra (Thermo Fisher Scientific, 2019[a]; Thermo Fisher Scientific, 2019[b]). The analysis of nitrogen did not highlight the presence of any significant signal (data not shown), in accordance with the very low nitrogen percentages determined via elemental analysis (**Table 3.1**). The biochar produced at 450°C showed a very broad carbon peak (**Figure 3.4A**), covering a larger range of binding energy compared to what was observed in the three other materials (**Figure 3.4B-D**). More specifically, binding energies typically associated with C-O-C (about 286 eV), C=O (about 287 eV) and O-C=O (about 288.5 eV) moieties were largely represented in the carbon peak of BC450, whilst much less chemical diversity was observed in BC650, BC850 and MAC, in agreement with their higher production temperature. Similar considerations can be deduced from XPS spectra of oxygen, which showed a much broader peak for BC450 (**Figure 3.4E**), compared to the others (**Figure 3.4F-H**), in any case covering the values of binding energies compatible with C=O (about 531.5 eV) and C-O (about 533.5 eV) groups. Quantitative data obtained from the normalized peak areas of XPS spectra (**Table S 3.10**) showed an increase in the carbon percentage and a corresponding decrease of oxygen with the rise in temperature from 450 °C to 650 °C, while no significant variations were

observed above this temperature. Interestingly, percentages of carbon and oxygen in the surface of biochar were very similar to the values determined by elemental analysis in the bulk materials (**Table 3.1**), suggesting a good degree of homogeneity.

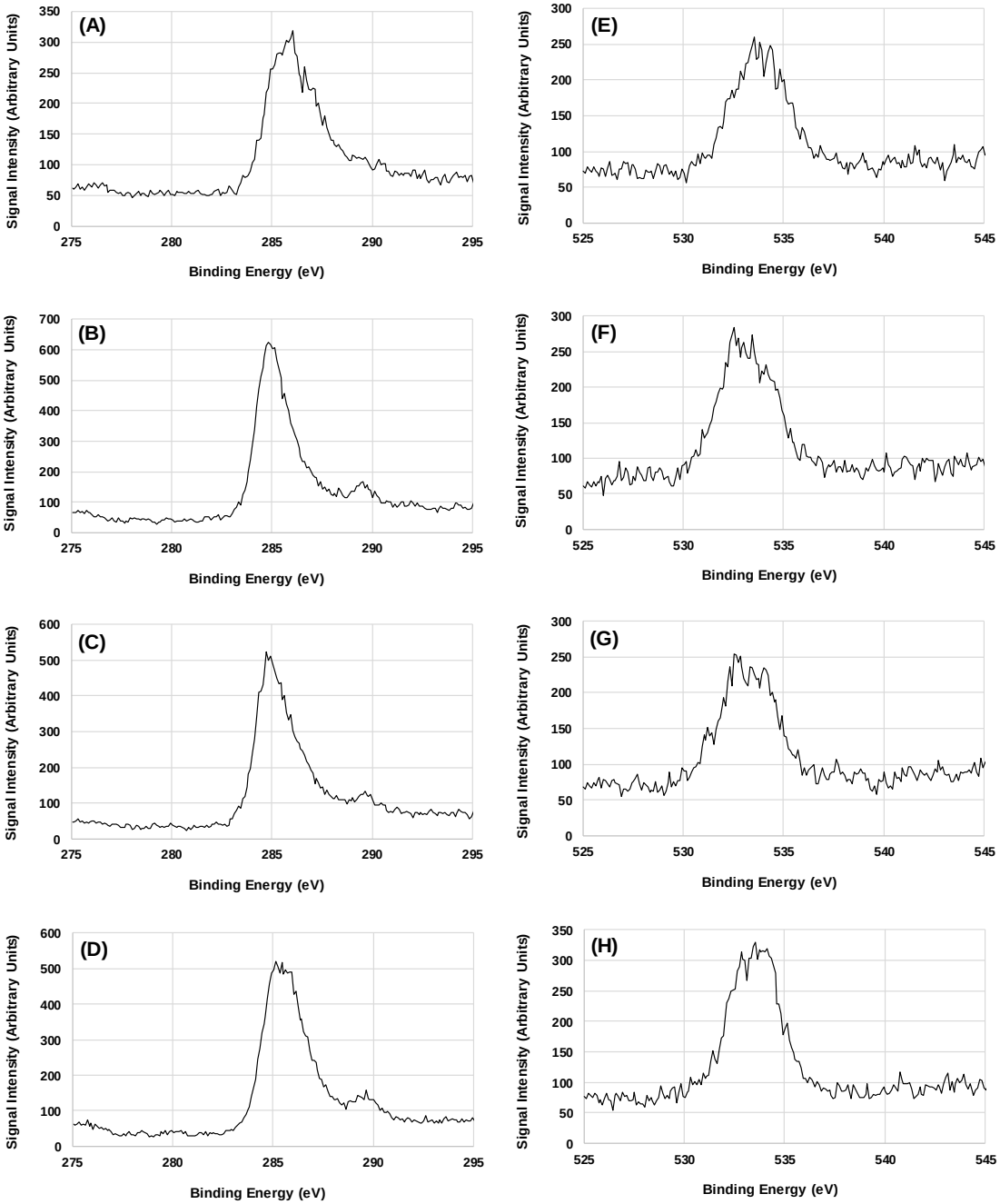

Figure 3.4. X-ray photoelectron spectroscopy spectra in the binding energy regions of carbon (A-D) and oxygen (E-H) of biochars produced by pyrolysis at 450 °C (A, E), 650 °C (B, F) and 850 °C (C, G), and of mineral commercial activated carbon (D, H).

5. FTIR analysis

Figure 3.5 illustrates the results of the FTIR analyses for BC450, BC650, BC850 and MAC,

obtained

in the wave number region between 1,800 and 600 cm^{-1}, which is the most sensitive to structural changes occurring in biochars as a function of the production temperature range investigated (Fu et al., 2012; Wang et al., 2015).

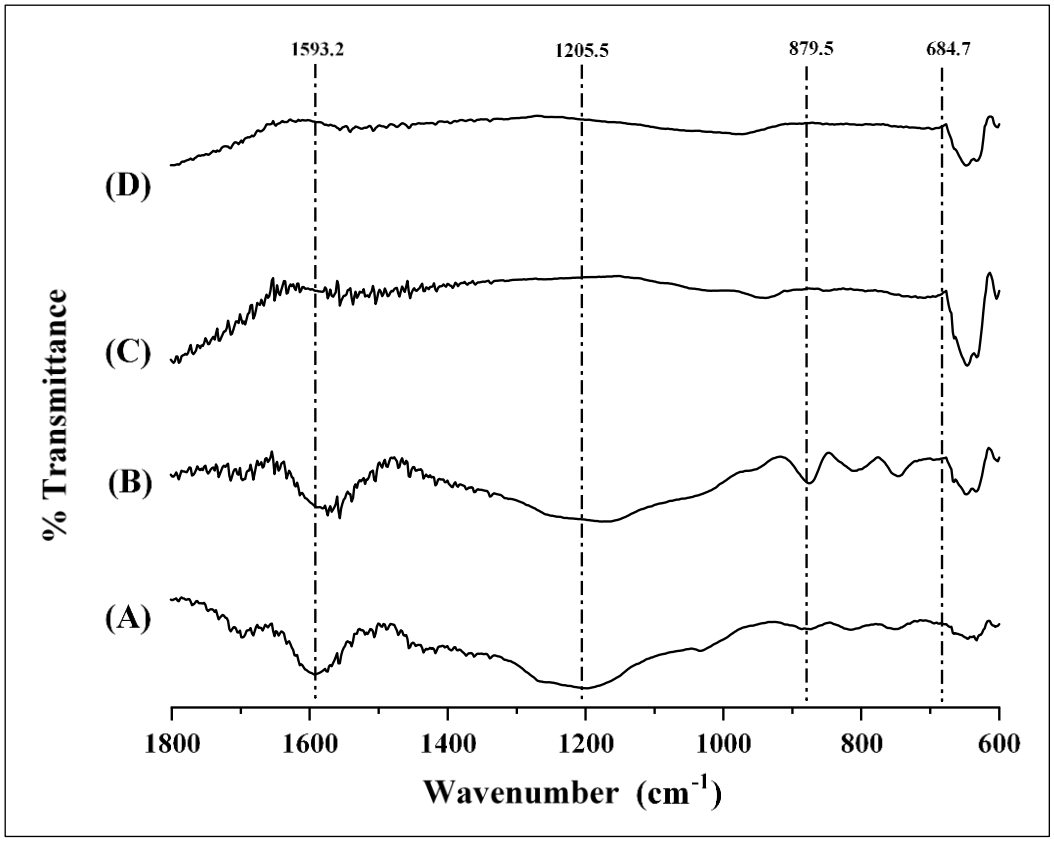

Figure 3.5. Fourier-transform infrared spectra of biochars produced by pyrolysis at 450 °C (A), 650 °C (B) and 850 °C (C), and of mineral commercial activated carbon (D).

The FTIR spectra of biochars reflected changes in their surface functional groups in relation to the different production temperatures. The spectroscopic assignments of the various FTIR absorption bands can be performed according to practical guidelines in literature for the interpretation of FTIR spectra (Coates, 2006). The FTIR spectrum of BC450 highlighted a band at about 1600 cm^{-1}, which can be attributed to the stretching of a C=O group conjugated with a C=C or an aromatic ring, as well as the aromatic ring itself. Stretching of aromatic C–O groups, related to the presence of the phenolic and/or ether moieties, is the cause of the broad absorption band centred at about 1205 cm^{-1} (Coates, 2006). This band was almost completely maintained in the BC650 spectrum, which also showed a shift to lower wavenumbers of the band at about 1600 cm^{-1}, probably due to the partial loss of polar functional groups and the simultaneous increase in aromatization. This latter modification was also evidenced by the increase of the absorptions in the wavenumber range 700-900 $cm^{-1,}$ which are related to the aromatic C-H out-of-plane bending. The further increase of the

pyrolysis temperature to 850°C conversely resulted in the loss of polar and aromatic groups up to the dominance of graphitic carbon (Liu et al., 2015), thus obtaining a FTIR spectra very similar to the one determined for MAC.

Overall, the FTIR findings are in agreement with the results of XPS discussed above, showing how BC650 possesses intermediate characteristics compared to the other materials tested, in terms of presence of polar group and degree of aromatization.

6. Ash

In biochars, ash percentages were in the narrow range of 1.74-2.30%, with the lowest value achieved at 650°C (**Table 3.3**). These values were comparable with that determined in VAC (2.13±0.04%), whereas a much higher ash content was found in MAC (8.02±0.03%). Literature data generally showed an increasing ash content with the rise in pyrolysis temperature (Zhao et al., 2013; Ahmad et al., 2014; Kearns et al., 2014). However, the extent of this increase is strongly influenced by the feedstock used for biochar production, due to the mineral quantity and organic matter combustion residues. Furthermore, ash content is obviously affected by the washing procedure of chars. As a result, a very wide range of values are reported in literature, even considering only vegetal feedstocks (0.3-58%) (Ahmad et al., 2014). Hence, ash percentages found in this study were among the lowest determined in previously published papers.

7. Water-extractable metals and PAHs

Concentrations of water-extractable metals and PAHs of biochars and MAC are shown in **Table 3.4** and **Table 3.5**, in comparison with values included in EN 12915-1/2009 (European Committee for Standardization, 2009), which provides limits for pollutant release from products used for the treatment of water intended for human consumption.

Table 3.4. Mean values (n=3) and standard deviations (in brackets) of water-extractable metals in biochars and mineral activated carbon. Values are compared with those reported in the European Regulation EN 12915-1/2009.

Metal	Unit	Blank	BC450	BC650	BC850	MAC	EN 12915-1
As	$\mu g\ L^{-1}$	<0.5[a]	<0.5[a]	<0.5[a]	<0.5[a]	11 (1)	10
Cd	$\mu g\ L^{-1}$	<0.5[a]	<0.5[a]	<0.5[a]	<0.5[a]	<0.5[a]	0.5
Cr	$\mu g\ L^{-1}$	<0.5[a]	0.6 (0.1)	0.5 (0.1)	1.0 (0.1)	<0.5[a]	5
Hg	$\mu g\ L^{-1}$	<0.1[a]	<0.1[a]	<0.1[a]	<0.1[a]	<0.1[a]	0.3
Ni	$\mu g\ L^{-1}$	<0.5[a]	2.2 (0.3)	<0.5[a]	1.4 (0.2)	1.3 (0.1)	15
Pb	$\mu g\ L^{-1}$	<0.5[a]	<0.5[a]	<0.5[a]	<0.5[a]	<0.5[a]	5
Sb	$\mu g\ L^{-1}$	<0.5[a]	<0.5[a]	<0.5[a]	<0.5[a]	1.2 (0.1)	3
Se	$\mu g\ L^{-1}$	<0.5[a]	<0.5[a]	<0.5[a]	<0.5[a]	<0.5[a]	3
Al	$\mu g\ L^{-1}$	8.1 (1.0)	7.5 (0.7)	28 (3)	232 (15)	207 (16)	n.s.
Fe	$\mu g\ L^{-1}$	<5[a]	<5[a]	8.0 (1.1)	12 (2)	<5[a]	n.s.
Mn	$\mu g\ L^{-1}$	3.2 (0.1)	37 (3)	34 (5)	21 (1)	3.4 (0.2)	n.s.
Cu	$mg\ L^{-1}$	<0.005[a]	<0.005[a]	<0.005[a]	<0.005[a]	<0.005[a]	n.s.
V	$\mu g\ L^{-1}$	<0.5[a]	<0.5[a]	<0.5[a]	<0.5[a]	1.4 (0.1)	n.s.
Zn	$\mu g\ L^{-1}$	12 (2)	35 (5)	16 (3)	21 (2)	10 (2)	n.s.
B	$mg\ L^{-1}$	0.02 (0.01)	0.05 (0.01)	0.04 (0.01)	<0.01[a]	<0.01[a]	n.s.
Na	$mg\ L^{-1}$	12 (1)	13 (1)	11 (2)	11 (1)	11 (1)	n.s.
K	$mg\ L^{-1}$	<0.3[a]	5.2 (1.0)	3.3 (0.7)	4.2 (0.3)	1.5 (0.3)	n.s.
Mg	$mg\ L^{-1}$	5.0 (0.8)	4.3 (0.4)	5.2 (0.8)	5.5 (0.61)	4.1 (0.5)	n.s.
Ca	$mg\ L^{-1}$	12 (2)	11 (1)	18 (3)	19 (2)	12 (1)	n.s.
Ba	$\mu g\ L^{-1}$	<10[a]	60 (3)	46 (2)	63 (5)	12 (1)	n.s.

[a] MDLs = method detection limits at signal-to-noise ratio of 3; n.s. = not specified.

Table 3.5. Mean concentration values (ng L^{-1}, n=3) and standard deviations (in brackets) of water-extractable PAHs in biochars and mineral activated carbon.

Compound	BC450	BC650	BC850	MAC
Naphthalene	0.67 (0.02)	0.40 (0.01)	n.d.	n.d.
Acenaphthene	0.38 (0.01)	<MQL	n.d.	n.d.
Acenaphthylene	0.48 (0.01)	<MQL	n.d.	n.d.
Fluorene	0.35 (0.01)	<MQL	n.d.	n.d.
Phenanthrene	7.0 (0.3)	2.92 (0.06)	1.28 (0.05)	2.24 (0.09)
Anthracene	0.35 (0.01)	n.d.	n.d.	n.d.
Fluoranthene*	0.53 (0.02)	0.33 (0.01)	0.23 (0.01)	0.50 (0.02)
Pyrene	0.34 (0.01)	<MQL	MQL	2.7 (0.1)
Benzo(a)anthracene	2.2 (0.1)	1.03 (0.05)	n.d.	n.d.
Chrysene	2.05 (0.09)	1.71 (0.08)	n.d.	n.d.
Benzo(b)fluoranthene*	0.79 (0.04)	MDL	n.d.	n.d.
Benzo(k)fluoranthene*	0.64 (0.03)	MDL	n.d.	n.d.
Benzo(a)pyrene*	0.89 (0.05)	MDL	n.d.	n.d.
Benzo (a, h) anthracene	2.0 (0.1)	1.51 (0.08)	n.d.	n.d.
Indeno (1,2,3-cd) pyrene*	2.4 (0.1)	1.8 (0.1)	n.d.	n.d.
Benzo (g, h, i) perylene*	1.66 (0.09)	1.05 (0.06)	n.d.	n.d.
Sum*	6.91	3.18	0.23	0.50

(*) Compounds regulated as sum in the EN 12915-1/2009. Maximum acceptable total concentration = 20 ng L^{-1}; n.d. = not detected. MDL = method detection limit; MQL = method quantification limit.

7. 1. Metals

All biochars complied with the EN 12915-1/2009 limits for metal release (European Committee for Standardization, 2009). In most cases, the data of **Table 3.4** evidenced values below the method quantification limits (MQLs) or comparable with blank contributions. The main exceptions were Al in BC850 and MAC, Mn and Ba in all biochars, as well as in MAC, the last found at 11 µg L^{-1}, which is slightly higher than the European Regulation limit. Ba and Mn were actually the only two metals exhibiting much higher leachable concentrations in biochars than MAC.

However, these metals are not included in the EN 12915-1/2009. No clear effect was observed for the release of heavy metals as a function of pyrolysis temperature, even though for Fe and particularly Al, a much higher leaching was determined in BC850 compared to BC450 (**Table 3.4**). The release of this latter metal was by far the greatest found in the investigated elements, suggesting a high native abundance in the feedstock. In this regard, it should be noted that Al was found

elsewhere to be the most abundant metal in sawdust (Sarkar et al., 2014). The much higher Al release by BC850 and MAC could be related to the high production temperature, which generally promotes the increase in surface area and porosity of the material, as well as the decrease in the surface oxygenated functional groups (Harvey et al., 2011; McBeath et al., 2011). In this regard, according to literature, surface area and porous structure of biochar seem to affect heavy metal adsorption less than oxygen-containing functional groups, which may exhibit strong interactions such as electrostatic attraction, ion-exchange and surface complexation (Tan et al., 2015).

As observed elsewhere, Na, K, Mg and Ca should be monitored in biochar leachate as possible causes of salinity increase in treated water, since these elements are naturally found at mg g^{-1} levels in biochar (Brewer et al., 2017). Concentrations observed in this study were comparable, or lower than those previously found in aqueous leachate of biochar produced from Atriplex species (Brewer et al., 2017). Moreover, Na, K, Mg and Ca concentrations found in biochar leachate were similar to those found for MAC, which are used for the treatment of drinking water without any significant contribution to their salinity.

7. 2. PAHs

As shown in **Table S 3.6** of the Supplementary material, the overall MQLs in extraction water were found in the range of 0.13 – 0.9 ng L^{-1}. These limits were fully suitable for PAH determination in the extraction water, according to EN 12915-1/2009 (European Committee for Standardization, 2009), which requires leachable concentrations $\leq$ 20 ng. L^{-1} for the sum of fluoranthene, benzo(b)fluoranthene, benzo(k)fluoranthene, benzo(a)pyrene, indeno (1,2,3-cd) pyrene and benzo(a)pyrene (**Table 3.5**). All sorbents showed leachable PAH concentrations from sub-ng L^{-1} to low- ng L^{-1} levels in accordance with the EN 12915-1/2009 limits. It must be noted that for all the investigated PAHs, leachable concentrations decreased as the production temperature of the biochar increased, in line with recently published results on 16 USEPA PAHs content in biochar produced at different temperatures (De la Rosa et al., 2019). Furthermore, phenanthrene was found to be the most abundant water-extractable PAH in all the biochars, in agreement with data reported elsewhere regarding biochar from wood biomass (Keiluweit et al., 2012).

III. Adsorption efficiency

The evaluation of AP_nEO and AP sorption by biochars and MAC (used as reference material) was performed by kinetic and isotherm analyses.

1. Kinetic test

Figure 3.6 illustrates the adsorption kinetics obtained with the four materials investigated for APs and AP_8EOs, which respectively represent the most hydrophobic and hydrophilic compounds considered in this study, whereas the complete removal dataset is shown in **Tables S3.11 – S3.14.** (paragraph **S.3.7.1** on the Supplementary material). Data shown in **Figure 3.6** clearly showed how the highest increase in sorption of APs and AP_8EOs was highlighted by passing from one to two hours of contact time.

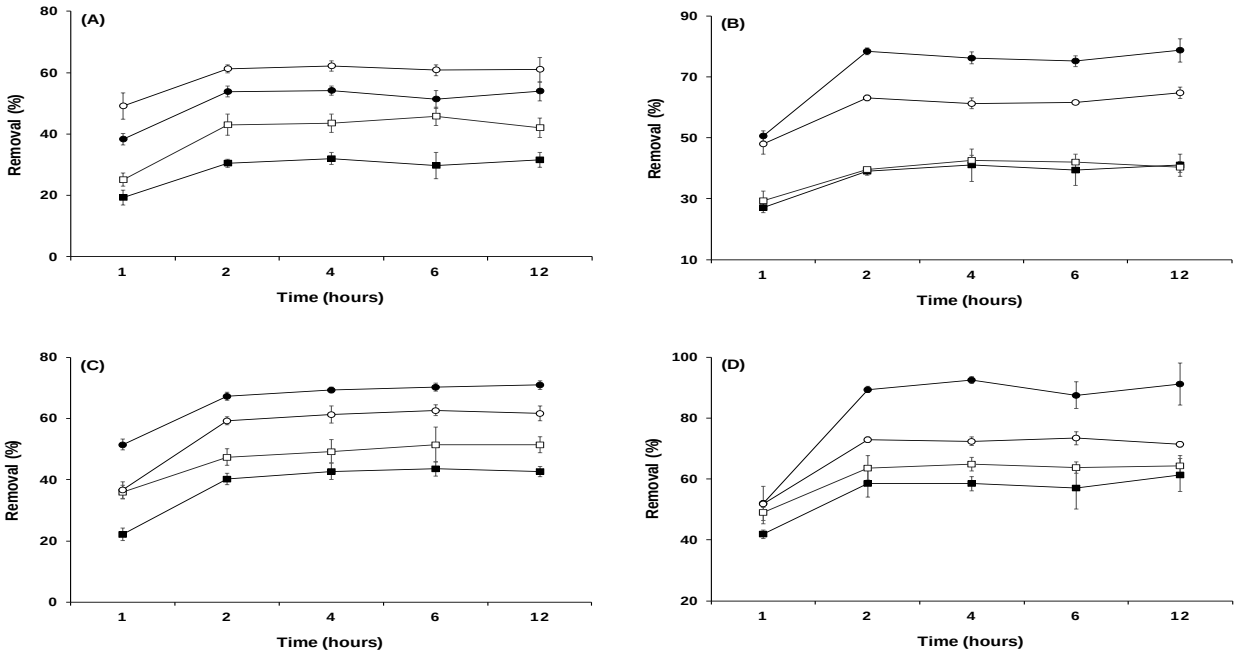

Figure 3.6. Removal of 4-t-OP (■), 4-t-OP8EO (□), 4-NP (●) and 4-NP8EO (○) at contact times of 1, 2, 4, 6 and 12 hours, provided by BC450 (A), BC650 (B), BC850 (C) and MAC (D). Concentrations of biochars = 10 mg L^{-1}; concentration of MAC = 1 mg L^{-1}. Concentrations of 4-t-OP, 4-NP and of technical mixtures containing 4-t-OP8EO and 4-NP8EO = 400 µg L^{-1}. Error bars represent standard deviations (n=3).

Two additional hours of contact time did not provide any further increase in the removal, except for 4-t-OP_8EO with BC650 (**Table S3.12**) and 4-t-OP_5EO for BC850 (**Table S3.13**), whereas contact times of 6 and 12 h did not offer any increase in removal. These results showed a fast adsorption kinetic for all carbons, in agreement with the fact that biochars were sieved at 45 µm and then purified by washing before being used in adsorption studies. According to the results of the adsorption kinetic study, a contact time of 4 h was selected for the isotherm test.

2. Isotherm analysis

Modelling the removal of organic micropollutants by adsorption isotherms is a widely accepted approach in the scientific community for evaluating and comparing the adsorption performance of sorbent materials, including carbons (Chen, 2015). Both Langmuir and Freundlich equations have been largely adopted for the investigation of sorption properties of biochar towards organic micropollutants in aqueous solution (Tan et al., 2015). The two equations were a good fit with the experimental data obtained, with determination coefficients (R^2) always higher than 0.92. However, in all cases the Langmuir model provided two different trends of C_e/Q_e values as a function of C_e, with comparable R^2 values. More specifically, much higher slopes of the regression lines and corresponding lower Q_m ($Q_{m,1}$) values were determined for the initial concentration ranges of 5-100 µg L^{-1} (for APnEOs) and 0.5-10 µg L^{-1} (for APs), compared to the higher ones ($Q_{m,2}$) obtained at 100-400 µg L^{-1} (for APnEOs) and 10-40 µg L^{-1} (for APs). Analogously, much lower values of the empirical constant k were calculated based on the higher concentration range compared to the lower one. **Table S3.15** illustrates the two Q_m data sets calculated by the linearized Langmuir equation, while the two series of k values are shown in **Table S3.16** (**paragraph S.3.7.2**) of the Supplementary material). The presence of two trends in the Langmuir isotherms has been demonstrated previously as generally valid for any experimental sorption isotherm such those obtained in this study, in which the mass adsorbed is a concave function of the equilibrium concentration that asymptotically approaches a maximum value (Sposito, 1982). Based on these considerations, it is evident that no physical significance should be attributed to the presence of the two trends of Ce/Qe vs. Ce.

The linearized Freundlich isotherm model fitted the experimental data by a single trend of log Qe vs. log Ce. **Table 3.6**. shows the K_F values determined by the linearized Freundlich equation, while the *n* data are reported in **Table S 3.16** (**paragraph S.3.7.2** of the Supplementary material).

Table 3.6. Mean (n=3) and standard deviations (in brackets) of Freundlich adsorption capacity (KF), calculated for biochars (BC450, BC650 and BC850) and mineral activated carbon (MAC) in the ranges 5–400 µg L^{-1} for APnEO technical mixtures, and in the ranges 0.5—40 µg L^{-1} for APs. Different letters within each line means statistically significant differences according to the Games-Howell non-parametric contrast test (P<0.05).

Analyte	K_F			
	BC450	BC650	BC850	MAC
4-t-OP	0.563 (0.008) a	1.05 (0.05) b	0.63 (0.02) a	9.4 (0.5) c
4-t-OP_2EO	0.40 (0.04) a	0.48 (0.02) a	0.586 (0.004) b	8.38 (0.08) c
4-t-OP_3EO	0.48 (0.06) a	0.53 (0.01) a	0.72 (0.01) b	10.0 (0.2) c
4-t-OP_4EO	0.50 (0.06) ab	0.442 (0.007) a	0.70 (0.02) b	9.9 (0.2) c
4-t-OP_5EO	0.42 (0.05) a	0.528 (0.002) a	0.63 (0.02) b	8.8 (0.2) c
4-t-OP_6EO	0.36 (0.04) ab	0.43 (0.01) a	0.464 (0.005) b	7.4 (0.2) c
4-t-OP_7EO	0.211 (0.008) a	0.214 (0.006) a	0.212 (0.006) a	6.1 (0.2) b
4-t-OP_8EO	0.166 (0.003) a	0.218 (0.006) b	0.213 (0.005) b	4.5 (0.2) c
4-NP	1.5 (0.2) a	2.07 (0.01) b	1.07 (0.04) a	26.2 (0.6) c
4-NP_2EO	0.84 (0.03) a	1.23 (0.03) b	1.11 (0.03) c	22.0 (0.4) d
4-NP_3EO	0.99 (0.08) ab	1.12 (0.04) a	0.79 (0.01) b	21.1 (0.2) c
4-NP_4EO	1.00 (0.07) ab	1.12 (0.03) a	0.712 (0.004) b	19.2 (0.2) c
4-NP_5EO	0.9 (0.2) a	0.870 (0.007) a	0.834 (0.004) a	15.98 (0.06) b
4-NP_6EO	0.52 (0.03) ab	0.619 (0.001) a	0.583 (0.008) b	12.9 (0.1) c
4-NP_7EO	0.44 (0.02) a	0.397 (0.003) a	0.375 (0.003) b	10.82 (0.04) c
4-NP_8EO	0.33 (0.02) ab	0.377 (0.002) a	0.366 (0.003) b	8.6 (0.2) c

Interestingly, the adsorption capacity parameters calculated by the two equations (i.e., $Q_{m,1}$ and $Q_{m,2}$; K_F) within each homologue series and material were quite well correlated ($0.67 \leq R^2 \leq 0.98$; $P<0.05$), highlighting similar trends of the adsorption capacity measured through the two parameters, as a function of the number of ethoxylate units.

Regardless of the physical meaning attributable to the Langmuir parameters Q_m and k, or their corresponding K_F and n of the Freundlich equation, it is nonetheless interesting to make some comments common to both isotherm equations. In this regard, according to literature, biochar can act as a sorbent of organic molecules through various mechanisms including the formation of hydrogen bonds, as well as electrostatic, π-π and hydrophobic interactions (Tan et al., 2015). The adsorption capacities of biochars, estimated by Q_m or K_F values, were much lower than those found

for MAC, irrespective of the compound considered, revealing the lower sorption performances of the former materials. Within each char, the sorption of the nonyl derivative (more hydrophobic) was higher than that of the corresponding octyl (less hydrophobic); furthermore, biochars and especially MAC showed the highest adsorption capacity for 4-NP, which represent the most hydrophobic compound among those investigated. These findings highlighted the presence of important hydrophobic interactions regulating the sorption of the investigated molecules on biochars and MAC. Therefore, in order to evaluate a possible relation between sorption capacity of the four materials investigated and the polarity of the target analytes, it is possible to plot the values of Q_m or K_F as a function of log K_{OW} of 4-t-OPnEOs and 4-t-OP. Conversely, for 4-NPnEOs contained in the IGEPAL®CO-520 technical mixture, it was not possible to draw a similar plot, since log K_{OW} values were not available for some branched nonyl oligomers (**Table S3.1**).

The trends observed for Q_m or K_F as a function of log K_{OW} of octyl derivatives were nearly overlapping and therefore only the plots of K_F values (which represent a single dataset) are reported. Accordingly, **Figure 3.7** illustrates the profile of K_F values as a function of log K_{OW} of 4-t-OP and 4-t-OP$_n$EOs. For all materials, the linear trend only partially fitted the K_F versus log K_{OW} data. More in detail, MAC exhibited linearity in the widest range of ethoxylation, from eight to four ethoxylate units, whilst compounds with a lower ethoxylation degree and 4-t-OP showed an erratic trend. On the whole, these findings are in accordance with the results of XPS and FTIR that evidenced the absence of aromaticity and polar functional groups for MAC, thus making hydrophobic interactions predominant. For biochars, the deviation from linearity started from 4-t-OP$_3$EO (BC450 and BC850) and 4-t-OP$_4$EO (BC650). These deviations may depend on the multiple interactions governing the sorption of organic compounds on chars.

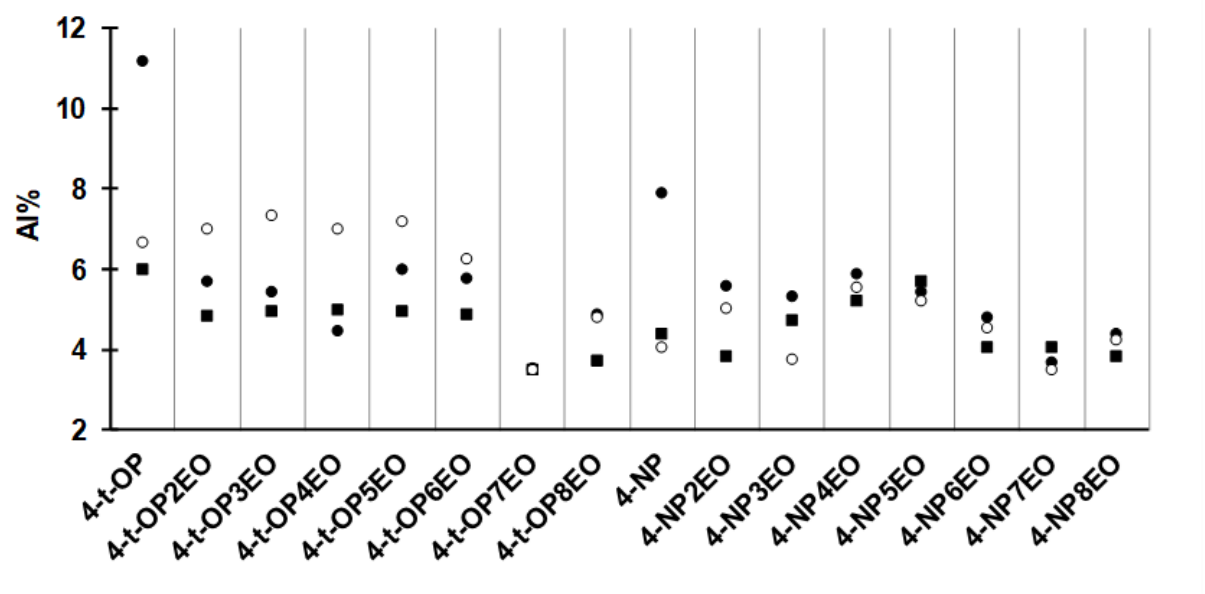

Figure 3.7. Mean values of relative adsorption index (AI%) determined for each target analyte, expressed as the percentage ratio between K_F values for a biochar and the virgin mineral activated carbon. BC450 (■); BC650 (●); BC850 (○).

Moreover, it is important to underline that the isothermal sorption experiments were conducted using a WWTP effluent which contains organic compounds differing from those investigated that are able to compete with the adsorption sites of the materials, thus making the data interpretation even more complex. Among the deviations from linearity observed in biochars for the K_F versus log Kow trend, it must also be observed that for BC450, and especially BC650 and BC850 (**Figures 3A-C**), the sorption capacities of 4-t-OP_8EO and 4-t-OP_7EO were approximately the same. This latter finding is probably related to the exclusion of the oligomers with 7-8 ethoxylate units from the pores of the biochars, which are for the most part in the micropore range. In fact, the molecular width of these oligomers (approximately from 3.25 to 3.50 nm) falls within the dimensional range of the mesopores. In this regard, it is interesting to note that in MAC, this exclusion phenomenon did not occur since the material is predominantly mesoporous (**Table 3.2**).

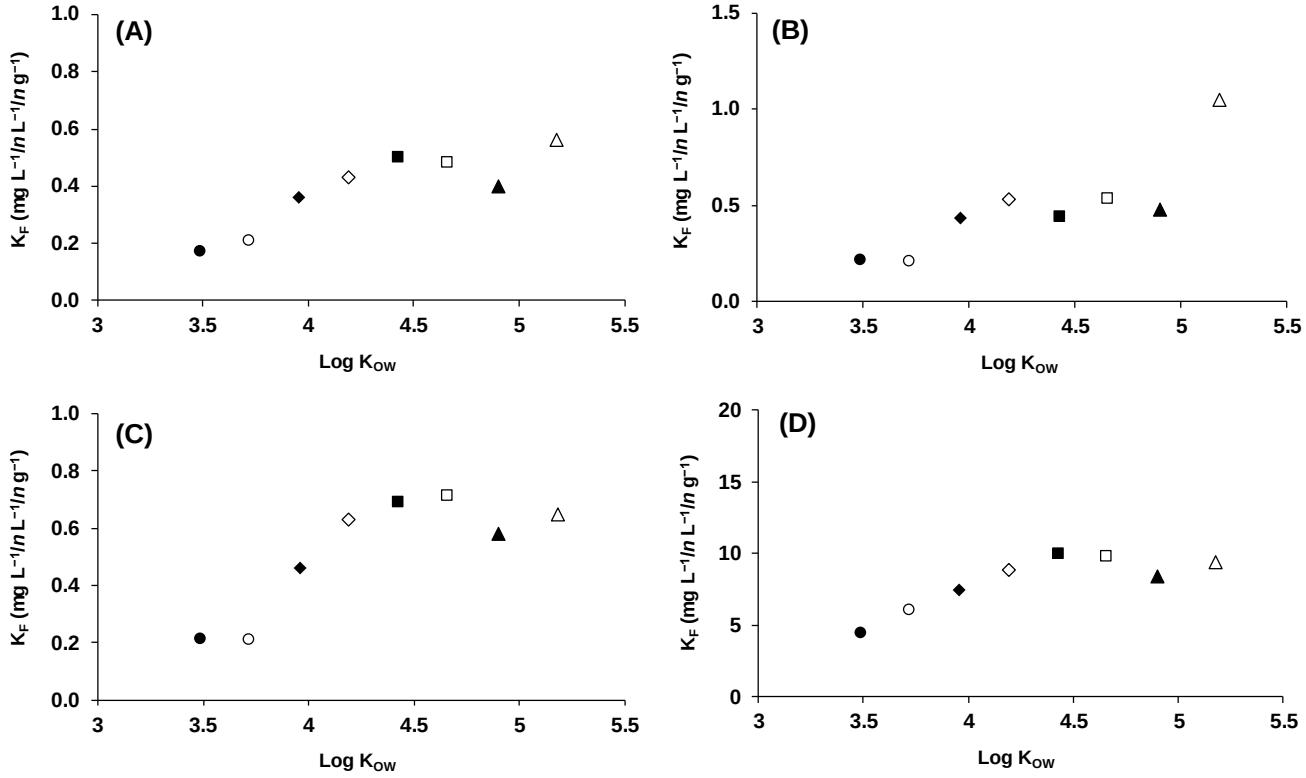

Figure 3.8. Trend of Freundlich adsorption capacity (K_F) as a function of log K_{OW} values for: 4-t-OP_8EO (●); 4-t-OP_7EO (○); 4-t-OP_6EO (◆); 4-t-OP_5EO (◇); 4-t-OP_4EO (■); 4-t-OP_3EO (□); 4-t-OP_2EO (▲); 4-t-OP (△). (A) BC450; (B) BC650; (C) BC850 and (D) MAC.

Considering the effect of the pyrolysis temperature on sorption estimated by the K_F values, the data reported in **Table 3.6** showed that in almost all cases BC450 exhibited the lowest sorption capacity, in agreement with its lower surface area and micro/mesoporosity development. For 4-t-OP and 4-NP – the smallest analytes within the group of molecules investigated (molecular width about 0.8-1.0 nm) – a sharp improvement of the sorption capacity was found from 450 °C to 650 °C, followed by a similar sharp decrease from 650 °C to 850 °C. This result is in full agreement with XPS and FTIR data which, as a whole, highlighted for BC650 the highest degree of aromatization (very important for sorption by π-π interactions) and the residual presence of polar functional groups that can contribute to sorption via the hydrogen bond and/or other polar interactions. More similar adsorption capacities were found for the other compounds, even though BC850 behaved slightly better for 4-t-OPnEOs with n=2-6, while BC650 was more effective for the corresponding nonyl derivatives.

3. Evaluation of sorption performances of biochars in comparison with MAC

Freundlich isotherm is empirical, whereas the Langmuir equation is based on very different model assumptions from the experimental conditions related to the adsorption of solvated molecules, especially in a real effluent WW such as the one used in this study. It is therefore evident that the model parameters of Langmuir (Q_m and k) and Freundlich (K_F and n) equations cannot be interpreted as fully significant values of adsorption capacity and intensity. However, these data can be compared with those obtained in the same experimental conditions using a reference sorbent material (i.e., MAC), and thereby obtaining more meaningful information for evaluating the removal performance of biochar. To this end, a relative adsorption index (AI%) can be calculated for each target compound as the percentage ratio of the adsorption capacities of biochars and MAC, using the K_F values for their evaluation (see **Figure 3.7**). AI% values were in the ranges of 3.5-6.0, 3.5-11.2 and 3.4-7.3, for BC450, BC650 and BC850, respectively. Overall, far higher AI% values were

obtained with BC650 for 4-t-OP (11.2%) and 4-NP (7.9%), which are listed in the Directive 2013/39/EU (European Parliament and Commission, 2013) as priority and priority hazardous substances and must therefore be considered of major environmental importance. Even though these sorption performances are 9-13 times lower than that of MAC, it should be stressed that they were obtained by a simple pyrolytic thermal conversion of a recycled biomass at a relatively low temperature (650°C), without any activation process. BC650 was also the best performing material for the sorption of 4-NPnEOs. However, the performance differences among materials were much more similar than those observed for APs, and approximately 17-25 times worse than MAC. Conversely, for 4-t-OPnEOs with n=2-5, the best removal performance was obtained with BC850, which provided a relative sorption performance approximately 14 times lower than MAC. BC850 was also the best performing material for t-OP_6EO, with a removal performance about 16 times lower compared to MAC and more similar to BC450, and especially BC650 (**Figure 3.6**). Still lower removal performances were found for 4-t-OP_8EO and above all for 4-t-OP_7EO, the latter showing the same sorption by the three biochars (**Table 3.6**).

4. Cost comparison between biochar and activated carbon

A market survey that involved the water potabilization companies of Tuscany (Italy) has shown that they obtain activated carbon at a wholesale price (i.e., 2.1-2.6 €/kg). The biochar produced in Italy is not currently used as water filtering material. However, the production of biochar from waste

vegetal biomass similar to those in this study used as feedstock of the pyrolysis process, is now starting up in Italy in the soil amendment market. According to the information provided by Romana Maceri Impianti S.r.l. (Arezzo, Italy), currently the largest biochar producer in Tuscany, this material is currently commercialized in the agricultural sector at a price of approximately 0.15 €/kg, which could of course be lowered in case of supplies comparable to those of activated carbons in WWTPs. Consequently, a price of biochar at least 16 times lower than that of activated carbon can be considered plausible, making biochar competitive with the marketed activated carbon, at least for the removal of APs, which, as mentioned above, have shown a sorption performance 9-13 times lower than that of MAC.

IV. Conclusion

For the first time, this research has provided information on sorption by biochar in real effluent WW of a mixture of AP_nEOs and APs which are very widespread micropollutants of environmental concern in WW and surface water. All biochars produced in this study using mixed coniferous and broad-leaved waste biomass, within a pyrolysis temperature range of 450-850 °C, complied with the EN 12915-1/2009 limits for metal and PAH leaching in water and provided a negligible contribution to the release of salts in the treated water.

The sorption of AP_nEOs and APs by BC450, BC650, BC850, and MAC showed a lower performance of biochar in comparison with activated carbon. The sorption by biochar was governed by multiple interaction mechanisms, which were more or less significant depending on the pyrolysis temperature and the resulting characteristics of the materials. In particular, BC650 showed the presence of surface aromatic domains and polar functionalities, together with a quite high surface area (319 m^2 g^{-1}), achieving the best sorption performance towards 4-t-OP and 4-NP (i.e., 9-13 times lower than those determined with MAC), which are the target analytes of the greatest environmental concern among those investigated. However, considering the cheaper market price of biochar compared to activated carbons (at least 16 times less expensive), the former can be considered commercially competitive with the latter and hence worth being further investigated for future applications in water and WW treatment. It should also be emphasized that the production and use of biochar from waste biomass is in line with the modern approach to resource management and the circular economy.

V. Bibliography

Ahmad, M., Lee, S. S., Rajapaksha, A. U., Vithanage, M., Zhang, M., Cho, J. S., Lee, S-E., Ok, Y. S., 2013. Trichloroethylene adsorption by pine needle biochars produced at various pyrolysis temperatures. Bioresour. technol. 143, 615-622.

Ahmad, M., Rajapaksha, A. U., Lim, J. E., Zhang, M., Bolan, N., Mohan, D., Vithanage, M., Lee, S. S., Ok, Y. S., 2014. Biochar as a sorbent for contaminant management in soil and water: a review. Chemosphere, 99, 19-33.

Brewer, C. E., Sarpong, K. A., Amiri, A., Smith, M. B., Idowu, O. J. Effects of Pyrolysis Conditions on Leaching of Salts from Halophyte Biochars. 2017 ASABE Annual International Meeting. ASABE, St. Joseph, MI, 2017, pp. 1.

Chen, X., 2015. Modeling of experimental adsorption isotherm data. Information, 6, 14-22.

Coates, J., 2006. Interpretation of infrared spectra, a practical approach. Encyclopedia of analytical chemistry: applications, theory and instrumentation.

De la Rosa, J. M., Sánchez-Martín, Á.M., Campos, P., Miller, A.Z., 2019. Effect of pyrolysis conditions on the total contents of polycyclic aromatic hydrocarbons in biochars produced from organic residues: Assessment of their hazard potential. Sci. Total Environ. 667, 578-585.

European Committee for Standardization. EN 12915:2009, Products used for the treatment of water intended for human consumption - Granular Activated Carbon, 2009.

European Council of Chemical Manufacturers' Federation. Test Method for Activated Carbon, 1986.

European Parliament and Commission. Directive 2013/39/EU of the European Parliament and of the Council of 12 August 2013 amending Directives 2000/60/EC and 2008/105/EC as regards priority substances in the field of water policy. Off. J. Eur. Union 2013; 226: 1-17.

European Parliament the Council. Directive 2003/53/EC of the European Parliament and of the Council of 18 June 2003 Amending for the 26th time Council Directive 76/769/EEC Relating to Restrictions on the Marketing and Use of Certain Dangerous Substances and Preparations (nonylphenol, nonylphenol ethoxylate and cement), 2003.

Fu, P., Hu, S., Xiang, J., Sun, L., Su, S., An, S., 2012. Study on the gas evolution and char structural change during pyrolysis of cotton stalk. J Anal Appl Pyrolysis 97, 130-136.

Harvey, O. R., Herbert, B. E., Rhue, R. D., Kuo, L-J., 2011. Metal Interactions at the Biochar-Water Interface: Energetics and Structure-Sorption Relationships Elucidated by Flow Adsorption Microcalorimetry. Environ. Sci. Technol. 45, 5550-5556.

Inyang, M., Dickenson, E., 2015. The potential role of biochar in the removal of organic and

microbial contaminants from potable and reuse water: A review. Chemosphere 134, 232-240.

Irfan, M., Chen, Q., Yue, Y., Pang, R., Lin, Q., Zhao, X., Chen, H., 2016. Co-production of biochar, bio-oil and syngas from halophyte grass (*Achnatherum splendens* L.) under three different pyrolysis temperatures. Bioresour. Technol. 211, 457-463.

Jian, X., Zhuang, X., Li, B., Xu, X., Wei, Z., Song, Y., Jiang, E., 2018. Comparison of characterization and adsorption of biochars produced from hydrothermal carbonization and pyrolysis. Environ. Technol. Innov. 10, 27-35.

Kearns, J. P., Wellborn, L. S., Summers, R. S., Knappe, D. R. U., 2014. 2,4-D adsorption to biochars: Effect of preparation conditions on equilibrium adsorption capacity and comparison with commercial activated carbon literature data. Water Res. 62, 20-28.

Keiluweit, M., Kleber, M., Sparrow, M. A., Simoneit, B. R. T., Prahl, F. G., 2012. Solvent-Extractable Polycyclic Aromatic Hydrocarbons in Biochar: Influence of Pyrolysis Temperature and Feedstock. Environ. Sci. Technol. 46, 9333-9341.

Liu, G., Zheng, S., Yin, D., Xu, Z., Fan, J., Jiang, F., 2006. Adsorption of aqueous alkylphenol ethoxylate surfactants by mesoporous carbon CMK-3. J. Colloid Interface Sci. 302, 47-53.

Liu, Y., He, Z., Uchimiya, M., 2015.Comparison of biochar formation from various agricultural by-products using FTIR spectroscopy. Mod. Appl. Sci. 9, 246.

McBeath, A. V., Smernik, R. J., Schneider, M. P. W., Schmidt, M. W. I., Plant, E.L., 2011. Determination of the aromaticity and the degree of aromatic condensation of a thermosequence of wood charcoal using NMR. Org. Geochem. 42, 1194-1202.

Sarkar, P., Sahu, S. G., Mukherjee, A., Kumar, M., Adak, A. K., Chakraborty, N., Biswas, S., 2014. Co-combustion studies for potential application of sawdust or its low temperature char as co-fuel with coal. Appl. Therm. Eng. 63, 616-623.

Sposito, G., 1982. On the use of the Langmuir equation in the interpretation of "adsorption" phenomena: II. The "two-surface" Langmuir equation. Soil Sci Soc Am J. 46, 1147-1152.

Tan, X., Liu, Y., Zeng, G., Wang, X., Hu, X., Gu, Y., Yang, Z., 2015. Application of biochar for the removal of pollutants from aqueous solutions. Chemosphere, 125, 70-85.

Thermo Fisher Scientific. XPS Elements Table - Carbon. 2019, https://xpssimplified.com/elements/carbon.php, accessed on 12 July 2019, 2019a.

Thermo Fisher Scientific. XPS Elements Table - Oxygen. 2019, https://xpssimplified.com/elements/oxygen.php, accessed on 12 July 2019, 2019b.

Wang, Z., Guo, H., Shen, F., Yang, G., Zhang, Y., Zeng, Y., Wang, L., Xiao, H., Deng, S., 2015. Biochar produced from oak sawdust by Lanthanum (La)-involved pyrolysis for adsorption of ammonium (NH_4^+), nitrate (NO_3^-), and phosphate (PO_4^{3-}). Chemosphere, 119, 646-653.

Xiao, F., Pignatello, J. J., 2015. Interactions of triazine herbicides with biochar: Steric and electronic effects. Water Res. 80, 179-188.

Zhang, W., Chang, Q. G., Liu, W. D., Li, B. J., Jiang, W. X., Fu, L. J., Ying, W. C., 2007. Selecting activated carbon for water and wastewater treatability studies. Environ. Prog. Sustain. 26: 289-298.

Zhao, L., Cao, X., Mašek, O., Zimmerman, A., 2013. Heterogeneity of biochar properties as a function of feedstock sources and production temperatures. J. Hazard. Mater. 256,1-9.

Zhu, X., Li, C., Li, J., Xie, B., Lü, J., Li, Y., 2018. Thermal treatment of biochar in the air/nitrogen

atmosphere for developed mesoporosity and enhanced adsorption to tetracycline. Bioresour. Technol.y 263, 475-482.

Part 4
Highlighting the effects of pyrolysis conditions and sludge ration on physiochemical properties of a sludge-based biochar and its activation using gasification waste by-product

I. Optimum parameters for producing biochar

The biochar properties are strongly related to the feedstock and pyrolytic conditions (pyrolysis time and temperature**). Table 4.1** presents the different conditions of the biochar synthesis that were established using a quality by design approach and its obtained results.

Twelve biochars produced from sawdust and sludge mixtures were characterized to demonstrate in one step the simultaneous variation of biochar synthesis parameters on its physicochemical properties and in the second step its adsorption efficiency. The determination of ash content, water-extractable metals and polycyclic aromatic hydrocarbons showed that all the produced biochars are not useful according to European Norm.

Table 4.1. Results of the quality by design used for the biochars production.

Exp.	Sawdust origin	Sludge type	Temperature	Contact time	Sludge percen-tage	BET surface area	Ash	As	Cd	Cr	Hg	Ni	Pb	Sb	Se	Sum of 6 PAHs*
			ºC	min	%	m²/g	(%)	ppb	ppb	ppb	ppb	ppb	ppb	ppb	ppb	(ng/L)
1	Oak		450	120	0	34.26	6	0.49	<0	7.7	<0	1.85	<0	0.27	0.01	165.1
2	Oak		650	60	0	336.3	10	0.14	<0	33.07	<0	<0	<0	0.04	<0	109.86
3	Poplar		850	120	0	551.5	8	0.39	<0	2.24	1.12	<0	<0	0.16	<0	20.86
4	Poplar	Calice	450	60	15	73.7	11	24.98	<0	66.23	0.1	3.8	<0	6.17	1.04	135.82
5	Oak	Vernio	650	120	15	258.30	22.5	0.69	<0	34.46	<0	<0	0.08	1.1	0.38	138.44
6	Poplar	Vernio	850	60	15	370.11	27.44	0.94	<0	18.22	<0	<0	0.12	3.25	1.57	29.39
7	Oak	Vernio	450	60	30	16.94	28.76	5.1	<0	18.56	<0	1.41	<0	4.2	2.05	0.855
8	Poplar	Calice	650	120	30	269.47	24.09	4.5	<0	69.12	0.02	<0	<0	2.7	0.43	5.426
9	Oak	Calice	850	60	30	300.14	26.65	2.43	<0	35.89	0.02	<0	<0	2.18	0.69	12.189
10	Poplar		850	120	0	680.14	7.86	0.56	<0	47.53	<0	<0	0.06	0.1	<0	23.5
11	Oak	Calice	850	60	30	319.04	26.98	2.62	<0	69.87	0.03	<0	<0	2.48	0.59	12.26
12	Poplar	Calice	650	120	30	285.11	21	3.45	<0	31.31	0.01	<0	<0	2.69	0.37	5.29
Limit*							15	10	0.5	5	0.3	15	5	3	3	20

II. Characterization of sludge based biochars

1. Porosimetry results

Figure 4.1 shows that the specific surface area increased with the increase of pyrolysis temperature, from 35 to 680 m^2g^{-1}, which was reported also in the literature for biochar obtained from vegetal or sludge feedstock (Pariyar et al. 2020). This increase is related to a complete carbonization of the materials at high temperature compared to the lower ones, where the carbonization is partial (Devi and Saroha, 2015). In fact, as shown in **Figure S4.1,** a pyrolysis temperature of 450°C created the lowest specific surface area (35, 73, 17 $m^2\ g^{-1}$) compared to biochars produced at 650°C and 850°C, where the volatilities of organic compositions increased. In fact, during the carbonization process, the volatilization and decomposition of organic matter produce the porosity of the biochar surface (Wang et al., 2018). The produced tars during the production of biochar and by increasing the

carbonization temperature from 450°C to 650°C and 850°C, transformed to pyrolytic gas which could enhance the micropores training in the surface of biochar (Jin et al., 2017).

As reported in the literature, biochar obtained from only woody biomass have a slightly higher specific surface area and specific pore volume than biochar derived from sludge (Wu et al., 2016). For example, the maximum of specific surface area and pore volume were reduced from 680 $m^2\ g^{-1}$ and 0.43 $cm^3\ g^{-1}$ to 370 $m^2\ g^{-1}$ and 0.225$cm^3\ g^{-1}$ for BC10 and BC6, obtained only poplar sawdust and poplar (85%) mixed with 15% of sewage sludge from Vernio WWTP at 850°C, respectively. Furthermore, micropores and mesopores total volume of the samples containing sludge were lower than those produced only from woody biomass. The highest surface area for biochar contained 30% of sludge was also obtained for the biochar produced at 850°C from oak and contained sludge from Calice WWTP (BC 11). This result could be also related to the highest pyrolysis temperature.

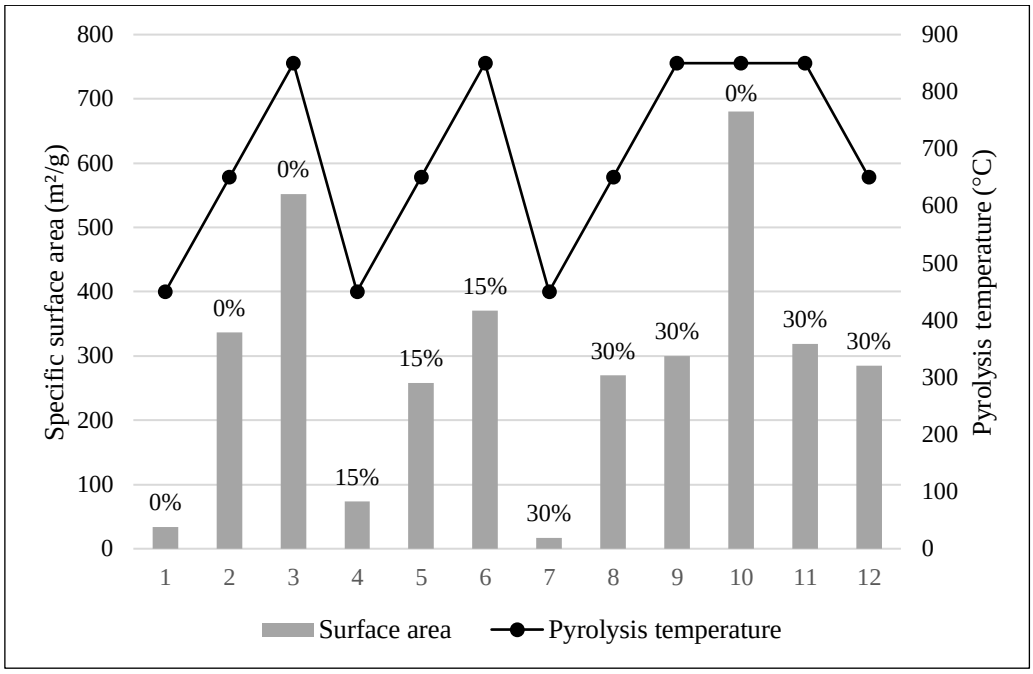

Figure 4.1. Influence of pyrolysis temperature on the biochars specific surface area.

2. Elemental analysis

According to the results of the elemental analysis shown in **Table 4.2**, different surface characteristics can be observed between the group of biochars prepared without sludge and the one obtained from sludge and woody biomasses mixtures at each temperature. The C content increased with the increase of pyrolysis temperature for different biochars which was verified in the literature (Chun et al., 2004). However, the O and H contents decreased with the increment of temperature as result of the weak bonds cracking (Demirbas, 2004). This decrease of H and O percentages could be explained also by the condensation of the hydroxyl groups at high pyrolysis temperature. The biochar basicity increased after loss of O at high temperature (Ahmad et al., 2012). Moreover, the

use of sewage sludge in the biochar production reduced the percentage of basic element (C, H and O) at each temperature (450, 650 and 850°C). The reduction of the C content in biochar derived from the mixture of woody biomass and sewage sludge is related to the high volatile matter and ash content of the sludge (Zielińska et al., 2015). The N percentage depended on the feedstock origins and decreased with the rise of temperature which was verified by many others works (Song and Guo, 2012). The N content was lower in biochars obtained only from woody materials (< 0.5%) compared with those containing sludge, which was reported in previous study done by Pariyar et al. (2020). No Sulphur content was reported in all biochars, this is explained by the abundance of vegetal source rich in lignin that has less or no Sulphur content also explained by the release of Sulphur as gas during the pyrolysis process (Lang et al. 2005; Lehman and Joseph, 2009). The H/C, O/C and (O + N)/C reports decreased with the increase of the pyrolysis temperature. The decrease of H/C and (O + N)/C ratio with pyrolysis temperature indicated an increase in aromaticity and a decrease in polarity by reduction of polar surface functional groups (Zhang et al., 2011; Ahmad et al., 2012; Chang et al., 2019). All biochars have very low H/C reports less than 0.4 indicating that produced biochars are chemically stable and characterize by an important degree of aromaticity (Enders et al., 2012).

Table 4.2. Elemental composition, atomic ratio, pH of the point zero charge and ash content.

	Composition (%)					Atomic ratio				
Biochar	N	C	H	S	O	H/C	O/C	(O+N)/C	pH_{pzc}	Ash content (%)
1	0.42	61.42	2.03	Nd	30.13	0.033	0.491	0.497	6.23	6
2	0.29	77.37	1.25	Nd	11.09	0.016	0.143	0.147	10.05	10
3	0.18	79.75	0.71	Nd	11.36	0.009	0.142	0.145	10.18	8
4	2.09	55.23	1.62	Nd	30.07	0.029	0.544	0.582	7.4	11
5	0.90	63.94	1.13	Nd	11.03	0.018	0.173	0.186	10.05	22.5
6	0.57	57.14	0.72	Nd	14.56	0.013	0.255	0.265	10.5	27.44
7	1.95	47.56	1.60	Nd	19.89	0.034	0.418	0.459	6.9	28.76
8	1.30	64.03	1.16	Nd	9.51	0.018	0.149	0.169	10.15	24.09
9	0.93	64.83	0.77	Nd	6.48	0.012	0.1	0.14	10.6	26.65
10	0.21	76.25	0.46	Nd	15.09	0.006	0.198	0.2	10.1	7.86
11	0.87	63.25	0.87	Nd	8.02	0.014	0.127	0.14	10.6	26.98
12	1.71	65.68	1.37	Nd	10.23	0.021	0.156	0.182	10.15	21

3. Point of zero charge

The basic surface character was proved also by the pH of the point of zero charge which is between 10 and 10.6 for biochars contained 30% of sludge except BC7 which has a pH_{pzc} equal to 6.9 (**Table 4.2**). Then these results suggest that the prepared biochars are positively charged when put in contact with WW, which has commonly lower pH values. Hence, the biochars should be suitable

for the adsorption of negatively charged molecules.

4. Ash content

Table 4.2 shows that the ash percentages varied from 6 to 29, which indicated the big change in the mineral contents of biochar derived from different compositions. All biochars containing sewage sludge have higher ash content (from 11 to 29%) compared to biochar obtained from only woody biomasses (less than 15%), which was also confirmed in the literature (Regkouzas and Diamadopoulos, 2019). The ash content increased with the rise of pyrolysis temperature in biochar produced from sludge (Hossain et al., 2011; Yuan et al., 2015. Zhang and Wang, 2016), as well as from other feedstocks (Novak et al., 2009; Al-Wabel et al., 2013). This is due to the removal of volatile constituents and the accumulation of non-volatile mineral elements (Cao and Harris, 2010). The highest ash content was obtained in BC7 derived from 70% oak sawdust and 30% of sludge at 450°C. This result could be explained by the high mineral fractions in the sewage sludge which is characterized by its complexity and constituents' diversity. The used sludge could contain high amount of silica and minerals constituents which increased the ash content.

5. Water extractable metals

The toxic impact of biochar derived or contained sewage sludge can be determined from the higher heavy metal contents. **Table 4.3** presents the result of metal leaching analysis of all biochars. Metal concentrations were in accordance with the European required standards (EN 12905 – 1), with the following exception: Cr in all biochars (except BC3); Sb in BCs 4, 6 and 7; As in BC4 and Hg in BC3. Contents of major elements, except K and Fe, increased by adding sewage sludge in the production of biochars. The increase in concentrations of the other metals was also observed with increasing the sludge percentage in the feedstock, with the exceptions of Pb and Ni.

Table 4.3. Water extractable metals.

	Na	Mg	K	V	Cr	Mn	Fe	Ni	Cu	Cd	As	Se	Sb	Hg	Pb
	ppm	ppm	ppm	Ppb	ppb	ppb	ppb	ppb	ppb	Ppb	ppb	ppb	ppb	ppb	ppb
1	<0.0	4.41	39.75	0.99	7.7	67.12	23.89	1.85	1.99	<0.0	0.49	0.01	0.27	<0.0	<0.0
2	<0.0	2.26	40.71	0.67	33.07	4.88	23.01	<0.00	<0.0	<0.0	0.14	<0.0	0.04	<0.0	<0.0
3	<0.0	1.69	58.05	0.29	2.24	<0.0	<0.0	<0.00	<0.0	<0.0	0.39	<0.0	0.16	1.12	<0.0
4	43.77	12.5	72.71	7.36	66.23	97.5	11.6	3.8	39.87	<0.0	24.98	1.04	6.17	0.10	<0.0
5	<0.0	1.92	29.58	1.93	34.46	5.22	8.89	<0.0	59.76	<0.0	0.69	0.38	1.1	<0.0	0.08
6	5.6	0.25	36.42	3.62	18.22	2.24	25.61	<0.0	<0.0	<0.0	0.94	1.57	3.25	<0.0	0.12
7	0.55	9.51	24.99	2.79	18.56	259.9	24.28	1.41	6.812	<0.0	5.10	2.05	4.2	<0.0	<0.0
8	18.3	1.54	44.67	3.71	69.12	1.67	<0.0	<0.00	<0.0	<0.0	4.5	0.43	2.7	0.02	<0.0
9	21.5	2.23	34.82	11.4	35.89	<0.0	<0.0	<0.0	<0.0	<0.0	2.43	0.69	2.18	0.02	<0.0
10	<0.0	7.59	24.27	2.85	47.53	1.93	8.911	<0.0	<0.0	<0.0	0.56	<0.0	0.1	<0.0	0.06
11	20.4	2.04	26.03	30.6	69.87	0.34	<0.0	<0.0	<0.0	<0.0	2.62	0.59	2.48	0.03	<0.0
12	27	2.34	36.68	3.83	31.31	0.96	133.62	<0.0	<0.0	<0.0	3.45	0.37	2.69	0.01	<0.0
Limit*					5			15		0.5	10	3	3	0.3	5

* European Regulation EN 12915-1/2009

At low temperature, the concentrations of all heavy metals were important as a result to the low volatilization of heavy metal. In fact, the first step of the pyrolysis is the evaporation of water and the degradation of organic matter (He et al., 2019). However, the high boiling point of heavy metal enhanced the amounts of these elements in biochar. Furthermore, the aptitude of heavy metal to transform from hydroxide and mineral salts into sulphides and oxides with higher thermal stability decreases their volatilization, at elevated temperature (Yuan et al., 2015). Besides, co-pyrolysis of sewage sludge with woody material influenced desired properties such as major elements, nutrients enrichment and fixed carbon concentrations which were demonstrated by Krueger et al. (2020). In fact, authors were reported that biochar obtained from sludge contained high metals concentrations then those obtained from vegetal and agricultural waste (Jin et al., 2017, Huang et al., 2017).

6. Water extractable PAHs

Results reported in **Table 4.4** showed that the total concentration of PAHs in biochar depended on the feedstock type and also the carbonization conditions. More in detail, PAHs concentrations decreased with the rise temperature. This behaviour is in agreement with findings elsewhere achieved for sludge-based biochar that showed an increase in PAHs concentrations for production temperatures from 200°C to 400-500°C and then their sharp decrease. Pyrolysis temperature strongly modifies the composition of biochar and its chemical structure, altering PAH formation and leaching. The increase in pyrolysis temperature up to about 500°C results in the loss of C, H, O and N from sludge, the formation of aromatic compounds, and their condensation into polyaromatic structures. The decrease of the leachable PAHs in biochar produced at pyrolysis temperatures above 500°C could be due to the volatilization of the amorphous phase and the nuclear condensation of

aromatic compounds in non-extractable sheet like structures with the augment of their retention in the biochar matrix. The sum of fluoranthene, benzo(b)fluoranthene, benzo(k)fluoranthene, benzo(a)pyrene, indeno(1,2,3-cd) pyrene and benzo(a)pyrene concentrations in biochar produced only from wood exceeded the European required standards (EN 12915-1/2009). However, the total concentrations of these six PAHs in biochars containing 30% of sewage sludge (7, 8, 9, 11 and 12) were lower than the required limits of leachable concentrations (20 ng/L).

Table 4.4. Water-extractable PAHs content in the prepared biochars

Biochar	1	2	3	4	5	6	7	8	9	10	11	12
Flu	26.2	28.7	3.92	8.8	7.8	12.4	0.40	2.53	0.99	4.6	4.08	2.55
B(b)Flu	56.4	15.5	0.43	55.01	55.7	0.54	0.045	0.10	0.143	0.29	0.72	0.057
B(k)Flu	0.28	3.1	0.14	0.16	n.d	0.14	0.038	0.046	0.086	0.25	0.16	0.032
B(a)Pyr	81.7	42.9	16.1	71.5	74.5	16	0.082	2.58	10.9	17.3	5.98	2.59
IPyr	n.d	12.6	n.d	n.d	n.d	n.d	n.d	n.d	n.d	0.46	n.d	n.d
BPyr	0.52	7.06	0.27	0.35	0.44	0.31	0.29	0.17	0.17	0.6	1.32	0.07
Sum*	165.1	109.86	20.86	135.82	138.44	29.39	0.855	5.426	12.289	23.5	12.26	5.299

* Sum of 6 leachable PAHs.
Flu: Fluorene; B(b)Flu: Benzo(b)fluoranthene; B(k)Flu: Benzo(k)fluoranthene; B(a)Pyr: Benzo(a) pyrene; IPyr: Indeno(1,2,3-cd)pyrene; BPyr: Benzo(g, h, i)perylene; n.d = not detected.

The reduction of the PAHs content could be effectuated by pyrolyzing the feedstock at high temperature (> 700°C) which modify the surface proprieties of biochar by improving the surface area (Czajczyńska et al., 2017) and decreasing the surface functional groups that enhance the biochar's adsorption capacity (Tang et al., 2019).

In summary, biochars contained sewage sludge and obtained at high temperature have higher BET surface area, are chemically stable and characterize by low leachable PAHs and an important degree of aromaticity will be used for the modification and adsorption tests.

III. Optimum parameters for biochars modification

The properties of all prepared biochars using a quality by design are not useful according to the European Regulation UNI EN 12915 – 1 regarding the high ash contents, metals and PAHs release. Therefore, the modification of biochar, surface characteristics and possible water leaching that enhance their performance is a necessity. Acidic modification is used usually to eliminate mineral impurities such as ash and metals, to increase also the surface acidic functional groups. The frequent used acids are sulfuric acid, phosphoric acid, nitric acid, hydrochloric acid, citric acid and oxalic acid (Vithanage et al., 2015; Aghababaei et al., 2017). However, in this work a new approach was proposed to modify biochar instead of the chemical agents previously located, which is the use of an acidic wood gasification WW for washing biochar. The characterization of this product is

mentioned in the **Supplementary S.4.2** part and **Table S4.2**.

The acidic washing of biochar is influenced by many parameters such as contact time and the biochar weight-to-gasification WW volume ratio adopted for the washing process. In fact, interesting physicochemical properties (high specific surface area, low ash content and metals leaching) of carbon adsorbents are strongly dependent on the distinct properties of the production processes. Therefore, a preliminary study of biochar modification using acidic gasification WW was carried out to optimize the treatment procedure. The evaluation of the optimum time used for washing biochar was carried out based on the variation of ash content and specific surface area with the washing time of BC7 and BC9. The choice of these two biochars based on their high ash content (28.76% in BC7 and 26.65% in BC9) and the lowest specific surface area for BC7. Different contact times were used;30 and 60 min for the treatment of BC7. Results present in **Table 4.5** showed that after 30 minutes an increase about 3.45 time of surface area more than the initial value was obtained then a reduction of this value to 10 m^2/g was registered after a contact time about one hour. This result could be explained by the polyphenols adsorption that could occur after the removal of inorganic impurities and ash from the surface blocked pores. However, for BC9, it was deduced that after one hour of washing (the longer time), there is no advantages for specific surface area. After 30 minutes of washing using the acidic water of BC9 the ash content reduced from 27% to 9% and to 8% after a contact time about one hour. However, for BC7, the ash content was reduced to 15% after 30 minutes and 17% after 60 minutes. Overall, these results showed that 30 minutes are the optimal washing time of biochar using the gasification WW.

Table 4.5. Effect of contact time on the specific surface area and ash content of biochars 7 and 9.

	Biochar 7			Biochar 9		
Contact time (min)	0	30	60	0	30	60
Specific surface area (m^2/g)	16.94	58.57	10.00	300.14	281.11	297.13
Ash content (%)	28.76	15.00	17.00	26.65	9.00	8.00

To optimize the ratio between the biochar weight and acidic product volume used for washing biochar, a filter pH monitoring has been performed after using the three ratios 1:10, 1:15 and 1:20 (w/v). **Table 4.6** shows that there is no significant effect of the biochar pH after washing using the three reports (W/V), hence, the lower volume of gasification WW was considered for further studies.

Table 4.6. Effect of the report biochar/ gasification wastewater on the pH value.

Biochar weight (g)	Volume of woody distillate (ml)	pH
1	10	3.97
1	15	3.85
1	20	3.65

Briefly, the process adopted in this study for the modification of biochar was a report 1/10 (w/v) (biochar/gasification WW) with a contact time of 30 minutes.

IV. Characterization of modified biochars

The use of the gasification WW reduced the ash content of biochar that contained ash percentages superior to the European norm (15%) and improved the specific surface area of sludge based biochars except BC6 as shown in the **Table 4.7**.

Table 4.7. Ash contents and BET surface areas of biochars 5, 6, 7, 8, 9, 10 and 11 before and after the acidic washing.

Simple	BC5	BC6	BC7	BC8	BC9	BC 10	BC 11
Ash content before washing (%)	22.50	27.44	28.76	24.09	26.65	7.86	26.98
Ash content after washing (%)	11.25	10.43	15.00	8.95	9.00	1.33	10.47
BET surface area before washing (m^2/g)	258.30	370.11	16.94	269.47	300.14	680.14	319.04
BET surface area after washing (m^2/g)	294.30	241.12	58.57	280.13	281.11	389.79	343.72

As illustrated in **Table 4.8**, the acid-washing using gasification WW and thermal activation of BCs 8 and 11 improved the specific surface area. This enhancement could be result from the elimination of the impurities and undesired constituents produced by the pre-carbonization treatment such as inorganic compounds and ash from the surface blocked pores (Liou and Wu, 2009). More in details, the specific surface area of BC11 increased from 319 to 459. 4 m^2/g and from 269.47 to 360.27 m^2/g for BC8. In fact, after the different modifications, micropore, mesopore and total pore volumes were also increased. Specific surface area and micropore total volume of BC8 and BC11 increased slightly after treatment with the gasification WW, this result was presented by the nitrogen adsorption desorption isotherms. In general, acidic treatment of biochar enhances the surface proprieties (Vithanage et al., 2015; Zhang et al. 2020) such as by surface carboxylic groups improvement which are suitable for increase the adsorption of various toxic elements such as sulfamethazine (Vithanage et al., 2015), Pd, Zn and Cu (Uchimiya et al., 2012) Cd and oxytetracycline (Aghababaei et al., 2017). Moreover, Biochar properties could be enhanced by activation that may be effectuated using gas or steam such as nitrogen, water vapor, CO_2 or air. This

enhancement could allow to the development of the specific surface area, surface reactivity, micro and mesoporosity (Rajapaksha et al., 2015). Gas activation could eliminate the impurities and undesired constituents produced by the incomplete combustion. This activation could change the surface functionality and reduce the availability of some surface functional groups such as the phenolic groups. Also, carboxylic acid could be degraded regarding its labile behaviour to gas activation inducing low oxidized char and a heavy metals remediations regarding the binding site that could be done by the carboxylic groups (Uchimiya et al., 2012; Pourret and Houben, 2018). Therefore, gas activation could induce to the production of biochar characterized by an extended surface area and a low polarity, thus the use of another modification is necessary in the case of positively functional groups requirement. The gasification WW and thermal activation enlarged the porosity of BCs 8 and 11 by increasing the micropore and mesopore total volumes by 72.72 and 36.37% for BC8 and by 73.07 and 9.57 % for BC11, respectively. However, ABC11 had higher pores volumes (0.151 cm^3 g^{-1}) compared to ABC8 (0.09 cm^3 g^{-1}) which could be related the pyrolysis conditions of BC11 at higher temperature (850°C) than BC8 (650°C). These results indicated the efficacy of gasification WW and above all thermal activation under nitrogen steam in the amelioration of the porosity of biochar containing 30% of sewage sludge.

Table 4.8. Porosimetry results of raw, washed and activated biochars 8 and 11.

Sample	BC8	WBC8	ABC8	BC11	WBC11	ABC 11
Specific surface area (m^2/g)	269.476	280.135	360.27	319.044	343.720	459.406
Micopores total volume (cm^3/g)	0.003	0.004	0.006	0.005	0.005	0.009
Mesopores total volume(cm^3/g)	0.062	0.060	0.085	0.087	0.068	0.095
Total volume (cm^3/g)	0.09	0.066	0.091	0.1043	0.110	0.151

SEM images of raw biochar, acidic-washed and activated biochars are shown in **Figure 4.2**. All samples presented an heterogeneous surface morphology and presented a wide range of organic and mineral elements in their structures without noticeable apparition of closely bound sludge-wood matrix. Different forms may observe in all biochars specially elongated shapes that is linked to the woody material which mainly consists of cellulose and hemicellulose (Zhang et al., 2020) and simply small formless particles that could be the sewage sludge biochar (Zhang et al., 2018). Forms resembling to honeycombs were observed in the surface after the acid washing which suggested the increase of the pore size and number that explained the improvement of porosity volumes and specific surface areas after the acid washing and thermal activation under nitrogen steam. These modifications of biochar exposed the porous structure and then enhanced its accessibility to the adsorbate elements. The acidic washing and activation of biochar reduced also the impurities that

should be responsible for the decrease of metals and ash content (**Table 4.7**). These results were confirmed using EDS, that explained also the different shape of biochar and their heterogeneity by their chemical composition. The EDS analysis performed on BC8 and BC11 confirmed the presence of C, O, Si, Al, Mg, Ca, P, K, S, Fe and Zn in the sewage sludge derived biochar (**Figure S4.2**), which was confirmed by the elemental analysis (**Table 4.2**).

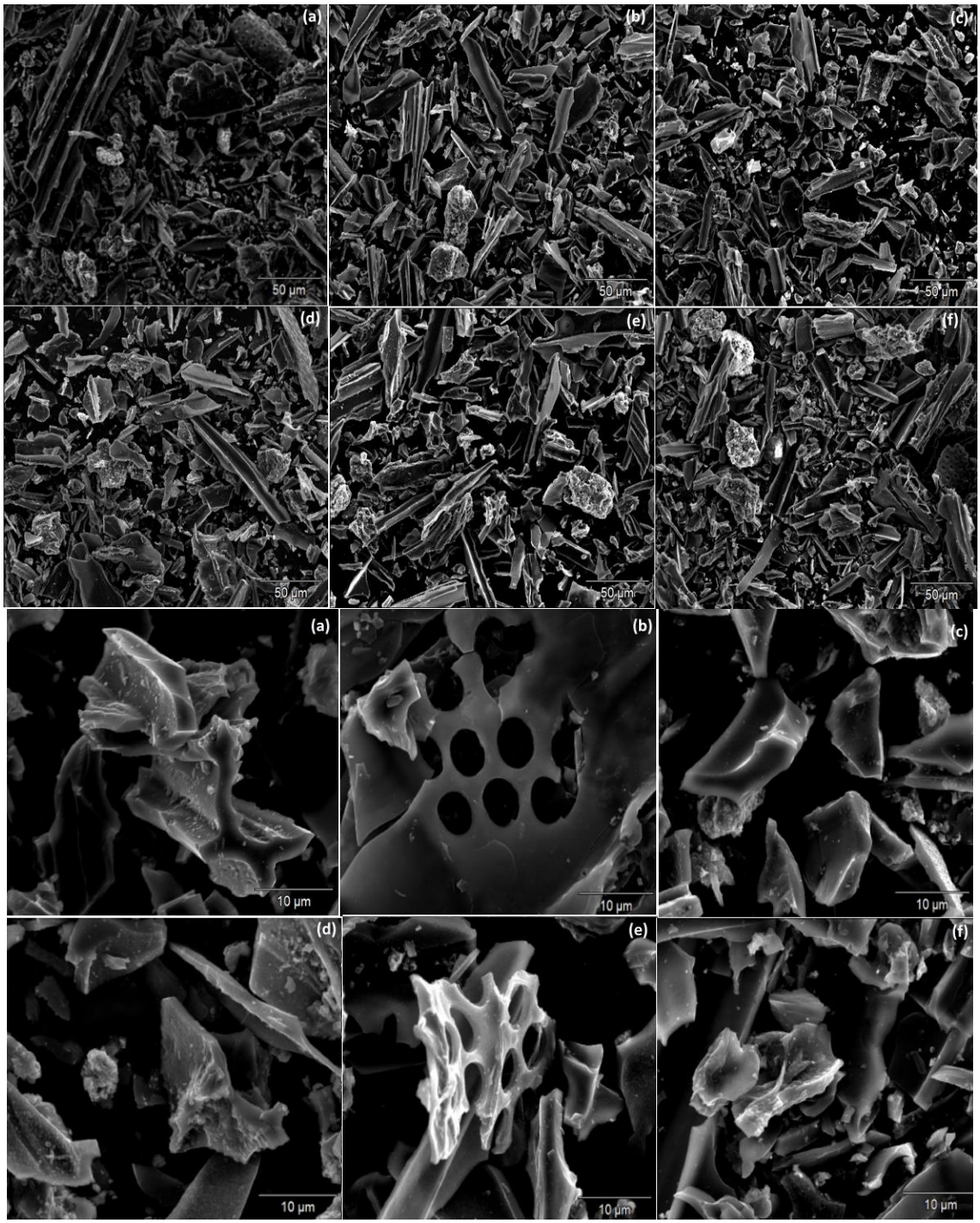

Figure 4.2. SEM of (a) Biochar 8, (b) acid washed biochar 8, (c) activated biochar 8, (d) biochar 11, (e) acid washed biochar 11, (f) activated biochar 11 (10 and 50 µm).

In many previous works, the washing of biochar after pyrolysis using a strong acid has been used for a goal of aqueous oxidation that may improve the surface characters such as the porous structure and surface acidity (Lin et al., 2012). The results are illustrated in **Figure 4.3** that showed pH_{pzc} values about 7.6 and 6.7 for ABC8 and ABC11 respectively. Since the mean value of pH of the effluent WW used in this study was in the range 7.5 and 8, it can be assumed that no significant charge was present at the surface of the ABCs.

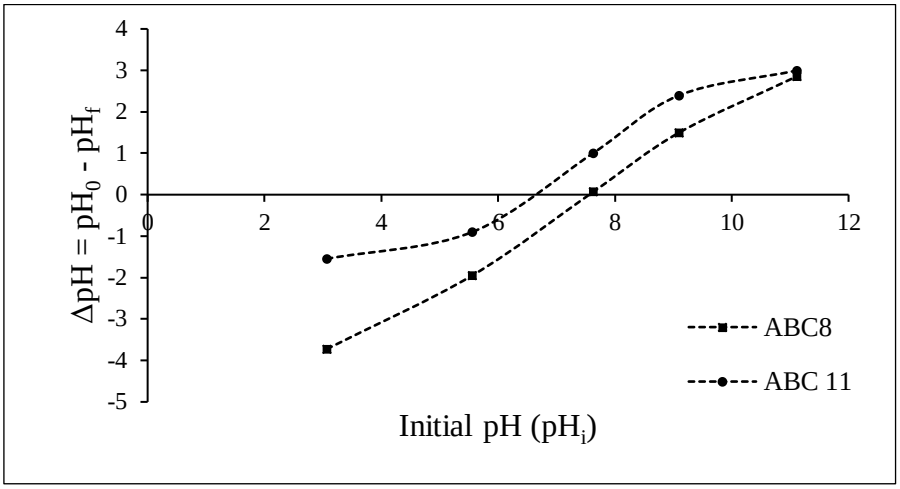

Figure 4.3. pH of the point of zero charge of the activated biochar 8 (ABC8) and activated biochar 11 (ABC11).

Moreover, after washing of biochar using acidic gasification WW, metal leaching decreased and their concentrations reduced under the required limits, especially for the Cr, As, Sb and Hg that were higher than the European norm before biochar modification (**Table 4.9**). The highest concentration was found for Cr is related specially to the sludge feedstock (Pantazopoulou et al., 2014; Angel Jessieleena et al., 2021), that decreased from 69 to 0.3 and 0.2 ppb for BC8 and BC11 respectively after acidic washing and thermal activation. In fact, different parameters could modify metals leaching such as pH of the water using for washing. Metals concentrations decrease with an alkaline pH, owing to the metal precipitation, however, an acidic pH improves the metals leaching (Regkouzas and Diamadopoulos, 2019). Indeed, the bioavailability of heavy metals may be affected by the interactions with organic matter or other elements (Hossain et al., 2011; Lu et al., 2013). However, As and Sb increased after the thermal activation but still below the required limits for metals leaching (**Table S4.1**). These results conform the usefulness of the used treatments to make the biochar useable according the norms.

The acid-washing that improved slightly the biochar porosity decreased the ash content less than the 15% as shown in **Table 4.7**. After acid-washing, the ash content reduced for the inorganic fractions (e.g., mineral oxides and soluble salt) loss. In fact, the important reducing of the metals after the washing and activation decreased the ash content that was also proved by the increasing of the specific surface area.

Table 4.9. Water metals and PAHs leaching of biochar 8 and biochar 11 before and after acid washing and activation.

Element	Unit	BC8	WBC8	ABC8	BC11	WBC11	ABC11	EN 12915-1
As	ppb	4.5	1.127	4.276	2.62	0.7	4.352	10
Cd	ppb	<0.000	0.045	<0.000	<0.000	<0.000	<0.000	0.5
Cr	ppb	69.12	0.93	0.341	69.87	1.786	0.215	5
Hg	ppb	0.02	0.064	0.103	0.03	<0.000	0.032	0.3
Ni	ppb	<0.000	0.403	<0.000	<0.000	2.255	<0.000	15
Pb	ppb	0.05	<0.000	<0.000	<0.000	1.122	<0.000	5
Sb	ppb	2.7	1.098	2.44	2.48	0.338	1.691	3
Se	ppb	0.43	<0.000	<0.000	0.59	0.032	0.085	3
Flu	ng/L	2.53	6		4.08	7.7		
B(b)Flu	ng/L	0.10	0.06		0.72	0.35		
B(k)Flu	ng/L	0.046	0.51		0.16	0.27		
B(a)Pyr	ng/L	2.58	7.37		5.98	8.22		
IPyr	ng/L	n.d	n.d		n.d	n.d		
BPyr	ng/L	0.17	0.09		1.32	0.28		
Sum*	ng/L	5.426	14.03		12.26	16.82		20

* Sum of 6 leachable PAHs.
Flu: Fluorene; B(b)Flu: Benzo(b)fluoranthene; B(k)Flu: Benzo(k)fluoranthene; B(a)Pyr: Benzo(a) pyrene; IPyr: Indeno(1,2,3-cd)pyrene; BPyr: Benzo(g, h, i)perylene; n.d = not detected.

The XRD pattern of WBC11, ABC 11and AC is shown in **Figure 4.4**. XRD analysis shows graphite structure in AB11 and AC (peaks at 2θ around 30 and 43). However, acidic washed BC11 does not contain any graphitic structure. This result conforms the effect of the acidic product and thermal activation processes on the apparition of graphitic structures in the biochar (Muegue et al., 2017). Moreover, WBC 11 and ABC 11 present peak at 2θ=31.6 were matching to quartz that could be related to the sewage sludge origin of the biochar, as mentioned in the work done by Rehman et al (Rehman et al.,2021), compared to the vegetal AC.

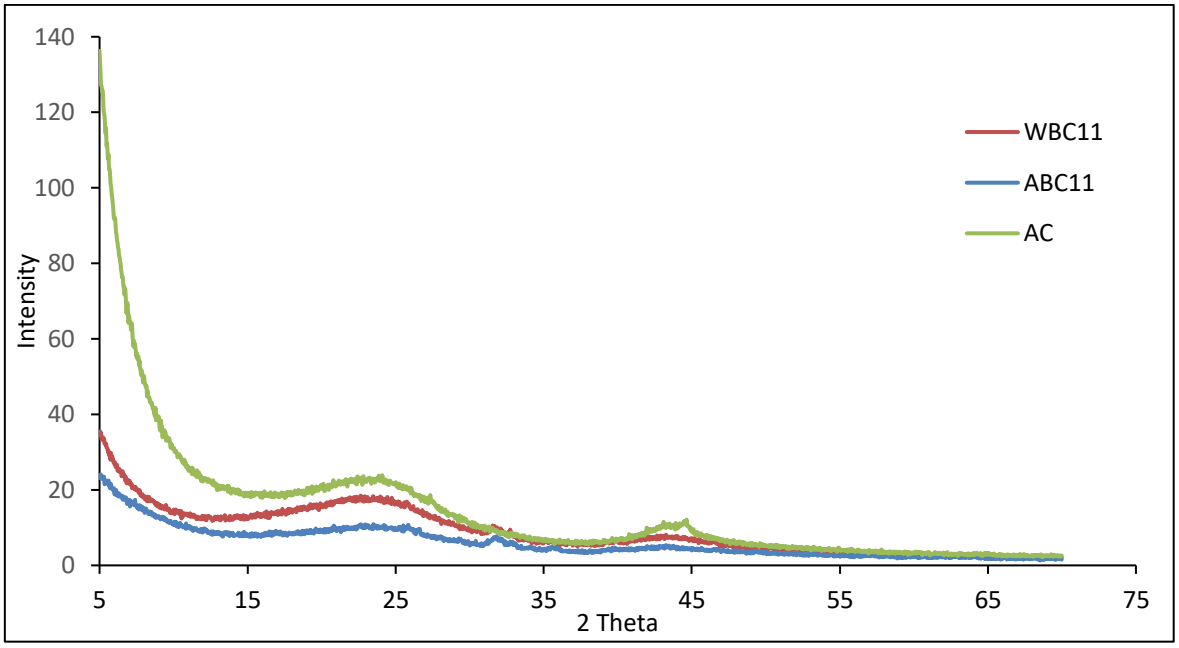

Figure 4.4. XRD of the acidic-washed biochar 11 (WBC11) and activated biochar 11 (ABC11) compared to the vegetal activated carbon.

V. Batch Adsorption of methylene blue

1. Kinetic study

The kinetic study showed that after 60 minutes the absorption balance of MB by the investigated biochars is reached (**Figure 4.5**). It is observable that high amount of MB was adsorbed within 5 min, this behaviour may be explained by the ion exchange or electrostatic attraction process that are commonly considered to acquire fast adsorption in which the equilibrium may be achieved after a low contact time.

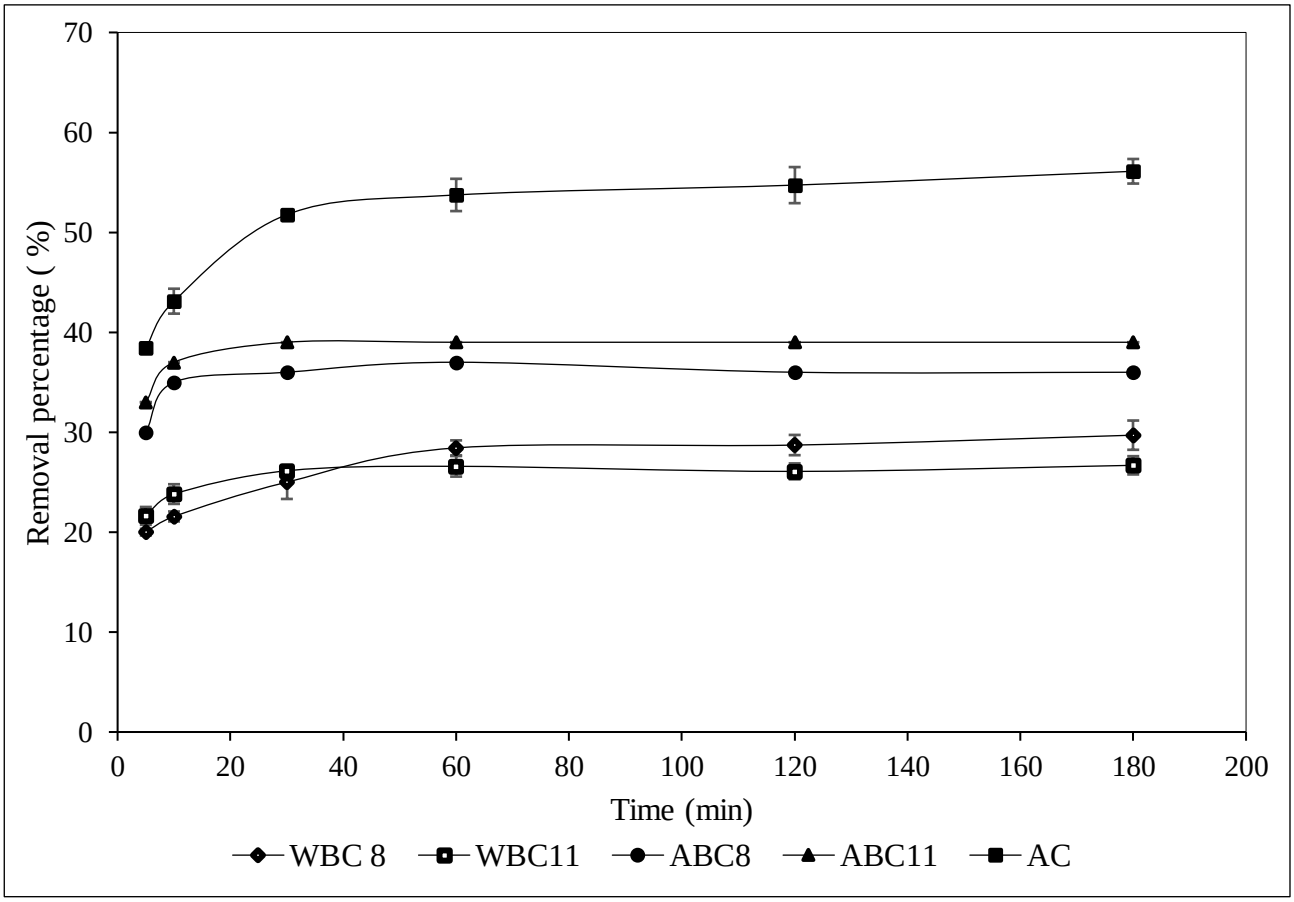

Figure 4.5. kinetic study of methylene blue sorption using biochars 8 and 11 after acid wash (WBC8 and WBC11), after acid wash and thermal activation (ABC8 and ABC11) compared to commercial activated carbon (AC).

For acid washed biochars, activated biochars and activated carbon, the pseudo-second order fits better the removal kinetic than the pseudo-first order model according to the determination coefficient (R^2> 0.99) (**Table 4.10**). The pseudo-second order model describes surface adsorption external liquid film diffusion and intra-particle diffusion. Thus, the MB adsorption is monitoring by chemical adsorption that includes electrons exchange between the dye cations and surface functional groups. The intra-particle diffusion model is used to analyse the adsorption mechanisms and rate control. The constant found by applying this model was different to zero, this result verified that various mechanisms can contribute and intervene in the adsorption process.

Table 4.10. Adsorption kinetic parameters.

			Pseudo-first model			Pseudo-second model			Intra-particle diffusion model		
Char	C_0 (mgL^{-1})	q_e,exp (mgg^{-1})	q_e,cal (mgg^{-1})	k_1 (min^{-1})	R^2	q_e,cal (mg g^{-1})	K_2 (gmg^{-1} min^{-1})	R^2	K_d (mg g^{-1} min$^{-0.5}$)	C (mg g^{-1})	R^2
WBC 8	25	4.92	2.95	0.16	0.964	4.98	0.30	0.999	0.15	3.91	0.823
	35	5.7	2.33	0.07	0.581	5.77	0.18	0.998	0.16	4.51	0.916
	50	6.75	3.85	0.06	0.778	6.84	0.08	0.996	0.33	4.23	0.997
	75	5.75	2.98	0.04	0.554	5.76	0.08	0.990	0.26	3.63	0.941
	100	6.75	3.80	0.07	0.811	6.84	0.09	0.998	0.31	4.41	0.972
WBC 11	25	5.47	3.11	0.07	0.818	5.55	0.11	0.998	0.26	3.56	0.978
	35	4.82	2.76	0.05	0.672	4.87	0.08	0.991	0.25	2.81	0.967
	50	6.72	5.89	0.08	0.911	7.45	0.02	0.945	0.77	1.31	0.740
	75	7.25	3.67	0.06	0.672	7.31	0.09	0.996	0.30	4.92	0.982
	100	7.25	3.20	0.072	0.651	7.29	0.13	0.998	0.24	5.46	0.877
ABC 8	25	23.5	11.93	0.03	0.406	23.36	0.02	0.98	1.04	14.41	0.802
	35	27.5	15.12	0.07	0.762	27.78	0.02	0.997	1.29	17.76	0.97
	50	27.5	9.28	0.09	0.667	27.62	0.07	0.999	0.46	24.05	0.987
	75	32.5	16.49	0.05	0.551	32.57	0.01	0.991	1.38	21.08	0.927
	100	40	15.02	0.07	0.542	40.16	0.03	0.999	1.08	31.83	0.723
ABC 11	25	41	19.08	0.06	0.6355	41.15	0.02	0.997	1.44	29.71	0.978
	35	35	18.75	0.05	0.632	35.21	0.01	0.993	1.67	21.74	0.961
	50	42.5	19.74	0.04	0.423	42.37	0.01	0.989	1.60	28.82	0.829
	75	42.5	21.03	0.06	0.619	42.73	0.01	0.995	1.71	28.92	0.977
	100	57.5	39.25	0.04	0.598	58.82	0.004	0.966	4.84	19.32	0.811

2.Isotherm study

The thermal activation increased the specific surface area, which improved the adsorption capacity of biochars. According to the isotherm's adsorption parameters shown in **Table 4.11**, and especially the correlation coefficients, Langmuir model fits better than the MB adsorption process compared to Freundlich model that was demonstrated by **Figure S4.3**. The MB sorption test showed that the adsorption capacity was improved by the thermal activation comparing to the acidic washing of biochar and became only around 3.5 and 5 time less than the activated carbon for ABC 11 and ABC 8 respectively. These results may be due to the improvement of pore structure in biochar after activation. Furthermore, the parameter 1/n found for the Freundlich isotherm model verified the adsorption heterogeneity factor, more details, the greater the expected heterogeneity corresponding to the smaller 1/n value. Heterogeneity factor for all biochars, activated biochars and activated

carbon were less than 0.5 this confirms that the adsorption is favourable (Shi et al., 2014).

Table 4.11. Mean (n = 3) and standard deviations (in brackets) of Langmuir (Q_m, K_L) Freundlich adsorption capacity (K_F) and correlation coefficient of Langmuir model calculated for biochar 8 and biochar 11 after acid wash (WBC8 and WBC11), after acid wash and thermal activation (ABC8 and ABC11) and commercial activated carbon (AC).

	Q_m (mg g^{-1})			K_L (mg g^{-1})			K_F (mg g^{-1})			R^2 range
	Mean	STD	RSD	Mean	STD	RSD	Mean	STD	RSD	
WBC8	6.9	0.2	2.9	0.50	0.10	20.0	1.91	0.05	2.6	0.966-0.99
WBC11	7.6	0.2	3.21	0.31	0.09	29.0	1.97	0.07	3.6	0.91-0.99
ABC8	43	3.0	6.27	0.06	0.01	14.3	2.95	0.08	2.7	0.915-0.96
ABC11	62	4.0	5.86	0.11	0.03	27.3	4.2	0.30	7.1	0.826-0.94
AC	214	2.0	0.88	0.53	0.03	5.7	10.12	0.09	0.9	0.99-0.995

After low contact time, the removal of MB increased; this increment could be related to the surface of BC that contains high vacant sites compared the MB molecules present in the reaction medium. The increase of the removal of MB could be explained by the high specific surface area and mesoroporosity that promoted the adsorption process. This result was proved in previous study done by Wang and Liu (2017). According the kinetic study (Second order), the MB removal process included chemical bonding and physical adsorption such as surface sorption, external liquid film diffusion and intra-particle diffusion mechanisms (Fan et al., 2017). The surface of BC may contain functional groups (O-H, C-O, N-H) that improved its binding with cationic molecules such as MB (Ahmed et al. 2019). Previous studies showed that the adsorption of MB onto co-pyrolyzed sludge and tea waste were managed by ion exchange, surface complexation, physical adsorption and external interactions, as verified by Fan et al. (2016) that demonstrated the important of ions exchange by showing the increase of the amount of leaching Ca^{2+}, Na^{+}, K^{+}, Mg^{2+}ions after reaching the equilibrium especially the $Ca^{2+}$and K^{+}.

The possible adsorption mechanisms of MB onto biochar derived from co-pyrolyzed of sewage sludge and biomasses were reported in literatures. Chen et al. (2019) studied the removal of MB onto sludge-rice husk based-biochar and verified that the adsorption involved by electrostatic interactions, π-π stacking interaction with the biochar sand interacting with O-H and C-O.

Hoslett et al. (2020) proved that the MB adsorption includes electrostatic attraction, hydrogen bonding and π-π interactions between attached methyl groups of the MB molecules and the π electrons of the graphitic surfaces in the biochars. Wei et al. (2019) demonstrated that the increase of pyrolysis temperature enhances the aromatic structure of BC then increase the π interactions.

This result was validated by Aksu and Akın. (2010) that proved the possible electrostatic attraction between biochar and MB molecules. Liu et al. (2019) studied the adsorption of Banana Pseudostem biochar towards MB, showed that hydrogen bending could be possible between the high amount of the sludge BC surface oxygen and the primary amine groups of MB molecules. This result was justified by Leng et al. (2015) that used sewage sludge biochar to adsorb MB and pointed out the important involving of the oxygen amount in the surface of biochar in the MB adsorption mechanisms. Liu et al. (2012) suggested the mechanisms of MB adsorption onto wine-processing waste sludge is based on the interactions between carboxyl and MB molecules that produce complex.

3.Comparison with other studies

To further explain and understand the adsorption performance of the prepared biochars in this study relative to previous works, the biochar production conditions, surface area, ash percentage, adsorption conditions and maximum adsorption capacity were compared with biochar prepared from mixture tea waste, rice husk, pine sawdust with sewage sludge using different ratio (Cheng et al., 2013; Fan et al., 2016; Chen at al., 2019). It is obvious that removal of MB depends of biochar preparation conditions such as the biomass-sewage sludge report, the 1/1 ratio decreased the sorption ability of biochar. An important critical point of view for biochar obtained from rice husk or pine sawdust mixed with sewage sludge have high ash contents (51.9 and 46% respectively) superior the required limits; thus, all biochars are not useful according the European Norms. Moreover, the adsorption using the biochar obtained from pine sawdust mixed with sludge and released at 30°C have the lower sorption capacity compared to the adsorption conducting at 25°C using the other biochars (Cheng et al., 2013). The sorption process using biochar made from tea waste mixed with sewage sludge was 10 g/L which is 25 time higher than the prepared materials in this study (Fan et al. 2016) while its maximum sorption capacity (Q_m) was 2.2 and 3.19 times less the Q_m of biochars obtained from sewage sludge mixed with poplar sawdust and oak sawdust respectively (ABC8 and ABC11 respectively). Thus, and as reported in **Table 4.12**, acidic washed and activated biochars obtained by mixture sewage sludge with oak sawdust and poplar sawdust have good adsorption capacities compared to the other sewage sludge based biochar. It can be concluded that the prepared biochars assumed as a good adsorbent to remove MB from aqueous solutions.

Table 4.12. Comparison with other studies.

Feedstock	Preparation conditions	BET (m^2g^{-1}) Ash %	Adsorption conditions	Qm (mg/g)	Ref.
Tea waste + sewage sludge	ratio of 1:1 300°C for 2h	No information	10g/L, 24h, pH 7, 45°C 50-150mg/L	19.38	Fan et al., 2016
Rice husk + Sewage sludge	Ratio 1:1 500 °C for 2 h	29.18 m²/g 51.9 %	0.1 g, 25h, 25°C, pH 6-7, 50-300mg/L	22.59	Chen et al., 2019
Pine sawdust + sewage sludge	Ratio 1:1 800˚C for 15 min.	168.27 m²/g 46%	1 g/L, 4h, 30°C, 20-50 mg/L	14.24	Cheng et al., 2013
Poplar sawdust + sewage sludge	Ratio 7:3 650°C for 2 h Acidic washing Pyrolysis 2h at 650°C	360.27 m²/g 14%	0.4g/L, 25°C, 1h 25-100 mg/L	43	This study
Oak sawdust + sewage sludge	Ratio 7:3 850°C for 1h Acidic washing Pyrolysis 2h at 650°C	459.406 m²/g 11%	0.4g/L, 1h, 25°C, 25-100 mg/L	62	This study

VI. Column adsorption study of real treated wastewater

Figure 4.6 shows the trend of the MB concentration during the passage of about 18 L of WW fortified with MB through the column. **Figure 4.6** shows also the dotted line indicating the initial concentration of MB in the treated water. The obtained data demonstrate a quantitative removal of the dye for the first 8 L of TWW, which correspond to approximately 413 mg of MB, or approximately 11.8 mg per g of biochar. Subsequently, the MB values exiting the column begin to increase until reaching, after the passage of a further 10 liters of water, the MB value determined in the water before treatment (i.e., about 52 mg / L).

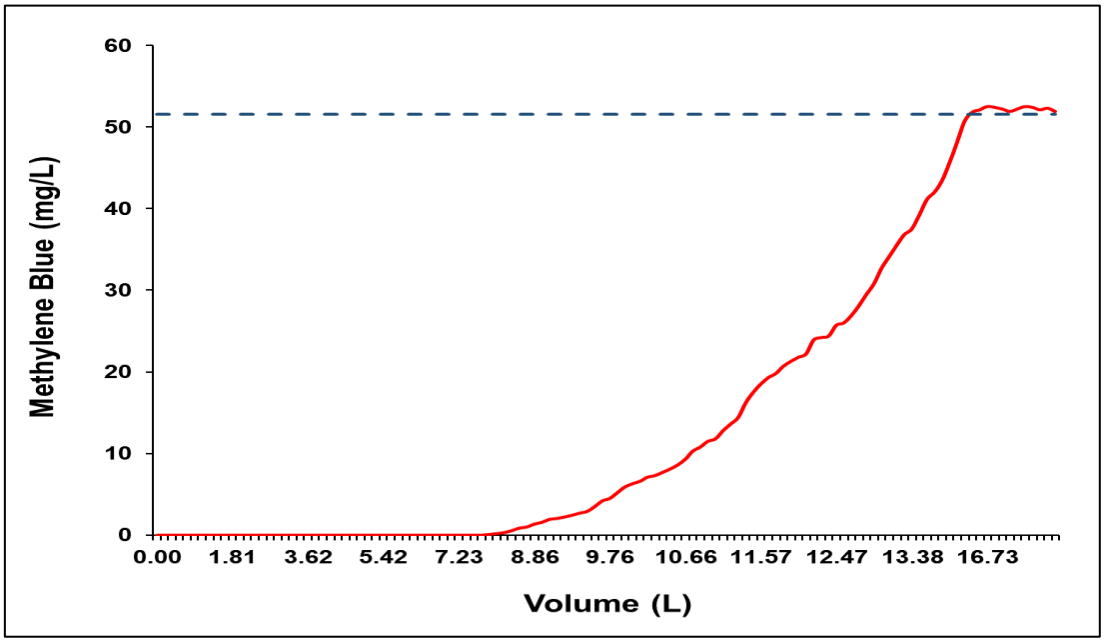

Figure 4.6. Column adsorption study.

VII. Biochar regeneration

ABC11 has higher adsorption capacity of MB than ABC8. The regeneration of biochar could be done by the adsorbate decomposition or desorption (Jia et al., 2016). The ABC11 was regenerated by thermal decomposition that reduces the adsorbate molecules less than the pore sized which favours their desorption (Hu et al., 2018). After one recycle of column adsorption, the BET surface area of ABC11 decreased from 459.4 to 386.99 m^2/g. The adsorbed molecules of MB and mico-pollutants brought by TWW were not totally destroyed or volatilized by the carbonization. The regeneration reduced the specific surface area by around 16% that is conforms the efficiency of ABC11 to be regenerated and used at least three times to remove MB from TWW (Liu et al., 2019). Thus, thermal generation could be efficient to reuse the biochar in MB without losing an important porosity and specific surface area therefore adsorption ability.

IX. Economic study

The use of this product instead of the commonly used acids reduces the cost of producing modified or activated biochar and may be an environment friendly. The regeneration results have also an economic benefit. According to Del Bubba et al. (2020) the cost of biochar is 16 times less than the AC in Italy. Moreover, in this study the washing was effectuated using a gasification WW. However, the activated biochar has MB adsorption capacity only about 3.5 and 5 time less than commercial activated carbon. These results confirm that in this work 3 goals were achieved; the management of sewage sludge by production of biochar and improvement of their surface properties and adsorption capacity by washing using a gasification WW instead of chemical products (acids, base, or organic products), as consequence, the price of biochar production was reduced in conventional treatment modifications of chars.

X. Conclusion

Results verified that biochar obtained from mixture sawdust / sewage sludge can cause threat to both human and environment safety considering its high ash content, metals and PAHs leaching values that above the standard limits EN 12905 − 1. Biochar surface proprieties and pollutant release depends essentially to the biochar feedstock types and synthesized conditions. Therefore, and to achieve the goal to reuse of sewage sludge to produce an efficient adsorbent support, the modification of biochar was necessary and was effectuated using an environmentally by product that is the WW of sawdust gasification. This acidic washing modification followed by a thermal activation was efficient to reduce ABC ash content and metals and PAHs leaching values bellow the

required limits. ABCs used for dyes adsorption showed an adsorption capacity of MB about 62 mg g^{-1}. ABC performances were lower by only 3.5 to 5 times than to commercial active carbon. A simultaneous removal of organic and MB from effluent were observed that are also crucial for their application in WW treatment.

These results verified the useful aspect of the prepared ABCs in WW treatment considering its high adsorption capacity of MB and also regarding the economic point of view of the low biochar production cost compared to the commercial AC.

XI. Bibliography

Aghababaei. A., Ncibi, M. C., Sillanpää, M., 2017. Optimized removal of oxytetracycline and cadmium from contaminated waters using chemically-activated and pyrolyzed biochars from forest and wood-processing residues. Bioresour. Technol. 239, 28-36.

Ahmad, M., Lee, S. S., Dou, X., Mohan, D., Sung, J. K., Yang, J. E., Ok, Y. S. 2012. Effects of pyrolysis temperature on soybean stover- and peanut shell-derived biochar properties and TCE adsorption in water. Bioresour. Technol. 118, 536–544.

Ahmed, M. J., Okoye, P. U., Hummadi, E. H., Hameed, B. H., 2019. High-performance porous biochar from the pyrolysis of natural and renewable seaweed (Gelidiella acerosa) and its application for the adsorption of methylene blue. Bioresour. Technol. 278, 159-164.

Aksu, Z., Akın, A. B., 2010. Comparison of Remazol Black B biosorptive properties of live and treated activated sludge. Chem. Eng. J. 165, 184-193.

Al-Wabel, M. I., Al-Omran, A., El-Naggar, A. H., Nadeem, M., Usman, A. R. A., 2013; Pyrolysis temperature induced changes in characteristics and chemical composition of biochar produced from conocarpus wastes, Bioresour. Technol. 131, 374–379.

Angel Jessieleena, A., Priyanka, M., Saravanakumar, M. P., 2021. Comparative study of Fenton, Fe^{2+}/NaOCl and Fe^{2+}/$(NH_4)_2S_2O_8$ on tannery sludge dewaterability, degradability of organics and leachability of chromium. J. Hazard. Mater. 402, 123495.

Cao, X., Harris, W., 2010. Properties of dairy-manure-derived biochar pertinent to its potential use in remediation. Bioresour. Technol. 101, 5222–5228.

Chang, R., Sohi, S. P., Jing, F., Liu, Y., Chen, J., 2019. A comparative study on biochar properties and Cd adsorption behavior under effects of ageing processes of leaching, acidification and oxidation. Environ. Pollut. 254, 113123.

Chen, S., Qin, C., Wang, T., Chen, F., Li, X., Hou, H., Zhou, M., 2019. Study on the adsorption of dyestuffs with different properties by sludge-rice husk biochar: Adsorption capacity, isotherm, kinetic, thermodynamics and mechanism. J. Mol. Liq. 285, 62–74.

Cheng, G., Sun, L., Jiao, L., Peng, L., Lei, Z., Wang, Y., Lin, J., 2013. Adsorption of methylene blue by residue biochar from copyrolysis of dewatered sewage sludge and pine sawdust. Desalin. Water Treat. 51, 7081–7087.

Chun, Y., Sheng, G., Chiou, G. T., Xing, B., 2004. Compositions and sorptive properties ofcrop residue-derived chars. Environ. Sci. Technol. 38, 4649–4655.

Czajczyńska, D., Anguilano, L., Ghazal, H., Krzyżyńska, R., Reynolds, A. J., Spencer, N., Jouhara, H., 2017. Potential of pyrolysis processes in the waste management sector. Therm. Sci. Eng. Prog. 3, 171–197.

Del Bubba, M., Anichini, B., Bakari, Z., Bruzzoniti, M.C., Camisa, R., Caprini, C., Checchini, L., Fibbi, D., El Ghadraoui, A., Liguori, F., Orlandini, S., 2020. Physicochemical properties and sorption capacities of sawdust-based biochars and commercial activated carbons towards ethoxylated alkylphenols and their phenolic metabolites in effluent wastewater from a textile district. Sci. Total Environ. 708, 135217.

Demirbas, A., 2004. Effects of temperature and particle size on bio-char yield from pyrolysis of

agricultural residues. J Anal Appl Pyrolysis. 72, 243–248.

Devi, P., Saroha, A. K., 2015. Effect of pyrolysis temperature on polycyclic aromatic hydrocarbons toxicity and sorption behaviour of biochars prepared by pyrolysis of paper mill effluent treatment plant sludge. Bioresour. Technol. 192, 312–320.

Enders, A., Hanley, K., Whitman, T., Joseph, S., Lehmann, J., 2012. Characterization of biochars to evaluate recalcitrance and agronomic performance. Bioresour. Technol. 114, 644–653.

Fan, S., Wang, Y., Wang, Z., Tang, J., Tang, J., Li, X., 2017. Removal of methylene blue from aqueous solution by sewage sludge-derived biochar: Adsorption kinetics, equilibrium, thermodynamics and mechanism. J. Environ. Chem. Eng. 5, 601-611.

Fan, S., Tang, J., Wang, Y., Li, H., Zhang, H., Tang, J., Wang, Z., Li, X., 2016. Biochar prepared from co-pyrolysis of municipal sewage sludge and tea waste for the adsorption of methylene blue from aqueous solutions: Kinetics, isotherm, thermodynamic and mechanism. J. Mol. Liq. 220, 432-441.

He, J., Strezov, V., Kan, T., Weldekidan, H., Asumadu-Sarkodie, S., Kumar, R., 2019. Effect of temperature on heavy metal(loid) deportment during pyrolysis of Avicennia marina biomass obtained from phytoremediation. Bioresour. Technol. 278, 214–222.

Hoslett, J., Ghazal, H., Mohamad, N., Jouhara, H., 2020. Removal of methylene blue from aqueous solutions by biochar prepared from the pyrolysis of mixed municipal discarded material. Sci. Total Environ. 714, 136832.

Hossain, M. K., Strezov, V., Chan, K. Y., Ziolkowski, A., Nelson, P. F., 2011. Influence of pyrolysis temperature on production and nutrient properties of wastewater sludge biochar. J. Environ. Manage. 92, 223 - 228.

Hu, H., Sun L., Jiang, B., Wu, H., Huang, Q., Chen, X., 2018. Low concentration Re (VII) recovery from acidic solution by Cu-biochar composite prepared from bamboo (Acidosasa longiligula) shoot shell. Miner. Eng. 124, 123-136.

Huang, H., Yang, T., Lai, F., Wu, G., 2017. Co-pyrolysis of sewage sludge and sawdust/rice straw for the production of Biochar. J Anal Appl Pyrolysis. 125, 61–68.

Jia, Y., Zong, Q., Zhang, M., Wang, Z.M., Zhang, L.H., 2016. Research progress in regeneration technology of activated carbon from flue gas desulfurization. Bull. China Ceram. Soc. 35, 815-818.

Jin, J., Wang, M., Cao, Y., Wu, S., Liang, P., Li, Y., Zhang, J., Zhang, J., Wong, M. H., Shan, S., Christie, P., 2017. Cumulative effects of bamboo sawdust addition on pyrolysis of sewage sludge: Biochar properties and environmental risk from metals. Bioresour. Technol. 228, 218–226.

Krueger, B. C., Fowler, G. D., Templeton, M. R., Moya, B., 2020.Resource recovery and biochar characteristics from full-scale faecal sludge treatment and co-treatment with agricultural waste. Water Res. 169, 115253.

Lang, T., Jensen, A. D., Jensen, P. A., 2005. Retention of organic elements during solid fuel pyrolysis with emphasis on the peculiar behavior of nitrogen. Energy Fuels. 19, 1631–1643.

Lehmann, J., Joseph, S. (Eds.). 2009. Biochar for environmental management (Vol. 1). London: Earthscan.

Leng, L. J., Yuan, X. Z., Huang, H. J., Shao, J. G., Wang, H., Chen, X. H., Zeng, G. M., 2015.

Biochar derived from sewage sludge by liquefaction: characterization and application for dye adsorption. Appl. Surf. Sci. 346, 223-231.

Lin, Y., Munroe, P., Joseph, S., Henderson, R., Ziolkowski, A., 2012. Water extractable organic carbon in untreated and chemical treated biochars. Chemosphere 87, 151-157.

Liu, S., Li, J., Xu, S., Wang, M., Zhang, Y., Xue, X., 2019. A modified method for enhancing adsorption capability of Banana Pseudostem biochar towards methylene blue at low temperature. Bioresour. Technol. 282, 48-55.

Liu, C. C., Li, Y. S., Chen, Y. M., Li, H. H., Wang, M. K., 2012. Removal of methylene blue from aqueous solution using wine-processing waste sludge. Water Sci. Technol. 65, 2191-2199.

Liou, T. H., Wu, S. J., 2009.Characteristics of microporous/mesoporous carbons prepared from rice husk under base- and acid-treated conditions. J. Hazard. Mater.171, 693-703.

Lu, H., Zhang, W., Wang, S., Zhuang, L., Yang, Y., Qiu, R., 2013. Characterization of sewage sludge-derived biochars from different feedstocks and pyrolysis temperatures. J Anal Appl Pyrolysis. 102, 137-143.

Muegue, L. C. D., González, J. C. A., Mesa, G. P., 2017. Characterization and Potential Use of Biochar for the Remediation of Coal Mine Waste Containing Efflorescent Salts. Sustainability 9, 2100.

Novak, J., Lima, I., Xing, B., Gaskin, J., Steiner, C., Das, K., 2009. Characterization of designer biochar produced at different temperatures and their effects on a loamy sand.Ann. Environ. Sci. 3, 195–206.

Pantazopoulou, E., Zebiliadou, O., Noli, F., Mitrakas, M., Samaras, P., Zouboulis, A., 2014. Utilization of phosphogypsum in tannery sludge stabilization and evaluation of the radiological impact. Bull Environ Contam Toxicol. 94, 352-357.

Pariyar, P., Kumari, K., Jain, M. K., Jadhao, P. S., 2020. Evaluation of change in biochar properties derived from different feedstock and pyrolysis temperature for environmental and agricultural application. Sci. Total Environ. 713, 136433.

Pourret, O., Houben, D., 2018.Characterization of metal binding sites onto biochar using rare earth elements as a fingerprint. Heliyon; 4, e00543.

Rajapaksha, A. U., Vithanage, M., Ahmad, M., Seo, D-C., Cho, J-S., Lee, S-E., Lee, S. S., Ok, Y. S., 2015. Enhanced sulfamethazine removal by steam-activated invasive plant-derived biochar. J. Hazard. Mater. 290, 43-50.

Regkouzas, P., Diamadopoulos, E., 2019.Adsorption of selected organic micro-pollutants on sewage sludge biochar. Chemosphere 224, 840-851.

Rehman, R. A., Qayyum, M. F., Haider, G., Schofield, K., Abid, M., Rizwan, M., Ali, S., 2021. The Sewage Sludge Biochar and Its Composts Influence the Phosphate Sorption in an Alkaline Calcareous Soil. Sustainability 13, 1779.

Shi, L., Zhang, G., Wei, D., Yan, T., Xue, X. D., Shi, S.S., Wei, Q., 2014.Preparation and utilization of anaerobic granular sludge-based biochar for the adsorption of methylene blue from aqueous solutions. J. Mol. Liq. 198, 334-340.

Song, W., Guo, M., 2012. Quality variations of poultry litter biochar generated at different pyrolysis

temperatures. J Anal Appl Pyrolysis. 94, 138–145.

Tang, Y., Alam, M. S., Konhauser, K. O., Alessi, D. S., Xu, S., Tian, W., Liu, Y., 2019. Influence of pyrolysis temperature on production of digested sludge biochar and its application for ammonium removal from municipal wastewater. J. Clean. Prod. 209, 927–936.

Uchimiya, M., Bannon, D. I., Wartelle, L. H., 2012. Retention of heavy metals by carboxyl functional groups of biochars in small arms range soil. J. Agric. Food Chem. 60, 1798-1809.

Vithanage, M., Rajapaksha, A. U., Zhang, M., Thiele-Bruhn, S., Lee, S. S., Ok, Y. S., 2015. Acid-activated biochar increased sulfamethazine retention in soils. Environ. Sci. Pollut. Res. 22, 2175-2186.

Wang, Z., Ma, X., Yao, Z., Yu, Q., Wang, Z., Lin, Y., 2018. Study of the pyrolysis of municipal sludge in N_2/CO_2 atmosphere. Appl. Therm. Eng. 128, 662–671.

Wang, Y., Liu, R., 2017. Comparison of characteristics of twenty-one types of biochar and their ability to remove multi-heavy metals and methylene blue in solution. Fuel Process. Technol. 160, 55-63.

Wei, J., Tu, C., Yuan, G., Liu, Y., Bi, D., Xiao, L., Lu, J., Theng, B. K. G., Wang, H., Zhang, L., Zhang, X., 2019. Assessing the effect of pyrolysis temperature on the molecular properties and copper sorption capacity of a halophyte biochar. Environ. Pollut. 251, 56-65.

Wu, H., Che, X., Ding, Z., Hu, X., Creamer, A. E., Chen, H., Gao, B., 2016. Release of soluble elements from biochars derived from various biomass feedstocks. Environ. Sci. Pollut. Res. 23, 1905–1915.

Yuan, H., Lu, T., Huang, H., Zhao, D., Kobayashi, N., Chen, Y., 2015. Influence of pyrolysis temperature on physical and chemical properties of biochar made from sewage sludge. J Anal Appl Pyrolysis. 112, 284-289.

Zhang, H., Tu, Y. J., Duan, Y. P., Liu, J., Zhi, W., Tang, Y., Xiao, L. S., Meng, L., 2020. Production of biochar from waste sludge/leaf for fast and efficient removal of diclofenac. J. Mol. Liq. 299, 112193.

Zhang, F., Wu, K., Zhou, H., Hu, Y., Sergei, P., Wu, H., Wei, C., 2018. Ozonation of aqueous phenol catalyzed by biochar produced from sludge obtained in the treatment of coking wastewater. J. Environ. Manage. 224, 376–386.

Zhang, J., Wang, Q., 2016. Sustainable mechanisms of biochar derived from brewers' spent grain and sewage sludge for ammonia-nitrogen capture. J. Clean. Prod. 112, 3927-3934.

Zhang, G., Zhang, Q., Sun, K., Liu, X., Zheng, W., Zhao, Y., 2011. Sorption of simazine to corn straw biochars prepared at different pyrolytic temperatures. Environ. Pollut. 159, 2594-2601.

Zielińska, A., Oleszczuk, P., Charmas, B., Skubiszewska-Zięba, J., Pasieczna-Patkowska, S., 2015. Effect of sewage sludge properties on the biochar characteristic. J. Anal. Appl. Pyrolysis. 112, 201-213.

Conclusion

Conclusion

This work aims to study the potential of the reuse of TWW in agriculture, to expand the range of the used crops and to assess the current situation of different effects. The work proposes solutions to the risks of soils, crops, water, users and consumers contamination through the production of new absorbents based on waste (vegetal and biosolids) which serve to reduce or eliminate the amount of micropollutants present in the TWW used for irrigation.

The work began by the use of TWW for the irrigation of olive and strawberry plants. Different morphological and biochemical parameters (chlorophyll pigments and soluble sugars) of plants were studied. Results showed that the irrigation using TWW increased the organic matter, total organic matter, metal and alkalinity of the soil (strawberry and olive substrates). Irrigation using TWW improved the morphological characteristic of plant by increasing the soil fertility, decreased the consummation of fresh water and reduced the use of fertilizers thus reduced the plants cultivation cost. However, the metal amounts increased in different substrates used for the olive and strawberry cultivation. In fact, a significant accumulation of iron in the substrate was registered. Cu, Zn, Mn, and Ni were the main metals translocated in plants. This behaviour is probably due to their involvement in the plant metabolism. Our study suggests the use of the dilution 40% of TWW to irrigate strawberries. This suggestion is based on the low concentration of heavy metals using this dilution and to the results found in term of morphological parameters in plant. However, our purpose is to reduce the use of fresh water, this could be achieved by using different methods such us the adsorption process to reduce micropollutants from the TWW.

The production of a low-cost adsorbent support by reusing high environmental concern waste was performed by the pyrolysis of sewage sludge to study their ability to removal copper ions from aqueous medium. To optimize the optimum conditions of copper adsorption using sewage sludge ash, a BOX-BEHNKEN Quality by Design was established by considering only one answer which is the adsorption capacity. The use of the quality by design approach allowed us to identify the optimum conditions for the use of ash as adsorbent material for copper which are a contact time about 69 min, a pH value equal to 4.2, an ash amount in the order of 0.1 g and a concentration of copper ions about 48 mg / L. These conditions were able to stimulate the adsorption capacity of sludge ash to reach an adsorption capacity of copper ions around 20 mg/g.

The third part, sawdust based biochars were produced and used for the removal of a mixture of ethoxylated alkylphenols and alkylphenolics from real WW. The production of biochar was effectuated by pyrolysis of sawdust in a furnace under inert atmosphere at 450. 650 and 850 °C for 60 min. All biochars produced in this study complied with the EN 12915-1/2009 limits for metal and PAH leaching in water and provided a negligible contribution to the release of salts in the

treated water. The increase of the pyrolysis temperature improved the surface area and carbon content, enhanced the production of graphitic layers and increased aromaticity degree verified by the decreasing of the H/C ratio. The pH of the point of zero charge was in the range 7.15 -7.78, these values verified the absence of sorption mechanisms based on ionic interactions in the experimental conditions adopted for the ethoxylated alkylphenols (which don't have any dissociable acid base groups) and alkylphenolics (which are neutral at the pH of the effluent WW equal to 7.46). The kinetics study of the adsorption of 4–t-octylphenol, 4-nonylphenol, ethoxylated 4t octylphenol and ethoxylated 4 nonylphenol using the prepared biochars and a mineral activated carbon showed that 4 h is the optimum contact time. Biochars showed a lower sorption performance compared to activated carbon. The best performance was found for biochar produced at 650 towards the alkylphenols which was about 9 to 13 times less efficient than the mineral activated carbon. However. considering the low cost of biochar comparing to activated carbon (at least 16 times less expensive), biochar can be used for future applications in water and WW treatment in line with the modern approach to resource management and the circular economy.

The aim of last part is the development of a "zero waste" circular strategy to manage sewage sludge through a thermal-conversion process for biochar production that was used in the sorption of organic micropollutants from real TWW. In order to optimize the thermal conversion conditions, an experimental design method has been established (i.e, temperature, contact time and relative percentage of vegetal biomass and biosolids). Results of biochar characterization showed that the surface area, micropores and mesopores total volume of the samples containing sludge were lower than those produced only from woody biomass. All sewage sludge based biochars have ash content above the EUROPEAN NORM except biochar 4 (containing only 15% of sludge) and have higher content compared to biochar obtained from only woody biomasses. Biochars contained 30% of sludge have pH_{pzc} between 9.6 and 10.4, then these results suggest the prepared biochars should be suitable for the adsorption of cationic molecules. Moreover, the sum of fluoranthene, benzo(b)fluoranthene, benzo(k)fluoranthene, benzo(a)pyrene, indeno (1,2,3-cd) pyrene and benzo(a)pyrene concentrations in biochars produced only from wood exceeded the European required standards (EN 12915-1/2009). However, the total concentrations of these six PAHs in biochars containing 30% of sewage sludge (7, 8, 9, 11 and 12) were lower than the required limits of leachable concentrations (20 ng/L). According to the European Regulation UNI EN 12915 - 1, some biochars are not useful. Thus, the modification of biochar is necessary to reduce metals and inorganic contents. The activation of biochar through physical or chemical method was used to enhance the BC8 and BC11 characteristics then their use in different fields such as adsorption or catalytic applications. In this work, a new approach for reducing the pores blockage by tars and the

metals contents has been proposed. More in detail, the biochar washing was performed using acidic gasification WW. The use of this product instead of the commonly used acids reduced the cost of producing modified/activated biochar. The modification of biochar with the acidic by product is environment friendly and considered as an economic solution. This modification reduced the ash and metal contents to be below the EN 12905-1 limits, and did not affect significantly the specific surface area. Biochars contained 30% of sewage sludge (8 and 11) were used in the removal of methylene blue from aqueous solutions then from real TWW. The comparison between the maximum adsorption capacities of biochar and activated carbon showed that the biochar are 18 to 21 time less efficient to remove methylene blue than activated carbon. Thus, improving the adsorption capacity of prepared biochar became a necessity that mostly done by activation. Therefore, a thermal activation of these biochars, performed at 650°C during 2h under nitrogen flow, improved the specific surface area and the pores size distribution. The methylene blue sorption test showed that the adsorption capacity was improved by the thermal activation comparing to the acidic washing and became only around 3.5 and 5 time less than the activated carbon for activated biochar 11 and activated biochar 8 respectively. This result proved that the activated biochar, derived from sawdust and sewage sludge, could represent an important added value economic and environmental.

As a conclusion, this work adopts a new strategy to manage sewage sludge through a thermal-conversion process for biochar production and its utilization as sorption media for WW purification. The innovative idea of this work was the use of a WW obtained from the gasification of plants, which is considered an eco-friendly solution for the possibility release of pollutants (metals) and ash content in sludge-based biochar in one hand. In the other hand, it is considered as an economic solution by reducing the cost of biochar activation or modification.

As prospective, it is will be important to integrate the activated biochar into phyto-purification plants to improve their removal efficiency against organic micro-pollutants and therefore their applicability in decentralized treatment contexts. Also, it is important to analyse the performance of the prepared biochar for electrochemical and electroanalytical applications.

Supplementary materials

Supplementary material of part 2

Table S2.1. Characteristics of the effluent wastewater.

Parameters	WWTP effluent
pH	6.54
CE (mS\cm)	7.65
TSS (mg\L)	30
COD (mg\L)	107
BOD_5 (mg\L)	37
P_{tot} (mg\L)	14.5
NH_4^+ (mg\L)	66
NO_3^- (mg\L)	8.0
Cl^- (mg\L)	720
SO_4^{2-} (mg\L)	603
Na^+ (mg\L)	2817
K^+ (mg\L)	175
Mg^{2+} (mg\L)	280
Ca^{2+} (mg\L)	242
HCO_3^- (mg\L)	240
Cu^{2+} (mg\L)	0.24
Fe^{2+} (mg\L)	6.6
Mn^{2+} (mg\L)	0.12
Zn^{2+} (mg\L)	5.8
Cd^{2+} (mg\L)	B.d.l.[a]
Cr^{3+} (mg\L)	2.1
Pb^{2+} (mg\L)	2.8

[a] Below detection limit

Table S2.2. Model coefficients

Name	Coefficient value
b_0	2.302
b_1	0,078
b_2	0,064
b_3	-7,874
b_4	1,93
b_{11}	0.993
b_{22}	0.596
b_{33}	7.151
b_{44}	-1.299
b_{12}	-0.0005
b_{13}	-0.239
b_{23}	-0.131
b_{14}	0.004
b_{24}	-0.058
b_{34}	-1.191

Table S2.3. Residue table

Next	Yelp.	Calk.	Difference	R-Student
1	2.675	3.749	-1.074	-0.670
2	2.704	3.907	-1.203	-0.753
3	2.503	3.879	-1.376	-0.882
4	2.504	4.035	-1.530	-0.987
5	20.715	18.004	2.710	1.844
6	21.694	18.641	3.053	2.135
7	1.411	2.735	-1.324	-0.845
8	1.412	2.412	-1	-0.632
9	0.950	-0.008	0.957	0.603
10	0.953	0.139	0.813	0.511
11	4.479	3.844	0.634	0.397
12	4.486	4.010	0.475	0.297
13	19.785	17.73	2.054	1.353
14	20.382	18.121	2.261	1.481
15	1.311	2.243	-0.932	-0.589
16	1.417	2.109	-0.692	-0.434
17	0.655	-0.453	1.108	0.706
18	0.905	-0.209	1.114	0.699
19	4.164	3.524	0.640	0.401
20	4.208	3.536	0.671	0.419
21	8.390	12.907	-4.517	-3.927
22	0.498	-0.459	0.956	0.596
23	14.546	19.151	-4.605	-4.023
24	2.351	1.012	1.331	0.844
25	2.696	2.302	0.393	0.174
26	2.698	2.302	0.395	0.174
27	2.695	2.302	0.392	0.173
28	2.697	2.302	0.394	0.174
29	2.563	4.307	-1.743	-0.783
30	2.567	4.455	-1.887	-0.850
31	2.77	4.358	-1.587	-0.711
32	2.11	0.026	2.083	0.943
33	4.054	3.018	1.035	0.459

Table S2.4. Maximum characteristics

Response	Response name	Value	Percentage %
X_1	Q_m	20.072	100
X_4	Desirability		100

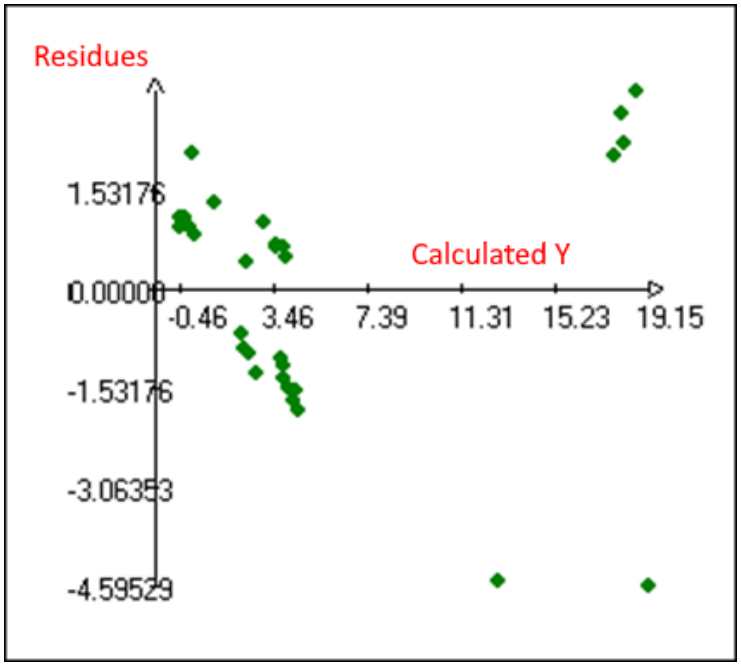

Figure S 2.1. Study of the residuals of response

Supplementary material of part 3

S.3.1 Reagents, standards and materials

Hydrochloric acid, phosphoric acid, methylene blue tri-hydrate and dichloromethane were purchased from Carlo Erba Reagents (Cornaredo, Milano, Italy). Phenol, sodium bicarbonate, calcium chloride, magnesium sulphate and isopropyl alcohol were obtained from Sigma-Aldrich (St. Louis, MO, USA).

Disodium hydrogen phosphate anhydrous was supplied by Panreac Quimica (Castellar del Vallès, Barcelona, Spain). Acetic acid was purchased from Romil (Waterbeach, Cambridge, UK). Reagent grade sodium thiosulfate and iodine were obtained from Labochimica (Campodarsego, Padova, Italy).

Concentrated nitric acid 70%, hydrogen peroxide 30% (trace metal analysis) and all standards (ICP-MS analysis grade) of elements investigated in the chars were supplied from Sigma-Aldrich.

LC–MS grade methanol (CH_3OH), water and ammonia (NH3 content >25%) were purchased from Sigma-Aldrich. Ultrapure water (resistivity > 18 MΩ) was obtained from a Milli-Q system (Millipore, Billerica, MA, USA).

EPA 610 PAH mixture (Supelco, St. Louis, MO, USA), containing the following polycyclic aromatic hydrocarbons: naphthalene (N), acenaphthene (Acy), acenaphthylene (Ac), fluorene (Fl), anthracene (A), phenanthrene (P), fluoranthene (Flu), pyrene (Py), benzo(a)anthracene (BaA), chrysene (Ch), benzo(b)fluoranthene (BbFlu), benzo(k)fluoranthene (BkFlu), benzo(a)pyrene

(BaPy), dibenzo(a,h)anthracene (BahA), indeno(1,2,3-cd)pyrene (Ipy) and benzo(ghi)perylene (BP), was employed. Naphthalene d-8 (N-d8), phenanthrene d-10 (P-d10), fluoranthene d-10 (Flu-d10), chrysene d-12 (Ch-d12), benzo(a)pyrene d-12 (BaPy-d12) and indeno(1,2,3-cd) pyrene d-12 (Ipy-d12) were purchased from Supelco. Reference standards of 4-tert-octylphenol (4-t-OP, purity 97 %, CAS: 140-66-9) and 4-(1-ethyl-1,4-dimethylpentyl)-phenol (4-NP, purity 99.9 %, CAS 142731-63-3) were obtained from Sigma-Aldrich. Since individual OP_nEO and NP_nEO with n>2 are unavailable as analytical standards, Triton™ X-45 and IGEPAL® CO-520 technical mixtures, purchased from Sigma-Aldrich, have been employed as reference standards of the two AP_nEO classes. These mixtures, respectively consisting of oligomers of 4-t-octylphenol polyethoxylates (4-t-OP_nEOs, with n=1–11) and 4-nonylphenol polyethoxylates (4-NP_nEOs, with n=2–8), were previously characterized by our team (see the reference [11] in the main text). According to this characterization, the relative percentages of the oligomers considered in this study (n=2-8) due to their much larger abundance, were the following. Triton™ X-45: n=2 – 14.3%; n=3 – 22.4%; n=4 – 21.9%; n=5 – 16.0%; n=6 – 10.5%; n=7 – 6.5%; n=8 – 3.6%. IGEPAL® CO-520: n=2 – 14.6%; n=3 – 18.3%; n=4 – 17.7%; n=5 – 14.4%; n=6 – 11.0%; n=7 – 7.9%; n=8 – 5.3%. Stock solutions of Triton™X-45 and IGEPAL® CO-520 (1 mg mL^{-1}) and APs (100 µg mL^{-1}) were prepared in LC–MS grade methanol and then stored in the dark at −20 °C. CAS numbers, structure formulas and Log K_{OW} values of the investigated APs and AP_nEOs are shown in **Table S3. 1**.

The GC column employed for PAH evaluation was an SLB®-5ms fused silica capillary (10 m × 0.10 mm, 0.10 µm film thickness) from Supelco. The SPE cartridge used for the evaluation of polycyclic aromatic hydrocarbons contents in char was the cartridge Strata C18-E (500 mg, 6 mL, 55 µm, 70 Å) from Phenomenex (Torrance, CA, USA). A LC pellicular column Kinetex® Biphenyl (Phenomenex, 100 mm × 3 mm, 2.6 µm particle size), was used for the evaluation of the removal of target compounds by biochars and activated carbon.

Table S3.1 – Compound names and acronyms (in bracket), CAS, structure formulas and log K_{OW} values of target analytes.

Compound Name	CAS	Structure formula	Log K_{OW} [a]
4-tert-Octylphenol (4-t-OP)	140-66-9	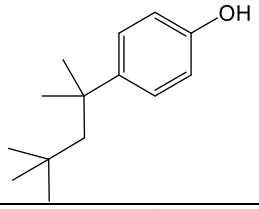	5.18
TRITON™X-45 (4-t-OP$_n$EO) Technical Mixture of 4-tert-octylphenolpolyethoxylate oligomers with ethoxylation number (n) equal to 2-8.	9002-93-1	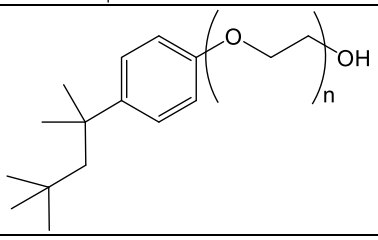	3.49-4.90 [b]
4-(1-Ethyl-1,4-dimethylpentyl)-phenol (4-NP)	142731-63-3	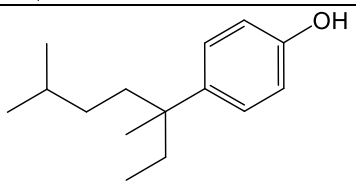	5.79
IGEPAL®CO-520 (4-NP$_n$EO) Technical Mixture of branched 4-nonylphenolpolyethoxylate oligomers with ethoxylation number (n) equal to 2-8.	68412-54-4	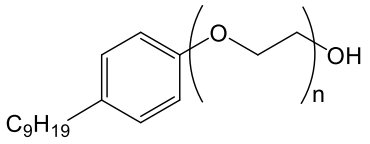	4.26-5.50 [c]

[a] Calculated using Advanced Chemistry Development (ACD/Labs) Software V11.02 (© 1994-2015 ACD/Labs). [b] Log K_{OW} range of 4-t-OP$_n$EO oligomers with n=2-8. [c] Log K_{OW} range of 4-NP$_n$EO oligomers with n=2-8 (when log K_{OW} of the branched oligomer was not available, the value concerning the corresponding compound with linear alkyl chain was reported).

S.3. 2 Characteristics of the effluent wastewater

The effluent WW used in this study was obtained from the Baciacavallo WWTP operating in the textile industrial district of Prato (Italy). The WW was characterized for the following parameters: pH, total suspended solids (TSS), chemical oxygen demand (COD), five-days biological oxygen demand (BOD_5), total nitrogen (N_{tot}), $N\text{-}NH_4^+$, $N\text{-}NO_3^-$, total phosphorus (P_{tot}), Cl^-, SO_4^{2-}, total hardness, total anionic surfactants (MBAS), total cationic surfactants (BiAS), and total surfactants. The characteristics of WW are shown in **Table S3.2**.

Table S3.2. Characteristics of the effluent wastewater used in this study. Values are mean of three determinations with corresponding standard deviations in bracket.

Parameter	Value
pH	7.46 (0.04)
TSS (mg/L)	1.1 (0.3)
COD (mg/L)	21 (4)
BOD_5 (mg/L)	<5
Ntot (mg/L)	10.8 (0.2)
$N\text{-}NH_4^+$ (mg/L)	1.5 (0.4)
$N\text{-}NO_3^-$ (mg/L)	7.6 (0.5)
P_{tot} (mg/L)	0.7 (0.1)
Cl^- (mg/L)	687 (21)
SO_4^{2-} (mg/L)	224 (18)
Total hardness (mg $CaCO_3$/L)	330 (11)
MBAS (mg/L)	0.21 (0.05)
BiAS (mg/L)	0.07 (0.01)
Total surfactants (mg/L)	0.29 (0.04)
4-t-OP (ng/L)	<95
4-t-OP_2EO (ng/L)	12 (2)
4-t-OP_3EO (ng/L)	10 (2)
4-t-OP_4EO (ng/L)	8 (2)
4-t-OP_5EO (ng/L)	7 (1)
4-t-OP_6EO (ng/L)	6 (1)
4-t-OP_7EO (ng/L)	< 5.5
4-t-OP_8EO (ng/L)	< 4.5
4-NP (ng/L)	58 (4)
4-NP_2EO (ng/L)	49 (5)
4-NP_3EO (ng/L)	37 (2)
4-NP_4EO (ng/L)	39 (3)
4-NP_5EO (ng/L)	31 (2)
4-NP_6EO (ng/L)	29 (2)
4-NP_7EO (ng/L)	33 (2)
4-NP_8EO (ng/L)	24 (2)

S.3.3 Metal analysis in recycled sawdust

Total Cd, Cr, Hg and Pb content in sawdust samples was determined by ICP-MS analysis, after acidic-oxidant digestion with trace metal grade reagents, using a microwave system ETHOS-1, (MILESTONE S.r.l., Bergamo, Italy) with pulsed-mode emission. Spontaneously dried sawdust (0.5 g) was treated with 2 mL of 30% hydrogen peroxide and 7 ml of 70% nitric acid, using the following microwave program: from ambient temperature to 180 °C in 10 min, and then isotherm at

180 °C for 10 min. After digestion, sawdust samples were taken up to 50 mL with Milli-Q water, filtered on 0.2 µm pore size PTFE filters, spiked with 1% Au 1000 mg L^{-1} solution and finally analysed by ICP-MS model 7700X (Agilent Technologies, Santa Clara, CA, U.S.A.) under the following experimental conditions: (i) plasma RF power 1450W, (ii) plasma gas flow (Ar) 15 L min^{-1} and (iii) auxiliary gas flow (Ar) 1.03 L min^{-1}. Total analysis time, including washing procedure of the system, was about 5 minutes. The entire procedure is programmed and automatically controlled by the MassHunter Workstation software for ICP-MS G7201B ver. B01.02 Build 349.8 patch 2 (Agilent Technologies).

For Cr(VI) analysis, 0.5 g of spontaneously dried sawdust were treated with 50 mL of a 0.01 M Na_3PO_4 solution (pH = 11.7) and heated for 5 min at 100 °C. The mixture was filtered through a 0.22 µm nylon membrane and injected for ion chromatographic analysis, which was performed with a Dionex 4000i (Dionex ThermoFisher, Sunnyvale, CA, USA) equipped with a spectrophotometric detector. Dionex IonPac column (AS7, 250 × 4.0 mm) and guard column (AG7, 50 × 4.0 mm) were used. The eluent, 250 mM $(NH_4)_2SO_4$ and 100 mM NH_4OH (pH 8.8), was delivered at 1 mL/min flow rate. Injection volume was 1000 µL. Detection was performed at 530 nm after post-column derivatization (750 µL reaction coil) with a 0.5 M H_2SO_4 solution with 2 mM DPC (10% CH_3OH). The flow rate of post-column reagent was 0.33 mL/min. Cr(VI) quantification was made by the standard addition method. The sawdust water content, measured by heating the material at 105°C for 1 h, together with the concentrations of selected toxic heavy-metals are shown in **Table S3.3**.

Table S3.3. Water content (%) and concentrations (mg kg^{-1}) of some toxic heavy-metals in recycled sawdust used for biochar production.

Parameter	Value
Water	9.1
Hg	<0.015[a]
Cd	1.1
Pb	0.9
Hexavalent Cr	<0.020[a]
Total Cr	1.3

[a] quantification limit

S.3. 4. Analysis of water extractable PAHs

The figure of merits of the instrumental method – i.e., limits of detection (IDLs), limits of quantification (IQLs), linearity and precision – obtained by replicated injections of standard solutions in dichloromethane, are shown in **Table S3.5**. IDLs and IQLs were taken as the minimum

concentrations of target analytes that give rise to a signal to noise ratio (S/N) equal to 3 and 10, respectively.

Table S3.4. GC-MS retention time (Rt), quantifier and qualifier ions of the investigated PAHs and selected labelled surrogate standards. The meaning of target analyte acronyms is reported in S1.

Compound	Rt [min]	Quantifier ion	Qualifier ion
N	3.5	128	127
Acy	4.4	152	151
Ac	4.5	153	154
Fl	4.9	165	165
P	5.7	178	176
A	5.8	178	176
Flu	7.0	202	200
Py	7.4	202	200
BaA	10.5	228	226
Ch	10.6	228	226
BbFlu	15.8	252	250
BkFlu	16.1	252	250
BaPy	18.0	252	250
Ipy	27.3	276	274
BahA	28.4	278	276
BP	29.8	276	274
N-d8	3.5	136	134
P-d10	5.7	188	184
Flu-d10	7.0	212	208
Ch-d12	10.5	240	236
BaPy-d12	18.0	264	260
Ipy-d12	27.3	288	284

The linearity was investigated by replicated analysis (n=5) of standard solutions from five calibration levels of PAHs. For each analyte concentration ranges were chosen starting from the IQLs up to three magnitude orders expressed as ng injected. Intra-day ($RSD\%_{intra}$) and inter-day ($RSD\%_{inter}$) precision were evaluated by ten replicated injections of standard solutions, at concentration levels twice higher than IQLs.

Table S3.5. Instrumental figure of merits of GC-MS analysis of PAHs. The meaning of target analyte acronyms is reported in S1.

Compound	IDL (ng injected)	Linearity range (ng injected)[a]	R^2	$RSD\%_{intra}$	$RSD\%_{inter}$
N	0.001	0.005 – 52.64	0.9996	2.1	2.8
Acy	0.001	0.004 – 52.98	0.9998	3.3	3.5
Ac	0.001	0.004 – 52.98	0.9994	2.4	2.8
Fl	0.001	0.005 – 5.40	0.9975	3.1	3.5
P	0.002	0.007 – 5.34	0.9996	3.5	3.8
A	0.002	0.007 – 5.37	0.9994	3.7	4.0
Flu	0.001	0.005 – 10.20	0.9994	3.2	3.3
Py	0.001	0.005 – 4.97	0.9987	3.4	3.5
BaA	0.003	0.01 – 26.63	0.9997	4.4	4.5
Ch	0.005	0.02 – 26.63	0.9994	4.2	4.4
BbFlu	0.004	0.015 – 10.87	0.9977	5.3	5.5
BkFlu	0.004	0.015 – 5.39	0.9983	5.1	5.4
BaPy	0.005	0.02 – 27.9	0.9995	4.8	5.2
BahA	0.008	0.03 – 29.16	0.9994	5.2	5.3
Ipy	0.006	0.025 – 26.75	0.9986	5.4	5.5
BP	0.008	0.030 – 3.15	0.9948	5.5	5.6
N-d8	0.001	0.005 – 51.37	0.9998	1.9	2.2
P-d10	0.002	0.007 – 5.52	0.9997	2.7	3.1
Flu-d10	0.001	0.005 – 12.33	0.9995	2.8	3.0
Ch-d12	0.005	0.02 – 24.53	0.9997	3.2	3.5
BaPy-d12	0.005	0.02 – 26.8	0.9993	4.2	4.8
Ipy-d12	0.006	0.02 – 21.15	0.9987	5.1	5.3

[a] The lower limits of the linearity ranges represent IQLs.

In order to evaluate the SPE apparent recovery, three 2 L aliquots of extraction water were fortified with labelled compounds (5 ng L-1 for N-d8, P-d10, Flu-d10 and Ch-d12 and 10 ng L-1 for BaP-d12 and Ipy-d12). The spiked samples were subjected to the SPE procedure, followed by the GC-MS analysis; the resulting mean areas (n=3) were compared to the mean areas (n=3) obtained by spiking 50 µL of dichloromethane with the same amounts of mass labelled compounds.

The following deuterated PAHs were used for calculating apparent recoveries: (i) N-d8 for N, (ii) P-d10or 3-ring PAHs, (iii) Flu-d10 for Flu, (iv) Ch-d12 for 4-ring PAHs, (v) BaP-d12 for 5-ring PAHs and (vi) Ipy-d12 for 6-ring PAHs. The recoveries of mass labelled analytes are detailed in **Figure S4**, and the detection (MDLs) and quantification (MQLs) limits of the whole analytical procedure are shown in **Table S3.6**. The overall MQLs in extraction water were found in the range of 0.13 – 0.9 ng L^{-1}.

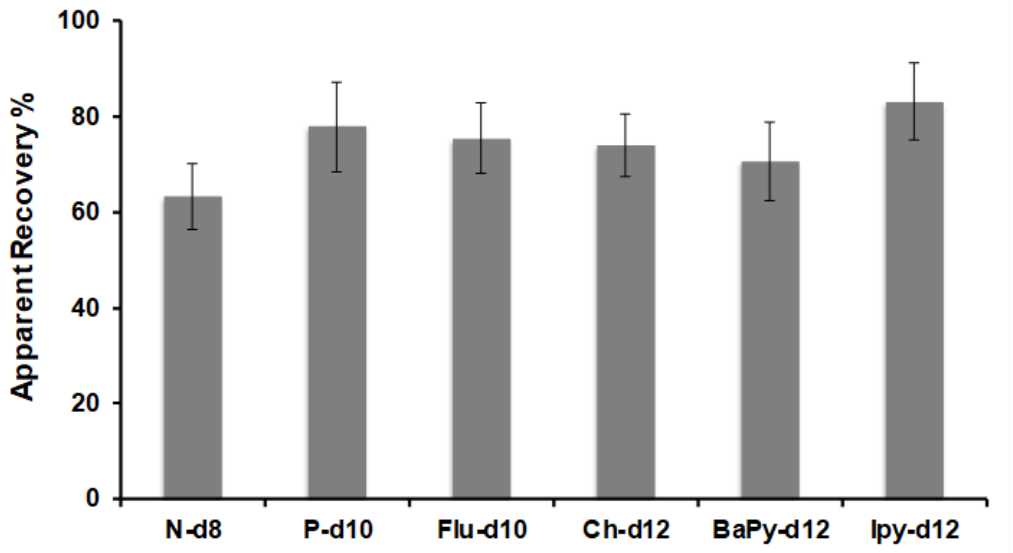

Figure S 3. 1 Mean percentage values of apparent recovery for the whole analytical procedure of PAH analysis. The meaning of target analyte acronyms is reported in the paragraph S 3.1.

Table S 3.6. Method detection (MDL) and quantification (MQL) limits (n=5) for the whole SPE-GC-MS procedure of PAH analysis. Values in bracket represent the standard deviation. The meaning of target analyte acronyms is reported in the paragraph S1.

Compound	MDL (ng L^{-1})	MQL (ng L^{-1})
N	0.050 (0.001)	0.20 (0.01)
Acy	0.032 (0.001)	0.13 (0.01)
Ac	0.032 (0.001)	0.13 (0.01)
Fl	0.040 (0.001)	0.16 (0.01)
P	0.056 (0.002)	0.22 (0.01)
A	0.056 (0.002)	0.22 (0.01)
Flu	0.042 (0.001)	0.17 (0.01)
Py	0.043 (0.001)	0.17 (0.01)
BaA	0.086 (0.004)	0.34 (0.02)
Ch	0.171 (0.008)	0.68 (0.03)
BbFlu	0.134 (0.007)	0.54 (0.03)
BkFlu	0.134 (0.007)	0.54(0.03)
BaPy	0.179 (0.009)	0.71 (0.04)
BahA	0.226 (0.012)	0.90 (0.05)
Ipy	0.188 (0.010)	0.75 (0.04)
BP	0.226 (0.013)	0.90 (0.05)

S.3. 5. LC-MS/MS analysis of APnEOs and APs

The LC-MS/MS analyses were performed on a Shimadzu chromatographic system, consisting of a low-pressure gradient quaternary pump Nexera X2 LC-30AD (pump 1) and one isocratic pump LC-20AD XR (pump 2), devoted to the delivery of the post-column positive ionization promoter. A CTO/20AC thermostatic column compartment equipped with the above-mentioned BP analytical column, a SIL-30AC auto injector equipped with a 50 µL sample loop, a DGU-20A 5R degassing unit and a CBM-20A module controller were also used. The entire chromatographic procedure is programmed and automatically controlled by the Analyst® software, version 1.6.2 (Sciex). LC analysis was carried out by injection of 100 µl sample at 50°C, on the BP column, using LC-MS grade water (A) and methanol (B), as eluents, at a flow rate of 0.8 mL min^{-1} and isocratic elution (85% B) for 4 min. During the whole LC run, the addition of a 300 mM ammonia solution in methanol (i.e., the positive ionization promoter) was post-column dispensed by pump 2 at 40 µL min^{-1}, by means of a three-way connector. Under the aforementioned experimental conditions, total analysis time per sample, including loop filling, was about 4.2 min.

The LC system was coupled with a 5500 QTrap mass spectrometer (Sciex, Ontario, Canada), equipped with a Turbo V® interface by an electro-spray (ESI) probe. MS/MS analysis was carried out using the Multiple Reaction Monitoring (MRM) mode by ESI, both in positive and negative ionization mode. The precursor and product ion pairs, as well as compound-dependent parameters, were optimized by direct infusion of diluted standard solution and are reported in **Table S3. 7**.

Table S3.7. LC Retention time (Rt, min) and optimized MS parameters for the detection of quantifier and qualifier ions of ethoxylated alkylphenols and alkylphenols. CE: collision energy (reported in bracket together with the related product ion). DP: declustering potential, EP: entrance potential, CXP: collision cell exit potential. The meaning of target analyte acronyms is reported in the paragraph S1.

Compound	Rt	Precursor ion	Product ions (CE)		DP	EP	CXP	
			Quantifier	Qualifier			Quantifier	Qualifier
4-t-OP[a]	1.16	205	133 (-35)	134 (-25)	-50	-5	-15	-15
4-t-OP_2EO[b]	1.60	312	183 (15)	121 (32)	40	5	10	10
4-t-OP_3EO[b]	1.79	356	227 (17)	121 (36)	40	5	20	10
4-t-OP_4EO[b]	2.00	400	271 (22)	383 (15)	40	5	25	10
4-t-OP_5EO[b]	2.19	444	315 (25)	427 (18)	40	5	9	12
4-t-OP_6EO[b]	2.39	488	471 (20)	359 (25)	40	5	13	10
4-t-OP_7EO[b]	2.60	532	515 (22)	133 (32)	40	5	14	15
4-t-OP_8EO[b]	2.83	576	133 (33)	559 (25)	40	5	15	15
4-NP[a]	1.37	219	133 (-45)	147 (-35)	-50	-5	-15	-13
4-NP_2EO[b]	1.93	326	183 (15)	121 (33)	45	12	15	13
4-NP_3EO[b]	2.19	370	227 (15)	121 (33)	45	12	15	15
4-NP_4EO[b]	2.44	414	271 (22)	397 (14)	45	12	30	35
4-NP_5EO[b]	2.68	458	315 (23)	441 (17)	45	12	13	13
4-NP_6EO[b]	2.93	502	485 (20)	359 (24)	45	12	15	30
4-NP_7EO[b]	3.22	546	529 (22)	133 (31)	45	12	17	15
4-NP_8EO[b]	3.57	590	133 (33)	573 (23)	45	12	15	13

[a] Monitored as $[M-H]^-$ ion; [b] Monitored as $[M + NH_4]^+$ adduct ion.

The first and the second most intense MRM transitions were used for analyte quantification and identification, respectively. Source-dependent parameters were optimized in flow injection analysis at optimal LC flow and mobile phase composition and were as follows: curtain gas 50, CAD gas medium, temperature 650°C, gas 1 40, gas 2 50, interface heater ON and ion spray voltage 3500 V and -4500 V in MRM(+) and MRM(-) mode, respectively. The polarity switching was performed as following specified: (i) from 0 to 1.5 min, MRM(-) for 4-t-OP and 4-NP monitoring and (ii) from 1.5 to 4 min, MRM(+) for 4-t-OPnEO (with n=2-8) and 4-NPnEO (with n=2-8) analysis.

Criteria proposed by the Commission Decision 2002/657/CE were adopted for identity confirmation. The positive identification is achieved when: (i) chromatographic retention time agrees within ±2%; (ii) relative abundance of the two transitions, selected as precursor ion and product ion, falls within the permitted tolerances for relative ion intensities using the LC-MS technique. Peak attribution and quantitative determination were performed using MultiQuant

software version 3.0.2 (Sciex). All statistical analyses were performed using SPSS® software, version 22 (SPSS Inc., Chicago, IL, USA).

The LC-MS/MS method was preliminary evaluated for instrumental limits of detection (IDLs) and quantification (IQLs), linearity, as well as intra-day and inter-day precision, by replicated injections of standard solutions of APs, Triton™X-45 and IGEPAL® CO-520 technical mixtures in Milli-Q water (**Table S3.8**). IDLs and IQLs were taken as the minimum concentrations of target analytes that give rise to a S/N equal to 3 and 10, respectively.

The linearity was investigated by replicated analysis (n=5) of standard solutions at ten different calibration levels. Concentration ranges from IQLs to 20–500 pg injected were chosen, depending on the response factor of the analyte considered, in order to cover a linearity range of about two magnitude orders. Determination coefficients (R^2) ≥0.9906 were obtained in all cases.

Intra-day ($RSD\%_{intra}$) and inter-day ($RSD\%_{inter}$) precision were evaluated by ten replicated injections of standard solutions, at concentration levels twice higher than IQLs. $RSD\%_{intra}$ and $RSD\%_{inter}$ values were found in the ranges of 1.8-4.6% and 2.4-5.6%, respectively.

The matrix effect was evaluated through the matrix matched calibration method, by spiking the matrix and Milli-Q water with the following concentration of APs, Triton™X-45 (4-t-OPnEO) and IGEPAL® CO-520 (4-NPnEO) technical mixtures. AP_nEOs technical mixtures: 0, 5, 10, 25, 50, 75, 100, 150, 200, 300 and 400 µg L^{-1}); APs: 0, 0.5, 1.0, 2.5, 5.0, 7.5, 10, 15, 20, 30 and 40 µg L^{-1}.

Table S3.8. Instrumental limits (pg injected) of detection (IDLs), and quantification (IQLs)[a], linearity range, determination coefficients (R^2), intra-day ($RSD\%_{intra}$) and inter-day ($RSD\%_{inter}$) relative standard deviation percentages (n=5) of the LC-MS/MS method. The meaning of target analyte acronyms is reported in the paragraph S3. 1.

Compound	IDL	Linearity range [a]	R^2	$RSD\%_{intra}$	$RSD\%_{inter}$
4-t-OP	2.90	9.50-500	0.9952	2.4	3.6
4-t-OP_2EO	0.10	0.35-75	0.9951	2.0	2.7
4-t-OP_3EO	0.05	0.20-110	0.9910	2.1	2.6
4-t-OP_4EO	0.04	0.15-110	0.9939	1.8	2.4
4-t-OP_5EO	0.07	0.25-80	0.9906	2.2	2.9
4-t-OP_6EO	0.14	0.45-50	0.9937	3.2	4.3
4-t-OP_7EO	0.16	0.55-35	0.9936	4.1	4.8
4-t-OP_8EO	0.13	0.45-20	0.9918	4.6	5.3
4-NP	1.70	5.50-500	0.9921	2.5	3.6
4-NP_2EO	0.63	2.10-75	0.9955	2.5	3.1
4-NP_3EO	0.32	1.05-90	0.9971	2.2	2.9
4-NP_4EO	0.18	0.60-90	0.9933	2.9	4.0
4-NP_5EO	0.26	0.90-75	0.9987	2.3	2.9
4-NP_6EO	0.45	1.50-55	0.9939	3.0	3.8
4-NP_7EO	0.66	2.20-40	0.9922	4.1	5.0
4-NP_8EO	0.45	1.50-30	0.9973	4.3	5.6

[a] The bottom limits of linearity range represent IQLs.

Direct injections (n = 3) of 50 µL of spiked purified matrix aliquots and Milli-Q reference solutions were performed, and the mean peak areas obtained were plotted as a function of the spiked concentrations. Matrix effect percentage (ME%) was defined as:

$$ME\% = (\frac{S_{matrix}}{S_{solvent}} * 100)\text{-}100$$

where S_{matrix} and $S_{solvent}$ are the slopes of the calibration lines in matrix and in Milli-Q water, respectively. ME% values higher or lower than zero indicate the presence of signal enhancement or suppression in comparison with the instrumental response observed in Milli-Q water (see **Table S 3. 9.**). However, absolute values of ME% ≤ 20% are commonly considered not significant. Data herein obtained for MAC evidenced a suppressive ME% values ranging from −4.0% to −11.4%, whereas for BC450-850, a signal enhancement, included between 0.8% and 19.1% was observed.

Table S3.9. Mean values (n=3) and standard deviations (in brackets) of matrix effect in biochars and activated carbon. The meaning of target analyte acronyms is reported in the paragraph S1.

Compound	Matrix Effect (%)			
	MAC	BC450	BC650	BC850
4-t-OP	-8.2 (0.7)	5.2 (3.7)	0.8 (2.3)	6.7 (3.4)
4-t-OP_2EO	-7.7 (0.5)	13.6 (1.9)	3.9 (1.4)	10.0 (1.3)
4-t-OP_3EO	-5.0 (0.2)	12.6 (2.5)	2.3 (1.6)	10.8 (1.5)
4-t-OP_4EO	-6.8 (0.4)	10.5 (2.9)	2.1 (0.7)	12.4 (1.0)
4-t-OP_5EO	-4.0 (0.5)	16.4 (2.4)	6.2 (1.2)	12.3 (1.8)
4-t-OP_6EO	-4.6 (0.5)	18.3 (3.7)	6.2 (1.1)	14.6 (2.0)
4-t-OP_7EO	-5.7 (0.4)	16.5 (3.3)	5.4 (1.0)	14.2 (2.4)
4-t-OP_8EO	-7.4 (0.3)	17.7 (4.2)	3.9 (2.3)	6.8 (1.9)
4-NP	-7.8 (0.6)	10.8 (4.2)	2.3 (1.7)	13.5 (3.9)
4-NP_2EO	-7.1 (0.3)	19.1 (3.5)	3.2 (1.1)	13.5 (1.5)
4-NP_3EO	-5.1 (0.5)	9.3 (2.7)	2.7 (1.3)	13.5 (1.7)
4-NP_4EO	-8.1 (0.6)	6.7 (4.5)	2.8 (1.4)	11.2 (1.2)
4-NP_5EO	-7.7 (0.2)	13.8 (4.8)	3.3 (1.9)	10.2 (0.8)
4-NP_6EO	-11.4 (1.0)	11.4 (5.3)	3.9 (1.8)	8.3 (1.1)
4-NP_7EO	-8.5 (0.7)	17.9 (6.2)	8.7 (4.5)	9.6 (3.9)
4-NP_8EO	-5.7 (1.2)	15.1 (6.3)	6.1 (5.0)	10.5 (5.7)

S3. 6. XPS analysis

Table S3.10. Experimental and corrected XPS areas, and relative percentages of carbon and oxygen determined in biochars produced at pyrolysis temperatures of 450°C (BC450), 650°C (BC650), 850°C (BC850), and in mineral activated carbon (MAC).

Char	C	$C_{corrected}$	O	$O_{corrected}$	C (%)	O(%)
BC450	731	2470	548	771	76.2	23.8
BC650	1294	4372	635	893	83.0	17.0
BC850	1195	4037	577	812	83.3	16.7
MAC	1359	4591	791	1113	80.5	19.5

S 3. 7. Isotherm adsorption tests

Complete datasets regarding Langmuir maximum sorption parameters (Q_m) and binding energy constants (k) are shown in **Table S3.17** and **Table S3.18**, respectively.

S 3. 7. 1. Kinetic adsorption tests

Complete removal datasets for APs and AP_nEOs are shown in **Tables S3.11-S3.14** for BC450, BC650, BC850 and MAC, respectively.

Table S3.11. Mean values (n=3) and standard deviation (in brackets) of removal percentages of APnEOs and APs from wastewater solutions (4-t-OP and 4-NP = 100 µg L^{-1}; technical mixtures containing APnEOs = 1 mg L^{-1}) by 10 mg L^{-1} of BC450 at different contact times. Within a same compound, values with the same letter are not statistically different (P>0.05) according to the Dunnett T3 non-parametric test. The meaning of target analyte acronyms is reported in the paragraph S 3.1.

Compound	Removal percentages				
	1h	2h	4h	6h	12h
4-t-OP	19 (2) a	30 (1) b	32 (2) b	30 (4) b	32 (2) b
4-t-OP_2EO	30 (6) a	45 (1) b	47 (2) b	47 (1) b	48 (2) b
4-t-OP_3EO	37 (3) a	53 (2) b	55 (3) b	53 (4) b	55 (1) b
4-t-OP_4EO	37 (2) a	51 (2) b	49 (5) b	51 (5) b	52 (2) b
4-t-OP_5EO	38 (3) a	52 (2) b	52 (2) b	52 (6) b	53 (4) b
4-t-OP_6EO	38 (2) a	53 (3) b	53 (3) b	53 (2) b	55 (1) b
4-t-OP_7EO	39 (2) a	52 (3) b	51 (3) b	53 (2) b	51 (1) b
4-t-OP_8EO	25 (2) a	43 (3) b	44 (3) b	46 (3) b	42 (3) b
4-NP	38 (2) a	54 (2) b	54 (2) b	51 (3) b	54 (3) b
4-NP_2EO	61 (3) a	79 (1) b	78 (2) b	79 (1) b	79 (2) b
4-NP_3EO	69 (4) a	81 (1) b	79 (3) b	82 (1) b	80 (4) b
4-NP_4EO	65 (2) a	80 (2) b	80 (3) b	82 (3) b	80 (3) b
4-NP_5EO	66 (2) a	82 (2) b	81 (1) b	81 (1) b	79 (2) b
4-NP_6EO	59 (2) a	71 (4) b	71 (4) b	72 (4) b	70 (2) b
4-NP_7EO	51 (2) a	64 (1) b	63 (2) b	64 (2) b	64 (3) b
4-NP_8EO	49 (4) a	61 (1) b	62 (2) b	61 (2) b	61 (4) b

Table S3.12. Mean values (n=3) and standard deviation (in brackets) of removal percentages of APnEOs and APs from wastewater solutions (4-t-OP and 4-NP = 100 µg L^{-1}; technical mixtures containing APnEOs = 1 mg L^{-1}) by 10 mg L^{-1} of BC650 at different contact times. Within a same compound, values with the same letter are not statistically different (P>0.05) according to the Dunnett T3 non-parametric test. The meaning of target analyte acronyms is reported in the paragraph S1.

Compound	Removal percentages				
	1h	2h	4h	6h	12h
4-t-OP	27 (2) a	39 (1) b	41 (5) b	39 (5) b	41 (4) b
4-t-OP_2EO	42 (6) a	62 (3) b	60 (2) b	62 (2) b	60 (1) b
4-t-OP_3EO	37 (1) a	56 (3) b	62 (7) b	63 (6) b	62 (4) b
4-t-OP_4EO	42 (4) a	65 (2) b	65 (4) bc	62 (5) c	66 (4) bc
4-t-OP_5EO	35 (2) a	59 (1) b	59 (3) b	60 (6) b	61 (3) b
4-t-OP_6EO	43 (1) a	57 (1) b	59 (2) bc	54 (1) b	57 (3) bc
4-t-OP_7EO	27 (3) a	38 (1) b	39 (3) b	39 (2) b	42 (3) b
4-t-OP_8EO	29 (3) a	40 (1) b	42 (2) c	42 (1) c	40 (2) bc
4-NP	51 (2) a	78 (1) b	76 (2) bc	75 (2) c	79 (4) bc
4-NP_2EO	61 (6) a	82 (2) b	80 (2) b	84 (2) b	80 (2) b
4-NP_3EO	50 (3) a	83 (1) b	82 (1) b	84 (1) b	83 (1) b
4-NP_4EO	64 (1) a	80 (1) b	80 (2) b	83 (1) b	83 (2) b
4-NP_5EO	64 (4) a	78 (2) b	80 (1) b	80 (2) b	80 (2) b
4-NP_6EO	53 (1) a	64 (5) b	64 (2) b	67 (4) b	67 (1) b
4-NP_7EO	40 (2) a	65 (1) b	66 (1) b	66 (3) b	67 (3) b
4-NP_8EO	48(3) a	63 (2) b	61 (3) b	62 (3) b	658 (1) b

Table S3.13. Mean values (n=3) and standard deviation (in brackets) of removal percentages of APnEOs and APs from wastewater solutions (4-t-OP and 4-NP = 100 µg L^{-1}; technical mixtures containing APnEOs = 1 mg L^{-1}) by 10 mg L^{-1} of BC850 at different contact times. Within a same compound, values with the same letter are not statistically different (P>0.05) according to the Dunnett T3 non-parametric test. The meaning of target analyte acronyms is reported in the paragraph S1.

Compound	Removal percentages				
	1h	2h	4h	6h	12h
4-t-OP	22 (2) a	40 (2) b	43 (2) b	43 (2) b	437 (2) b
4-t-OP_2EO	44 (2) a	63 (2) b	62 (4) b	66 (2) b	65 (2) b
4-t-OP_3EO	44 (3) a	64 (5) b	67 (4) b	68 (2) b	70 (2) b
4-t-OP_4EO	46 (3) a	68 (3) b	66 (1) b	69 (3) b	68 (3) b
4-t-OP_5EO	46 (3) a	65 (1) b	67 (1) c	66 (4) bc	65 (2) bc
4-t-OP_6EO	43 (2) a	63 (1) b	66 (4) bc	66 (2) c	64 (4) bc
4-t-OP_7EO	39 (2) a	56 (1) b	55 (1) b	56 (2) b	56 (1) b
4-t-OP_8EO	36 (2) a	47 (3) b	49 (4) b	52 (6) b	51 (3) b
4-NP	52 (2) a	67 (1) b	69 (1) bc	70 (1) c	71 (1) c
4-NP_2EO	56 (4) a	81 (1) b	81 (1) b	79 (3) b	80 (2) b
4-NP_3EO	67 (1) a	82 (1) b	84 (1) bc	86 (1) c	86 (1) c
4-NP_4EO	68 (1) a	84 (1) b	85 (1) b	85 (1) b	86 (2) b
4-NP_5EO	52 (2) a	76 (1) b	74 (3) b	77 (2) b	80 (3) b
4-NP_6EO	50 (4) a	71 (1) b	72 (2) b	72 (2) b	74 (2) b
4-NP_7EO	42 (2) a	66 (2) b	67 (2) b	68 (2) b	68 (3) b
4-NP_8EO	37 (3) a	59 (1) b	61 (3) bc	63 (2) c	62 (2) bc

Table S3.14. Mean values (n=3) and standard deviation (in brackets) of removal percentages of APnEOs and APs from wastewater solutions (4-t-OP and 4-NP = 100 µg L^{-1}; technical mixtures containing APnEOs = 1 mg L^{-1}) by 1 mg L^{-1} of MAC at different contact times. Within a same compound, values with the same letter are not statistically different (P>0.05) according to the Dunnett T3 non-parametric test. The meaning of target analyte acronyms is reported in the paragraph S1.

Compound	Removal percentages				
	1h	2h	4h	6h	12h
4-t-OP	42 (1) a	58 (4) b	58 (2) b	57 (7) b	61 (5) b
4-t-OP2EO	57 (4) a	76 (1) b	78 (4) b	76 (3) b	78 (1) b
4-t-OP3EO	62 (2) a	80 (1) b	81 (1) b	80 (2) b	81 (1) b
4-t-OP4EO	62 (3) a	78 (1) b	78 (2) b	78 (1) b	79 (1) b
4-t-OP5EO	57 (5) a	73 (1) b	76 (3) bc	76 (2) c	75 (2) bc
4-t-OP6EO	52 (3) a	73 (3) b	71 (2) b	72 (1) b	72 (6) b
4-t-OP7EO	48 (5) a	69 (3) b	69 (2) b	68 (1) b	67 (5) b
4-t-OP8EO	49 (4) a	64 (4) b	65 (2) b	64 (2) b	64 (3) b
4-NP	52 (6) a	89 (1) b	92 (1) b	87 (4) b	91 (7) b
4-NP2EO	65 (1) a	87 (1) b	88 (2) b	89 (3) b	87 (3) b
4-NP3EO	71 (3) a	91 (1) b	90 (5) b	91 (1) b	939 (1) b
4-NP4EO	63 (4) a	90(1) b	90 (1) b	90 (1) b	92 (1) b
4-NP5EO	53 (3) a	87 (1) b	87 (1) b	87 (3) b	88 (4) b
4-NP6EO	63 (4) a	84 (1) b	84 (2) b	83 (4) b	84 (2) b
4-NP7EO	51 (4) a	78 (4) b	80 (1) b	79 (4) b	80 (4) b
4-NP8EO	52 (1) a	73 (1) b	72 (1) b	73 (2) b	71 (1) b

S.3.7.2 Isotherm adsorption tests

Complete datasets regarding Langmuir maximum sorption parameters (Q_m) and binding energy constants (k) are shown in **Table S3.15** and **Table S3.16**, respectively.

Table S3.15. Mean values (n=3) standard deviation (in brackets) of maximum sorption parameters (Q_m) as estimated by Langmuir adsorption-isotherm linear equation in the ranges 5–100 µg L^{-1} ($Q_{m,1}$ - Range 1) and 100–400 µg L^{-1} ($Q_{m,2}$ - Range 2) of APEOs technical mixtures and APs for 10 mg L^{-1} and 1 mg L^{-1} of biochars and mineral activated carbon, respectively. The meaning of target analyte acronyms is reported in the paragraph S1.

Analyte	Adsorption Maxima (Q_m) mg g^{-1}							
	$Q_{m,1}$ - Range 1				$Q_{m,2}$ - Range 2			
	BC450	BC650	BC850	MAC	BC450	BC650	BC850	MAC
4-t-OP	3.8 (0.1)	6.2 (0.2)	5.3 (0.1)	103 (10)	11 (1)	17.2 (0.9)	24 (3)	386 (9)
4-t-OP2EO	0.89 (0.06)	1.29 (0.08)	1.43 (0.02)	16.6 (0.6)	3.4 (0.3)	5.2 (0.3)	5.5 (0.3)	47 (1)
4-t-OP3EO	1.56 (0.04)	2.0 (0.1)	2.0 (0.1)	24 (2)	6.6 (0.5)	7.2 (0.3)	7.86 (0.09)	60.7 (0.2)
4-t-OP4EO	1.53 (0.05)	2.2 (0.1)	1.94 (0.05)	24 (2)	6.3 (0.1)	7.7 (0.5)	7.8 (0.2)	53 (2)
4-t-OP5EO	1.18 (0.07)	1.64 (0.02)	1.5 (0.1)	17.1 (0.8)	4.9 (0.1)	5.6 (0.3)	5.3 (0.2)	39 (1)
4-t-OP6EO	0.74 (0.05)	0.92 (0.05)	1.0 (0.1)	11.1 (0.4)	2.74 (0.08)	2.8 (0.1)	3.7 (0.5)	25.5 (0.6)
4-t-OP7EO	0.42 (0.01)	0.40 (0.01)	0.37 (0.05)	6.8 (0.1)	1.82 (0.06)	1.1 (0.1)	1.3 (0.2)	16.6 (0.1)
4-t-OP8EO	0.20 (0.01)	0.25 (0.01)	0.25 (0.02)	3.7 (0.1)	0.83 (0.09)	0.72 (0.03)	0.95 (0.06)	7.5 (0.4)
4-NP	6.8 (0.2)	8.8 (0.4)	9.6 (0.6)	164 (13)	20.7 (0.7)	31 (2)	42 (2)	625 (27)
4-NP2EO	1.47 (0.09)	1.75 (0.09)	1.83 (0.03)	17.8 (0.5)	5.5 (0.1)	7.6 (0.7)	7.6 (0.2)	73 (2)
4-NP3EO	1.9 (0.1)	2.2 (0.1)	2.0 (0.1)	23 (2)	6.5 (0.2)	10 (0.4)	8.1 (0.7)	78 (2)
4-NP4EO	1.96 (0.07)	1.90 (0.04)	2.0 (0.2)	20.3 (0.7)	6.8 (0.2)	9.0 (0.2)	8.7 (0.9)	68.6 (0.5)
4-NP5EO	1.37 (0.02)	1.40 (0.08)	1.40 (0.06)	15.5 (0.2)	5.1 (0.2)	6.3 (0.2)	6.9 (0.5)	54.8 (0.1)
4-NP6EO	0.97 (0.04)	1.00 (0.08)	1.0 (0.1)	11.8 (0.1)	3.9 (0.2)	4.1 (0.3)	4.2 (0.3)	41.3 (0.2)
4-NP7EO	0.56 (0.02)	0.58 (0.05)	0.55 (0.04)	8.4 (0.2)	2.9 (0.1)	2.2 (0.1)	2.36 (0.08)	34.5 (0.1)
4-NP8EO	0.41 (0.01)	0.41 (0.01)	0.41 (0.01)	5.6 (0.1)	1.3 (0.1)	1.40 (0.06)	1.67 (0.09)	20.2 (0.3)

Table S3.16 Mean values (n=3) standard deviation (in brackets) of binding energy constants (k) as estimated by Langmuir adsorption-isotherm linear equation in the ranges 5–100 µg L^{-1} (k_1 - Range 1) and 100–400 µg L^{-1} (k_2 - Range 2) of APEOs technical mixtures and APs for 10 mg L^{-1} and 1 mg L^{-1} of biochars and mineral activated carbon, respectively. The meaning of target analyte acronyms is reported in the paragraph S1.

Analyte	Binding energy constants (k)							
	k_1 - Range 1				k_2 - Range 2			
	BC450	BC650	BC850	MAC	BC450	BC650	BC850	MAC
4-t-OP	0.132 (0.01)	0.188 (0.02)	0.106 (0.01)	0.094 (0.02)	0,008 (0.01)	0.0104 (0.00)	0.004 (0.00)	0.008 (0.00)
4-t-OP_2EO	7.437 (3.45)	0.856 (0.07)	0.997 (0.06)	1.602 (0.18)	0,029 (0.01)	0.0594 (0.01)	0.075 (0.01)	0.157 (0.00)
4-t-OP_3EO	0.684 (0.17)	0.507 (0.04)	0.902 (0.16)	1.217 (0.25)	0,029 (0.01)	0.0413 (0.01)	0.045 (0.00)	0.119 (0.01)
4-t-OP_4EO	0.776 (0.16)	0.296 (0.03)	0.865 (0.02)	1.301 (0.26)	0,043 (0.01)	0.0391 (0.01)	0.044 (0.00)	0.165 (0.01)
4-t-OP_5EO	0.962 (0.31)	0.661 (0.02)	1.192 (0.26)	1.947 (0.32)	0,069 (0.00)	0.0649 (0.01)	0.072 (0.01)	0.247 (0.01)
4-t-OP_6EO	1.752 (0.40)	1.398 (0.17)	1.419 (0.24)	3.413 (0.31)	0,080 (0.00)	0.1100 (0.01)	0.085 (0.02)	0.363 (0.03)
4-t-OP_7EO	1.456 (0.06)	2.004 (0.21)	2.569 (1.19)	6.096 (0.91)	0,156 (0.02)	0.1338 (0.03)	0.097 (0.03)	0.561 (0.04)
4-t-OP_8EO	5.361 (0.77)	6.254 (0.10)	0.127 (0.02)	12.31 (0.25)	0,009 (0.00)	0.3242 (0.01)	0.009 (0.00)	1.754 (0.01)
4-NP	0.374 (0.12)	0.415 (0.03)	5.960 (0.58)	0.235 (0.02)	0,107 (0.00)	0.0265 (0.02)	0.194 (0.03)	0.023 (0.00)
4-NP_2EO	2.127 (0.33)	2.218 (0.42)	1.763 (0.12)	7.007 (0.39)	0,120 (0.01)	0.1688 (0.03)	0.133 (0.01)	0.415 (0.03)
4-NP_3EO	1.753 (0.18)	1.289 (0.05)	0.946 (0.13)	4.786 (0.70)	0,125 (0.00)	0.0937 (0.00)	0.067 (0.01)	0.340 (0.03)
4-NP_4EO	1.522 (0.20)	1.899 (0.11)	0.830 (015)	5.340 (0.61)	0,119 (0.02)	0.0986 (0.00)	0.051 (0.01)	0.363 (0.01)
4-NP_5EO	2.449 (0.38)	2.363 (0.29)	2.041 (0.20)	7.474 (0.30)	0,095 (0.01)	0.0956 (0.01)	0.088 (0.01)	0.363 (0.01)
4-NP_6EO	1.825 (0.32)	2.618 (0.46)	2.455 (0.42)	8.013 (0.10)	0,084 (0.01)	0.1052 (0.01)	0.092 (0.02)	0.412 (0.01)
4-NP_7EO	5.693 (0.77)	4.233 (0.74)	4.185 (0.77)	9.273 (0.09)	0,244 (0.06)	0.1089 (0.01)	0.083 (0.00)	0.397 (0.01)
4-NP_8EO	4.900 (0.60)	7.725 (0.31)	7.094 (0.88)	15.97 (0.84)	0,008 (0.06)	0.2394 (0.01)	0.169 (0.01)	0.725 (0.01)

The complete dataset regarding the Freundlich adsorption parameters (n) is shown in **Table S 3.17**.

Table S3.17. Mean (n=3) and standard deviations (in brackets) of Freundlich adsorption intensity (*n*) parameters, calculated for biochars (BC) produced at 450, 650, 850°C, and mineral activated carbon (MAC), in the ranges 5–400 µg L^{-1} for AP_nEO technical mixtures, and in the ranges 0.5–40 µg L^{-1} for APs. See Table 1 for the meaning of target analyte acronyms.

		N		
Compound	BC450	BC650	BC850	MAC
4-t-OP	2.12 (0.033)	2.15 (0.046)	1.86 (0.021)	1.57 (0.040)
4-t-OP_2EO	2.07 (0.052)	1.62 (0.038)	1.61 (0.031)	1.75 (0.034)
4-t-OP_3EO	1.83 (0.062)	1.65 (0.020)	1.82 (0.037)	1.86 (0.036)
4-t-OP_4EO	1.87 (0.092)	1.47 (0.013)	1.75 (0.008)	1.91 (0.049)
4-t-OP_5EO	1.80 (0.097)	1.61 (0.007)	1.78 (0.096)	1.92 (0.054)
4-t-OP_6EO	1.92 (0.064)	1.83 (0.035)	1.70 (0.024)	1.96 (0.026)
4-t-OP_7EO	1.71 (0.014)	2.00 (0.030)	2.06 (0.260)	1.97 (0.044)
4-t-OP_8EO	2.10 (0.027)	2.12 (0.045)	2.06 (0.033)	2.05 (0.026)
4-NP	2.35 (0.137)	1.83 (0.014)	1.55 (0.043)	1.45 (0.009)
4-NP_2EO	1.78 (0.061)	1.54 (0.066)	1.53 (0.027)	1.68 (0.007)
4-NP_3EO	1.79 (0.063)	1.55 (0.020)	1.56 (0.019)	1.75 (0.045)
4-NP_4EO	1.70 (0.048)	1.64 (0.030)	1.56 (0.020)	1.80 (0.021)
4-NP_5EO	1.86 (0.037)	1.83 (0.048)	1.75 (0.024)	1.91 (0.010)
4-NP_6EO	1.75 (0.054)	1.83 (0.020)	1.82 (0.032)	1.88 (0.011)
4-NP_7EO	2.12 (0.041)	2.05 (0.022)	2.04 (0.035)	1.80 (0.023)
4-NP_8EO	1.95 (0.025)	2.10 (0.023)	2.05 (0.056)	1.90 (0.057)

Supplementary material of part 4

S.4.1 sewage sludge-based biochar characterization

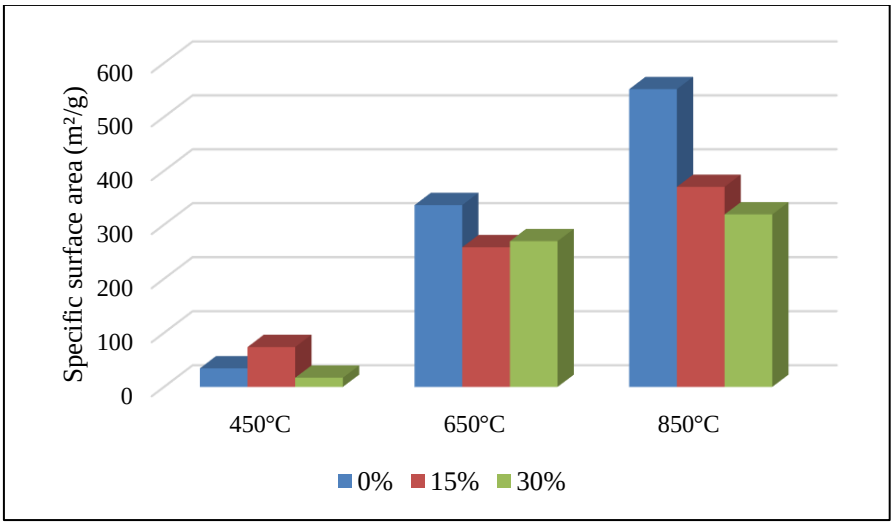

Figure S4.1. Effect of the percentage of sewage sludge on the biochars specific surface area.

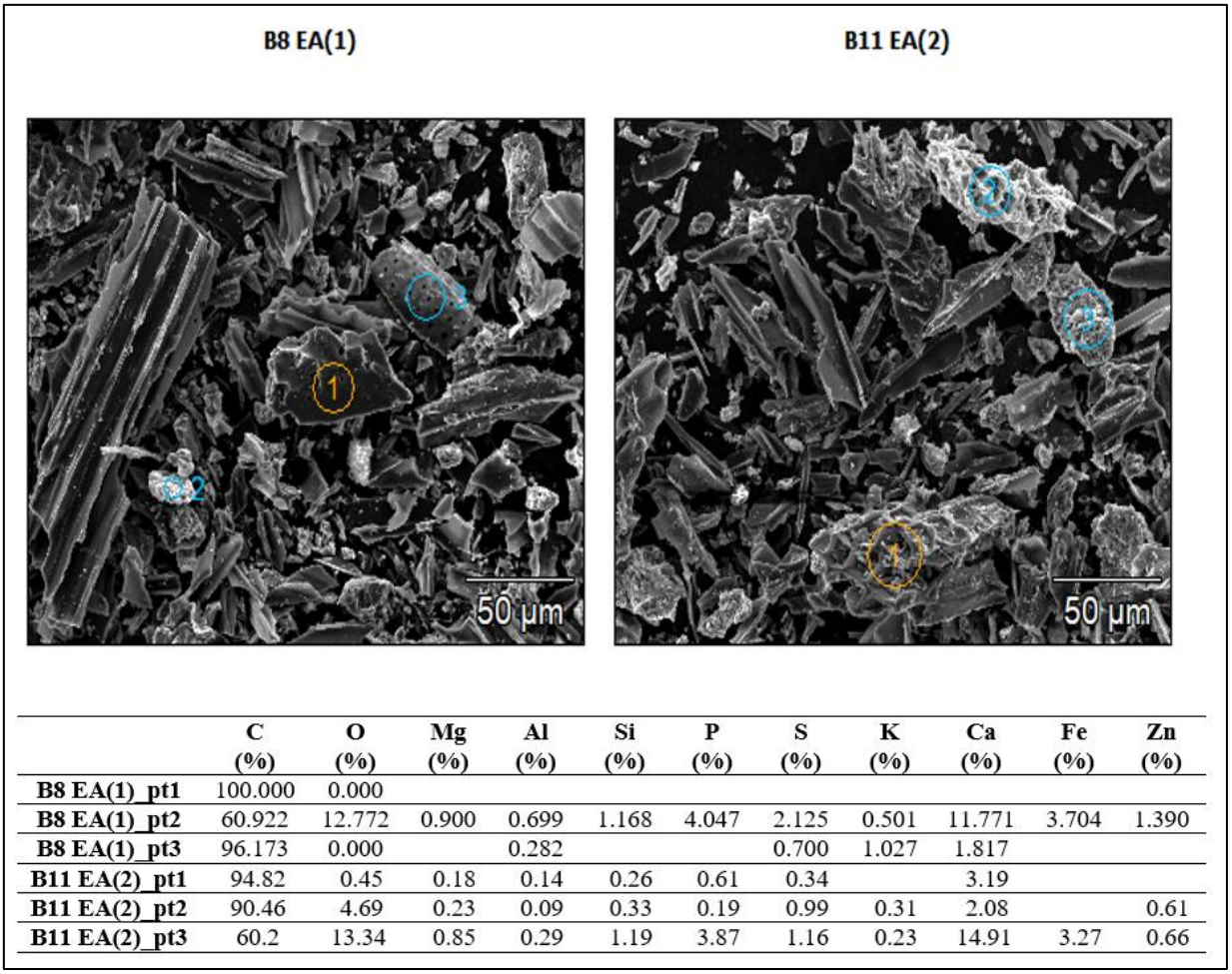

	C (%)	O (%)	Mg (%)	Al (%)	Si (%)	P (%)	S (%)	K (%)	Ca (%)	Fe (%)	Zn (%)
B8 EA(1)_pt1	100.000	0.000									
B8 EA(1)_pt2	60.922	12.772	0.900	0.699	1.168	4.047	2.125	0.501	11.771	3.704	1.390
B8 EA(1)_pt3	96.173	0.000		0.282			0.700	1.027	1.817		
B11 EA(2)_pt1	94.82	0.45	0.18	0.14	0.26	0.61	0.34		3.19		
B11 EA(2)_pt2	90.46	4.69	0.23	0.09	0.33	0.19	0.99	0.31	2.08		0.61
B11 EA(2)_pt3	60.2	13.34	0.85	0.29	1.19	3.87	1.16	0.23	14.91	3.27	0.66

Figure S4.2. SEM-EDS qualitative analysis of biochar 8 and biochar 11.

Table S4.1. Water extractable metals after acidic treatment

Biochar	Cr (ppb)	Ni (ppb)	As (ppb)	Se (ppb)	Cd (ppb)	Sb (ppb)	Hg (ppb)	Pb (ppb)
5	0.89	1.651	0.115	0.098	<0.000	0.067	<0.000	0.646
6	0.616	3.77	0.068	<0.000	<0.000	0.076	<0.000	3.375
8	0.93	0.403	1.127	<0.000	0.045	1.098	0.064	<0.000
10	0.437	1.533	0.034	<0.000	<0.000	<0.000	<0.000	4.501
11	1.786	2.255	0.7	0.032	<0.000	0.338	<0.000	1.122
EN12915-1	5	15	10	3	0.5	3	0.3	5

S.4.2 Characterization of the wood gasification wastewater

The wood vinegar is extracted from native woodland plant essences through the distillation of wood with its own physiological water, through the pyrolysis process. The wood vinegar is produced to be used exclusively in agriculture as an adjuvant for plant development and soil revitalizing agent. The wood vinegar is totally natural product that is rich in active ingredients in particular polyphenols and tannins. The acid character (**Table S4.1**), natural origin and cheap production of the wood vinegar allow its use for the modification of biochar instead of the traditional chemical products.

Table S4.2. Gasification wastewater characteristics.

Parameter	Value
pH	2.8 – 3.5
Density	1.05 kg/L
Acetic acid	2/2.6%
Total phenols	2.900/ 3.020 mg/kg
Tannins	13 - 26 g/kg
Heavy metals	< 1 mg/ kg

S4.3. Batch Adsorption of methylene blue

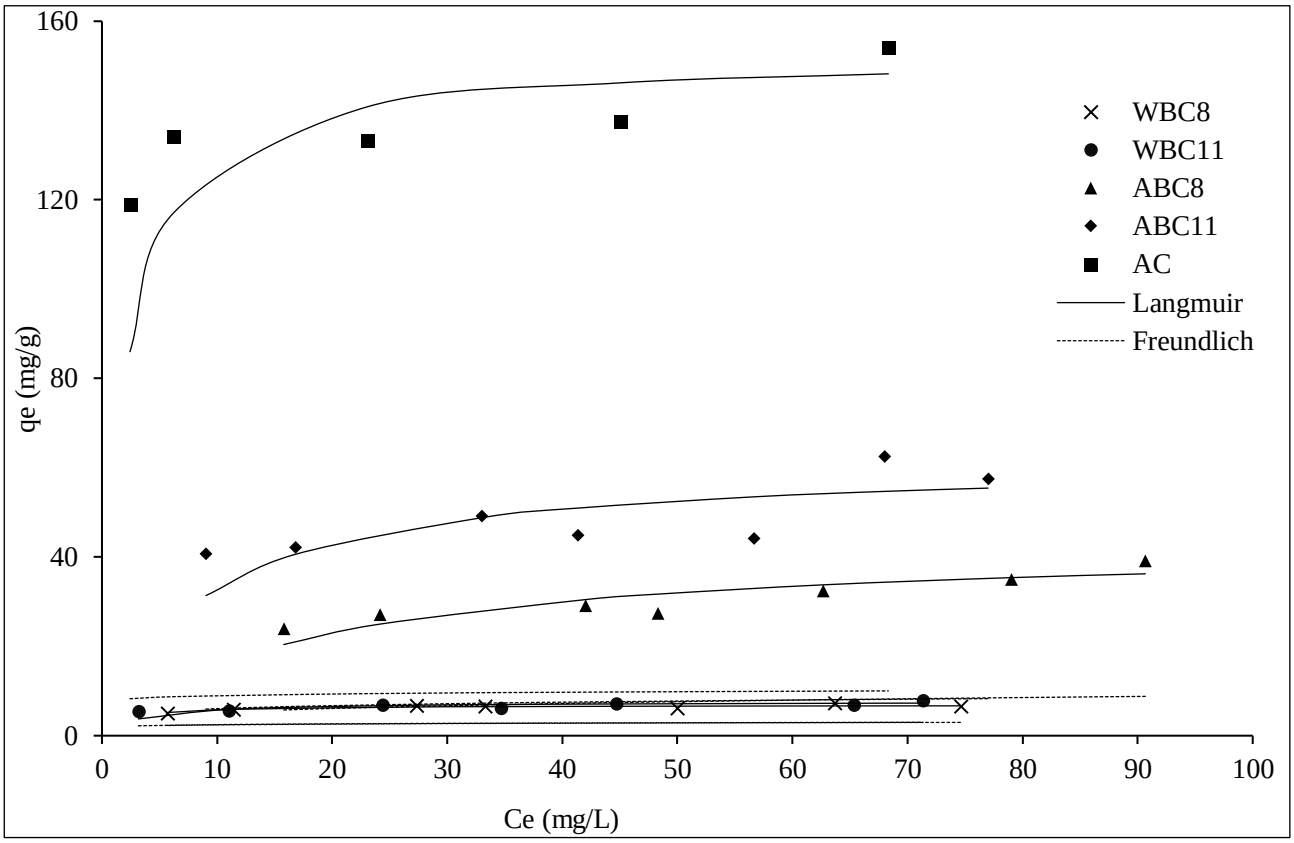

Figure S4.3. Experimental data of adsorption isotherm of methylene blue for biochar 8 and biochar 11 after acid washing (WBC8 and WBC11) and after acid washing and thermal activation (ABC8 and ABC11) compared to commercial activated carbon (AC) and adaptation of Langmuir models and Freundlich.

Résumé

Plusieurs périmètres agricoles irrigués par les eaux usées traitées (EUT) ont été établis en Tunisie dans le cadre de la stratégie de la conservation des eaux douces et de la recherche des sources hydriques alternatives. Afin d'évaluer les performances de l'utilisation des EUTs, caractérisées par des teneurs élevées en métaux lourds, pour l'irrigation des cultures agricoles à haute valeur ajoutée, les fraisiers et les oliviers ont été cultivés dans des petites échelles. Les résultats relatifs aux différentes propriétés chimiques et physiques du sol, à la croissance des plantes, au rendement et à la qualité des fruits suggèrent la possibilité de la courte réutilisation du EUTs dans l'irrigation des olives et l'utilisation de la dilution 60% (40% EUT) pour l'irrigation des fraisiers. Les niveaux de métaux dans le sol, les plantes et les fruits ont augmenté mais sans dépasser les limites autorisées. Cependant, le traitement supplémentaire des EUTs est désirable dans le but d'assurer une plus grande sécurité environnementale et santé publique lors de leur utilisation. Dans ce cadre, la production des matériaux carbonés (biochar) à faible coût capable de réduire, par adsorption, les concentrations des micropolluants tels que les métaux lourds, les colorants, les alkylphénols et les alkylphénols éthoxylés, contenus dans les EUTs. L'idée innovante de ce travail est représentée par la production de biochar par pyrolyse des déchets de bois mélangés à des pourcentages significatives de boues biologiques provenant des stations d'épuration. De plus, dans le but d'activer chimiquement le matériau, les eaux usées issues du processus de gazéification de la biomasse ligneuse ont été utilisées, conduisant à une réduction significativement des teneurs en cendres et en métaux et en hydrocarbures aromatiques polycycliques extractibles à l'eau, permettant ainsi l'utilisation du biochar comme un support adsorbant pour le traitement des eaux, conformément à UNI EN 12915-1. Les résultats obtenus à partir des études menées dans cette thèse de doctorat montrent que les biochars préparés uniquement à partir des déchets végétaux (sciure de bois) et d'un mélange de boue d'épuration et de sciure de bois peuvent être considérés comme des adsorbants appropriés pour l'élimination de différents types de micropolluants organiques des eaux usées. En fait, en raison de leurs surfaces spécifiques et de ses capacités d'adsorption, les biochars préparés peuvent être une alternative durable aux adsorbants commerciaux tels que le charbon actif, capable d'offrir des avantages environnementaux et économiques en réduisant la quantité de boues d'épuration dont il faut disposer et en minimisant le coût de production des matériaux adsorbants.
Mots clés : Eaux usées traitées ; Boues d'épuration ; Irrigation ; Polluants ; Biochar ; Adsorption.

Riassunto

Diversi perimetri agricoli irrigati con acque reflue trattate (ART) sono stati istituiti in Tunisia nel quadro della strategia per la conservazione delle acque dolci e la ricerca di fonti idriche alternative. Al fine di valutare le prestazioni dell'uso di ART, caratterizzate da alti livelli di metalli pesanti, per l'irrigazione di colture agricole ad elevato valore aggiunto, fragole e olivi sono stati coltivati su piccola scala. I risultati relativi alle diverse proprietà chimico-fisiche del suolo, alla crescita delle piante, alla resa e alla qualità dei frutti suggeriscono la possibilità di un breve riutilizzo delle ART nell'irrigazione dell'olivo e l'uso della diluizione 60% (40% ART) per l'irrigazione delle fragole. I livelli di metalli nel suolo, nelle piante e nei frutti sono aumentati ma non hanno superato i limiti consentiti. Tuttavia, il trattamento aggiuntivo delle ART è auspicabile nel tentativo di garantire una maggiore sicurezza ambientale e salute pubblica durante il loro utilizzo. In questo quadro, la produzione di materiali carboniosi a basso costo (biochar) in grado di ridurre, per adsorbimento, le concentrazioni di microinquinanti come metalli pesanti, coloranti, alchilfenoli e alchilfenoli etossilati, contenuti nelle ART. L'idea innovativa di questo lavoro è rappresentata dalla produzione del biochar mediante pirolisi di biomasse legnose di scarto miscelate con significative percentuali di fanghi biologici derivanti da impianti di depurazione. Inoltre, ai fini dell'attivazione chimica del materiale, è stata utilizzata un'acqua di risulta derivante dal processo di gassificazione di biomasse legnose, che si è dimostrata idonea a ridurre in modo significativo i contenuti di ceneri e di metalli e idrocarburi policiclici aromatici estraibili con acqua, rendendo i biochar idonei al loro utilizzo come mezzi adsorbenti per il trattamento delle acque, ai sensi della UNI EN 12915-1. I risultati ottenuti dagli studi condotti in questa Tesi di Dottorato dimostrano che i biochar preparati da soli rifiuti vegetali (segatura) e da una miscela di fanghi di depurazione e segatura possono essere considerati adsorbenti idonei per la rimozione dalle acque reflue di diversi tipi di microinquinanti organici. Infatti, per le loro superfici specifiche e per le loro capacità di adsorbimento, i biochar preparati possono essere un'alternativa sostenibile agli assorbenti commerciali come il carbone attivo, in grado di offrire vantaggi ambientali ed economici, riducendo da un lato la quantità di fanghi di depurazione che devono essere smaltiti e dall'altro minimizzando il costo di produzione dei materiali adsorbenti.
Parole chiave: Acque reflue trattate; Fanghi di depurazione; Irrigazione; Inquinanti; Biochar; Adsorbimento.